RANDOM VIBRATION OF DEGRADING SYSTEMS WITH GENERAL HYSTERETIC BEHAVIOR

A Dissertation Presented to

the Faculty of the School of Engineering and Applied Science

University of Virginia

In Partial Fulfillment

of the requirements for the Degree of

Doctor of Philosophy in Civil Engineering

by

Mohammad Noori

August 1984

APPROVAL SHEET

This Dissertation is submitted in partial fulfillment of the requirements for the degree of

Doctor of Philosophy in Civil Engineering

Mohammad Noori

AUTHOR

This Dissertation has been read and approved by the examining committee:

Dissertation Advisor

Accepted for the School of Engineering and Applied Science:

Dean of Engineering and Applied Science

Date: August 1984

ABSTRACT

Three mathematical models which are capable of representing general degradation behavior of hysteretic structural elements, including hysteresis pinching, as a function of hysteretic energy dissipation are presented. Two of the models are series models consisting of Bouc-Baber-Wen smooth hysteresis with two "slip-lock" elements. One of these slip-lock elements is designated as the BN and the other one as NB model. The third model has a single form and is designated as Single Element Pinching (SEP) model.

Behavior of a SDOF system of each model under cyclic and general loading is studied and the obtained results illustrate the versatility of all three models in reproducing various types of general degradation including pinching hysteretic behavior.

With the assumption of gradual degradation equivalent linearization solutions are obtained for these models for zero mean excitation case. Linearization for BN and SEP models are obtained in closed form and for NB model linearization is derived numerically. Nonstationary RMS response statistics obtained for zero mean excitaion, compare well with response statistics computed using Monte Carlo simulation. Comparison for NB and SEP models are better than those for BN model.

Response analysis of a SDOF system of BN and SEP model, subjected to nonzero mean input excitation is studied and approximate solutions are obtained by subtracting mean responses from the governing stochastic differential equations and then

applying equivalent linearization. The response predictions of the linearized model compare well for the SEP model and reasonably well for BN model. At all levels of excitation, the linearized models predict qualitatively the response of the system.

To Nahid, my wife, my helpmate, my companion and my friend. To you, my dear, who has faithfully supported me in this work by giving me inner strength, by your great sacrifices and devotion. No one knows how hard these years went by for you and my lovely son, Heeman. No one can understand how you sacrificed your health, your time, and all you could, for me. I could not do this work alone and without you. Words can not fully express my appreciation for what you have done for me. To you, at this moment of accomplishment, I hereby dedicate this work.

To Heeman, my son, who has reminded me in profound ways that research and wrinting are not the only things in life; who showed to me in many ways and terms where the real meaning of life lies. I apologize to you my son, for missing all those great moments that I could have spent and enjoyed with you. You taught me great lessons about unselfishness, sacrifice and true love. I admire your great patience, my son. So I hereby dedicate this work to you.

To Hooman, my newborn son. When I was finishing the final chapter of this work, you began the first chapter of your life. You were a great source of encouragement and hope for me in finishing and completing this work. So I hereby dedicate this work to you.

ACKNOWLEDGMENT

In completing the final phase of my graduate study, I wish to take this opportunity to express my sincere appreciation and gratitude to those people in my life who made this accomplishment possible. First and foremost, I want to thank my wonderful wife, Nahid, for her patience and understanding throughout my years of graduate study. Thank you for your love gifts. Without your sacrifice and encouragements this accomplishment would not be possible. And my son Heeman, thank you for your patience, love and undestanding. I have been richly blessed by a wife and a son who deserve much credit for this success, and to whom I dedicate this work.

There are others I wish to acknowledge and thank because of their unselfish support, guidance, help, encouragement, and input along the way. I should express my gratitude and appreciation for untiring efforts and benign guidance of Dr. Thomas T. Baber, my thesis advisor, in supporting me with ideas, help, and encouragement in this work through to the end. Thank you for introducing me to the wonderful world of probability, stochastic processes and random vibration. I say thank you in a deep and sincere way. I also want to express my appreciation to the other members of the doctoral committee. To Dr. Furman W. Barton, for his excellent teaching and friendly advices. He has been an admired and respected teacher and friend during my attendance at the University of Virginia. To Dr. Richard T. Eppink for his teaching, guides, comments and friendly discussions. To Dr. Kazakos from whom I learned a great deal about stochastic

processes. To Dr. Lois Mansfield for serving on my committee. I would also like to thank Dr. Richard L. Jennings from whom I learned a lot, through his excellent teaching. He was always available for consultation, friendly advice, discussion, and help. He has been an admired teacher and friend as well.

I wish to acknowledge the Academic Computing Center at the University of Virginia for generously provided computer funds for this work. Also my appreciation goes to the National Science Foundation for sponsoring this research.

Last but not least by any means, many thanks to my newborn son, Hooman, whose birth was a great source of inspiration for me in completing this work in time.

TABLE OF CONTENTS

CHAPTER PAGE

LIST OF FIGURES

LIST OF SYMBOLS

The following symbols are used in this thesis:

α = ratio of post-yield/pre-yield stiffness;

β = energy dissipation parameter of hysteretic restoring force;

γ = shape parameter of hystertic restoring force; also a variable of integration;

$\Gamma(.)$ = gamma function:

Δ = variable of integration;

δ_η = degradation rate for η;

δ_λ = degradation rate for λ;

δ_1 = degradation rate for 1;

δ_ξ = degradation rate for ξ;

δ_σ = degradation rate for σ;

δ_A = degradation rate for A;

δ_a = degradation rate for a;

δ_{ij} = kronelcker delta;

ε = hysteretic energy dissipation;

ζ = critical viscous damping ratio for the system;

ζ_1 = parameter controlling the magnitude of pinching in SEP model;

ζ_{1_0} = initial value of ζ_1;

ζ_2 = parameter controlling severity of pinching in SEP model;

η = stiffness degradation parameter in hysteretic restoring force;

η_0 = initial value of η;

θ = variable of integration;

λ = parameter controlling the magnitude of pinching in NB model; also a parameter that affects the severity of pinching in SEP model;

λ_0 = initial value of λ;

μ_i = mean value of response variable y_i;

μ_u = mean value of u;

μ_u = mean value of u;

μ_z = mean value of z;

μ_{u1} = mean value of u_1;

μ_{u2} = mean value of u_2;

μ_ε = mean value of ε;

ν = strength degradation parameter in hysteretic restoring force;

ν_0 = initial value of ν;

ξ = parameter controlling severity of pinching in NB model;

ξ_0 = initial value of ξ;

ρ_{23} = correlation coefficient between $\dot{u}$ and z (in SEP);

$\rho_{3\dot{4}}$ = correlation coefficient between $\dot{u}_1$ and z (in BN and NB);

= series summation;

σ = parameter controlling severity of pinching in BN model;

σ_0 = initial value of σ;

σ_i = rms response variable y_i;

σ_u = rms value of u;

$\sigma_{\dot{u}}$ = rms value of $\dot{u}$;

σ_z = rms value of z;

σ_{u1} = rms value of u_1;

σ_{u2} = rms value of u_2;

$\phi(.)$ = Gaussian cumulative distribution function;

ω_0 = natural frequency of nonlinear system;

A = hysteretic parameter affecting initial slope and yield level;

A_0 = initial value of A;

a = parameter controlling the magnitude of pinching in BN model;

a(t) = input base acceleration;

$\underset{\sim}{B}$ = right hand side vector of response covariance matrix equation;

b_{ij} = the nonzero term of matrix $\underset{\sim}{B}$;

BBW = Bouc-Baber-Wen smooth hysteresis model;

BN = Baber-Noori model;

C_{ei} = equivalent linearized damping coefficient;

E[.] = expected value;

erf(.) = error function;

$\underset{\sim}{f}$ = vector of Gaussian white noise excitation input;

f(z) = slip-lock function;

$\underset{\sim}{G}$ = linearized system matrix;

g(z) = continuous function approximation of δ function;

$g(y_2, y_3)$ = nonlinear hysteretic restoring force in SEP model;

$g_i(y_3, \dot{y}_4)$ = nonlinear function in the governing stochastic differential equation for BN and NB model;

h(z) = a function controlling dz/du vs z behavior in SEP model;

k = tangent stiffness;

K_{ei} = equivalent linearized stiffness coefficient;

K_0 = constant excitation power spectral density;

NB = Noori-Baber model;

n = parameter of hysteretic element, controls shape;

p = a parameter that affects magnitude of pinching in SEP model;

q = total restoring force;

q_L = a linear post-yield restoring force;

q_H = hysteretic restoring force;

$\underset{\sim}{S}$ = one time response covariance matrix;

SEP = Single Element Pinching model;

sgn(.) = signum function;

T = transpose;

u = displacement relative to the base;

u_1 = relative displacement of BBW component in Bn and NB models;

u_2 = relative displacement of slip-lock element in BN and NB;

$\underset{\sim}{v}$ = array of nonzero mean response variables;

$\underset{\sim}{y}$ = vector of response variables;

$\underset{\sim}{\dot{y}}$ = 1st order nonlinear governing stochastic differential equation for the system;

z = nonlinear hysteretic restoring force function;

z_{max} = ultimate value of z.

CHAPTER 1

INTRODUCTION

The destructive and many times disastrous effects of the forces of nature such as floods, earthquakes, gusty winds, and sea waves have always been a matter of significant concern to structural engineers. In these and numerous other cases, systems of engineering interest are subject to dynamic excitations which are basically random in nature. Examples range from systems acted upon by aerodynamic and fluid dynamic forces to machine induced noise environment.

The importance of incorporating natural hazard loadings, such as earthquakes, into engineering design criteria is well recognized. Traditionally the random dynamic characteristics of these forces have been replaced by "equivalent" static analysis and loadings, and the response of the structure under actual stochastic inputs has been obtained by theoretical studies based on deterministic methods. These methods have serious limitations due to the highly random nature of hazard loadings, and the accuracy of such an approach may prove inadequate in the presence of design constraints. The random nature of these loadings indicates that a probabilistic approach to analysis and design is necessary. The random nature of earthquake phenomena, for example, can be realistically represented only by stochastic mathematical models. Analyses that have used actual recorded data of particular earthquakes are equivalent to deterministic approach, and cannot be used to develop response statistics.

Although the deterministic aspects of these analyses become less restrictive when effects of a large number of past earthquakes are studied, the opportunity to investigate response for a spectrum of reconstructed earthquakes is limited by the relatively small number of existing records of strong motion earthquakes.

One thus is led to choose stochastic model representations of these types of random inputs and responses as an appropriate alternative approach. Numerous researchers have considered this possibility (4, 27, 87, 94, 127, 59, 123, 150, 114), and research continues in this area.

Analysis of structural systems to seismic excitations and other natural hazard loadings, is not an easy task. The response of structural systems to high intensity random loadings such as strong ground shaking, often exceeds the elastic range. The result is a highly nonlinear behavior due to yielding and subsequent energy dissipation through hysteresis. The inelastic response can be accompanied by strength and/or stiffness degradation. The exact nature of the system degradation is a function of structural materials and configuration which varies with the type of structure. Degradation can be quite important since it might lead to progressive weakening and total failure of structures. Therefore, the dynamic analysis of hysteretic, degrading structures under random excitation is a challenging task and employing proper analytical tools in dealing with the problem is essential.

The yielding behavior of hysteretically degrading structures has been described by linear models by most researchers. This simplified representation generally lacks the tractability necessary for even approximate analysis under random excitation. Other proposed hystereses, such as smooth hysteresis models, do not take into account hysteretic loop pinching behavior associated with many structural systems. To the knowledge of the author, no work has been done for developing a mathematical model for random vibration analysis of loop pinching hysteresis.

Another problem of considerable engineering interest is the nonzero mean response of hysteretic systems under random excitation. Practically, no work has been done on the nonzero mean response of hysteretic structures. Recently analytical procedures to allow response analysis of smooth hysteresis models under nonzero mean excitation have been developed by Baber (12). This work was based on the approach introduced by Spanos (127).

It is the objective of this thesis to study the problem of zero and nonzero mean response analysis of hysteretic structures, with general hysteretic behavior, subject to random vibration. The stochastic model considered for the base excitation here is a temporally modulated Gaussian white noise which has pertinent properties of seismic excitation. In Chapter 2, mathematical bases for developing general hysteretic models will be discussed and several nonlinear hysteretic models with the capability of reproducing loop-pinching and general deterioration are introduced. In Chapter 3, techniques for nonlinear random

vibration are discussed and a generalized equivalent linearization method as extended by Baber and Wen (15) is reviewed. A linearized form of the general hysteresis models of Chapter 2 is presented which has been derived without Krylov-Bogoliubov assumption. Zero mean numerical studies on the proposed models and nonstationary stochastic response of the proposed nonlinear models subject to temporally modulated Gaussian white noise is also presented. In Chapter 4, the problem of the nonzero mean response of hysteretic systems under random excitation is discussed and the application to general hysteresis models is presented. Numerical studies which verify the capabilities and range of apllicability of the proposed general hysteresis models, comparison of response statistics from linearized model and Monte Carlo simulation, for both zero mean and nonzero mean problems, have been included in the corresponding chapters. In Chapter 5, conclusions, remarks and suggestions are given. General theory and background for each individual topic has been included in the content of each chapter.

CHAPTER 2

MATHEMATICAL MODELS FOR STRUCTURAL HYSTERESIS

2.1- Introduction:

For years structural engineers have used differential equations to predict the behavior of structures subjected to dynamic loadings. In case of linear elastic behavior, the form of the differential equation has been accepted and the parameters in these equations, representing physical properties, have by various means been determined . The equations, along with the parameters they contain, constitute a mathematical model of the physical structure in question. The results of the studies on the dynamic response of linear systems have even gradually been incorporated into structural design procedures and codes.

In case of high excitations, such as strong ground motion, the response of structual systems exceeds the elastic range. As a result of yielding, the structure dissipates energy through hysteresis. The inelastic response can be accompanied by strength and/or stiffness degradation. The exact nature of the system degradation is a function of the structural materials and configuration which varies with the type of structure. Degradation can be quite important since it might lead to progressive weakening and total failure of structures. To predict this kind of response, mathematical models are needed that can predict the energy absorption, hysteretic response, and the resulting system evolution through degradation. Constructing such models requires in general, the deployment of systematic

modeling procedures.

2.2- Models for General Structural Hysteresis:

Ideally, the analytic modeling of inelastic behavior of structural systems requires a force-deformation relationship that can produce the true behavior of the structure at all displacement levels and strain rates. This is a difficult requirement in view of the number and variety of parameters which contribute to the hysteresis of different types of structural systems. Moreover, complete derivation of material models which can adequately predict different types of stress states for any desired material and configuration, requires more information than is currently available on the dynamic behavior of materials (104, 124, 107, 23, 69). Hence, in practice, simplified hysteresis models are usually selected to estimate dynamic response in the inelastic range. This is particularly true when response to stochastic excitations is required. Otherwise Monte Carlo simulation with a large number of sample functions may be the only feasible solution algorithm.

A number of approximate structural hysteresis models for inelastic dynamics, under deterministic or random excitation, have been developed.

The usual method of characterizing the behavior of a structural member under dynamic loading, for example cyclic loading, is to specify its force-deformation relation on first loading, called the skeleton curve, supplemented by a rule to

obtain unloading and reloading curves. The bilinear model of classical plasticity which exhibits a sharp transition from elastic to plastic state and linear hardening, is perhaps the simplest and most widely used model for inelastic behavior of structural elements under cyclic loading or high intensity excitation. Kinematic and isotropic hardening are two examples of rules to obtain unloading and reloading. Bilinear model has been used by many researchers in the analysis of dynamic response to complex deterministic as well as random excitations. Caughy (28, 29, 30), Iwan and Lutes (72), Kobori et al (85, 86), Husid (62), Goto and Iemura (51), Lutes and Takemiya (95), Roberts (118), Lutes and Lilhanand (94), Iwan and Gates (70), Tansirikongkol and Pecknold (140), Lutes (92), Popoff, jr (112), Iyengar and Dash (77), Mitani et al (102), Lutes and Jan (93), and Asano and Iwan (9), have used this model for different classes of problems and for obtaining approximate solutions in random vibration analysis, utilizing various techniques such as Gaussian closure and equivalent linearization. Additional studies have been performed on the stochastic response of elasto-plastic yield model, which is a special case of bilinear yield model, to seismic excitation by Kaul and Penzien (83), Penzien and Liu (110), Karnopp and Brown (81), Karnopp and Scharton (82), Liu (89), Vanmarcke and Veneziano (147), Grossmayer (54), Vanmarcke (145), Chopra and Lopez (37), and Yamada and Kawamura (153). The bilinear model fails to represent actual material behavior and is computationally inefficient because it requires one to keep track of all stiffness transition

points.

Other types of hysteresis models have also been used in analysis of deteriorating and nondeteriorating systems. For nondeteriorating systems, in an effort to simulate a smooth transition into the plastic range, many researchers have proposed algebraic expressions to be used as skeleton curves. The most well known example of this class is probably the Ramberg-Osgood relationship used by several researchers to predict inelastic response of structural systems (99). The Ramberg-Osgood model coupled with Masing's rule for unloading and reloading, give a continuous transition from elastic to inelastic states. This model however, suffers from many limitations. For example, it is difficult to include stiffness degradation. From a computational viewpoint, it is a tedious model to use, because it specifies deformation as a function of force and therefore, determination of force given deformation requires iterative techniques. Also the model as presented originally is not suitable for random excitations (23). Jennings (80), Iemura (63) and Iwan (67) have proposed other smooth models which are basically variations of Ramberg-Osgood model. A number of researchers proposed smoothly varying hysteresis models. Iwan (65), proposed a smooth model based upon a series of parallel coulomb and spring elements. Bouc's (26) hysteresis was used for analysis of single degree of freedom systems subjected to white noise excitation by Wen (150, 152).

Consideration of system degradation has also been investigated by numerous researchers. This introduces further

complications into the modeling of hysteresis, because it is necessary to choose an index of structural response which is indicative of the rate of degradation and the extent of nonlinearity of the response. This index is not a unique one, however, it should reflect the duration and severity of the nonlinear response. Gates (47), and Iwan and Gates (72) studied the seismic response of Iwan's model to specific sample earthquakes. Takeda et al (139) proposed a trilinear model for hysteretic behavior of reinforced concrete structures. The degradation in this model is governed by the maximum displacement. Penzien and Liu (110), and Liu (89) obtained approximate response statistics for a single degree of freedom system trilinear model by Monte Carlo simulation. Iemura (63) proposed a degrading bilinear model based on low cycle fatigue damage ratios and obtained mean square response statistics under filtered white noise by a variation of equivalent linearization. Shih and Lin (122) used a functional relationship proposed by Hata and Shibata to study vertical seismic load effect on hysteretic columns. Many other researchers in the response of hysteretic systems to random or complex deterministic excitations have developed other types of piecewise linear or smoothly varying hysteresis. Ozdemir (107) developed a model for describing hysteretic behavior of nonlinear elements. This model was used by Ozdemir (107) and Bhatti and Pister (23) for nonlinear transient dynamic analysis of frames with energy absorbingdevices. Baber and Wen (15, 14) developed an extension of Bouc's (26) model to represent degrading systems. This model

is a smooth hysteretic model capable of representing stiffness, strength or combined degradation as a function of total energy dissipated by hysteretic action. The model was applied by Baber and Wen (15, 16) to analyze multidegree of freedom shear beam, and discrete hinge structures subjected to random excitations. Sues et al (136, 137) used Baber and Wen model for seismic performance evaluation of buildings but with maximum deformation incurred in each cycle, instead of energy dissipation, as the index for measuring degradations. Ang and Wen (6) used Baber and Wen model for prediction of structural damage under random earthquake excitations.

Most of the available hysteresis models are unable to represent more complex forms of yielding behavior in which the hysteresis loop associated with successive cycles of loading show a progressive decrease in stiffness and energy dissipation as well as pinching behavior. Experimental investigations have demonstrated the existence of such deteriorating and pinching behavior. Such behavior may be associated with high shear loads and slippage of longitudinal reinforcement in reinforced concrete structures, with the behavior of cross braced steel frames, with cyclically loaded piles, or repeated loading of timber diaphragms to cite a few cases. Numerous examples of this type of behavior are reported in the literature (3, 7, 10, 21, 22, 51, 58, 64, 98, 101, 102, 104, 105, 108, 115, 124, 137, 141-143, 147, 152, 153).

Hysteresis loop pinching models which have been previously proposed, have been simple, but relatively inaccurate and constructed largely empirically (10, 17, 18, 45, 101, 121, 134,

153). Such models do not appear promising for random vibration (13), since they typically require several rules for their description which are not easily stated in a form compatible with available solution methods.

2.3- Proposed General Structural Hysteresis Models:

In this study three general degradation models are proposed. The first two models incorporate the previous smooth system deteriorating element by Bouc as modified by Baber and Wen (BBW) in series with slip-lock elements developed by Baber and Noori (BN) and Noori and Baber (NB). The third model is a single element pinching model (SEP) developed by modifying BBW smooth hysteresis element. In all three cases, the form of the model has been chosen to be suitable for equivalent linearization for random vibration analysis.

In this chapter, the mathematical basis for the development of these models is discussed. A thorough deterministic dynamic response study on the capabilities of the models, types of degradations obtainable under cyclic loadings, deterioration parameters, etc. is then presented. Behavior of the models under random vibration is discussed in Chapters 3 and 4.

2.4- Mathematical Basis for Developing Pinching Models:

The nonlinear system under study is a single degree of freedom system. The governing differential equation of motion is

$$\ddot{u} + 2\zeta\omega_0\dot{u} + q(u,t) = a(t) \qquad [2.1]$$

where 'u' is the displacement of the mass relative to the base, a(t) is the input base acceleration, and q(u,t) is the restoring force given by

$$q = \alpha\omega_o^2 u + (1-\alpha)\omega_o^2 z = q_L + q_H \qquad [2.2]$$

α is the ratio of post-yield/pre-yield stiffness. 'z' is the hysteretic restoring force which will be presented in detail for each of three proposed models in the following sections. The first component of the restoring force, q_L, is the linear post-yield restoring force, and the second component, q_H, is the hysteretic restoring force.

2.4.1- Slip-Lock Pinching Models:

In this section the mathematical basis for the development of two slip-lock models, Baber-Noori model (BN), and Noori-Baber model (NB), will be discussed. A single degree of freedom system for these two models is shown in Figure 2.1.

The Baber-Bouc-Wen (BBW) smooth hysteresis model is capable of reproducing a wide variety of inelastic, hysteretic, degrading behavior with a wide range of cyclic energy dissipation (14, 15, 27, 136, 137). For the two slip-lock models under study, the hysteretic restoring force model of BBW is presented in the form

$$\dot{z} = \{A\dot{u}_1 - \nu[\beta|\dot{u}_1||z|^{(n-1)}z + \gamma\dot{u}_1|z|^n]\}/\eta \qquad 2.3$$

where β, γ, and 'n' determine the hysteresis shape, and A controls the tangent stiffness. The parameters A, ν and η are varied as a function of the response history to introduce system

deterioration. In this work the dissipated hysteretic energy, $\varepsilon(t)$ is considered as a measure of response duration and severity, as in the work by Baber and Wen. The degradation parameters A, ν, η and other deteriorations parameters will be defined as functions of dissipated energy. The deterioration is chosen as

$$\begin{aligned} A &= A_0 - \delta_A \varepsilon \\ \nu &= \nu_0 + \delta_\nu \varepsilon \\ \eta &= \eta_0 + \delta_\eta \varepsilon \end{aligned} \qquad [2.4]$$

where A_0, η_0, and ν_0 are the initial values of the degradation parameters, and δ_A, δ_η, and δ_ν are parameters which control the rate of degradation of initial tangent stiffness, stiffness, and strength respectively. Here these rates are chosen as constants. Also in Equation [2.4]

$$\begin{aligned} \varepsilon &= \int_{u_o}^{u_f} q_H du = (1-\alpha)\omega_0^2 \int_{u_o}^{u_f} z\, du \\ &= (1-\alpha)\omega_0^2 \int_{t_o}^{t_f} (z.u)\, dt \end{aligned} \qquad [2.5]$$

Detailed study of the BBW model is presented in References (14, 15, 150).

Equation [2.3] is one of example of a number of hysteretic models which take the general form

$$\dot{z} = g(\dot{u}, z, t) \qquad [2.6]$$

models of this form have been found to be quite useful in random vibration analysis, because of their expression in a compact

mathematical form. Generally, the functions will be piecewise differentiable, at best.

In order to add hysteresis loop pinching capability, a time dependent slip-lock element as shown schematically in Figures 2.1 and 2.2(b) is incorporated in series with the BBW smooth hysteresis element as given by Equation [2.3]. The mathematical form of the "slip-lock" element for each of the two models BN and NB will be as follows.

2.4.1.1- Slip-Lock Element in Baber-Noori Model:

The slip-lock element in BN model is given by the differential equation

$$\dot{u}_2 = f(z).\dot{z} \qquad [2.7]$$

where 'z' is the restoring force defined by Equation [2.3]. Equation [2.7] can be written in the form

$$du_2/dz = f(z) \qquad [2.8]$$

Equation [2.8], which defines the behavior of the slope of the function in Figure 2.2(b) suggests the following properties for the function f(z)

(a) f(z) is an at least piecewise continuous function which is independent of the sign of z and u_2.

(b) f(z) is zero, or nearly zero everywhere, except within a small region near z=0, where it has a sharp peak as shown in Figure 2.3. In the limit, as the

stiffness during slipping goes to zero, f(z) approaches the Dirac delta function. In practical situations, a large but finite peak value is expected.

For practical modeling purposes, it is convenient to choose f(z) of the form

$$f(z) = 2a.g(z) \qquad [2.9]$$

where g(z) is chosen to have an area of 1, in order to allow a total slip of '2a', i.e., it is a continuous function approximation of Dirac delta function. Thus, it is seen that g(z) has the form of a unimodal probability density function, symmetric about z=0. The magnitude of slip 'a' is computed, as are the other deterioration parameters, as a function of the response history. Herein, 'a' is given as

$$a = \delta_a \varepsilon \qquad [2.10]$$

where δ_a is a parameter which controls the amount of pinching as a function of the energy dissipated. Any function with properties discussed above can be considered as a suitable model for g(z). In the present work the Gaussian density function,

$$\dot{u}_2 = 2a/(\sqrt{2\pi}\ \sigma).\exp\{-\ z^2/(2\sigma^2)\}\cdot \dot{z} \qquad [2.11]$$

is used for mathematical tractability. A small value of σ in Equation [2.11] creates the sharp peak needed by the pinching model. Equation [2.11] will give a slip of '2a' as 'z' changes sign. For more general degradation, parameter σ can be taken as

$$\sigma = \sigma_0 + \delta_\sigma \varepsilon \qquad [2.12]$$

In the present study σ is considered as a constant parameter with a small value relative to the ultimate value of 'z'. Equations [2.1], [2.3]-[2.5], [2.7], [2.10] and [2.11] complete the BN pinching hysteresis model.

2.4.1.2- Slip-Lock Element in Noori-Baber Model:

In the second proposed model, instead of a differential equation form, the slip-lock element is defined in a relatively simpler analytic form as follows

$$u_2 = \lambda \cdot \arctan(z/\xi) \qquad [2.13]$$

where 'z' is defined by Equation [2.3].

In this model, parameter λ controls the slipping magnitude and the severity of pinching, and ξ is a small parameter which controls and is a measure of the rate of change of the pinching. The sharpness of pinching is controlled by this parameter. These two parameters are defined as two linear functions of dissipated energy as follows

$$\lambda = \delta_\lambda \varepsilon$$
$$\xi = \xi_0 + \delta_\xi \varepsilon \qquad [2.14]$$

where ε is given by Equation [2.5]. Equations [2.1], [2.3], [2.5], [2.13] and [2.14] complete the definition of NB model.

This element has a behavior very similar to the BN slip-lock element. However, because u_2 is given directly as an algebraic function of z, it is more tractable mathematically.

This results in reduction of the number of operations involved for numerical studies in deterministic case. Moreover, in random vibration analysis, the mathematical form of the model is suitable for approximate analysis and its relatively simple form reduces the simulation costs. Comparison of the two models is presented in numerical studies in this chapter as well as in random vibration analysis of the proposed models in Chapters 3 and 4.

2.4.2- Numerical Studies on the Behavior of Proposed Series Models:

In order to investigate the capabilities of the proposed slip-lock series models in representing hysteretic pinching as well as general degradation behavior, ranges of the parameters for the control of pinching and also for comparing the performance of each of the two slip-lock models, several studies were conducted. The numerical studies reported in this section were undertaken to verify the behavior of the models under cyclic and general loadings. Initially, it was necessary to develop tractable schemes for numerical simulation of the nonlinear systems by digital computer, both for verification of the model behavior under general loading, and for subsequent Monte Carlo simulation during random vibration analysis.

Consider the governing equations for the two series models. It can be noted that for the BN slip-lock model, Equations [2.3] and [2.11] contain derivatives on the right hand side which are of the highest order of the particular variable involved. If it

is assumed that u, u_1 and u_2 all have the same algebraic sign due to the absence of any intermediate mass between the smooth system and slip-lock elements, then this problem is easily taken care of. In the case of NB model

$$u_2 = [(\lambda\xi)/(\lambda^2 + z^2)]\,\dot{z} \qquad [2.15]$$

due to explicit form of the integral the difficulties existing with the numerical integration of the BN model will not be encountered. Noting that for these two models

$$\text{or} \qquad \begin{aligned} u &= u_1 + u_2 \qquad (a) \\ \dot{u}_2 &= \dot{u} - \dot{u}_1 \qquad (b) \end{aligned} \qquad [2.16]$$

and setting up $\operatorname{sgn}(\dot{u}_1) = \operatorname{sgn}(\dot{u})$ in accordance with the assumption, will give the following relation for BN model upon substitution of [2.3] and [2.15] into [2.10]

$$\dot{u}_1 = (\dot{u}/\eta)/\Big[1 + 2a/(\sqrt{2\pi}\sigma).\exp(-z^2/2\sigma^2).\{A - \nu[\beta \operatorname{sgn}(\dot{u})|z|^{(n-1)}z + \gamma|z|^n]\}\Big] \qquad [2.17]$$

For NB model, substitution of [2.3] and [2.15] into [2.16] results similarly

$$\dot{u}_1 = (\dot{u}/\eta)/\Big[1 + (\lambda\xi)/(\lambda^2 + z^2).\{A - \nu[\beta \operatorname{sgn}(u)|z|^{n-1}z + \gamma|z|^n]\}\Big] \qquad [2.18]$$

Once u_1 is obtained in this manner, it is straightforward to obtain u_2 and z, in the case of BN model, by substitution into [2.16] and [2.3], respectively. For the NB case, z can be obtained in the same way, but u_2 is easily obtained directly from [2.15]. Although Equations [2.17] and [2.18] contain a

derivative of u it is not the highest order derivative of u in the problem, so numerical values are available at each time step. Thus, Equations [2.1]-[2.5], [2.16] and [2.17] for the BN model and [2.1]-[2.5], [2.16] and [2.18] for the NB model form two sets of simultaneous ordinary differential equations which are equivalent to the original sets but more suitable for numerical purposes.

It should be mentioned here that by substituting Equations [2.17] or [2.18] into Equation [2.3] a single element pinching model can be obtained but the resulting equations will have a very complicated form and are not mathematically tractable.

The excitation a(t) in Equation [2.1] can be any specifiable function. For the purpose of model verification in this section, a(t) will be taken as a Gaussian white noise. Discussion on the input noise with regard to the random vibration analysis will be presented in the next chapter.

In the studies reported in this chapter and in this work, degradation of BBW system parameters, A, ν and η will not be considered, except for a number of examples to show the capability of models in reproducing combined strength and stiffness degradation as well as pinching behavior. As an example on the capabilities of BBW smooth model, two plots of the response of a SDOF system of this model have been presented in Figure 2.4. Figure 2.4 (a) illustrates combined stiffness and strength degradation under a cyclic displacement with amplitude of 2.5. Degradation rate is slow for this case and parameter

values of $\delta_A = \delta_\eta = \delta_\nu = 0.004$ are considered. Figure 2.4(b) shows similar behavior with higher rate of degradation and with parameter values of $\delta_A = \delta_\eta = \delta_\nu = 0.01$. More examples on degradation of these parameters as well as capabilities of BBW system have been reported extensively elsewhere (15, 136). Here, the emphasis will be on the study of pinching behavior of the proposed models.

2.4.2.1- Numerical Studies on the Baber-Noori Model:

In the studies for the BN model, only the parameter 'a' was degraded and 'σ' was kept as constant.

First to verify the type of degradation behavior obtainable by this model, behavior of a single degree of freedom system model under cyclic displacement u_1 was obtained by numerical integration with parameter values $A_0 = 1$, $\beta = \gamma = 0.5$, and $\sigma = 0.08$. The deterioration parameter $\delta_a = 0.1$ was chosen, with all other parameters taken as constant. With $u_1(t)$ a known sinusoidal function, $\dot{u}_2$, $\dot{z}$ and $\dot{u}$ all follow from Equations [2.3], [2.11] and [2.16], following differentiation of $u_1(t)$. Figure 2.5 shows the response of the smooth system, slip-lock and series models, which comprise the BN model. To verify the behavior of the nonlinear differential equation set [2.1]-[2.5],[2.10],[2.15] and [2.16], and also to illustrate more fully the effect of varying δ_a and σ, several single sample plots of z versus u were obtained under white noise excitation. Plots of runs for several cycles of model for a low pinching rate, $\delta_a = 0.1$ and $\sigma = 0.1$, and high pinching rates

where $\delta_a = 0.5$ and $\sigma = 0.1$, $\delta_a = 0.5$ and $\sigma = 0.2$ are shown in Figures 2.6(a)-(c). In all cases shown, the viscous damping ratio $\nu = 0.1$. The plots shown in Figure 2.6 are fairly rough, since they are based on a limited number of data points, but the anticipated behavior is observed. It can be seen that severity of pinching increases by increasing δ_a, and the sharpness of pinching varies inversely with σ.

Figure 2.7 illustrates the capability of this model in reproducing pinching behavior under a cyclic displacement, as given above, along with combined strength and stiffness degradation. The two cases shown in Figure 2.7(a) and 2.7(b) are for a moderate pinching rate with the pinching parameter values of $\sigma_0 = 0.07$, $\delta_a = 0.3$, and $\delta_\sigma = 0.009$. The stiffness and strength degradation rates for the two cases are similar to those used in Figure 2.4(a) and (b) respectively. To demonstrate a more general pinching behavior σ has been set to vary according to Equation [2.12].

2.4.2.2- Numerical Studies on the Noori-Baber Model:

A similar study for the verification of the capabilities of NB nonlinear pinching model was performed. Behavior of a single degree of freedom system was studied to investigate the deterioration obtainable by the NB model as well as to compare its capabilities with the preceeding BN model. Here, the deterministic studies and comparisons are reported. Comparison under random vibration analysis will be discussed in next chapters.

Similar to previous case, u_1 was set to vary cyclically. With $u_1(t)$ a known function, 'z' can be evaluated from Equation [2.3] following differentiation of u_1. In this case, $u_2(t)$ is directly evaluated from Equation [2.13] and u_2 is obtained following integration of z. u then follows from summation of u_1 and u_2. Because of the simple analytic form of u_2 in Equation [2.13], the number of variables to be integrated in this case, is less than the one for BN model. Therefore, fewer operations are involved for integration in each time step. This reduces the computation cost as compared with preceeding model.

Parameter values of $A_0 = 1$, $\beta = \gamma = 0.5$ were considered for BBW component in this case. Figure 2.8(a) and (b) show two plots of the response of slip-lock elemnt in this model with low and high degree of pinching sharpnesses respectively. This model in series with BBW smooth element comprise the NB model. The pinching parameters considered for these plots were, $\xi_0 = 0.05$, $\delta_\lambda = 0.2$, and $\delta_\xi = 0.0$ for Figure 2.8(a), and $\xi_0 = 0.01$, $\delta_\lambda = 0.2$, and $\delta_\xi = 0.0$ for Figure 2.8(b). In Figure 2.9 the behavior of NB model under a cyclic displacement similar to the one used in preceeding case, is illustrated. Figure 2.9(a) with parameters $\xi_0 = 0.35$, $\delta_\lambda = 0.2$, and $\delta_\xi = 0.0$ shows a low pinching case, whereas Figure 2.9(b) with parameter values of $\xi_0 = 0.125$, $\delta_\lambda = 0.5$, and $\delta_\xi = 0.0$ represents a high pinching rate behavior of this model. For verification of behavior of nonlinear system defined by differential equations [2.1]-[2.5], [2.13], and [2.15] and to study the effect of

varying λ and ξ several single sample plots of 'z' versus 'u' were obtained under white noise excitation. Plots of several cycles of these responses are illustrated in Figures 2.10(a)-(d). These plots are for the cases with low pinching sharpness, where $\xi_0 = 0.3$, with two different rates of low and high pinching severity of $\delta_\lambda = 0.2$, Figure 2.10(a), and $\delta_\lambda = 0.5$, Figure 2.10(b). And also for high pinching sharpness where $\xi_0 = 0.15$, with two different rates of low and high pinching severity of $\delta_\lambda = 0.2$, Figure 2.10(c), and $\delta_\lambda = 0.5$, for Figure 2.10(d). As these plots show, the severity of pinching in this model increases with λ and the sharpness of pinching varies inversely with ξ.

To show the general hysteretic behavior capability of NB model in representing pinching as well as stiffness and/or strength deterioration, behavior of a SDOF system of the model under cyclic displacement was considered where BBW parameters were allowed to deteriorate. Figure 2.11(a)-(d) show a combined strength and stiffness degradation accompanied with pinching behavior. Figure 2.11(a) and (b) are for low degradation rates of BBW element with $\delta_\eta = \delta_\nu = \delta_A = 0.004$, and for pinching parameter values of $\xi_0 = 0.05$, $\delta\lambda = 0.2$, Figure 2.11(a), and a sharper pinching with $\xi_0 = 0.1$, $\delta_\lambda = 0.2$, Figure 2.11(b). Whereas Figures 2.11(c) and (d) are for higher degradation rates of BBW with $\delta_A = \delta_\eta = \delta_\nu = 0.001$, and with pinching parameters for two cases of low and high pinching sharpness similar to those in Figure 2.11(a) and (b).

2.4.3- Single Element Pinching Hysteresis Model:

The third model, as shown schematically in Figure 2.12, is an extension of BBW hysteresis model which has been generalized such that it can reproduce loop-pinching hysteresis as well. In order to incorporate loop-pinching capability in the BBW model, the following modification is considered for the hysteretic restoring force equation

$$\dot{z} = h(z).\{A\dot{u} - [\beta|\dot{u}||z|^{(n-1)}z + \gamma\dot{u}|z|^{n}]\}/\eta \qquad [2.19]$$

The mathematical approach for the development of a suitable h(z) function is based on the study of the behavior of the slope of restoring force, i.e., dz/du versus 'z', for the two proposed slip-lock models introduced in preceeding sections.

Consider first the behavior of dz/du vs 'z' for the original smooth element hysteresis of BBW. A plot of this type has been shown in Figure 2.13. In this discussion consider the case n = 1. Figure 2.13 represents a nondeteriorating case. In the BBW model, three parameters η, ν, and A are defined to incorporate stiffness, strength or combined degradation respectively. The effect of variation of these three parameters on the dz/du versus 'z' plot, as z/z_{max} changes, have been shown in Figure 2.14. As can be observed, in each cycle degradation is introduced by reduction of initial value of slope, Figure 2.14 (a), ultimate value of z, Figure 2.14(b), or both, Figure 2.14(c). For all three cases in Figure 2.14 a cyclic displacement with amplitude of 2.5 was used. In order to incorporate pinching behavior as

well, it is necessary to establish an additional variability as shown in Figure 2.15. In the case when no other degradation occurs, the effect of pinching on the variation of dz/du vs 'z' is that, as 'z' changes sign, dz/du decreases to a certain desired level, and then starts increasing until it becomes asymptotic to the original slope in the non-pinching smooth hysteresis case. The extent of slope decrease value of 'z' at which the initial slope is effectively regained depends on the amount and rate of pinching in the model.

To verify that the suggested variation of dz/du does, indeed, occur, consider the dz/du vs 'z' behavior plots for slip-lock models introduced earlier. Figure 2.16 shows this plot for a SDOF BN model subjected to a cyclic displacement with amplitude of 2.5. Figure 2.16(a) and 2.16(b) represent the two cases of low and high pinching respectively. The slope behavior shown in Figure 2.16(b) corresponds to the loop-pinching behavior illustrated in Figure 2.5(c). In these two cases, parameters 'a' and σ both vary according to Equations [2.10] and [2.12], with the parameterr values of $\sigma_0 = 0.07$, $\delta_a = 0.1$, and $\delta_\sigma = 0.009$, for Figure 2.16(a), and $\sigma_0 = 0.07$, $\delta_a = 0.4$, and $\delta_\sigma = 0.03$, for Figure 2.16(b). Figure 2.17(a) and (b) represent similar study for NB model under the same input displacement. Parameters λ and ξ follow the Equation [2.14]. Pinching parmeter values for each case are $\lambda_0 = 0.$, $\delta_\lambda = 0.1$, $\xi_0 = 0.1$, and $\delta_\xi = 0.0$, for Figure 2.17(a), and $\lambda_0 = 0.$, $\delta_\lambda = 0.4$, $\xi_0 = 0.02$, and $\delta_\xi = 0.$, for Figure 2.17(b). These plots have been obtained by considering no deterioration for BBW component

of the models. Slope behaviors shown in Figures 2.17(a) and (b) relate to the cyclic behavior of NB model as illustrated in Figures 2.19(a) and (b).

From these plots it is possible to infer the desired properties of the slope variation which will be the basis for developing a suitable function h(z).

(a) In the initial (starting from rest) loading, no pinching occurs.

(b) In the first pinching cycle the value of dz/du drops sharply near z = 0. In the following cycles the reduction slows down, but the range of 'z' for which a significant decrease in stiffness occurs spreads.

(c) In each cycle slope is low near z = 0, then increases relatively rapidly as 'z' increases. This rapid increase slows as the original slope is approached. As 'z' finally approaches ultimate value, the slope sharply decreases and reaches zero at the appropriate z_{max}, which may or may not change with time.

(d) The slope reaches the non-pinching slope and 'z' should reach the same ultimate value even at high pinching rate although large displacement may be required to reach z_{max}.

Considering these observations and criteria, h(z) is taken as a function which has a small, but nonzero value near z = 0., but

approaches 1 as z increases. How rapidly h(z) approaches 1 with increasing z depends upon the desired amount of pinching. A simple mathematical form with the desired properties is

$$h(z) = 1 - \zeta_1 \exp(-z^2/\ \zeta_2{}^2) \qquad [2.20]$$

In this equation ζ_1 and ζ_2 can be established so that a plot of dz/du vs 'z' computed from Equation [2.19] will have a form similar to the slip-lock models plotted in Figure 2.16 and 2.17. In Equation [2.20] ζ_1 is a parameter that controls the magnitude of initial drop in slope. This parameter should vary such that the magnitude of initial drop increases relatively rapidly during the beginning cycles but approaches a maximum value $\zeta_1 < 1$ after several cycles. ζ_2 is introduced to control the rate of change of the slope. For the current work, ζ_1 is expressed as an exponential function of dissipation energy

$$\zeta_1 = \zeta_{1_0}(1 - \exp[-p\varepsilon]) \qquad [2.21]$$

so that at the beginning cycles there is a noticeable drop in the magnitude of initial slope but as time progresses, the rate of drop will decrease. ζ_2 is established in such a way that it is a function of both energy dissipation and ζ_1, and is given, for the present work by

$$\zeta_2 = \xi(\lambda + \zeta_1) \qquad [2.22]$$

where

$$\xi = \xi_0 + \delta_\xi \varepsilon \qquad [2.23]$$

Initially, when the energy dissipated and therefore ζ_1 is zero,

ζ_2 will have a nonzero starting value. In these equations, ε is the dissipation energy as given by Equation [2.5], 'p' is a constant parameter that contributes to the control of the rate of initial drop in slope, ζ_{1_0} is a parameter that is a measure of the total slip, ξ also contributes to the control of the amount of pinching and λ is a small parameter that controls the rate of change of ζ_2 as ζ_1 changes. Figure 2.18 show the variation of a sample function of ζ_1 versus energy and ζ_2 as a function of ζ_1 for the single element pinching model subjected to a cyclic displacement. Both plots have been obtained under a cyclic displacement with amplitude of 2.5. Pinching parameter values used here are $\zeta_1 = 0.8$, $p = 1$, $\xi_0 = 0.2$, $\delta_\xi = 0.1$, and $\lambda = 0.06$. In Figure 2.19 the effect of the variation of ζ_1 on pinching is plotted where ζ_2 is kept constant. As can be seen, ζ_1 controls the amount of initial drop in slope, and therefore the rate of pinching, in successive cycles. For this plot values of $\zeta_{1_0} = 0.7$, $p = 0.06$, and $\zeta_2 = 0.3$ were used. Figure 2.20 represents the variation of ζ_2 when ζ_1 is kept constant. This figure shows that ζ_2 controls the rate of change of slope variation in each cycle, as the slope approaches its original level. It also provides a smooth behavior for the change in slope and prevents a sudden drop in value of 'z' before 'z' gets to ultimate level. Parameter values of $\zeta_1 = 0.6$, $\xi_0 = 0.2$, $\delta_\xi = 0.05$, and $\lambda = 0.06$ were used to plot this figure. Figure 2.21 illustrates the variation of dz/du vs 'z' for the single element pinching model subjected to a cyclic displacement as described for preceeding plots. In this figure,

ζ_1 and ζ_2 both vary according to Equations [2.21]-[2.23] and for the two cases of low and high pinching rates. In Figure 2.21(a), low pinching case, parameter values of $\zeta_{10} = 0.65$, $p = 1$, $\xi_0 = 0.2$, $\delta_\xi = 0.01$, and $\lambda = 0.06$ are used, and for Figure 2.21(b), high pinching case, values of $\zeta_{10} = 0.85$, $p = 1$, $\xi_0 = 0.2$, $\delta_\xi = 0.03$, $\lambda = 0.06$ are considered. Loop-pinching behavior of this model under cyclic displacement, corresponding to these two slope behaviors, are shown in Figures 2.23(a) and (b) respectively. A comparison between Figure 2.21(a) and (b) and Figures 2.16 and 2.17 shows similarity in slope behavior for the single element pinching model and the two series models and therefore indicates the capability of this model in reproducing similar pinching behavior. Further detailed comparison between this model and the other two proposed models is presented in numerical studies of the model in this chapter and in random vibration analyses using the proposed models.

2.4.4- Numerical Studies on the Single Element Pinching Model:

In order to verify the capabilities of the single element pinching model (SEP), numerical studies were performed. The study presented on the similarity in the behavior of dz/du vs 'z' for this model and the two slip-lock models indicated that this model would be capable of reproducing pinching behavior in the same manner as the other two series models. Following studies illustrate and verify this behavior as well as advantages of this model as compared with the other two proposed models. Further studies and comparisons under random vibration analysis will be

introduced in next chapters.

To investigate degradation behavior of a single degree of freedom system of this model, a known sinusoidal function with an amplitude increasing with time, as shown in Figure 2.22, was used for u(t). The right hand side of equation for restoring force, [2.18], contain $\mathring{u}$, but $\mathring{u}$ is available at time t as a result of the numerical integration. Alternately, under cyclic displacement, a program of u(t) values can be differentiated to provide values of $\mathring{u}$. Thus numerical values are directly available at each time step for the SEP model. The analytical complexity is hence reduced by the SEP formulation as compared with either of the two series models. This reduces the computation time involved and is one of the advantages of the SEP model. The significance of this feature is better understood and is more valueable in the random vibration and statistical analysis, as will be seen later.

In the studies reported here, parameter values of $A_0 = 1$, $\beta = \gamma = 0.5$ were considered. Figures 2.23(a) and (b) illustrate the loop pinching behavior of SEP model under the cyclic displacement shown in Figure 2.22. Figure 2.23(a) represents a low pinching rate case with pinching parameter values of $\zeta_{10} = 0.8$, $\lambda = 0.05$, $\xi_0 = 0.2$ and $\delta_\xi = 0.01$. Figure 2.23(b) shows a high pinching rate behavior with parameters $\zeta_{10} = 0.95$, $\lambda = 0.3$, $\xi_0 = 0.2$, and $\delta_\xi = 0.01$. For both cases a viscous damping ratio of 1% was considered.

To verify the behavior of nonlinear system defined by

Equations [2.5] and [2.19]-[2.23] and to study the effect of varying pinching parameters, several single sample plots of 'z' vs u were obtained under white noise excitation. Plots of several cycles of these responses are illustrated in Figures 2.24(a) and (b). Figure 2.24(a) shows a case for low pinching rate, with parameter values $\zeta_{1_0} = 0.8$, $\lambda = 0.05$, $\xi_0 = 0.2$, and $\delta_\xi = 0.01$, whereas Figure 2.24(b) represents a high pinching case with parameter values of $\zeta_{1_0}=0.95$, $\lambda = 0.3$, $\xi_0 = 0.2$, and $\delta_\xi = 0.01$. As these plots indicate, severity of pinching increases with ζ_1 and the sharpness inceases with ζ_2.

The general hysteretic behavior of the SEP model and its ability to reproduce pinching combined with stiffness and strength degradation, was verified by considering the behavior of a SDOF system of this model, as shown in Figure 2.12, under cyclic displacement as shown in Figure 2.22. Figure 2.25(a) and (b) illustrate this behavior. In Figure 2.25(a), a plot with low degradation rates for strength and stiffness with parameter values of $\delta_A = \delta_\eta = \delta_\nu = 0.001$ is shown. And Figure 2.25(b) represents a strength and stiffness deterioration with higher rate and with parameter values of $\delta_A = \delta_\eta = \delta_\nu = 0.004$. For both cases a high pinching rate was considered with pinching parameter values of $\zeta_{1_0}= 0.9$, $\xi_0 = 0.2$, $\lambda = 0.06$, and $\delta\xi = 0.01$.

Studies performed on deterministic behavior of the SEP model indicate that the model is very well capable of reproducing various types of degradation behavior. Further studies on the

three proposed models as well as comparison of the statistical responses of the models will be presented in the following chapters.

CHAPTER 3

RANDOM VIBRATION OF PROPOSED HYSTERESIS MODELS

3.1- Introduction:

Basically three elements are involved in the analysis of the response of nonlinear dynamical systems to stochastic excitations. The first of these is to obtain mathematical models that provide the best representatives for particular materials and configurations. Such models, however, generally lack the tractability necessary for even approximate analysis under random vibration, except by Monte Carlo simulation (MCS). Instead of such specialized material models, researchers in random vibration analysis or response to complex deterministic excitations have developed simplified models for hysteresis and degradation. A thorough review of the hysteresis models used in random vibration studies as well as complex deterministic studies was presented in the preceeding chapter. Several models capable of reproducing general hysteretic, degrading behavior were then proposed. Random vibration analysis using the proposed models is the subject of this chapter.

Besides the material model, the dynamic response analysis of hysteretic degrading structures under stochastic excitation requires excitation models which possess the relevant properties of natural hazard excitations. Moreover, mathematical techniques are needed which would allow practical response estimates to be obtained. These two latter conditions can be fulfilled by proper seismic excitation models and approximate solution techniques.

3.2- Stochastic Model of Seismic Excitations:

Formulation of the stochastic model for seismic response of hysteretic, degrading structures is complete when a proper stochastic model for base excitation is described. This model should possess the pertinent properties of seismic excitation. Considerable work has been done in the area of describing seismic excitation by random process models and the existing models can be classified according to the characteristics of the ground acceleration that is generated. In one group of models and inputs used, the aceleration is stationary (27, 41, 42, 50, 53, 55, 59, 96, 106, 109, 119, 149) Gaussian white noise is the simplest random process model of this group. Bycroft (27) was one of the first to suggest the use of Gaussian white noise with its flat power spectral density. Realistically earthquakes are not stationary and do not have a flat power spectrum. However, stationary white noise can be a satisfactory approximation for wide band excitation, when the excitation spectrum varies slowly in the vicinity of the natural frequency of the structural system. This will be used as an approximation for seismic excitation in the current study. Numerous researchers have investigated ways of introducing temporal variation and frequency dependence into stochastic excitation models. Several stationary models that produce variable spectral density of ground acceleration, consistent with the observation for real earthquakes, have been proposed (35, 60, 91, 120). Yet other models approximate nonstationary acceleration processes by introducing time varying amplitude (4, 25, 49, 57, 79, 110, 112,

113).

Nonwhite stationary Gaussian excitation is obtained by passing a Gaussian white noise through one or more linear filters. These models, which are simple both in concept and execution, allow convenient digital computer processing. Housner and Jennings' model (60) developed simulated ground acceleration by filtering a white sequence of Gaussian random numbers that is equally spaced in time. The process is stationary until interrupted at an empirically predetermined time. Lutes and Lilhamand (94) proposed that seismic excitations be passed through a high pass as well as the customary low pass filter to eliminate the unbounded drift which could otherwise occur.

Temporally modulated excitation can be introduced in two ways. One way is to multiply the white noise by a deterministic temporally varying function before passing it through the appropriate filters. The second approach is to multiply the filtered excitation by the temporal factor before being passed through the system. Several such deterministic envelopes have been proposed. The model of Amin and Ang (4) and the model of Shinozuka and Sato (123) for example, filter a white input, and a time multiplier function is included to induce nonstationarity. A significant innovation of the Shinozuka and Sato model was to select a filter to insure that the variance function for the associated ground velocity, in addition to ground acceleration, would eventually tend toward zero. Liu (90) developed nonstationary excitation models with time varying frequency

content, based on Priestley's concept of evolutionary spectral density (110). A number of other authors have used and developed nonwhite-nonstationary models (40, 47), simulation of probability density of ordinates to simulate random processes with various probability density functions (24), or other empirical models (61). Recently, several researchers have proposed ARMA based models for seismic excitation (36).

Thus, a series of models are available for stochastic representation of seismic excitation. For further detail on the available stochastic models one may refer to Levy et al (87), Spanos (128), To (141), and references (31, 35). In the present work, only Gaussian process models will be considered. Filtering and temporal modulation of the input noise excitation can be easily incorporated into the model and are discussed elsewhere (15).

3.3- Approximate Techniques for Nonlinear Random Vibration Analysis:

Formulation of mathematical models for random vibration of hysteretic systems is not a difficult task, however, due to the high order of nonlinearity involved it is difficult to solve these models in closed form. For this reason, the class of nonlinear random vibration problems which are currently amenable to exact solution is quite limited. The available exact solutions are restricted only to simple systems under Gaussian white noise excitations (83), and the construction of the exact steady-state probability density function for a limited class of

nonlinear systems (33 ,34). Therefore, various researchers have developed and employed approximate analytical techniques in the investigation of yielding systems. At present several basic approaches are used in the study of stochastically excited nonlinear systems. These include formulation of Fokker-Plank-Kolmogorov (FPK) equation of the nonlinear system and using various techniques to obtain approximate solution of this equation, the perturbation approach, normal mode approach, and equivalent linearization. Other techniques such as an extended statistical linearization (19), and approaches for computing the distribution of a random variable via Gaussian quadrature rules (100) have also been proposed. Other methods for approximate random vibration analysis exist and have been discussed in references such as (7, 31, 69, 116, 117, 146). There are two fundemental approaches:

(a) Formulate the exact FPK forward (or Kolmogorov backward) diffusion equations and manipulate it to obtain solutions.

(b) Work directly with the stochastic differential equation.

Techniques such as the perturbation method have led to numerous asymptotic solutions in the deterministic case, but in the stochastic case only the first order terms are saved. The primary limitations of the perturbation method are that the nonlinearity must be small and numerical implementation for MDOF systems is difficult. By formulating the FPK equation, solution for certain restricted classes of problems can be obtained. This

approach can be used to obtain exact solution for certain cases (32) or to get approximate response statistics either by eigenfunction expansion (150, 130), finite element solution of the related Pontriagin equation (20), or any of the variety of closure methods such as Gaussian closure which replace an indefinite moment with a finite moment problem (39, 77, 78). Non-Gaussian closure techniques have also been proposed by some researchers (38, 103). In the equivalent linearization approach, the strategy is to replace the nonlinear system of stochastic differential equations with some members of a class of linear systems, the corresponding solutions of which are obtainable. This linear system should be similar, in some sense, to the original nonlinear system (56). The solution to the linear system is then taken as an approximate solution to the original nonlinear system of equations. The technique of equivalent linearization has been widely studied. This method was initially developed independently by Caughey (30) and Booton. The method has been generalized by Foster (46) and by Iwan and Yang (76). Atalik and Utku (11), Iwan (66), Iwan and Patula (74), Spanos (125, ,126, 129), Spanos and Iwan (133), Mason (97), Gates (48), Beaman and Hedrick (19), Baber and Wen (16), Ahamdi (1), Sues et al (136, 137), Pires et al (111), Asano (9), and Ang and Wen (6) have used this technique and have shown that, if properly formulated, the method can be extended in a relatively straightforward manner to MDOF and degrading systems. Application of this method to infinite dimensional responses of continuous structures have been reported as well (2). It should

be pointed out that the minimization of the equation difference with respect to the linear parameters does not necessarily guarantee that a minimization of the solution difference has been achieved, and this may be considered a drawback of averaging methods (97). Caughey (28-30) was the first to apply equivalent linearization to hysteretic systems, by replacing the bilinear hysteretic SDOF system with a linearized system. He used the Krylov-Bogoliubov (KB) approach which is most satisfactory for small nonlinearities and has been shown to underestimate the RMS response for nearly elasto-plastic systems (72). Application of this approach for finding statistical characteristics of the response of hysteretic structures with strong nonlinearity, for example near yielding, does not lead to accurate results. Kobori et al (85) improved this approach by considering the effect of the scatter of frequency and fluctuation of the center of hysteretic oscillation on the RMS displacements of bilinear systems with severe nonlinearity, and by introducing a drift parameter into the linearized response. Iwan and Spanos (75) developed a technique for finding the approximate envelope response statistics of a narrow-band SDOF nonlinear oscillator subject to unmodulated white noise as it approaches steady-state from zero initial conditions. This method first uses equivalent linearization and the narrow-bandness of the response to derive an approximate first order differential equation for the envelope response. The associated FPK equation is then solved by eigenfunction expansion for the transition probability density of the envelope response. Wen (152) realized that by using Bouc's

hysteresis, the linearization could be completed in closed form without the KB approximation and the resulting zero time lag covariance matrix response obtained by this approach are satisfactory for SDOF nearly elasto-plastic systems at all response levels. Baber and Wen (15) proved that the same linearization technique can be applied to both stiffness and strength deteriorating hysteretic systems. They obtained close agreement between the zero time lag covariance matrix response from linearized system and Monte Carlo simulation (MCS), for SDOF and MDOF shear beam models and extended the application to discrete hinge MDOF systems. Baber and Noori (13) applied this approach to a SDOF pinching, hysteretic system and were able to obtain accurate results, verified by MCS, without resorting to KB assumption. A thorough review and discussion of equivalent linearization can be found in references (15, 117, 129).

3.4- Stochastic Equivalent Linearization of the Proposed Models:

Response statistics for the SDOF systems described in Chapter 2 cannot be obtained in closed form because of the nonlinear form of the models. On the basis of the equation error due to substitution of an equivalent linear system, coefficients for equivalent linear systems are derived. This will be done for the three proposed models in the following subsections.

3.5- Equivalent Linearization of the Slip-Lock Models:

The special form of the nonlinear hysteretic models presented in Chapter 2 permits the linearization of the

equations, without resorting to the KB approximation. In the following subsections zero mean solutions by the method of equivalent linearization (15, 152) for the proposed models is presented.

3.5.1- Linearization of Baber-Noori Slip-Lock Model:

The original set of nonlinear equations [2.1]-[2.5], [2.10], and [2.11] is replaced by a linearized approximate set of equations. first let

$$\begin{aligned} y_1 &= u \\ y_2 &= \dot{u} \\ y_3 &= z \\ y_4 &= u_1 \\ y_5 &= u_2 \end{aligned} \qquad [3.1]$$

Then the governing nonlinear equations can be rewritten as

$$\begin{aligned} \dot{y}_1 &= y_2 && (a) \\ \dot{y}_2 &= -\alpha\omega_0^2 y_1 - 2\zeta\omega_0 y_2 - (1-\alpha)\omega_0^2 y_3 + a(t) && (b) \\ \dot{y}_3 &= \{A\dot{y}_4 - [\beta|\dot{y}_4||y_3|^{(n-1)}y_3 + \gamma|y_3|^n\dot{y}_4]\}/\eta && (c) \\ \dot{y}_4 &= y_2 - \dot{y}_5 && (d) \\ \dot{y}_5 &= 2a/(\sqrt{2\pi}\sigma)\exp[-y_3^2/(2\sigma^2)] \\ &\quad \{A\dot{y}_4 - [\beta|\dot{y}_4||y_3|^{(n-1)} + \gamma\dot{y}_4|y_3|^n]\}/\eta && (e) \end{aligned} \qquad [3.2]$$

These general system equations may be written in the matrix form

$$g(\underset{\sim}{y}, \dot{\underset{\sim}{y}}) = \underset{\sim}{f} \qquad [3.3]$$

Assuming zero mean response, the third and fifth of

Equations [3.2] can be replaced by the linearized forms

$$\dot{y}_3 = C_{e3}\dot{y}_4 + K_{e3}y_3$$
$$\dot{y}_5 = C_{e5}\dot{y}_4 + K_{e5}y_3 \qquad [3.4]$$

Where, according to Atalik and Utku (11), Iwan and Mason (73), Baber and Wen (15)

$$C_{ei} = E[\partial g_i(\underset{\sim}{y})/\partial \dot{y}_4]$$
$$K_{ei} = E[\partial g_i(\underset{\sim}{y})/\partial y_3] \qquad i=3,5 \qquad [3.5]$$

If it is assumed that y_3 and y_4 are jointly Gaussian, Equation [3.5] can be evaluated in closed form, given the response statistics σ_3, σ_4 and $\rho_{3,4}$. Derivation of C_{ei} and K_{ei} in terms of the response statistics are given in Appendix A. It is advantageous, to rewrite Equation [3.4] together with [3.2(d)] in the form

$$\dot{y}_3 = [C_{e3}/(1+C_{e5})]y_2 + [K_{e3} - C_{e3}K_{e5}/(1+C_{e5})]y_3 \qquad (a)$$
$$\dot{y}_4 = [1/(1+C_{e5}))]y_2 - [K_{e5}/(1+C_{e5})]y_3 \qquad (b)$$
$$\dot{y}_5 = [C_{e5}/(1+C_{e5})]y_2 + [K_{e5}/(1+ C_{e5})]y_3 \qquad (c) \qquad [3.6]$$

to eliminate derivatives from the right hand side. Equations [3.2(a)], [3.2(b)], and [3.6] form a set of simultaneous stochastic differential equations which may be written symbolically in matrix form as

$$\underset{\sim}{\dot{y}} + \underset{\sim}{G}\,\underset{\sim}{y} = \underset{\sim}{f} \qquad [3.7]$$

Postmultiplying Equation [3.7] by y^T, taking expected values and

adding the resulting equation to its transpose, gives the following result

$$\dot{\underset{\sim}{S}} + \underset{\sim}{G}\cdot\underset{\sim}{S} + \underset{\sim}{S}\cdot\underset{\sim}{G}^T = \underset{\sim}{B} \qquad [3.8]$$

where,

$$\underset{\sim}{S} = E[\underset{\sim}{y}\cdot\underset{\sim}{y}^T] \qquad (a)$$

and [3.9]

$$\underset{\sim}{B} = E[\underset{\sim}{f}\cdot\underset{\sim}{y}^T] + E[\underset{\sim}{y}\cdot\underset{\sim}{f}^T] \qquad (b)$$

The desired response statistics are obtained by solving Equation [3.8] for the zero time lag covariance matrix $\underset{\sim}{S}$. If it is assumed that f(t) is a zero mean Gaussian white noise with constant power spectral density K_0, then it may be shown that $\underset{\sim}{B}$ matrix has only one nonzero term (15). Therefore elements of B can be written as

$$b_{ij} = \delta_{i2}\delta_{2j}2\pi K_0 \qquad [3.10]$$

where δ_{ij} is the Kronecker delta.

The system of equations defined by [3.8] is a system of nonlinear ordinary differential equations, because $\underset{\sim}{G}$ depends on the response statistics $\underset{\sim}{S}$, which can be solved by numerical integration in the time domain. At each time step the response statistics

$$\sigma_3^2 = E[y_3^2]$$
$$\sigma_4^{\cdot 2} = E[\dot{y}_4^2] \qquad [3.11]$$

and

$$\rho_{34}^{\cdot} = E[y_3 \dot{y}_4]/(\sigma_3 \sigma_4^{\cdot})$$

are needed to update G. σ_3^2 is obtained as part of $\underset{\sim}{S}$, while using Equation [3.6(b)] gives

$$\sigma_4^{\cdot 2} = [1/(1+C_{e5})^2]\{\sigma_2^2 - 2K_{e5}\rho_{23}\sigma_2\sigma_3 + K_{e5}^2\sigma_3^2\}$$

$$\rho_{34}^{\cdot} = [1/(1+C_{e5})][\rho_{23} - K_{e5}\sigma_3/\sigma_2] \qquad [3.12]$$

A fixed-point iteration approach is used to compute the values of σ_4 and ρ_{34} to assure convergence as the covariance matrix elements start to build up. Convergence occurs very rapidly at the first few iteration steps. If the model includes system degradation, then several parameters (A, ν, η and a) may be functions of the response history. Closed form incorporation of these added complications into the model is difficult. However, it has been found to be a reasonable approximation to updat the degradation parameters at each time step, replacing ε in Equation [2.4] and [2.10] by its expected value μ_ε (14, 15). Taking expected values of Equation [2.5] gives

$$\dot{\mu}_\varepsilon = (1-\alpha)\omega_0^2 E[\dot{u}z] = (1-\alpha)\omega_0^2 s_{23} \qquad [3.[3]$$

where s_{23} is an element of the covariance matrix $\underset{\sim}{S}$. Differential equation [3.13] is integrated inparallel with Equation [3.8] to allow updating of the degradation parameters, and complete the evaluation of the $\underset{\sim}{G}$ matrix.

3.5.2- Linearization of Noori-Baber Slip-Lock Model:

In this case, the nonlinear equations [2.1]-[2.5], [2.13], and [2.14] which represent the NB model are replaced by a linearized approximate set of equations. Using the same relationships established in [3.1], the governing nonlinear equations may be rewriten as

$$\begin{aligned}
\dot{y}_1 &= y_2 && \text{(a)}\\
\dot{y}_2 &= -\alpha\omega_0^2\, y_1 - 2\zeta\omega_0\, y_2 - (1-\alpha)\omega_0^2 y_3 + a(t) && \text{(b)}\\
\dot{y}_3 &= \{A\dot{y}_4 - \nu[\beta|\dot{y}_4||y_3|^{(n-1)}y_3 + \gamma|y_3|^n\dot{y}_4]\}/\eta && \text{(c)}\\
\dot{y}_4 &= y_2 - \dot{y}_5 && \text{(d)}\\
\dot{y}_5 &= [\lambda\xi/(\xi^2 + y_3^2)]\{A\dot{y}_4 - [\beta|\dot{y}_4||y_3|^{(n-1)}y_3 \\
&\qquad + \gamma\dot{y}_4|y_3|^n]\}/\eta && \text{(e)}
\end{aligned} \qquad [3.14]$$

Equations [3.14] and [3.2] are similar except for the last equation, (e). This general system of equations can also be written in the form of Equation [3.3]. With assumption of zero mean response, Equations [3.14] (c) and (e) can be replaced by the equivalent linearized form

$$\begin{aligned}
\dot{y}_3 &= C_{e3}'\dot{y}_4 + K_{e3}'y_3\\
\dot{y}_5 &= C_{e5}'\dot{y}_4 + K_{e5}'y_3
\end{aligned} \qquad [3.15]$$

where the equivalent linearization coefficients are defined by Equation [3.5]. Assuming that y_3 and $\dot{y}_4$ are jointly Gaussian random variables, coefficients C_{e3} and K_{e3} are evaluated in closed form, given the response statistics σ_3, $\sigma_{\dot{4}}$, and $\rho_{3\dot{4}}$. Evaluation for these coefficients was presented in preceeding

section. Expected values for C_{e5}' and K_{e5}' however, can not be obtained in closed form. These expected values can be reduced to a single Gauss-Laguerre quadrature (135) in this case and are evaluated numerically. Details of these evaluations are provided in Appendix B. Equation [3.15] along with [3.14(d)] are rewritten in a form similar to [3.6] to eliminate derivatives from the right hand side

$$\begin{aligned} y_3 &= [C_{e3}/(1+C_{e5}')]\, y_2 + [K_{e3} - C_{e3}K_{e5}'/(1+C_{e5}')]y_3 && \text{(a)} \\ y_4 &= [1/(1+C_{e5}')]y_2 - [K_{e5}'/(1+C_{e5}')]y_3 && \text{(b)} \\ y_5 &= [C_{e5}'/(1+C_{e5}')]y_2 + [K_{e5}'/(1+C_{e5}')]y_3 && \text{(c)} \end{aligned} \qquad [3.16]$$

Equations [3.14] (a) and (b), and [3.16] form a set of simultaneous stochastic differential equations with the matrix form given by [3.7] and [3.8]. Response statistics for this case can be obtained following the same procedure discussed for solving Equation [3.8] for BN model. In this case however, coefficients C_{e5} and K_{e5} in Equation [3.12] should be replaced by C_{e5}' and K_{e5}' respectively, for evaluation of $\sigma_4'^2$ and ρ_{34}' in each time step.

Incorporation of system degradation, and evaluation of $\underset{\sim}{G}$ matrix and response statistics in this regard, will also be similar to the procedure discussed for BN model.

3.6- Equivalent Linearization of Single Element Pinching Model:

In the case of the single element pinching hysteresis model,

the number of operations involved in linearization procedure is reduced. Let

$$\begin{aligned} y_1 &= u \\ y_2 &= \dot{u} \\ y_3 &= z \end{aligned} \qquad [3.17]$$

Then the governing Equations [2.1], [2.2], [2.19], and [2.20] are rewritten in the form

$$\begin{aligned} \dot{y}_1 &= y_2 && (a) \\ \dot{y}_2 &= -\alpha\omega_0{}^2 y_1 - 2\zeta\omega_0\, y_2 - (1-\alpha)\omega_0{}^2 y_3 + a(t) && (b) \\ \dot{y}_3 &= [1-\zeta_1 \exp(-y_3{}^2/\zeta_2{}^2)]. && (c) \\ & \quad \{A y_2 - \nu\,[\beta\,|y_2|\,|y_3|^{(n-1)} y_3 + \gamma\,|y_3|^n y_2]\}/\eta \end{aligned} \qquad [3.18]$$

Equations [3.18] can be written in the matrix form

$$\underset{\sim}{y} + g(\underset{\sim}{y}) = \underset{\sim}{f} \qquad [3.19]$$

with zero mean response assumption, Equation [3.18(c)] may be replaced by the linearized form

$$\dot{y}_3 = C_{e3}{}' y_2 + K_{e3}{}' y_3 \qquad [3.20]$$

where the equivalent coefficients $C_{e3}{}'$ and $K_{e3}{}'$ are defined by Equation [3.5].

Given the assumption of jointly Gaussian distribution for y_2 and y_3, and given the response statistics σ_2, σ_3 and ρ_{23}, Equation [3.5] can be evaluated in closed form. Derivation of $C_{e3}{}'$ and $K_{e3}{}'$ in terms of response statistics are given in

Appendix C. In Equation [3.20] derivatives are only on the left hand side. Therefore, Equations [3.18] (a) and (b) and [3.20] can be easily transformed into the form given by [3.8]. Again, the system of equations defined by [3.8] is a system of first order nonlinear differential equations which can be solved by numerical integration. To update $\underset{\sim}{G}$ matrix, response statistics

$$\begin{aligned} \sigma_3^2 &= E[y_3^2] \\ \sigma_2^2 &= E[y_2^2] \\ \rho_{23} &= E[y_2 y_3] / (\sigma_2 \sigma_3) \end{aligned} \qquad [3.21]$$

are needed at each time step. σ_2^2, σ_3^2 and $E[y_2 y_3]$ are all obtained as part of S in this case. Hence, as can be seen, number of steps involved for the numerical integration in each time step, is noticeably less than the one for the two series models. This reduces the computation cost and is an advantage of this model over the other two proposed models.

To incorporate system degradation, a procedure similar to that discussed for the two series models is utilized. Equation [3.14] will be solved concurrently with Equation [3.8] to allow updating the deterioration parameters, and to complete the evaluaion of the G matrix.

3.7- Numerical Studies

In the preceeding chapter, the capabilities and behavior of proposed nonlinear pinching models under cyclic and general loadings were verified. The numerical studies which follow here, have been conducted to investigate the relative validity of the

approximate random vibration analysis by equivalent linearization, assuming zero mean response. A number of studies on single degree of freedom systems will be considered in the following subsections. In these approximate response analysis of the proposed models to random input, a stationary white noise input is considered. Filtering and modulation of the input noise excitation can be easily incorporated into the model and are discussed elsewhere (15).

3.7.1- Approximate Response Analysis of Baber-Noori Model:

Consider first the nonstationary response of the BN slip-lock pinching model. Starting with zero initial conditions, the zero time lag covariance matrix response of the single degree of freedom BN oscillator to stationary white noise input was computed. Response estimates were obtained using 100 samples of Monte Carlo simulation, and the linearized approximate model, for several values of input power spectral density K_0, and for $\delta_a = 0.1$, and $\delta_a = 0.5$. System viscous damping ration of =0.02 was chosen, with all other parameters as discussed in section 2.4.2.1. RMS displacements σ_u, velocities $\sigma_{\dot{u}}$, and hysteretic restoring force values, σ_z compare well for low pinching rate of $\delta_a = 0.1$, as shown in Figures 3.1-3.3. The constituent element displacements σ_{u1} and σ_{u2} are reasonably well estimated for low to moderate excitation levels, but for higher excitation levels σ_{u1} is underestimated and σ_{u2} is overestimated as shown in Figures 3.4 and 3.5. The system degradation, as measured by the total energy dissipation μ_ε is

underestimated slightly, with the underestimation increasing as K_0 increases, as shown in Figure 3.6.

At higher pinching rate, with a value $\delta_a = 0.5$, σ_u is closely estimated by the linearized model, but $\sigma_{\dot{u}}$ is somewhat overestimated at high excitation levels as shown in Figures 3.7 and 3.8, and σ_z is overestimated for much of the time, following an initial period of underestimation as can be seen in Figure 3.9. The overestimation of $\sigma_{\dot{u}}$ indicates that the kinetic energy, and energy dissipated due to damping will be overestimated, with a consequent loss in hysteretic energy. This judgement is verified by the plots for σ_{u1}, σ_{u2}, and energy dissipation μ_ε as shown in Figures 3.10-3.12. As these plots indicate σ_{u1} and μ_ε are underestimated for all excitation levels and σ_{u2} is underestimated for high levels of excitation.

3.7.2- Approximate Response Analysis of Noori-Baber Model:

The studies for the approximate response analysis of the NB system to random input were performed with two purposes in mind, first, to investigate the capabilities of this model, second, to look for any advantage or disadvantage of this model as compared with the BN model.

The computation time needed to obtain approximate responses, which in this case required use of Gauss-Laguerre quadrature numerical integration scheme, was about the same as needed for the linearization analysis of BN model. However, the simulation time was noticeably less and consequently the computation cost

for checking the accuracy of the results was lower.

In order to compute the zero time lag covariance matrix response, the nonstationary response analysis of a SDOF system of NB model, to a stationary white noise input beginning at $t = 0.$, was considered. Response estimates in this case were also obtained using 100 samples of Monte Carlo simulation, and the linearized approximate model. Several values of input power spectral density K_0, with maximum excitation level of $K_0 = 1.0$, twice the highest level considered for BN model, were considered. Two cases of low pinching rate with parameter values of $\xi_0 = 0.35$ and $\delta_\lambda = 0.2$, and high pinching with coresponding parameter values of $\xi_0 = 0.125$, and $\delta_\lambda = 0.5$, were chosen. System viscous damping ratio of $= 0.02$ was used, with all other parameter values as discussed in section 2.4.2.2. RMS displacements σ_u, velocities $\sigma_{\dot{u}}$, and hysteretic restoring force values σ_z compare well for low pinching rate at all excitation levels, as shown in Figures 3.13-3.15. RMS displacements for constituent elements σ_{u1}, is reasonably well estimated for low to moderate excitation levels as shown in Figure 3.16. σ_{u2} is well estimated for much of the time for low to moderate level and reasonably well estimated for very high level of excitation as can be seen from Figure 3.17. The system degradation, as indicated by the mean value of total dissipated energy μ_ε, is very well estimated upto very high level of excitation as shown in Figure 3.18.

At higher rate of pinching, with parameters given

above, σ_u, $\sigma_{\dot{u}}$ and σ_z are still very well estimated even at very high levels of excitation as shown in Figures 3.19-3.21 except that peak starting values of σ_z is underestimated at very high excitation level. RMS displacement for σ_{u1} is reasonably well estimated for low excitation level and is underestimated for much of the time for higher values of excitation, with underestimation increasing as K_0 gets larger, as shown in Figure 3.22. σ_{u2} however, is well estimated even at very high levels of excitation, as shown in Figure 3.23. Estimation of the mean value of total energy dissipation is satisfactory upto high levels of excitation and is reasonable for very high excitation levels, as shown in Figure 3.24.

Studies presented here for NB model indicate that the performance of this model in estimating various response statistics is somewhat better than the BN series model. Accuracy of the results obtained by the NB model, especially at very high levels of excitations, are more accurate in general than those obtained from the BN model.

3.7.3- Approximate Response Analysis of SEP Model:

Similar studies were performed to compute the zero time lag covariance matrix response of SDOF single element pinching model. In these studies nonstationary response statistics were obtained under stationary white noise input beginning at zero initial conditions. Same number of samples were used in Monte Carlo simulation of the model.

In order to be able to make a comparison between this model and the two series models and also to investigate the capabilities of this model several values of input power spectral density K_0, were considered.

It was observed that the computation time needed for approximate response analysis and for simulation were significantly lower than the one for either the BN or NB model. This is due to the mathematical form of the model and consequent reduction in the number of variables involved for numerical integration process. This advantage makes this model particularly suitable for random vibration analysis.

Two cases of low pinching with pinching parameter values of $\zeta_{10} = 0.8$ and $\lambda_0 = 0.05$, and high pinching with parameter values of $\zeta_{10} = 0.9$ and $\lambda_0 = 0.15$ were considered for RMS response analysis of this model. A system damping ratio of $\zeta = 0.02$ was chosen, with all other parameter values as discussed in section 2.4.2.3. Behavior of a single sample, with similar pinching characters, under white noise excitaion is illustrated in Figure 2.24 in Chapter 2. RMS displacements σ_u, and velocities $\sigma_{\dot{u}}$ compare very well for low pinching rate and all levels of excitation as illustrated in Figures 3.25 and 3.26. RMS prediction of hysteretic restoring force compares well for low excitation level, but underestimates the peak value of z for intermediate excitation levels as shown in Figure 3.27. Mean value of the total energy dissipation μ_ε, which is a measure of system degradation is estimated very well at all excitation levels as shown in Figure 3.28.

For the high pinching case, with parameter values as given above, displacements σ_u and velocities $\sigma_{\dot{u}}$ are estimated reasonably well for all levels of excitation as illustrated in Figures 3.29 and 3.30. The hysteretic restoring force σ_z, is estimated closely for low excitation level, but underestimates the peak values for intermediate and high level of excitation as can be observed from Figure 3.31. It should be noticed that in the case of predecting the restoring force with the SEP model somewhat differnt character of the response is obtained. As can be seen from Figures 3.27 and 3.31, the SEP model displays much more severe stiffness degradation than do the BN and NB models. Estimation of the mean value of total energy dissipation is quite good for all excitation levels as shown in Figure 3.32.

CHAPTER 4

NONZERO MEAN RANDOM VIBRATION ANALYSIS OF SYSTEMS WITH PINCHING HYSTERESIS.

4.1- Introduction and Background:

In the preceeding chapters, severl models for the deterministic and stochastic response of degrading structures, with general hysteretic behavior were presented. Equivalent linearization formulations to predict the zero time lag covariance matrix, for SDOF systems utilizing these models were derived. The approximate solution obtained compared reasonably well with Monte Carlo simulation.

In random vibration analysis of hysteretic systems, attention has been focused on the zero mean response to stochastic excitation. Little work has been done on the nonzero mean response of hysteretic and degrading structures. Spanos (127, 131) and Spanos and Chen (132) considered the response of a nonhysteretic system with nonsymmetric force deformation characteristics. This problem is closely related to the nonzero mean response problem even under zero mean excitation. The theoretical tools for extension of equivalent linearization to nonzero mean problem is also available. Baber and Wen (15) extended the linearization theorem of Atalik and Utku (11) to the nonzero mean case. Spanos (127, 131) developed a relatively more straightforward approach to linearization of nonzero mean problems by subtracting the mean response from the governing stochastic differential equations. This computation was based on

the assumed Gaussian distribution for the response. A nonsymmetric zero mean problem is obtained by this approach, which can be solved by equivalent linearization techniques. Baber (12) applied Spanos' approach to linearize the BBW smooth system subjected to nonzero mean excitation, with energy based degradation. It is the objective of this chapter to employ the equivalent linearization technique to obtain approximate nonzero mean solutions of Baber-Noori series pinching model and the single element pinching model. A linearization solution for the Noori-Baber model in nonzero mean case must be obtained numerically. This requires development of proper algorithms and selection of a suitable numerical scheme. Therefore, although the zero mean results for the NB model indicates that this model is a promising series model, nonzero mean analysis of this system will be omitted herein.

The nonzero mean response analysis os structures is of considerable engineering interest, even under apparently zero mean excitations, such as earthquakes. Anderson and Bertero (5) considered the loss of symmetry in girder yielding under the action of gravity loads, and used this phenomenon as a justification for introducing curvature based ductility ratios in studying the seismic response of multistory steel frames. Baber (12) considered this point as motivation for nonzero mean random vibration analysis of BBW smooth hysteresis model. To illustrate this point, consider a single story, one bay frame shown in Figure 4.1, subjected to earthquake excitation. As Figure 4.1(a) shows, this frame will yield antisymmetrically at the beam column

joints in the absence of gravity effects. By contrast, inclusion of gravity effects results in loss of symmetry and may lead to the nonsymmetric yield mechanism of Figure 4.1(b). Even if the mechanism of Figure 4.1(b) is not developed, studies indicate that complete reversal of hysteretic action will not occur (5). In the most severe instances, repeated cycles may lead to incremental deformation at the yield "hinges," each of which has a prefered yield action. Hence, the accumulated inelastic action may lead to stochastic "shakedown" . In a multistory frame, not all stories will form mid-member hinges (5, 12). Design moments near the base will be largely controlled by lateral, for example seismic, loads. In higher stories, gravity loads will have a greater effect upon the design.

It is difficult to analyze multi-component frame structures under a combination of gravity load and seismic base acceleration at this time. Baber and Wen (14, 15) suggested one possible formulation, which can be extended to the nonzero mean case provided the necessary response statistics can be obtained for the constituent hysteretic elements, and given suitable model assembly and solution techniques. This chapter includes the research on the response analysis of single degree of freedom Baber-Noori and single element pinching models to nonzero mean random excitations. Extension of the work to multidegree of freedom models is not considered herein.

4.2- Nonzero Mean Analysis of Baber-Noori Model:

The system to be considered here is a single degree of

freedom oscillator as described by the nonlinear differential equation set

$$\ddot{u} + 2\zeta\omega_0\dot{u} + q(u,t) = a(t) \qquad [2.1]$$

$$q = \alpha\omega_0{}^2 u + (1-\alpha)\omega_0{}^2 z \qquad [2.2]$$

$$\dot{z} = \{A\dot{u}_1 - [\beta|\dot{u}_1||z|^{(n-1)}z + \gamma\dot{u}_1|z|^n]\}/\eta \qquad [2.3]$$

$$u_2 = [2a/(\sqrt{2\pi}\sigma)]\exp(-z^2/(2\sigma^2))\dot{z} \qquad [2.11]$$

and

$$u = u_1 + u_2 \qquad [2.16(a)]$$

where a(t) is, by assumption, a nonzero mean stochastic process. The response is given as

$$\underset{\sim}{v}^T = \{u,\ \dot{u},\ z,\ u_1,\ u_2,\ \varepsilon\}^T \qquad [4.1]$$

where ε is the hysteretic energy dissipated at time t and defined by Equation [2.5]. The system degradation has the form defined by Equations [2.4] and [2.10].

Equations [2.3], [2.11], and [2.16(a)] lead to the set of stochastic differential equations

$$\dot{u}_1 = \dot{u}/\{1 + [2a/(\sqrt{2\pi}\sigma)]\exp(-z^2/(2\sigma^2))h(\dot{u}, z)\} \qquad [2.17]$$

$$\dot{u}_2 = \dot{u} - \dot{u}_1 \qquad [2.16(b)]$$

$$\dot{z} = h(\dot{u}, z)\dot{u}_1 \qquad [2.3\text{-}1]$$

where

$$h(\dot{u}, z) = \{A - \nu[\beta\,\mathrm{sgn}(\dot{u})|z|^{(n-1)}z + \gamma|z|^n]\}/\eta \qquad [2.3\text{-}2]$$

Equations [2.1], [2.2], [2.17], [2.16(b)], [2.3-1], and [2.3-2] provide a convenient form for numerical simulation of BN model response when the appropriate deterioration rule has been

selected.

4.2.1- Equivalent Linearization Solution of Baber-Noori Model

Before proceeding with the linearization, it is convenient to reduce the governing equations [2.1], [2.2], [2.3], [2.11], and [2.16(a)] to the first order differential equation set

$$\begin{aligned}
\dot{v}_1 &= v_2 \\
\dot{v}_2 &= -\alpha\omega_0{}^2 v_1 - 2\zeta\omega_0 v_2 - (1-\alpha)\omega_0{}^2 v_3 + a(t) \\
\dot{v}_3 &= \{A\dot{v}_4 - [\beta|\dot{v}_4||v_3|^{(n-1)}v_3 + \gamma\dot{v}_4|v_3|^n]\}/\eta \\
\dot{v}_4 &= v_2 - \dot{v}_5 \\
\dot{v}_5 &= [2a/(\sqrt{2\pi}\sigma)]\exp[-v_3{}^2/(2\sigma^2)]. \\
&\quad \{A\dot{v}_4 - \nu[\beta|\dot{v}_4||v_3|^{(n-1)}v_3 + \gamma\dot{v}_4|v_3|^n]\}/\eta
\end{aligned} \qquad [4.2]$$

where

$$v_i = y_i + \mu_i; \qquad i=1,5 \qquad [4.3]$$

and y_i's are given by Equation [4.1]

Since a(t) is, by assumption, a nonzero mean random process, it is necessary to compute expected values μ_i, namely

$$\begin{aligned}
\dot{\mu}_1 &= \mu_2 \\
\dot{\mu}_2 &= -\alpha\omega_0{}^2\mu_1 - 2\zeta\omega_0\mu_2 - (1-\alpha)\omega_0{}^2\mu_3 + \mu_F \\
\dot{\mu}_3 &= \{A\mu_4 - \nu[\beta E_1 + \gamma E_2]\}/\eta \\
\dot{\mu}_4 &= \mu_2 - \mu_5 \\
\dot{\mu}_5 &= [2a/(\sqrt{2\pi}\sigma)]\{AE_3 - \nu(\beta E_4 + \gamma E_5)\}/\eta
\end{aligned} \qquad [4.4]$$

where

$$
\begin{aligned}
\mu_F &= \text{nonzero mean for input excitation} \\
E_1 &= E[\,|v_3|^{(n-1)} v_3 \,|\dot{v}_4|\,] \\
E_2 &= E[\,|v_3|^{n} \dot{v}_4\,] \\
E_3 &= E[\exp(-v_3^{\,2}/(2\sigma^2))\,\dot{v}_4] \\
E_4 &= E[\exp(-v_3^{\,2}/(2\sigma^2))\,|v_3|^{(n-1)} v_3\,|\dot{v}_4|\,] \\
E_5 &= E[\exp(-v_3^{\,2}/(2\sigma^2))\,|v_3|^{n}\dot{v}_4]
\end{aligned}
\qquad [4.5]
$$

Subtracting equations [4.4] from [4.2] and using $y_i = v_i - \mu_i$, results in the nonsymmetric zero mean problem

$$
\begin{aligned}
\dot{y}_1 &= y_2 && \text{(a)} \\
\dot{y}_2 &= -\alpha\omega_0^{\,2} y_1 - 2\ \omega_0 y_2 - (1-\alpha)\omega_0^{\,2} y_3 + \hat{a}(t) && \text{(b)} \\
\dot{y}_3 &= \{A\dot{y}_4 - \nu\,[\beta\big[\,|y_3+\mu_3|^{(n-1)}(y_3+\mu_3)\,|\dot{y}_4+\dot{\mu}_4|\,- && \text{(c)} \\
&\qquad E_1\big] + \gamma\big[|y_3+\mu_3|^{n}(\dot{y}_4+\dot{\mu}_4) - E_2\big]\ ]\}/\eta \\
\dot{y}_4 &= y_2 - y_5 && \text{(d)} \\
\dot{y}_5 &= [2a/(\sqrt{2\pi}\sigma)]\{A[(\dot{y}_4+\dot{\mu}_4)\cdot \\
&\qquad \exp(-[y_3+\mu_3]^2/(2\sigma^2)) - E_3] && \text{(e)} \\
&\qquad -\nu\beta[\,|y_3+\mu_3|^{(n-1)}(y_3+\mu_3)\,|\dot{y}_4+\dot{\mu}_4|\,\cdot \\
&\qquad \exp(-[y_3+\mu_3]^2/(2\sigma^2)) - E_4] \\
&\qquad -\nu\gamma[\,|y_3+\mu_3|^{n}(\dot{y}_4+\dot{\mu}_4) - E_5]\}/\eta
\end{aligned}
\qquad [4.6]
$$

In [4.6] it is convenient to rewrite E_i; i=1,2,3,4,5, as functions of y_i by appropriate substitution.

If it is assumed that the y_i are jointly distriuted Gaussian random variables, at time t, then following Kazakov (84), Atalik and Utku (11), and Mason (97), the nonlinear equations [4.6] (c) and (e) can formally be replaced by the linearized equations

$$\dot{y}_3 = C_{e3}\dot{y}_4 + K_{e3}y_3 + (\nu/\eta)[\beta E_1 + \gamma E_2]$$
$$\dot{y}_5 = C_{e5}\dot{y}_4 + K_{e5} - [2a/(2\pi\sigma\eta)]E_3 + (\nu/\eta)[\beta E_4 + \gamma E_5] \qquad [4.7]$$

where

$$C_{ei} = E[\partial g_i(y_3, \dot{y}_4)/\partial \dot{y}_4]$$
$$K_{ei} = E[\partial g_i(y_3, \dot{y}_4)/\partial y_3] \quad i=3,5 \qquad [4.8]$$

and $g_i(y_3, \dot{y}_4)$ are the right hand sides of equations [4.6] (c) and (e) respectively.

It is apparent that a difficulty exists in Equations [4.4] for the mean responses, and [4.6] or [4.17] for the zero mean response. The expected value μ_4 appears on the right hand sides of equations [4.4] and [4.6]. Moreover, the second order response statistics $\sigma_4^{*2} = E[\dot{y}_4^2]$ and $\rho_{3\dot{4}} = E[y_3\dot{y}_4]/(\sigma_3\sigma_4^*)$ are required, along with $\mathring{\mu}_4$ to evaluate the expected values in equations [4.5] and [4.8]. In short, $\mathring{\mu}_4$, σ_4^{*2} and $\rho_{3\dot{4}}$ are implicit variables, which must be determined by iteration, before solution can be proceed at each step. The linearized equations can be rewritten as

$$\mathring{y}_1 = y_2$$
$$\mathring{y}_2 = -\alpha\omega_0^2 y_1 - 2\zeta\omega_0 y_2 - (1-\alpha)\omega_0^2 y_3 + \hat{a}(t)$$
$$\mathring{y}_3 = C_1 y_2 + K_1 y_3 \qquad [4.9]$$
$$\mathring{y}_4 = C_2 y_2 + K_2 y_3$$
$$\dot{y}_5 = C_3 y_2 + K_3 y_3$$

where

$$C_1 = C_{e3}/(1+C_{e5}) \qquad K_1 = K_{e3} - C_{e3}K_{e5}/(1+C_{e5})$$
$$C_2 = 1/(1+C_{e5}) \qquad K_2 = -K_{e5}/(1+C_{e5}) \qquad [4.10]$$
$$C_3 = C_{e5}/(1+C_{e5}) \qquad K_3 = K_{e5}/(1+C_{e5})$$

Equations [4.9] are summarized in matrix form as

$$\dot{\underset{\sim}{y}} + \underset{\sim}{G}\,\underset{\sim}{y} = \underset{\sim}{a}^* \qquad [4.11]$$

where

$$\underset{\sim}{a}^* = \{0\,|\,a\,|\,0\,|\,0\,|\,0\,|\,0\}$$

Postmultiplying [4.11] by $\underset{\sim}{y}^T$, taking expected values and adding the result to its transpose gives the ususal result

$$\dot{\underset{\sim}{S}} + \underset{\sim}{G}\,\underset{\sim}{S} + \underset{\sim}{S}\,\underset{\sim}{G}^T = \underset{\sim}{B} \qquad [4.12]$$

where, $S = E[\underset{\sim}{y}\,\underset{\sim}{y}^T]$ and $\underset{\sim}{B} = E[\underset{\sim}{a}^*\underset{\sim}{y}^T + \underset{\sim}{y}\,\underset{\sim}{a}^{*T}]$. If $\hat{\underset{\sim}{a}}(t)$ is taken as a zero mean Gaussian white noise input with power spectral density K_0, then

$$b_{ij} = \delta_{2i}\delta_{j2}2\pi K_0 \qquad [4.13]$$

where δ_{ij} is the Kronelcker delta. Equations [4.12] together with [4.4] form as set of equations to be jointly solved by numerical integration, for the responses $\underset{\sim}{\mu}_y$ and $\underset{\sim}{S}$. It remains to evaluate the expected values in [4.5] and [4.8]. these require the joint one time distributions of y_3 and $\dot{y}_4$. Assuming that y_3 and $\dot{y}_4$ are jointly Gaussian, it is necessary to have μ_3, σ_3, $\dot{\mu}_4$, $\sigma_{\dot{4}}$, and $\rho_{3\dot{4}}$, in order to evaluate the expressions at each time step. μ_3 and σ_3 are obtained from the previous numerical integration step. Squaring the fourth of

equations [4.9] and taking expected values gives

$$\sigma_4^2 = C_2^2\sigma_2^2 + 2C_2K_2\rho_{23}\sigma_2\sigma_3 + K_2^2\sigma_3^2 \qquad [4.14]$$

while postmultiplying that equation by y_3 and taking expected values gives

$$\rho_{34}^{\cdot} = (C_2\rho_{23}\sigma_2\sigma_3 + K_2\sigma_3^2)/(\sigma_3\sigma_4^{\cdot}) \qquad [4.15]$$

Thus $\sigma_4^{\cdot}$ and $\rho_{34}^{\cdot}$ can be determined directly from the linearized equations.

Direct determination of $\dot{\mu}_4$ is also possible in principle. Using equations [2.17], [2.16(b)], and [2.3-1] gives

$$\dot{\mu}_4 = E[v_2/\{1+[2a/(\sqrt{2\pi}\sigma)]\exp(-v_3^2/(2\sigma^2)).\ h(v_2, v_3)\}] \qquad [4.16]$$

If v_2 and v_3 are jointly Gaussian, the right-hand side of [4.16] can hypothetically be determined in terms of available response statistics. Unfortunately, the form of [4.16] is difficult to evaluate in closed form, or even to reduce to a numerical quadrature for one variable. Alternately, the last two of equations [4.2] can be solved to give

$$\dot{v}_4 = v_2 - [2a/(\sqrt{2\pi}\sigma)]\exp(-v_3^2/(2\sigma^2)).\ \{A\dot{v}_4 - \nu[\beta|\dot{v}_4||v_3|^{(n-1)}v_3 + \gamma\dot{v}_4|v_3|^n]\}/\eta \qquad [4.17]$$

whence, taking expected values, gives

$$\dot{\mu}_4 = \mu_2 - [2a/(\sqrt{2\pi}\sigma)]E[\exp(-v_3^2/(2\sigma^2)). \qquad [4.18]$$

$$\{A\dot{v}_4 - [\beta|\dot{v}_4\|v_3|^{(n-1)}v_3 + \gamma\dot{v}_4|v_3|^n]\}/\eta$$

Equation [4.18] is of the form

$$\dot{\mu}_4 = \mu_2 - g(\mu_3, \dot{\mu}_4, \sigma_3, \sigma_4^{\cdot}, \rho_{34}^{\cdot}) \qquad [4.19]$$

and can be solved using a fixed point problem approach if convergence can be demonstrated. Alternately, numerical solution using Newton-Raphson or secant method is possible at each step. Since $\dot{\mu}_4$ evolves slowly in time, previous values provide excellent starting guesses, so rapid convergence is achieved. Moreover, the form of [4.18] is more suitable than Equation [4.16] for closed form evaluation. In the work presented here, Equation [4.18] and the secant method was used to update $\dot{\mu}_4$ at each step. Having iteratively determined $\dot{\mu}_4$ at each step, equations [4.5] and [4.8] can then be evaluated, setting up the next time step. The expected values in equations [4.5] and [4.8] are quite lengthy, and details of their evaluations are given in Appendix D. Closed form solution has been obtained for odd values of 'n' only. For even, or non-integer values of 'n', the equations can be reduced to doubly infinite numerical quadratures in one variable. The integrals possess a single cusp in this instance, so two-sided application of Gauss-Laguerre quadrature is suitable.

In this work, system deterioration is obtained by adding Equation [2.5] to the set of stochastic differential equations for the response and using

$$A = A_0 - \delta_A\varepsilon$$

$$\nu = \nu_0 + \delta_1 \varepsilon \qquad [2.4]$$

$$\eta = \eta_0 + \delta_\eta \varepsilon$$

and

$$a = \delta_a \varepsilon \qquad [2.10]$$

For simulation, equations [2.5], [2.4], and [2.10], together with equations [2.1], [2.2], [2.17], [2.16(b)], [2.3-1], and [2.3-2] complete the set to be solved. In the linearization solutions, substitution of [2.1] and [2.2], and [2.4] and [2.10] into [4.2] before linearization, considerably complicates the problem. However, if system deterioration is assumed to be evolving slowly, it is possible to approximately take expected values of [2.5], [2.4] and [2.10], resulting

$$\dot{\mu}_\varepsilon \doteq (1-\alpha)\omega_0^2 E[\dot{u}z] \qquad [4.20]$$

and

$$\begin{aligned} \mu_A &\doteq A_0 - \delta_A \mu_\varepsilon \\ \mu_\nu &\doteq \nu_0 + \delta_1 \mu_\varepsilon \\ \mu_\eta &\doteq \eta_0 + \delta_\eta \mu_\varepsilon \\ \mu_a &\doteq \delta_a \mu_\varepsilon \end{aligned} \qquad [4.21]$$

Then A, ν , η and 'a' are replaced in the equations [4.4], [4.6], [4.7], [4.8], [4.17], and [4.18] by their approximate expected values at the present time as computed by equations [4.20] and [4.21]. This procedure was applied in zero mean analysis of this model and the other two proposed models with considerable success, and is also implemented herein.

4.3- Nonzero Mean Analysis of Single Element Pinching Model

The system to be studied in this case is a single degree of freedom oscillator as described by the nonlinear stochastic differential equation set given by equations [2.1], [2.2] and

$$\dot{z} = h(z).\{A\dot{u} - \nu[\beta|\dot{u}||z|^{(n-1)}z + \gamma\dot{u}|z|^{n}]\}/\eta \qquad [2.19]$$

where

$$h(z) = 1 - \zeta_1 \exp(-z^2/\zeta_2^2) \qquad [2.20]$$

and expressions for ζ_1 and ζ_2 are given by equations [2.20] and [2.21] in Chapter 2. In this case, similar to nonzero mean study for BN model, a(t) in Equation [2.1] is a nonzero mean stochastic process. The system response is given as

$$\underset{\sim}{v}^T = \{u, \dot{u}, z, \varepsilon\}^T \qquad [4.22]$$

where ε epresents the hysteretic energy dissipated at time t and defined by Equation [2.5]. The system degradation has the form defined by equations [2.4], [2.10] and [2.21]-[2.23]. The form of the model provides a very convenient form for numerical simulation of the response to random excitation. It also simplifies the linearization process relative to the BN series model. This will be shown in the following section.

4.3.1- Equivalent Linearization Solution of SEP Model:

To proceed with the linearization of the SEP the governing equations [2.1], [2.2], [2.19], and [2.20] are reduced to the following first order nonlinear differential equation set

$$\dot{v}_1 = v_2$$

$$\dot{v}_2 = -\alpha\omega_0^2 v_1 - 2\zeta\omega_0 v_2 - (1-\alpha)\omega_0^2 v_3 + a(t) \qquad [4.23]$$
$$\dot{v}_3 = [1 - \zeta_1 \exp(-v_3^2/(\zeta_2^2))] \cdot \{A v_2 - \nu[\beta |v_2||v_3|^{(n-1)} v_3 + \gamma |v_3|^n v_2]\}/\eta$$

where

$$v_i = y_i + \mu_i \quad ; \qquad i = 1,3 \qquad [4.24]$$

and v_i are given by Equation [4.22]. As above, it is necessary to compute expected values μ_i, namely

$$\begin{aligned} \mu_1 &= \mu_2 \\ \mu_2 &= -\alpha\omega_0^2 \mu_1 - 2\zeta\omega_0 \mu_2 - (1-\alpha)\omega_0^2 \mu_3 + \mu_F \\ \mu_3 &= \{A\mu_2 - \nu(\beta E_1' + \gamma E_2')\}/\eta - \\ &\quad (\zeta_1/\eta)\{A E_3' - \nu(\beta E_4' + \gamma E_5')\} \end{aligned} \qquad [4.25]$$

where

$$\begin{aligned} \mu_F &= \text{nonzero mean for input excitation} \\ E_1' &= E[|v_3|^{(n-1)} v_3 |v_2|] \\ E_2' &= E[|v_3|^n v_2] \\ E_3' &= E[\exp(-v_3^2/\zeta_2^2) v_2] \\ E_4' &= E[\exp(-v_3^2/\zeta_2^2) |v_3|^{(n-1)} v_3 |v_2|] \\ E_5' &= E[\exp(-v_3^2/\zeta_2^2) |v_3|^n v_2] \end{aligned} \qquad [4.26]$$

Subtraction of equations [4.25] from [4.23] and letting $y_i = v_i - \mu_i$, yields the nonsymmetric zero mean problem

$$\dot{y}_1 = y_2 \qquad (a)$$
$$\dot{y}_2 = -\alpha\omega_0^2 y_1 - 2\zeta\omega_0 y_2 - (1-\alpha)\omega_0^2 y_3 + \hat{a}(t) \qquad (b)$$
$$\dot{y}_3 = \Big[A y_2 - \nu[\beta\{|y_3+\mu_3|^{(n-1)}(y_3+\mu_3)|y_2+\mu_2| - E_1'\} + \gamma\{y_3+\mu_3^n(y_2+\mu_2) - E_2'\}]\Big]/\eta - (\zeta_1/\eta).$$

$$\Big[A[(y_2+\mu_2)\exp(-[y_3+\mu_3]^2/\zeta_2^2) - E_3'] - \nu\cdot \qquad [4.27]$$
$$\beta[|y_2+\mu_2||y_3+\mu_3|^{(n-1)}(y_3+\mu_3)\cdot \qquad (c)$$
$$\exp(-[y_3+\mu_3]^2/\zeta_2^2) - E_4'] - \nu\cdot$$
$$\gamma[|y_3+\mu_3|^n(y_2+\mu_2)\exp(-[y_3+\mu_3]^2/\zeta_2^2) - E_5']\Big]$$

In Equation [4.27] E_i', $i = 1,2,3,4,5$ can be rewritten as functions of y_i by appropriate substitution.

If the y_i are assumed to be jointly distributed Gaussian random variables, at time t, then the nonlinear Equation [4.27(c)] can be replaced by the equivalent linearized form

$$\dot{y}_3 = C_e y_2 + K_e y_3 + (\nu/\eta)[\beta E_1' + \gamma E_2'] - \qquad [4.28]$$
$$(\zeta_1/\eta)[-AE_3' + \nu(\beta E_4' + \gamma E_5')]$$

where

$$C_e = E[\partial g(y_2,y_3)/\partial y_2]$$
$$K_e = E[\partial g(y_2,y_3)/\partial y_3] \qquad [4.29]$$

and $g(y_2,y_3)$ is the right hand side of Equation [4.27(c)]. Since the derivatives of μ_i do not appear on the right hand side of equations [4.25] or [4.27], the difficulty that existed in linearization of BN model does not arise. Also, the second order response statistics $\sigma_2^2 = E[y_2^2]$, σ_3 and $E[y_2y_3]$ needed for evaluating $\rho_{23} = E[y_2y_3]/(\sigma_2\sigma_3)$ can be directly determined as elements of the covariance matrix at each time step. Therefore, no iterative approach is needed for evaluating these terms. This is a major advantage of the SEP model and reduces the computation cost invloved noticeably.

Equation [4.28], together with equations [4.27] (a) and (b), can be symbolically written in the matrix form given by Equation [4.11]. Similarly, covariance equation defined by [4.12] can be obtained. Equation [4.12] together with [4.25] form a set of equations to be jointly solved by numerical integration, for the response statistics $\underset{\sim}{\mu}_v$ and $\underset{\sim}{S}$. Hence, it remains to evaluate expected values given in [4.26] and [4.29]. Assuming that y_2 and y_3 are jointly distributed Gaussian random variables, μ_3, σ_3, μ_2, σ_2 and ρ_{23} are needed in order to evaluate these expected values at each time step. μ_2 and μ_3 are obtained from the previous numerical integration step. σ_2^2, σ_3^2 and $E[y_2y_3]$ are also evaluated as elements of covariance matrix at each time step. Therefore ρ_{23} is easily obtained as well. Other parameter values needed to evaluate C_e, K_e and the remaining expected values which require knowledge of mean and zero time lag covariance matrix terms are obtained from Equation [4.25] and [4.12]. Detailed derivations of the expected values in equations [4.26] and [4.29] are given in Appendix E. Closed form solutions are possible for odd values of 'n' only. For even, or non-integer values of 'n', the equations can be reduced to doubly infinite numerical quadratures in one variable. The integrals have a single cusp in this case as well, therefore two-sided appliction of Gauss-Laguerre quadrature is suitable.

In this study, system degradation is obtained by adding equations [2.4], [2.5], and [2.21]-[2.23] to the set of stochastic differential equations for the response. For simulation, these equations along with equations [2.1], [2.2],

[2.19], and [2.20] complete the set to be solved. In the linearization solutions, substitutions of [2.1], [2.2] and [2.4], [2.5], [2.21]-[2.23] into [4.23] will complicate the problem. However, if variation of degradation parameters are slow, these parameters may be treated approximately as constants at any time step. Hence, approximating the expected values of [2.4] and [2.21]-[2.23] by first order approximation results in equations [4.20] and the first three equations in [4.21] and

$$\begin{aligned} \mu_{\xi} &\doteq \xi_0 + \delta_{\xi}\mu_{\varepsilon} \\ \mu_{\zeta_1} &\doteq \zeta_{1_0}[1 - \exp(-p\mu_{\varepsilon})] \\ \mu_{\zeta_2} &\doteq \mu_{\xi}(\mu_{\lambda} + \mu_{\zeta_1}) \end{aligned} \qquad [4.30]$$

Expected values computed by equations [4.20], the first three equations in [4.21] and equations [4.30] at the present time, will replace the degradation parameters A, , η, ξ, $_1$ and $_2$ in the governing equations. A similar procedure was used in the analysis of BN model in this chapter and zero mean analysis of the proposed models.

4.4- Numerical Studies for Nonzero Mean Analysis

In order to demonstrate the applications of the linearization solutions for nonzero mean excitation of the two models discussed in this chapter, the response of a single degree of freedom system utilizing each model was considered. These analyses were limited to a pinching system without considering any other form of degradation, since inclusion of other degradations adds no additional complication. In these studies

system parameters of $A_0 = \eta_0 = \nu_0 = n = 1$, $\beta = \gamma = 0.5$, $\alpha = .04762$, $\omega_0 = 1$, and $\zeta = \%2$ were used. The power spectral density for the input excitation was set at three levels of $K_0 = 0.1$, low excitation, $K_0 = 0.2$, moderate level excitation, and $K_0 = 0.4$, for relatively high level of excitation. The excitation mean was allowed to vary, taking values of μ_F ranging from 0.2 to 0.8 with 0.2 increment. For the system modeled, these excitation means correspond to 20% to 80% of z_{ult}, where z_{ult} is the limiting magnitude of the hysteretic restoring force upon first loading. Both constant mean and noise excitations were applied to the system at the initial condition at $t = 0$. In the following subsections response statistics obtained for each model are presented.

4.4.1- Numerical Results for Baber-Noori Model

Several studies were conducted using the BN series model. First, to verify the behavior of the model under nonzero mean random input excitation and also for subsequent Monte Carlo simulation, several single sample plots of 'u' vs 'z' were obtained under white noise excitation for a SDOF system system model. This single sample simulation also illustrated more fully the effect of varying pinching parameters δ_a and σ. For this response a power spectral density (PSD) of 0.1 was used. Plots of runs for $\delta_a = 0.1$, $\sigma = 0.08$ with excitation mean of 0.2, $\delta_a = 0.3$, $\sigma = 0.08$ with excitation mean of 0.4 and $\delta_a = 0.1$, $\sigma = 0.08$ with mean excitation of 0.8 are shown in Figures 4.2(a)-(c). The plots shown in Figures 4.2 illustrate the

anticipated behavior. Having verified the capabilities of the nonlinear pinching model under nonzero mean excitation, the approximate response analysis of the system was considered. Figures 4.3(a)-(e) illustrate the mean response computation for displacement, μ_u, corresponding to several different values of μ_F, low, moderate, and high levels of excitations and subjected to different values of pinching rates. Figures 4.3(a) and (b) show the plots for low level of excitation, 0.1, with low and high pinching rates of $\delta_a = 0.1$, and $\delta_a = 0.5$ respectively. Figures 4.3(c) and (d) illustrate the respective plots for moderate excitation level of 0.2, with low pinching rate of $\delta_a = 0.1$, and medimum rate of $\delta_a = 0.25$. Figure 4.3(e) shows the case of high excitation level with one pinching rate of $\delta_a = 0.1$. The solid curves are the responses computed by equivalent linearization, while the dotted line curves are results of 100 samples of Monte Carlo simulation. The four plots in each figure correspond to $\mu_F = 0.2$, 0.4, 0.6, and 0.8. Mean responses for the displacement, μ_u obtained by linearization compare very well with Monte Carlo simulation at low pinching rate at all mean levels and also at high pinching rate for the mean values of $\mu_F = 0.2$ and 0.4. For the high pinching case the response is underestimated by the linearization. Figures 4.4, 4.5, 4.6, 4.7, and 4.8 show the mean response computations for u, z, u_1, u_2 and ε corresponding to the same values of μ_F, excitation levels and pinching rates as discussed for μ_u. In Figures 4.4 and 4.5 solid line curves represent the linearization results for the mean velocity response, μ_u, and

mean hysteretic restoring force prediction, μ_z, and points indiced by the symbols 'o' and 'x' are results of simulion with 100 samples, at $\mu_F = 0.2$ and $\mu_F = 0.8$ respectively. As can be seen from Figures 4.4(a)-4.4(d), comparison between linearization and simulation results for mean response of velocity is fairly good for mean excitation levels of upto 0.2 and in both cases of low and high pinching. However, for higher mean excitation levels there is not a good agreement between these results, in the presence of a high level of pinching. One source of this problem may be the numerical integration. Selecting a smaller time step might improve the result somewhat. As Figures 4.5(a)-(e) indicate, the agreement between linearization and Monte Carlo simulation results for mean response of hysteretic restoring force are very good for low pinching rate at all mean excitation levels, Figures 4.5(a), (c) and (e). In the case of high pinching rate, agreement is good for low value of mean excitation, $\mu_F = 0.2$, whereas for $\mu_F = 0.8$ response is overestimated, as can be observed from Figures 4.5(b) and (d). Considering next the mean displacement response u_1 of the smooth element component. At the low pinching rate predicted responses compare reasonably well at all values of mean excitation and both levels of PSD, as Figures 4.6(a), (c) and (e) indicate. For the high pinching rate system, μ_{u1} responses are underestimated at all mean excitation values and for both low and moderate excitation PSD levels, as shown in Figures 4.6(b) and (d). Mean displacement responses for the slip-lock element component of model, μ_{u2} is shown in Figure 4.7. As these plots

indicate, the agreement between the linearization and simulation results for u_2 is not, in general, good. However, the trends of the response are correct, except at high pinching. One reason for this problem can be found in the numerical technique used to evaluate the equivalent linearization coefficients. Moreover, the problem due to numerical integration, may have additional influence. It seems questionable at first glance, that satisfactory agreement between MCS and linearization estimates for μ_u would be obtained when agreement between the constituent parts is not obtained. However, μ_u is obtained from integration of the differential equation of motion, while μ_{u1} and μ_{u2} are obtained from additional equations. It seems likely that small systematic errors in computation of μ_{u1} and μ_{u2} are contributing to the poor agreement in the latter case. Also it should be noticed that the difference between the order of the magnitude of μ_{u1} and μ_{u2} is so large (maximum value of about 16 for μ_{u1} and about 0.6 for μ_{u2}), that the magnitude of μ_2 response will not have significant effect on the total response. Results for the mean energy dissipation response, as shown in Figure 4.8(a)-(e), indicate that there is a very good agreement between the linearization and simulation results for all excitation levels, for both low and high pinching rates, and for all values of mean excitation. Only for the case of high pinching and at high value of mean excitation the linearization solution slightly underestimates the response. Figures 4.9, 4.10, 4.11, 4.12, and 4.13 illustrate the RMS response computations for u, u, z, u_1, and u_2 under the same conditions

discussed for the mean responses. Figures 4.9(a)-(e) indicate that there is a reasonably good comparison between the linearization and simulation trends for the RMS displacement responses, but numerical estimates are not particularly good. In all the cases shown, responses are underestimated for low values of mean excitation, $\mu_F = 0.2$, and overestimated for high values, $\mu_F = 0.8$. A somewhat better numerical comparison is observed for the RMS velocity response results. Although the responses are slightly overestimated for all excitation levels and mean excitation values, the important response trends are accounted for. These comparisons are shown in Figures 4.10(a)-(e). Results for the RMS hysteretic force response are shown in Figure 4.11. As can be seen from Figures 4.11(a)-(e), value of σ_z decreases as μ_F increases. This behavior is in agreement with the predicted mean values for 'z' as shown in Figure 4.5. This phenomenon occurs since, if μ_z is close to 1 and $z_{ult} = 1$, the standard deviation of z will be smaller than if μ_z is near zero. For σ_z and for the low as well as high pinching case, the responses are generally overestimated by the linearization for low excitation level and at both low and high values of mean excitation. However, as the excitation level increases the overestimation becomes smaller and there is relatively good agreement between the linearization and simulation results at high excitation level, as shown in Figure 4.11(e). Results for the RMS displacement response of smooth element as shown in Figure 4.12 indicate generally poor agreement for all excitation levels, for low and high pinching rates and at

all values of mean excitation, for much of the time. The RMS response for slip-lock element component of the model, as shown in Figure 4.13, for low pinching rate, at any level of excitation and for all values of μ_e, are significantly overestimated.

In general, it may be stated that first order response statistics are more closely estimated than are second order statistics, and that primary quantities u, $\dot{u}$, and z are more adequately characterized than the secondary quantities u_1 and u_2. It is important to mention here that the advantage of linearization over the Monte Carlo simulation is that response statistics can be predicted fairly closely at a reasonable cost by the equivalent linearization. But here, in the nonzero mean analysis of this model, the iteration approach used for the computation of equivalent linearization coefficients makes the computer runs expensive and comparable to the simulation. This is one of the disadvantages of the slip-lock model for nonzero mean analysis. This problem is not encountered in nonzero mean analysis of the SEP model as will be seen in the following section.

4.4.2- Numerical Results for Single Element Pinching Model

Similar studies were performed for the response analysis of the single element pinching model with the same purposes in mind. To verify the behavior of the model under nonzero mean random excitation several single sample plots of 'u' vs 'z' were obtained under white noise excitation for a SDOF system model.

This single sample simulation shows the effect of varying pinching parameters ζ_1 and λ as well. In this study, power spectral density values of 0.1 and 0.2 were used. Plots of runs for power spectral density of 0.1 are shown in Figures 4.14(a) and (b) and the plots for power spectral density of 0.2 are given in Figures 4.15(a) and (b). In both cases shown in figures 4.14 and 4.15 a very high level of pinching with $\zeta_{10} = 0.95$ and $\lambda = 0.15$ subjected to mean excitation value of $\mu_F = 0.2$ and 0.6 is considered. In Figures 4.14 a value of viscous damping ratio of 0.02 is used whereas in Figure 4.15 a corresponding value of 0.1 is considered. Both these figures illustrate the capability of the model in reproducing a pinching hysteresis behavior under a general loading.

Results for the approximate response analysis via equivalent linearization for a SDOF system using the SEP model are illustrated in Figures 4.16-4.22. In these studies three levels of excitation with two different rates of low and high pinching for each case were considered. Also the statistics in this case have been obtained for a longer duration of t = 100 seconds. The values of pinching parameters and pinching rates are established such that the type of behavior obtained in each case is comparable to corresponding studies for the BN model as illustrated in figures 4.3-4.13. This will make the comparison between the two models easier. Figures 4.16(a)-(e) show mean response computation for displacement, μ_u. The results for linearization are in a very good agreement with Monte Carlo simulation for all excitation levels, all pinching rates and all

values of mean excitation. The agreement between the two results is much better for this model than for BN series model for the high pinching high excitation level case. This can be observed by comparing these results with the corresponding results for the BN model as shown in Figure 4.3. A noticeable instability may be observed for the high excitation, high pinching case beyond 65-70 seconds as shown in Figure 4.16(e), but the trends of the response are accounted for. Similar instabilities however, are also observed in some other response statistics results for the SEP model in high pinching, high excitation studies as will be seen. The instability starts quite suddenly when the responses have reached a stationary level. This abrupt behavior is almost certainly due to a numerical problem and is not part of the physical behavior that has been modelled. Plots shown in Figures 4.17(a)-(e) ilustrate the mean response evaluations for velocity, μ_u. Agreement between linearization and simulation results for this case is also acceptable and better than corresponding results for BN model shown in Figure 4.4. Similar discussion as mentioned for mean response of u is valid for the results shown in Figure 4.17(e). Figures 4.18(a)-(e) show mean response values for restoring force. In this case as well, there is a very good agreement between the approximate and simulation results for all excitation levels, all pinching rates and all values of mean excitation. Agreement between the approximate and simulation results in this case is generally better than the corresponding comparison for the BN model. Figures 4.19(a)-(e) shows the results for the mean energy dissipation. The agreement

between the approximate values and the simulated responses is very good for low as well as high pinching and at all excitation levels. There is only a slight underestimation at highest level of mean excitation, as these results indicate.

RMS response statistics for u, $\dot{u}$, and z are presented in Figures 4.20-4.22. Figures 4.20(a) and (b) indicate that for low excitation level there is a good agreement between the linearization and simulation results for RMS displacement response for all values of mean excitation and for both cases of low and high pinching. It is important to point out here that even at low level of excitation a fair amount of yielding (inelastic action) is taking place. Therefore the good agreement between the approximate results and the simulation results obtained by the SEP model in nonzero mean analysis should be considered with this fact in mind. For moderate excitation level and for all pinching levels and all values of mean excitation, responses are slightly underestimated by linearization. This is shown in Figures 4.20(c) and (d). For high level of excitation, at all pinching rates, and all values of mean excitation, results will be overestimated as shown in Figure 4.20(e). Comparing these results with the corresponding results for the BN model, as shown in Figure 4.9, indicate a somewhat better agreement for the response statistics obtained by the SEP model. Plots shown in Figure 4.21(a)-(e) show the RMS response for the velocity. As can be seen, the results are underestimated for all levels of excitations, all values of mean excitations and for both low and high pinching rates. Underestimation increases as the excitation

level increases as well as with the increase in pinching. As can be seen, the instability observed in similar results for the BN model, shown in Figure 4.10, does not occur in this case. This is an advantage of the SEP model in this regard. RMS responses for hysteretic restoring force are presented in Figures 2.22(a)-(e). For the low excitation level, at both low as well as high pinching rates and for all values of mean excitation computations show indicate slight underestimation as obsereved from Figure 4.22(a) and (b). For moderate excitation level, for low pinching and at all values of mean excitation there is a good agreement between the approximate and simulation results as shown in Figure 4.22(c). For moderate excitation level, for high pinching case and for all mean excitation values there is a slight underestimation in the results. This is illustrated in Figure 4.22(d). For high level of excitation, for both cases of low and high pinching rates and for all values of mean excitation, responses are underestimated as indicated in Figure 4.22(e). It is also interesting to see that the value of σ_z decreases as μ_F increases. This behavior agrees well with the predicted mean values for z as shown in Figure 4.18. This is due to the same reason discussed in the study of σ_z for the BN model and the same argument can be applied here. Comparison of these results with those of BN model, shown in Figure 4.11, illustrate a better agreement in results for the SEP mode. Also similar to the results for σ_u, instability observed in the results shown in Figure 4.11 for the BN model is not observed here.

Studies for the proposed single element pinching model suggest that such models may be more suitable for random vibration analysis than the slip-lock series models. An important feature of the SEP is its single rather than series form. This reduces the number of varables involved for computation in the mean and RMS response analysis and therefore reduces the computation costs significantly. As discussed in sections 3.5.3 and 4.3, the explicit form of the equation for the derivatives allows for considerable simplification in evaluating the equivalent linear system coefficients. Moreover, comparison of the computed statistical results show a somewhat better agreement, in general, between linearization and simulation solutions for the SEP model than for the BN model; especially for nonzero mean excitations.

The numerical studies presented here, apply to the situation where the mean and random loads are from the same source. In a more general case, the mean and random loads may have different origins. Such is the case for the gravity-seismic ground motion, or current-wave action combinations. In such situations, the equilibrium state under the mean excitation alone is taken as the initial condition for the random vibration analysis. This study is not considered here. However, study of this type for smooth hysteresis model can be found in reference (11).

CHAPTER 5

SUMMARY, CONCLUSIONS AND REMARKS

5.1- Summary and Conclusions:

The intent of the research presented herein was to develop mathematical models capable of representing general degradation behavior of a hysteretic structural element, including hysteretic pinching, as a function of energy dissipation. These models were required to meet the additional condition of mathematical tractability so that they can be used for approximate solution with the available methods of nonlinear random vibration analysis.

Three mathematical models for hysteresis with pinching are presented in Chapter 2, two series slip-lock models and one single element hysteresis model. These are all relatively versatile models which are capable of a variety of degrading behaviors, and hysteresis shapes. Behavior of the proposed models under cyclic as well general loadings illustrates the capability of all these models in reproducing a wide range of degradation behavior including hysteretic pinching. A mathematical approach for developing hysteresis models with general degradation behavior is also presented in Chapter 2. The single element model which seems to be a more tractable model as compared with the two series models is developed based on this mathematical technique. This method provides a basis for

developing even wider choice of models.

In Chapter 3, random vibration analysis of the proposed models is studied. Due to the highly nonlinear character of the models of Chapter 2, closed form solution of these models is not possible. It is shown in chapter 3 however, that the mathematical forms of the models are suitable for approximate solution by the method of equivalent linearization without recourse to the Krylov-Bogoliubov approximation. The linearized models are used to obtain zero time lag covariance matrix response. In random vibration analysis of chapter 3, mean excitation and mean responses are assumed to be zero. The response statistics are also computed using Monte Carlo simulation. The response predictions of the linearized models for RMS displacement, velocity and hysteretic restoring force are reasonably good for all degradation and excitation levels. The constituent element responses, and the hysteretic energy dissipation is closely modeled at low to moderate excitation levels for BN series model, and for low to high levels for NB series model. Also for the single element pinching model mean energy dissipation is closely modeled at low to high excitation levels.

At all levels, the linearized models predict qualitatively the response of the system. In random vibration analysis, agreement between the results of Monte Carlo simulation and linearized models is somewhat better for single element pinching and NB series model than for the BN slip-lock model.

In Chapter 4, the random vibration analysis of the proposed models is extended to the more general case of nonzero mean excitations and responses. Equivalent linearization models for two of the proposed systems, BN series model and single element pinching, is preseted for the response of a single degree of freedom system with general hysteretic behavior to a nonzero mean excitation. The nonstationary response statistics are obtained by numerical integration of the linearized equations. Mean responses computed using these two models are in fairly good agreement, for BN model, and very good agreement, for the single element pinching model, with the results of Monte Carlo simulation. Covariance matrix responses predict the response in the case of single element model, or the BN series model, prediction is fairly good for some of the RMS responses but the linearized results either underestimate or overestimate the response magnitudes in other cases. However, the response trends are predicted reasonably well.

5.2- Suggestions and Recommendations

As illustrated and discussed in preceeding chapter, the main objective of the research presented in this thesis was to develop mathematical models which are capable of representing general degradation behavior of a hysteretic structural element, including hysteresis pinching for both deterministic as well as random vibration analysis. While the present work indicates that the proposed models are quite useful in this respect, a number of areas remain for further study.

1. Studies reported here were limited to the response analysis of a single degree of freedom oscillator. However, application of these models as part of a multidegree of freedom system is possible and theoretical ground work exists for this extension (14,15). Considering the nonzero mean analysis reported herein, application of these models to MDOF case will allow consideration of nonzero mean effects such as wind, current or gravity loads upon the response of inelastic systems.

2. Models proposed here may be used to incorporate the physically observed phenomenon of hysteresis loop pinching into the random vibration analysis of hysteretic structures. Thus the modeling technique proposed herein has potential application to the random vibration of reinforced concrete structures, or braced steel frames. In order to properly model the restoring force behavior of a real structure, it is necessary to determine appropriate values for hysteresis loop shapes as well as pinching parameters of the proposed models. For this purpose, proper systems identification techniques are available (43, 44) and have been investigated for system identification of BBW smooth model (130). Effort in this regard will be a major contribution.

3. Hysteretic degradation behavior as well as pinching,

have been assumed as a function of energy dissipation in this work. In order to properly model the hysteretic behavior of real structural elements, modifications to this assumption might be necessary. Consideration of the degradation as a function of maximum displacement in each cycle may be a suitable assumption. Results for this alternative approach are available for BBW model (137) and seem to be promising.

4. Studies reported here were limited to approximate response prediction under zero and nonzero mean excitation. The mean square response is only one of several quantities of interest, however, and does not provide information concerning such items as maximum structural response, or total energy dissipation demands upon the structure caused by an excitation of particular intensity and duration. These quantities are of interest in seismic design. Analysis of this problem can be accomplished by consideration of first passage time problem. Therefore, evaluation of first passage estimates are quite important in case of hysteretically degrading as well as pinching system. One of the problems which will be encountered in this analysis will be selection of a suitable probability distribution for the response, which is strongly non-Gaussian in this case. Some ground work exist for attempting this effort (14,92).

5. The approach used for linearization in the nonzero mean analysis was based on the technique suggested by Spanos (122, 131) and used by Baber (11). This approach suggested the subtraction of mean responses from the governing stochastic differential equations. However, an alternative approach is subtracting the mean responses after performing the linearization. It would be interesting to see a comparison of the results for these two approaches.

6. The studies performed for the nonzero mean analysis were limited to two of the three models, BN and SEP. However, as the results for zero mean studies indicate, prediction of RMS responses for NB model are somewhat better than those corresponding to BN model. Therefore, nonzero mean solution should obtained for this model as well in order to achieve a better judgement on the possible source of the problems with the results for BN model.

7. Also requiring additional work are

   a- The computational problems included in the solution

   b- Considering the application of more general and improved statistical linerization techniques such as the approach proposed by Beaman and Hedrick (18)

   c- Consideration of some promissing numerical

schemes for approximating the distribution of a random variable, such as the method suggested by Meyers (95).

8. In the work discussed herein, it has been assumed that hysteresis pinching is essentially a slipping phenomenon at force reversal which is ideally modelled by a slip-lock model or an equivalent SEP model. Additional pinching can be attributed to general stiffness degradation during unloading stages of a cycle. Such degradation may be described mathematically using the constructive techniques used to establish the SEP model, and should be investigated.

BIBLIOGRAPHY

1. Ahmadi, G., "Mean Square Response of a Duffing Oscillator to a Modulated White Noise Excitation by the Generalized Method of Equivalent Linearization," Journal of Sound and Vibration, Vol. 71, pp. 9-15, 1980.

2. Ahmadi, G., Tadjbakhsh, I., and Farshad, M., "On the Response of Nonlinear Plates to Random Loads," Acoustica, Vol. 40, pp. 316-322, 1978.

3. Aleman, M.A., Meinheit, D.F., and Jirsa, J.O., "Influence of Lateral Beams on the Behavior of Beam-Column Joints," Proceedings of the Sixth World Conference on Earthquake Engineering, New Delhi, India, 1977, Vol.3, pp. 3089-3094.

4. Amin, M., and Ang, A. H-S., "Nonstationary Stochastic Model of Earthquake Motions," Journal of the Engineering Mechanics Division, ASCE, Vol. 94, No. EM2, pp. 559-583, April 1968.

5. Anderson, J.C., and Bertero, V.V., "Seismic Behavior of Multistory Frames Designed by Different Philosophies," Earthquake Engineering Research Center, Report No. EERC-69/11, University of California, Berkeley, California, October 1969.

6. Ang, A. H-S., and Wen, Y.K., "Prediction of Structural Damage Under Random Earthquake Excitations," Presented at the Winter Annual Meeting, ASME, Phoenix, Arizona, November 14-19, 1982. Reprinted in Earthquake Ground Motion and Its Effects on Structures, ASME, AMD-Vol. 53, pp. 91-107, 1982.

7. Aoyama, H., Umemura, H., and Minamino, H., "Tests and Analyses of SRC Beam-Column Subassemblages," Proceedings of the Sixth World Conference on Earthquake Engineering, New Delhi, India, 1977, Vol. 3, pp. 3081-3088.

8. Apetaur, M., and Opticka, F., "Linearization of Non-Linear Stochastically Excited Dynamic Systems," Journal of Sound and Vibration, Vol. 86, No. 4, pp. 563-585, 1983.

9. Asano, K., and Iwan, W.D., "An Alternative Approach to the Random Response of Bilinear Hysteretic Systems," Earthquake Engineering and Structural Dynamics, Vol. 12, pp. 229-236, 1984.

10. Atalay, B., and Penzien, J., "Inelastic Cyclic Behavior of

Reinforced Concrete Flexural Members," Proceedings of the Sixth World Conference on Earthquake Engineering, New Delhi, India, 1977, Vol. 3, pp. 3062-3068.

11. Atalik, T.S., and Utku, S., "Stochastic Linearization of Multidegree of Freedom Nonlinear Systems," Earthquake Engineering and Structural Dynamics, Vol. 4, pp. 411-420, 1976.

12. Baber, T.T., "Nonzero Mean Random Vibration of Hysteretic Systems," Accepted for Publication in the Journal of the Engineering Mechanics Division, ASCE. Will appear in issue of July 1984.

13. Baber, T.T., and Noori, M.N., "Random Vibration of Pinching, Hysteretic Systems," Technical Report on Grant No. CEE 81-12584, Submitted to National Science Foundation. Also, Report No. UVA-526378-CE84-102, September, 1983.

14. Baber, T.T, and Wen, Y.K., "Random Vibration of Hysteretic Degrading Systems," Journal of the Engineering Mechanics Division, ASCE, Vol. 107, No. EM6, PP. 1069-1087, December 1981.

15. Baber, T.T., and Wen, Y.K., "Stochastic Equivalent Linearization for Hysteretic, Degrading, Multistory Structures," Civil Engineering Studies, Structural Research Series No. 471, University of Illinois, Urbana, Illinois, December 1979.

16. Baber, T.T., and Wen, Y.K., "Stochastic Response of Multistory Yielding Frames," Earthquake Engineering and Structural Dynamics, Vol. 10, pp. 403-416, June 1982.

17. Banon, H., Biggs, J.M., and Irvine, H.M., "Seismic Damage in Reinforced Concrete Frames," Journal of the Structural Division, ASCE, Vol. 107, No. ST9, pp. 1713-1729, September 1981.

18. Banon, H., and Veneziano, D., "Seismic Safety of Reinforced Concrete Members and Structures," Earthquake Engineering and Structural Dynamics, Vol. 10, pp. 179-193, 1982.

19. Beaman, J.J., and Hedrick, J.K., "Improved Statistical Linearization for Analysis and Control of Non-Linear Stochastic Systems: Part 1: An Extended Statistical Linearization Technique," Journal of Dynamic Systems, Measurement and Control, Transactions ASME, Vol. 103, pp. 14-21, March 1981.

20. Bergman, L.A., "Moments of Time to First Passage of the

Linear Oscillator," Ph.D. Thesis, Department of Civil Engineering, Case Western Reserve University, August 1979.

21. Bertero, V.V., and Brokken, S., "Infills in Seismic Resistant Buliding," Journal of the Structural Division, ASCE, Vol. 109, No. 6, pp. 1337-1362, June 1983.

22. Bertero, V.V., Popov, E.P., and Wang, T.T., "Hysteresis Behavior of R/C Flexural Members with Special Web Reinforcement," Earthquake Engineering Research Center, Report No. EERC-74/09, University of California, Berkeley, California, August 1974.

23. Bhatti, M.A., and Pister, K.S., "Transient Response Analysis of Structural Systems with Nonlinear Behavior," Computers and Structures, Vol. 13, pp. 181-188, 1981.

24. Bily, M., and Cacko, J., "Simulation of Random Processes with Various Probability Density Functions," Journal of Sound and Vibration, Vol. 81, No. 3, pp. 393-403, 1982.

25. Bogdanoff, J.L., Goldberg, J.E., and Bernard, M.C., "Response of a Single Structure to the Random Earthquake-Type Disturbance," Bulletin, Seismological Society of America, Vol. 51, No. 2, pp. 293-310, April 1961.

26. Bouc, R., "Modele Mathematique d'Hysteresis," Acustica, Vol. 24, pp. 16-25, Marseille, France.

27. Bycroft, G.N., "White Noise Representation of Earthquakes," Journal of the Engineering Mechanics Division, ASCE, VOl. 86, No. EM2, pp. 1-16, April 1960.

28. Caughey, T.K., "Random Excitation of a System with Bilinear Hysteresis," Journal of Applied Mechanics, Transactions ASME, Vol. 27, pp. 649-652, December 1960.

29. Caughey, T.K., "Sinusoidal Excitation of a System with Bilinear Hysteresis," Journal of Applied Mechanics, Transactions ASME, Vol. 27, pp. 640-643, December 1960.

30. Caughey, T.K., "Equivalent Linearization Techniques," Journal of the Acoustical Society of America, Vol. 35, No. 11, pp. 1706-1711, November 1963.

31. Caughey, T.K., "Nonlinear Theory of Random Vibration," Advances in Applied Mechanics, Vol. 11, pp. 209-253, 1971.

32. Caughey, T.K., "Derivation and Application of the Fokker-Plank Equation to Discrete Nonlinear Dynamic Systems

Subjected to White Random Excitation," Journal of the Acoustical Society of America, Vol. 35, No. 11, pp. 1683-1692, November 1963.

33. Caughey, T.K., and Ma, F., "The Steady-State Response of a Class of Dynamical Systems to Stochastic Excitation," Journal of Applied Mechanics, Transactions ASME, Vol. 49, pp. 629-632, September 1982.

34. Caughey, T.K., and Ma, F., "The Exact Steady-State Solution of a Class of Non-Linear Stochastic Systems," International Journal of Non-Linear Mechanics, Vol. 17, No. 3, pp. 137-142, 1982.

35. Caughey, T.K., and Stumpf, H.J., "Transient Response of a Dynamic System under Random Excitation," Journal of Applied Mechanics, Transactions ASME, Vol. 28, No. 4, pp. 563-566, December 1961.

36. Chang, M.K., Kwiatkowski, J.W., and Nau, R.F., "ARMA Models for Earthquake Ground Motion," Earthquake Engineering and Structural Dynamics, Vol. 10, pp. 651-662, 1982.

37. Chopra, A.K., and Lopez, O.A., "Evaluation of Simulated Ground Motions for Predicting Elastic Response of Long Period Structures and Inelastic Response of Structures," Earthquake Engineering and Structural Dynamics, Vol. 7, pp. 383-402, 1979.

38. Crandall, S.H., "Non-Gaussian Closure for Random Vibration of Non-Linear Oscillator," International Journal of Non-Linear Mechanics, Vol. 15, pp. 303-313, 1980.

39. Dash, P.K., and Iyengar, R.N., "Analysis of Randomly Time Varying Systems by Gaussian Closure Technique," Journal of Sound and Vibration, Vol. 83., No. 2, pp. 241-251, 1982.

40. Deb Chaudhury, A. and Gasparini, D.A., "Response of MDOF Systems to Vector Random Excitation," Journal of the Engineering Mechanics Division, ASCE, Vol. 108, No. EM2, pp. 367-385, April 1982.

41. Der Kiureghian, A., "A Response Spectrum Method for Random Vibrations," Earthquake Engineering Research Center, Report No. EERC-80/15, University of California, Berkeley, California, June 1980.

42. Der Kiureghian, A., "A Response Spectrum Method for Random Vibration Analysis of MDF Systems," Earthquake Engineering and Structural Dynamics, Vol. 9, pp. 419-435, 1981.

43. Distefano, N., and Pena-Pardo, B., "System Identification of Frames under Seismic Loads," Journal of Engineering Mechanics Division, ASCE, Vol. 102, No. EM2, pp. 313-330, April 1976.

44. Distefano, N., and Rath, A., "Modeling and Identification in Nonlinear Structural Dynamics, I- One Degree of Freedom Models," Report No. EERC-74/15, University of California, Berkeley, California, December 1974.

45. Filippou, F.C., Popov, E.P., and Bertero, V.V., "Modeling of R/C Joints under Cyclic Excitations," Journal of the Structural Engineering, ASCE, Vol. 109, No. 11, pp. 2666-2684, November 1983.

46. Foster, E.T., "Semilinear Random Vibrations in Discrete Systems," Journal of Applied Mechanics, Transactions ASME, Vol. 35, pp. 560-564, 1968.

47. Gasparini, D.A., "Response of MDOF Systems to Nonstationary Random Excitation," Journal of the Engineering Mechanics Division, ASCE, Vol. 105, No. EM1, pp. 13-27, February 1979.

48. Gates, N.C., "The Earthquake Response of Deteriorating Systems," Report No. EERL 77-03, Earthquake Engineering Research Laboratory, California Institute of Technology, Pasadena, California, March 1977.

49. Goldberg, J.E., "Bogdanoff, J.L., and Sharpe, D.R., "The Response of Simple Nonlinear Systems to a Random Disturbance of the Earthquake Type," Bulletin, Seismological Society of America, Vol. 54, No. 1, pp. 263-276, 1964.

50. Goldman, L.E., Rosenblueth, E., and Newmark, N.M., "A Seimic Design of Elastic Structures on Firm Ground," Transactions ASCE, Vol. 120, pp. 782-802, 1955.

51. Gosain, N.K., and Jirsa, J.O., "Bond Deterioration in Reinforced Concrete Members under Cyclic Loads," Proceedings of the Sixth World Conference on Earthquake Engineering, New Delhi, India, 1977, Vol. 3, pp. 3049-3055.

52. Goto, H., and Iemura, H., "Earthquake Response Characteristics of Deteriorating Hysteretic Structures," Proceedings of the Sixth World Conference on Earthquake Engineering, New Delhi, India, 1977, Vol. 2, pp. 1106-111.

53. Grigoriu, M., "Mean-Square Structural Response to Stationary Ground Acceleration," Journal of the Engineering Mechanics Division, ASCE, Vol. 107, No. EM5, pp. 969-986, October

1981.

54. Grossmayer, R.L., "Stochastic Analysis of Elasto-Plastic Systems," Journal of the Engineering Mechanics Division, ASCE, Vol. 107, No. EM1, pp. 97-116, February 1981.

55. Grossmayer, R.L., and Iwan, W.D., "A Linearization Scheme for Hysteretic Systems Subjected to Random Excitation," Earthquake Engineering and Structural Dynamics, Vol. 9, pp. 171-185, 1981.

56. Hadjian, A.H., "Re-evaluation of Equivalent Linear Models for Simple Yielding Systems," Earthquake Engineering and Structural Dynamics, Vol. 10, pp. 759-767, 1982.

57. Hammond, J.K., "On the Response of Single and Multidegree of Freedom Systems to Nonstationary Random Excitations," Journal of Sound and Vibration, Vol. 7, pp. 393-416, 1968.

58. Higashi, Y., Ohkubo, M., and Ohtsuka, M., "Influence of Loading Excursions on Restoring Force Characteristics and Failure Modes of Reinforced Concrete Columns," Proceedings of the Sixth World Conference on Earthquake Engineering, New Delhi, India, 1977, Vol. 3, pp. 3127-3132.

59. Housner, G.W., "Characteristics of Strong Motion Earthquakes," Bulletin, Seimological Society of America, Vol. 37, No. 1, pp. 19-31, January 1947.

60. Housner, G.W., and Jennings, P.C., "Generation of Artificial Earthquakes," Journal of the Engineering Mechanics Division, ASCE, Vol. 90, No. EM1, pp. 113-150, February 1964.

61. Hsu, T-I., and Bernard, M.C., "A Random Process for Earthquake Simulation," Earthquake Engineering and Structural Dynamics, Vol. 6, pp. 347-362, 1978.

62. Husid, R., "The Effect of Gravity on the Collapse of Yielding Structures with Earthquake Excitation," Proceedings of the Fourth World Conference on Earthquake Engineering, Santiago, Chile, Vol. 2, A-4, pp. 31-44, 1969.

63. Iemura, H., "Earthquake Response of Stationary and Deteriorating Hysteretic Structures," Department of Civil Engineering, Kyoto University, Kyoto, Japan, May 1977.

64. Ikeda, A., Yamada, T., Kawamura, S., and Fujii, S., "State of the Art of Precast Concrete Technique in Japan," Proceedings of a Workshop on Earthquake-Resistant Reinforced Concrete Building Construction, University of California, Berkeley, California, July 11-15, 1977, Vol. 2, pp.

770-788.

65. Iwan, W.D., "The Response of Simple Stiffness Degrading Structures," Proceedings of the Sixth World Conference on Earthquake Engineering, New Delhi, India, 1977, Vol. 2, pp. 1094-1099.

66. Iwan, W.D., "A Generalization of the Concept of Equivalent Linearization," International Journal of Non-Linear Mechanics, Vol. 8, pp. 279-287, 1973.

67. Iwan, W.D., "The Distributed Element Concept of Hysteretic Modeling and Its Application to Transient Response Problems," Proceedings of the Fourth World Conference on Earthquake Engineering, Santiago, Chile, 1969, Vol. 2, A-4, pp. 45-47.

68. Iwan, W.D., "On A Class of Models for the Yielding Behavior of Continuous and Composite Systems," Journal of Applied Mechanics, Transactions ASME, Vol. 34, pp. 612-617, September 1967.

69. Iwan, W.D., "Application of Non-Linear Analysis Techniques," Applied Mechanics in Earthquake Engineering, the Applied Mechanics Division, ASME, AMD, Vol. 8, pp. 135-161, 1974.

70. Iwan, W.D., and Gates, N.C., "Estimating Earthquake Response of Simple Hysteretic Structures," Journal of the Engineering Mechanics Division, ASCE, Vol. 105, No. EM3, pp. 391-405, June 1979.

71. Iwan, W.D., and Gates, N.C., "The Effective Period and Damping of A Class of Hysteretic Structures," Earthquake Engineering and Structural Dynamics, Vol. 7, pp. 199-211, 1979.

72. Iwan, W.D., and Lutes, L.D., "Response of the Bilinear Hysteretic System to Stationary Random Excitation," Journal of the Acoustical Society of America, Vol. 43, No. 3, pp. 545-552, 1968.

73. Iwan, W.D., and Mason, A.B., Jr., "Equivalent Linearization for Systems Subjected to Non-Stationary Random Excitation," International Journal of Non-Linear Mechanics, Vol. 15, pp. 71-82, 1980.

74. Iwan, W.D., and Patula, W.D., "The Merit of Different Error Minimization Criteria in Approximate Analysis," Journal of Applied Mechanics, Transactions ASME, Vol. 39, pp. 257-262, March 1972.

75. Iwan, W.D., and Spanos, P-T.D., "Response Envelope Statistics for Nonlinear Oscillators with Random Excitation," Journal of Applied Mechanics, Transactiona ASME, Vol. 45, pp. 170-174,, 1978.

76. Iwan, W.D., and Yang, I-M., "Application of Statistical Linearization Techniques to Nonlinear Multidegree of Freedom Systems," Journal of Applied Mechanics , Transactions ASME, Vol. 39, pp. 545-550, June 1972.

77. Iyengar, N.R., and Dash, P.K., "Stochastic Analysis of Yielding Systems," Journal of the Engineering Mechanics Division, ASCE, Vol. 104, EM2, pp. 383-398, April 1978.

78. Iyengar, N.R., and Dash, P.K., "Study of the Random Vibration of Nonlinear Systems by the Gaussian Closure Technique," Journal of Applied Mechanics, Transactions ASME, Vol. 45, No. 2, pp. 393-399, June 1978.

79. Iyengar, N.R., and Iyengar, K.T., "A Nonstationary Random Process Model for Earthquake Accelerations," Bulletin, Seismological Society of America, Vol. 59, No. 3, pp. 1163-1188, June 1969.

80. Jennings, P.C., "Response of Yielding Structures to Stationary Generated Ground Motion," Proceedings of the Third World Conference on Earthquake Engineering, Auckland, New Zealand, 1965, Vol. 2, pp. 783-796.

81. Karnopp, D., and Brown, R.N., "Random Vibration of Multidegree of Freedom Hysteretic Structures," Journal of Acoustical Society of America, Vol. 42., No. 1, pp. 54-59, 1967.

82. Karnopp, D., and Scharton, T.D., "Plastic Deformation in Random Vibration," Journal of the Acoustical Society of America, Vol. 39, No. 6, pp. 1154-1161, 1966.

83. Kaul, M.K., and Penzien, J., "Stochastic Seismis Analysis of Yielding Offshore Towers," Journal of the Engineering Mechanics Division, ASCE, Vol. 100, No. EM5, pp. 1026-1038, October 1974.

84. Kazakov, I.E., "Statistical Analysis of Systems with Multi-Dimensional Non-Linearities," Automation and Remote Control, Vol. 26, pp. 458-464, 1965.

85. Kobori, T., Minai, R., and Suzuki, Y., "Statistical Linearization Techniques of Hysteretic Structures to Earthquake Excitations," Bulletin of the Disaster Prevention Research Institute, Kyoto University, Vol. 23, parts 3-4,

No. 215, pp. 111-135, December 1973.

86. Kobori, T., Minai, R., and Suzuki, Y., "Nonstationary Random Response of Bilinear Hysteretic Systems," Theoretical and Applied Mechanics, Vol. 24, pp. 143-152, 1974.

87. Levy, R., Kozin, F., and Moorman, R.B., "Random Processes for Earthquake Simulation," Journal of the Engineering Mechanics Division, ASCE, Vol. 97, No. EM2, pp. 495-517, April 1971.

88. Lin, Y.K., Probabilistic Theory of Structural Dynamics, Robert E. Krieger Publishing Company, New York, 1976.

89. Liu, S.C., "Earthquake Response Statistics of Nonlinear Systems," Journal of the Engineering Mechanics Division, ASCE, Vol. 95, No. EM2, pp. 397-419, April 1969.

90. Liu, S.C., "Evolutionary Power Spectral Density of Strong Motion Earthquakes," Bulletin, Seismological Society of America, Vol. 48, No. 1, pp. 299-306, 1970.

91. Liu, S.C., "Statistical Analysis and Stochastic Simulation of Ground Motion Data," The Bell System Technical Journal, pp. 2273-2298, December 1968.

92. Lutes, L.D., "Approximate Techniques for Treating Random Vibration of Hysteretic Systems," Journal of the Acoustical Society of America, Vol. 48, No. 1, pp. 299-306, 1970.

93. Lutes, L.D., and Jan, T.S., "Stochastic Response of Yielding Multi-Story Structures," Journal of the Engineering Mechanics Division, ASCE, Vol. 109, No. 6, pp. 1403-1418, December 1983.

94. Lutes, L.D., and Lilhand, K., "Frequency Content in Earthquake Simulation," Journal of the Engineering Mechanics Division, ASCE, Vol. 105, No. EM1, pp. 143-158, February 1979.

95. Lutes, L.D., and Takemiya, H., "Random Vibration of Yielding Oscillators," Journal of the Engineering Mechanics Division, ASCE, Vol. 100, No. EM2, pp. 343-358, April 1974.

96. Madsen, P.H., and Krenk, S., "Stationary and Transient Response Statistics," Journal of the Engineering Mechanics Division, ASCE, Vol. 108, No. EM4, pp. 622-635, August 1982.

97. Mason, A.B., Jr., "Some Observations on the Random Response of the Linear and Nonlinear Dynamical Systems," Earthquake

Engineering Research Laboratory, Report No. EERL 79-01, California Institute of Technology, Pasadena, California, January 1979.

98. Matsui, C., and Mitani, I., "Inelastic Behavior of High Strength Steel Frames Subjected to Constant Vertical and Alternating Horizontal Loads," Proceedings of the Sixth World Conference on Earthquake Engineering, New Delhi, India, 1977, Vol. 3, pp. 3169-3174.

99. McNiven, H.D., and Matzen, V.C., "A Mathematical Model to Predict the Inelastic Response of a Steel Frame: Formulation of the Model," Earthquake Engineering and Structural Dynamics, Vol. 6, pp. 189-202, 1978.

100. Meyers, M.H., "Computing the Distribution of a Random Variable Via Gaussian Quadrature Rules," The Bell System Technical Journal, Vol. 61, No. 9, pp. 2245-2261, 1982.

101. Minai, K., and Wakabayashi, M., "Seismic Resistance of Reinforced Concrete Beam-and-Column Assemblages with Emphasis on Shear Failure of Column," Proceedings of the Sixth World Conference on Earthquake Engineering, New Delhi, India, 1977, Vol. 3, pp. 3101-3106.

102. Mitani, I., Makino, M., and Matsui, C., "Influence of Local Buckling on Cyclic Behavior of Steel Beam-Columns," Proceedings of the Sixth World Conference on Earthquake Engineering, New Delhi, India, 1977, Vol. 3, pp. 3175-3180.

103. Nakazimo, T., "On the State Estimation for Non-Linear Dynamic Systems," International Journal of Control, Vol. 11, pp. 683-695, 1970.

104. Newmark, M.N., and Rosenblueth, Fundamentals of Earthquake Engineering, Prentice Hall, Inc., Englewood Cliffs, New Jersey, 1971.

105. Ohmori, N., "The 18-Storied Shiinamachi Building, Cast-in-Field Reinforced Concrete Systems," Proceedings of a Workshop on Earthquake-Resistant Reinforced Concrete Building Construction, University of California, Berkeley, California, July 11-15, 1977, Vol. 2, pp. 756-769.

106. Ozaki, M., and Ishiyama, Y., "An Evaluation Method for the Earthquake Rersistant Capacity of Reinforced Concrete and Steel Reinforced Concrete Columns," Proceedings of the Sixth World Conference on Earthquake Engineering, New Delhi, India, 1977, Vol. 3, pp. 3107-3112.

107. Ozdemir, H., "Nonlinear Transient Dynamic Analysis of Yielding Stauctures," Ph.D. Dissertaion, Division of Structural Engineering and Structural Mechanics, Department of Civil Engineering, University of California, Berkeley, California, 1976.

108. Park, R., and Paulay, T., Reinforced Concret Structures, John Wiley and Sons, Inc., New York, 1975.

109. Penzien, J., "Applications of Random Vibration Theory in Earthquake Engineering," Bulletin of the International Institute of Seismology, Vol. 2, pp. 47-69, 1965.

110. Penzien, and Liu, S.C., "Nondeterministic Analysis of Nonlinear Structures Subjected to Earthquake Excitations," Proceedings of the Fourth World Conference on Earthquake Engineering, Santiago, Chile, 1969, Vol. 1, A-1, pp. 114-129.

111. Piers, J.E., Wen, Y.K., and Ang, A. H-S., "Stochastic Analysis of Liquefaction under Earthquake Loading," Civil Engineering Studies, Structural Research Series No. 504, Department of Civil Engineering, University of Illinois, Urbana, Illinois, April 1983.

112. Popoff, A., Jr., "Soft Story Concept Applied at St. Joseph Health Care Center, Tacoma, Washington," Proceedings of a Workshop on Earthquake-Resistant Reinforced Concrete Building Construction, University of California, Berkeley, July 11-15, 1977, Vol. 2, pp. 742-755.

113. Priestley, M.B., "Evolutionary Spectra and Nonstationary Processes," Journal of the Royal Statistical Society, B, Vol. 27, pp. 204-237, 1965.

114. Rajagopalan, A., and Taylor, R.E., "Dynamics of Offshore Structures, Part 2: Stochastic Averaging Analysis," Journal of Sound and Vibration, Vol. 83, No. 3, pp. 417-431, 1982.

115. Razani, R., "Proposed Standard Method for Dynamic Testing of Reinforced Concrete Members and for Presentation of Test Results," Proceedings of the Sixth World Conference on Earthquake Engineering, New Delhi, India, 1977, Vol. 3, pp. 2919-2921.

116. Roberts, J.B., "Response of Nonlinear Mechanical Systems to Random Excitation, Part 1: Markov Methods," Shock and Vibration Digest, Vol. 13, No. 3, pp. 17-28, March 1981.

117. Roberts, J.B., "Response of Nonlinear Mechanical Systems to

Random Excitation, Part 2: Equivalent Linearization and Other Methods," Shock and Vibration Digest, Vol. 13, No. 4, pp. 15-29, April 1981.

118. Roberts, J.B., "The Response of an Oscillator with Bilinear Hysteresis to Stationary Random Excitation," Journal of Applied Mechanics, Transactions ASME, Vol. 45, pp. 923-928, December 1978.

119. Rosenblueth, E., and Bustamente, J.I., "Distribution of Structural Response to Earthquakes," Journal of the Engineering Mechanics Division, ASCE, Vol. 88,, No. EM3, Proceeding Paper 3177, June 1962.

120. Ruiz, P., and Penzien, J., "Probabilistic Study of the Behavior of Structures During Earthquakes," Report No. EERC-69/03, Earthquake Engineering Research Center, University of California, Berkeley, California, 1969.

121. Saatcioglu, M., Derecho, A.T., and Corley, W.G., "Modelling Hysteretic Behavior of Coupled Walls for Dynamic Analysis," Earthquake Engineering and Structural Dynamics, Vol. 11, pp. 711-726, 1983.

122. Shih, T-Y., and Lin, Y.K., "Vertical Seismic Load Effect on Hysteretic Columns," Journal of the Engineering Mechanics Division, ASCE, Vol. 108, No. EM2, pp. 242-254, April 1982.

123. Shinozuka, M., and Sato, Y., "Simulation of Nonstationary Random Processes," Jouranl of the Engineering Mechanics Division, ASCE, Vol. 93, No. EM1, pp. 11-40, February 1967.

124. Sozen, M.A., "Hysteresis in Structural Elements," Applied Mechanics in Earthquake Engineering, ASME Annual Meeting, Applied Mechanics Division, Vol. 8, pp. 63-98, 1974.

125. Spanos, P-T. D., "Stochastic Analysis of Oscillator with Non-Linear Damping," International Journal of Non-Linear Mecahnics, Vol. 13, pp. 249-259, 1978.

126. Spanos, P-T. D., "Hysteretic Structural Vibrations under Random Load," Journal of the Acoustical Society of America, Vol. 65, pp. 404-410, 1979.

127. Spanos, P-T. D., "Formulation of Stochastic Linearization for Symmetric or Asymetric MDOF Nonlinear Systems," Journal of Applied Mechanics, Transactions ASME, Vol. 47, No. 1, p. 209, March 1980.

128. Spanos, P-T. D., "Probabilistic Earthquake Energy Equations," Journal of the Engineering Mechanics Division, ASCE, Vol. 106, No. EM1, pp. 147-159, February 1980.

129. Spanos, P-T. D., "Stochastic Linearization in Structural Dynamics," Applied Mechanics Review, Vol. 34, No. 1, pp. 1-8, January 1981.

130. Spanos, P-T. D., "A Method for Analysis of Non-Linear Vibrations Caused by Modulated Random Excitation," International Journal of Non-Linear Mechanics, Vol. 16, No. 1, pp. 1-10, 1981.

131. Spanos, P-T.D., "Stochastic Linearization for Dynamic Systems with Asymetric Nonlinearities," Engineering Mechanics Research Laboratory Report No. 1126, University of Texas at Austin, Texas, September 1978.

132. Spanos, P-T. D. and Chen, T.W., "Random Response to Flow-Induced Forces," Jurnal of the Engineering Mechanics Division, ASCE, Vol. 107, No. EM6, pp. 1173-1190, December 1981.

133. Spanos, P-T. D., and Iwan, W.D., "On the Existence and Uniqueness of Solutions Generated by Equivalent Linearization," International Journal of Non-Linear Mechanics, Vol. 13, pp. 71-78, 1978.

134. Stanton, J.F., and McNiven, H.D., "Toawrds an Optimum Model for the Response of Reinforced Concrete Beams to Cyclic Loads," Earthquake Engineering and Structural Dynamics, Vol. 11, pp. 299-312, 1983.

135. Stroud, A.H., and Secrest, D., Gaussian Quadrature Formulas, Prentice Hall, Inc., Englewood Cliffs, New Jersey, 1966.

136. Sues, R.H., and Wen, Y.K., and Ang, A. H-S., "Stochastic Seismic Performance Evaluation of Buildings," Civil Engineering Studies Structural Research Series, No. 506, Department of Civil Engineering, University of Illinois, Urbana, Illinoois, May 1983.

137. Sues, R.H., Wen, Y-K., and Ang, A. H-S., "Safety Evaluation of Structures to Earthquakes," Proceedings of the Symposium on Probabilistic Methods in Structural Engineering, ASCE, St. Louis, Missouri, October 26-27, 1981, pp. 358-377.

138. Suzuki, T., and Ono, T., "An Experimental Study on Inelastic Behavior of Steel Members Subjected to Repeated Loading," Proceedings of the Sixth World Conference on Earthquake Engineering, New Delhi, India, 1977, Vol. 3, pp.

3163-3168.

139. Takeda, T., Sozen, M.A., and Nielsen, N.N., "Reinforced Concrete Response to Simulated Earthquake," Journal of Structural Division, ASCE, Vol. 96, No. ST12, pp. 2257-2573, December 1970.

140. Tansirikongkol, V., and Pecknold, D.A., "Approximate Modal Analysis of Bilinear MDF Systems," Journal of the Engineering Mechanics Division, ASCE, Vol. 106, No. EM2, pp. 361-375, April 1980.

141. To, C.W.S., "Non-Stationary Random Response of A Multi-Degree-of-Freedom System by the Theory of Evolutionary Spectra," Journal of Sound and Vibration, Vol. 83, No. 2, pp. 273-291, 1982.

142. Thompson, K.J., and Park, R., "Stress-Strain Model for Prestressing Steel with Cyclic Loading," Bulletin of the New Zealand National Society for Earthquake Engineering, Vol. 12, No. 4, pp. 209-218, November 1980.

143. Umebara, H., and Jirsa, J.O., "Short Rectangular RC Columns under Bidirectional Loadings," Journal of the Structural Division, ASCE, Vol. 110, No. 3, pp. 605-619, March 1984.

144. Umemura, H., Shimazu, T., Tadehara, S., Konishi, T., and Abe, Y., "Experimental Study on Reinforced Concrete Columns with Double Spiral Web Reinforcements," Proceedings of the Sixth World Conference on Earthquake Engineering, New Delhi, India, 1977, Vol. 3, pp. 3113-3119.

145. Vanmarcke, E.H., "Structural Response to Earthquake Seismic Risk and Engineering Decision," C. Lomnitz, and Rosenblueth, eds., Elsevier Publishing Co., Amsterdam, Netherlands, 1976.

146. Vanmarcke, E.H., "Some Recent Developments in Random Vibration," Applied Mechanics Review, Vol. 32, pp. 1197-1202, 1979.

147. Vanmarcke, E.H., and Veneziano, D., "Probabilistic Seismis Response of Simple Systems," Proceeding of the Fifth World Conference on Earthquake Engineering, Rome, Italy, 1973, Vol. 2, pp. 2851-2863.

148. Viwathanatepa, S., Popov, E.P., and Beretero, V.V., "Effects of Generalized Loadings on Bond of Reinforcing Bars Embedded in Confined Concrete Blocks," Earthquake Engineering Research Center, Report No. EERC-79/22, University of California, Berkeley, california, August 1979.

149. Ward, H.S., "Analog Simulation of Earthquake Motions," Journal of the Engineering Mechanics Division, ASCE, Vol. 91, No. EM5, pp. 173-190, October 1965.

150. Wen, Y.K., "Method for Random Vibration of Hysteretic Systems," Journal of the Engineering Mechanics Division, ASCE, Vol. 102, No. EM2, pp. 249-263, April 1976.

151. Wen, Y.K., "Approximate Method for Nonlinear Random Vibration," Journal of the Engineering Mechanics Division, ASCE, Vol. 101, No. EM4, pp. 389-401, August 1975.

152. Wen, Y.K., "Equivalent Linearization for Hysteretic Systems under Random Excitation," Journal of Applied Mechanics, Transactions ASME, Vol. 47, March 1980.

153. Yamada, M., and Kawamura, H., "Response Capacity Method for Earthquake Response Analysis of Hysteretic Structures," Earthquake Engineering and Structural Dynamics, Vol. 8, pp. 299-313, 1980.

154. Yamada, M., Kawamura, H., Katagihara, K., and Moritaka, H., "Cyclic Deformation Behavior of Reinforced Concrete Shear Walls," Proceedings of the Sixth World Conference on Earthquake Engineering, New Delhi, India, 1977, Vol. 3, pp. 3075-3080.

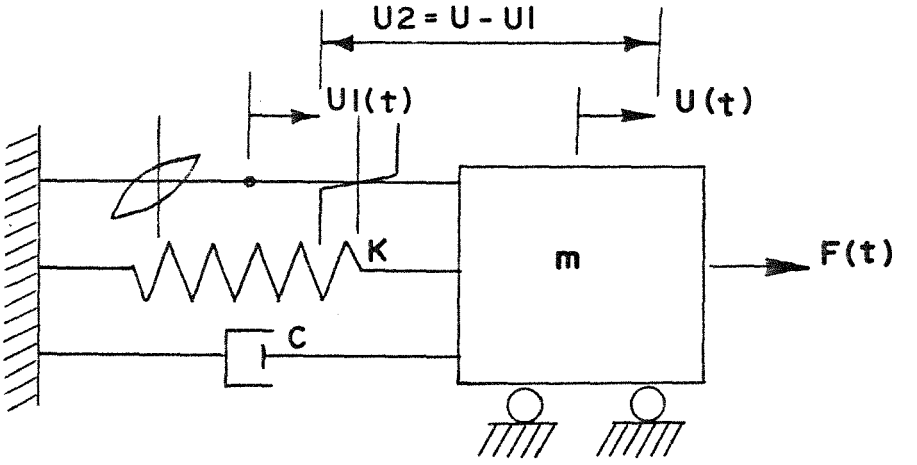

FIG. 2.1 - SDOF SYSTEM MODEL FOR B-N AND N-B ELEMENT.

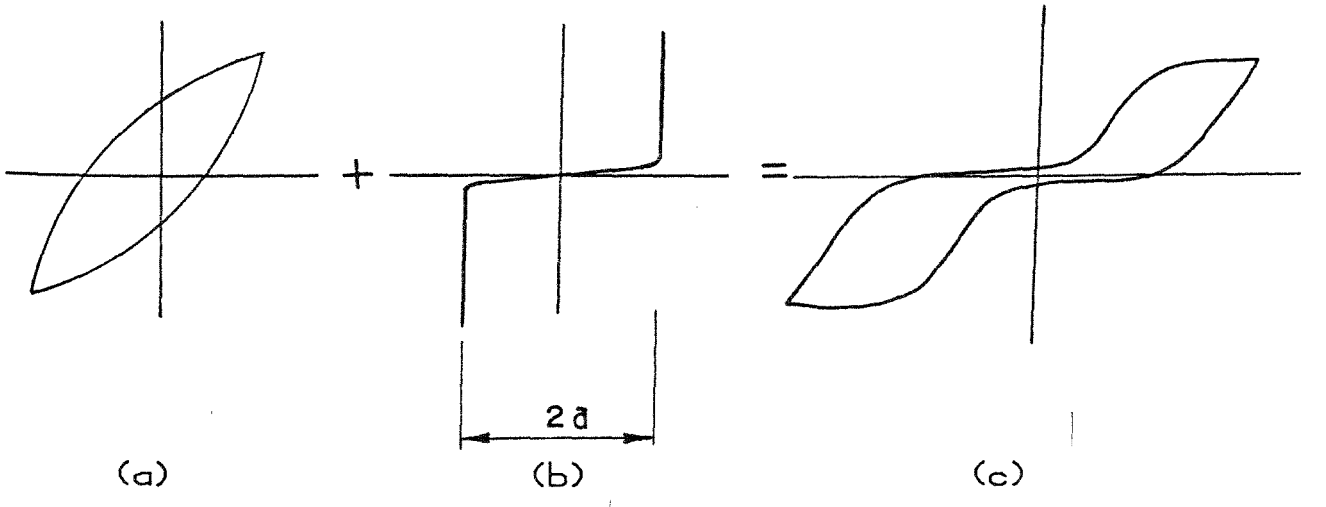

FIG. 2.2 - SLIP-LOCK SERIES HYSTERESIS.

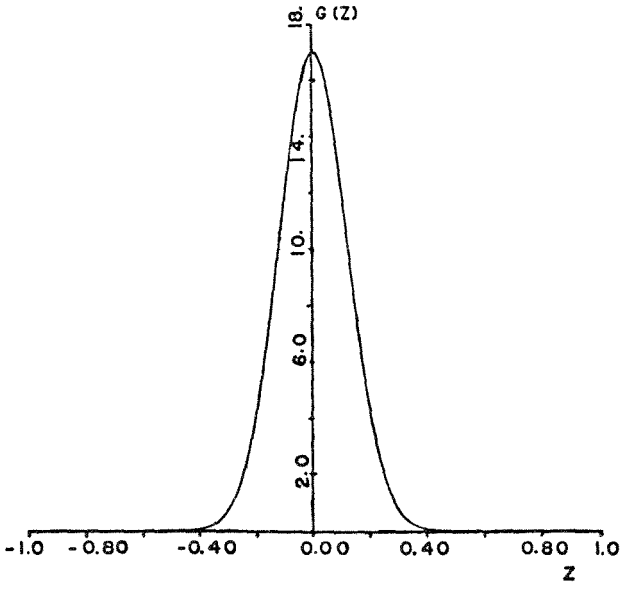

FIG. 2.3 - THE SLIP-LOCK FUNCTION IN B-N MODEL.

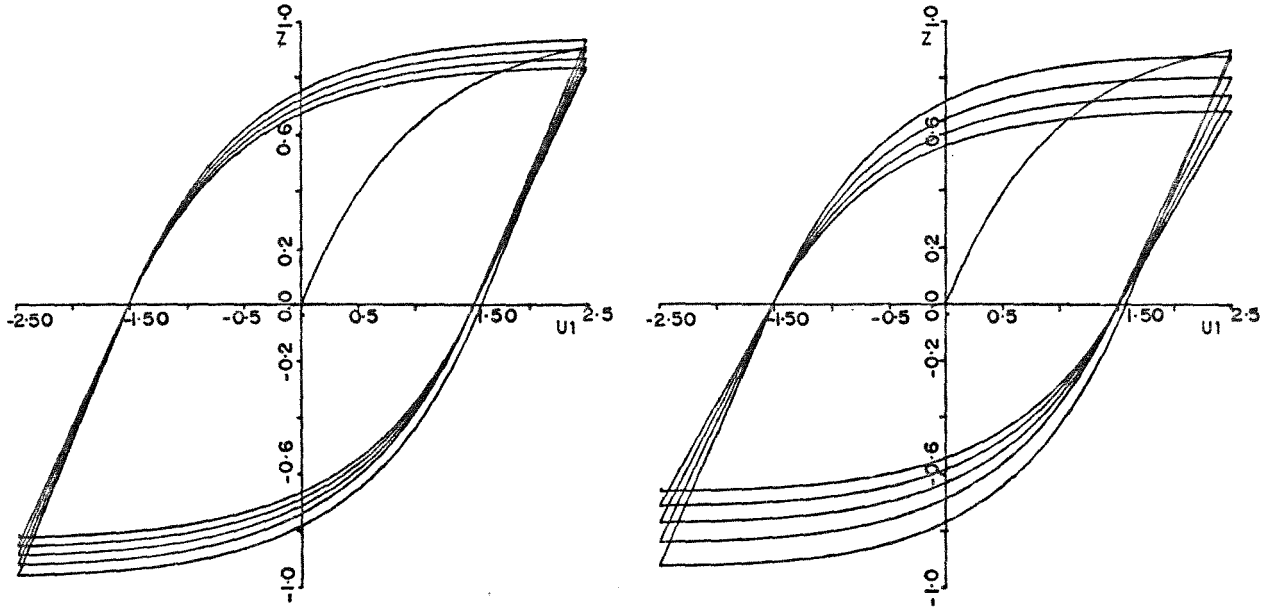

(a) LOW DEGRADATION RATE.
$\delta_A = \delta\eta = \delta\nu =$ 0.004.

(b) HIGH DEGRADATION RATE.
$\delta_A = \delta\eta = \delta\nu =$ 0.01.

FIG. 2.4 - SMOOTH HYSTERESIS UNDER COMBINED STRENGTH AND STIFFNESS DEGRADATION. PSD = 2.5.

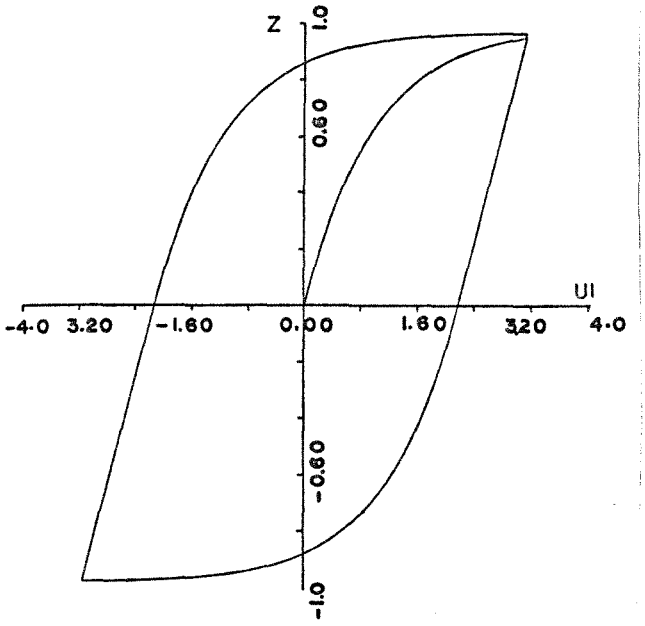

(a) SMOOTH HYSTERESIS ELEMENT

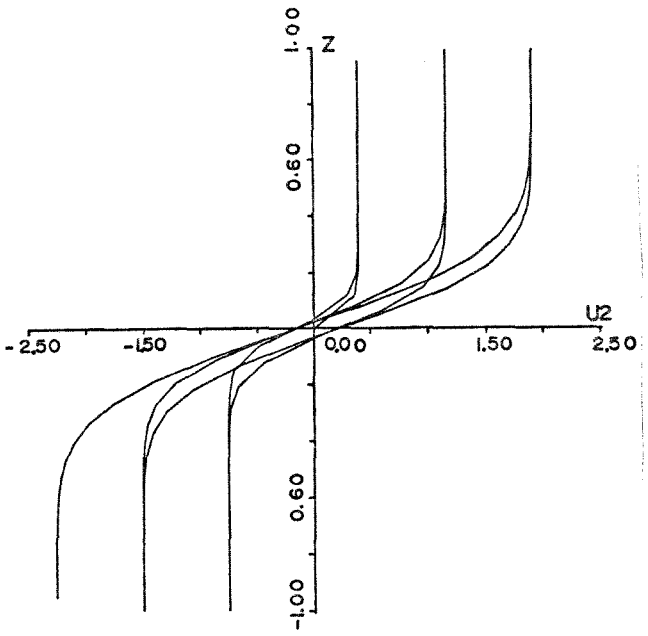

(b) SLIP-LOCK ELEMNT (B-N)

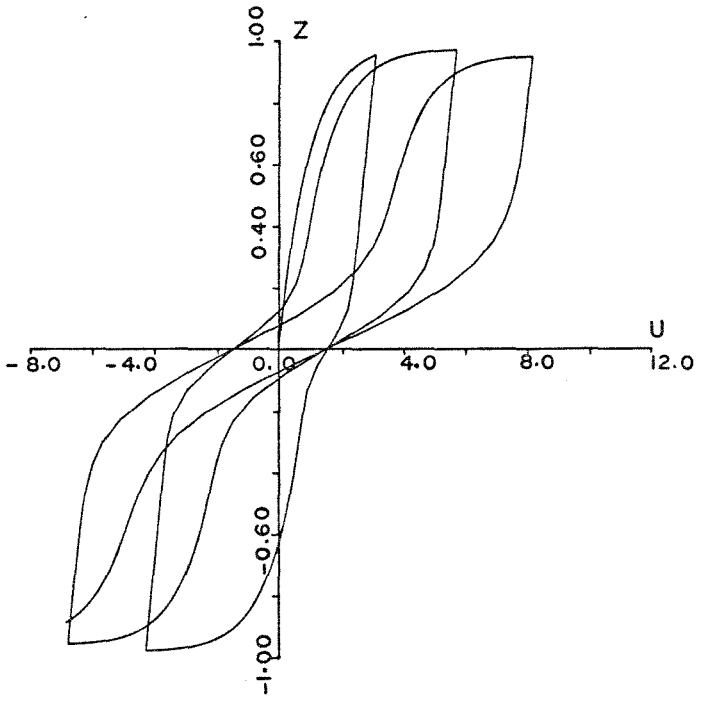

(c) LOOP-PINCHING BEHAVIOR UNDER CYCLIC DISPLACEMENT.

FIG. 2.5 - BEHAVIOR OF B-N MODEL AND ITS CONSTITUENT ELEMENTS UNDER CYCLIC INPUT DISPLACEMENT.

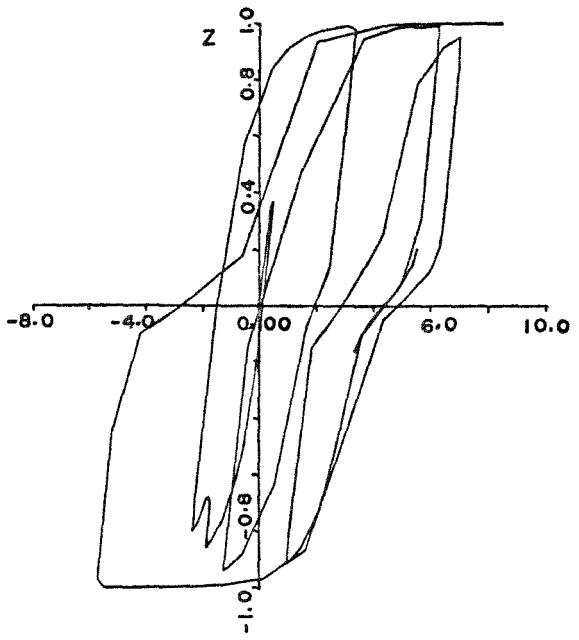

(a) σ = 0.1 AND δa = 0.1.

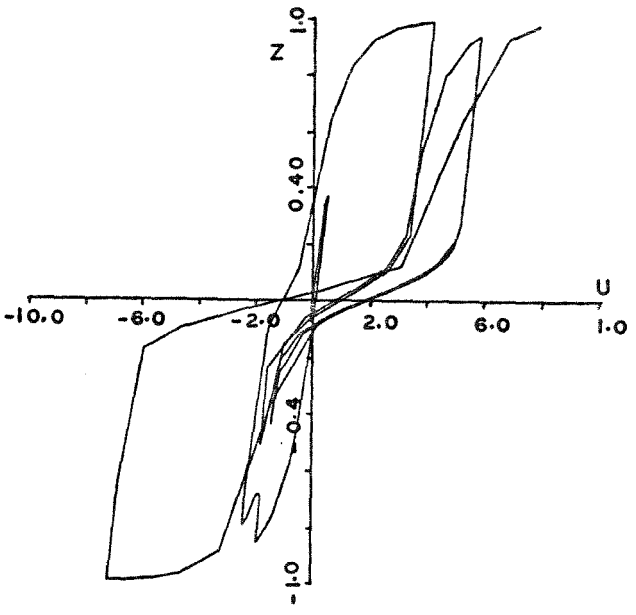

(b) σ = 0.1 AND δa = 0.5.

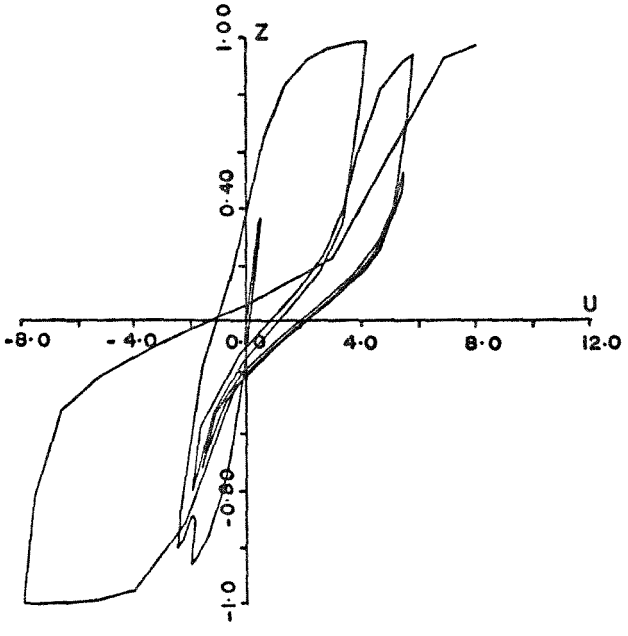

(c) σ = 0.2 AND δa = 0.5.

FIG. 2.6 - PINCHING BEHAVIOR OF B-N MODEL UNDER WHITE NOISE INPUT EXCITATION, PSD = Ø.2 AND ζ = Ø.1.

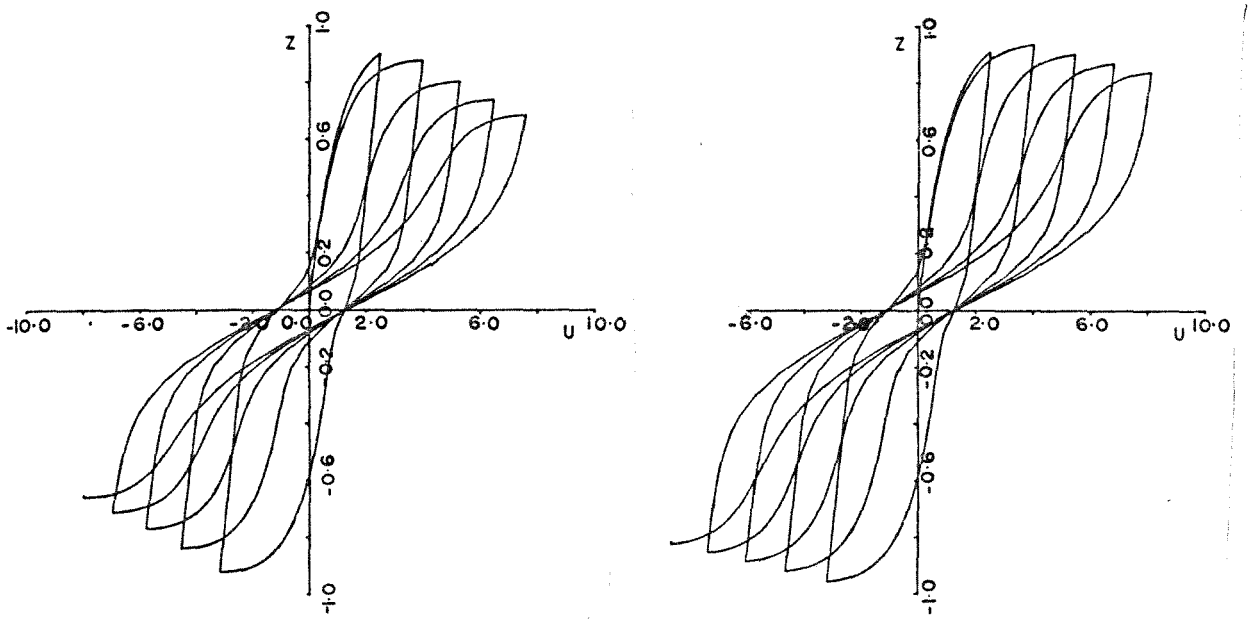

(a) LOW DEGRADATION RATE.

(b) HIGH DEGRADATION RATE.

FIG. 2.7 – PINCHING BEHAVIOR OF B-N SERIES MODEL UNDER COMBINED STRENGTH AND STIFFNESS DEGRADATION. δ_a = Ø.3, σ = .Ø7, AND δ_σ = Ø.ØØ9.

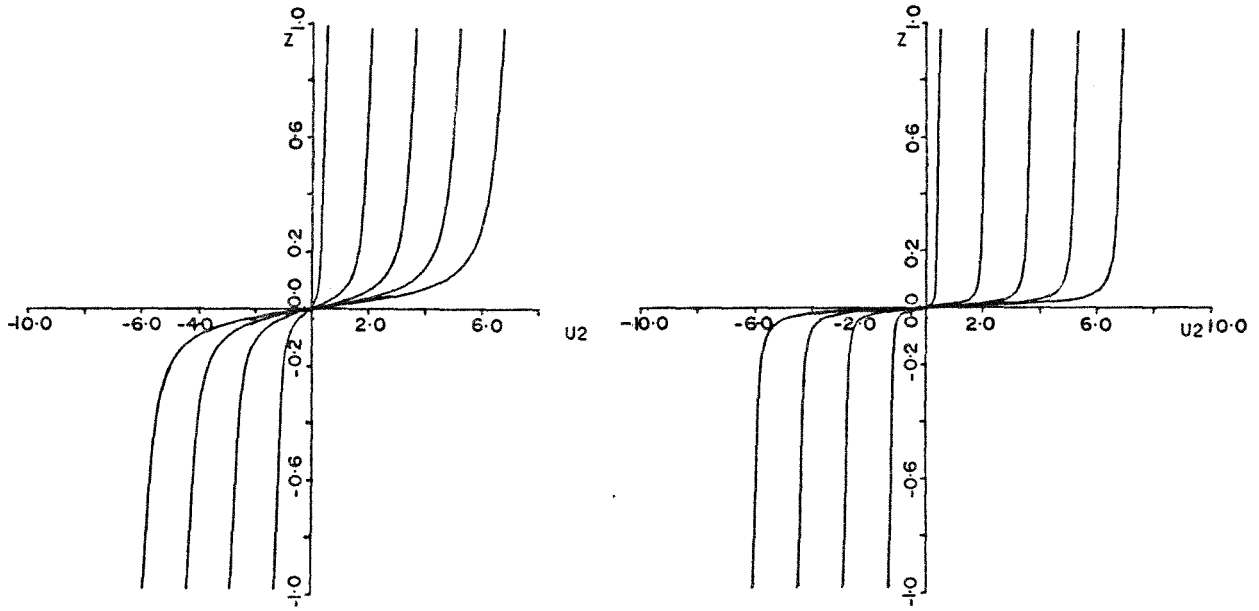

(a) λ_o = 0.0, ξ_o = .05

(b) λ_o = 0.0, ξ_o = .01.

FIG. 2.8 – SLIP-LOCK ELEMENT FOR N-B MODEL. δ_ξ = Ø.Ø, δ_λ = Ø.2.

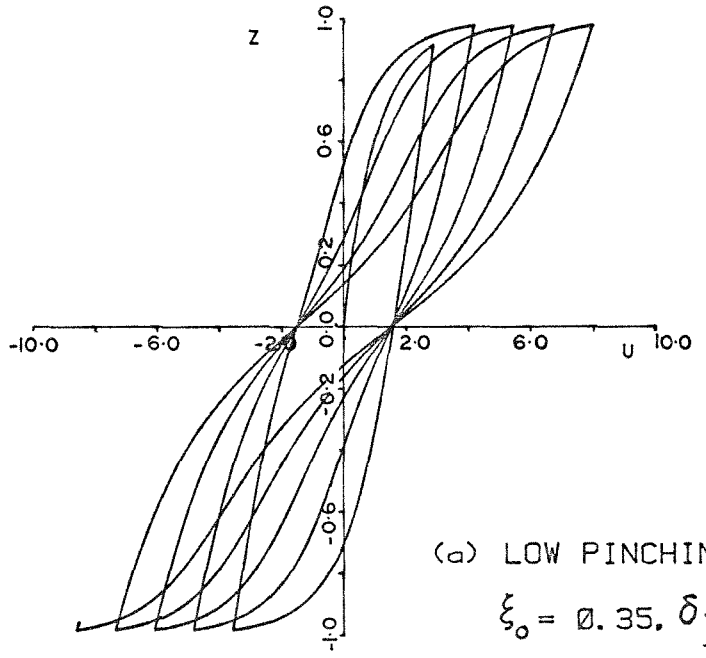

(a) LOW PINCHING RATE, $\lambda_o = 0.0$, $\xi_o = 0.35$, $\delta_\lambda = 0.2$, $\delta_\xi = 0.0$.

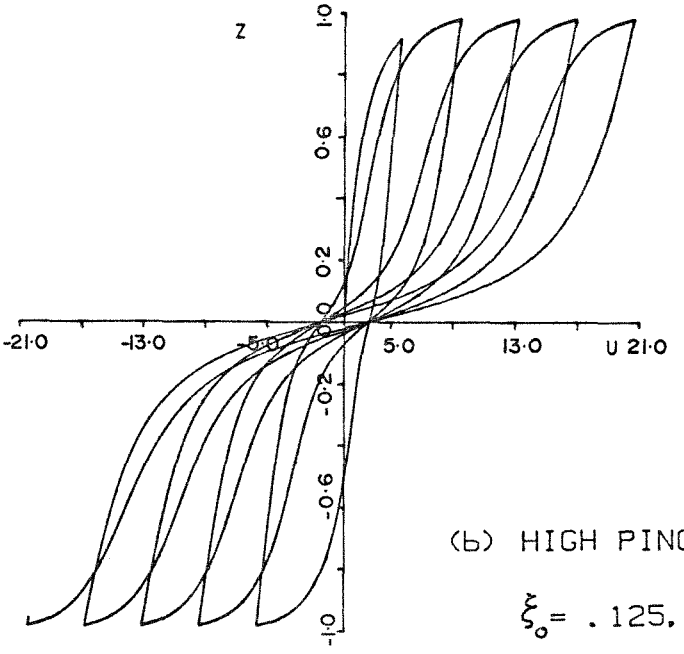

(b) HIGH PINCHING RATE, $\lambda_o = 0.0$, $\xi_o = .125$, $\delta_\lambda = 0.5$, $\delta_\xi = 0.0$.

FIG. 2.9 - LOOP-PINCHING BEHAVIOR OF N-B MODEL UNDER CYCLIC DISPLACEMENT.

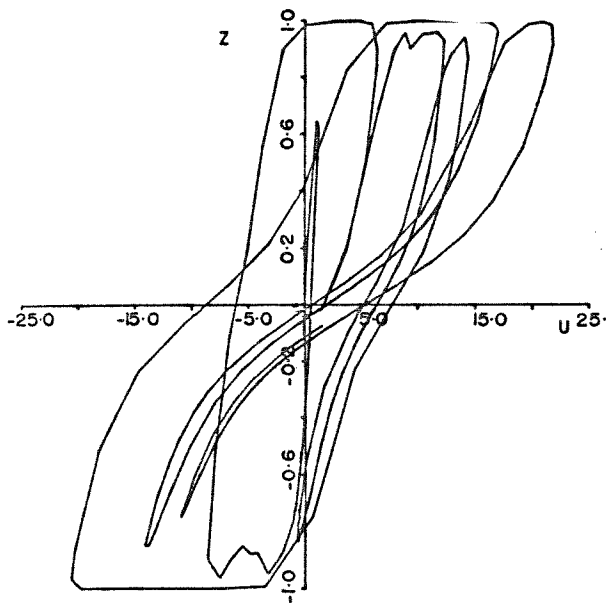

(a) $\xi_o = 0.3$. AND $\delta_\lambda = 0.2$.

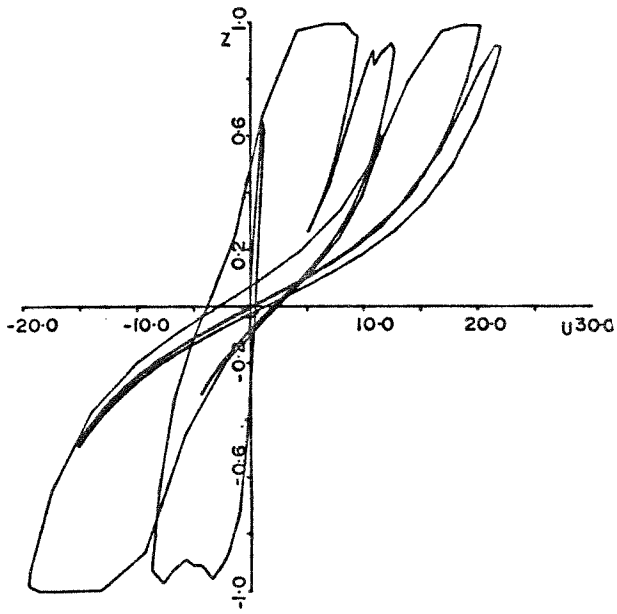

(b) $\xi_o = 0.3$. AND $\delta_\lambda = 0.5$.

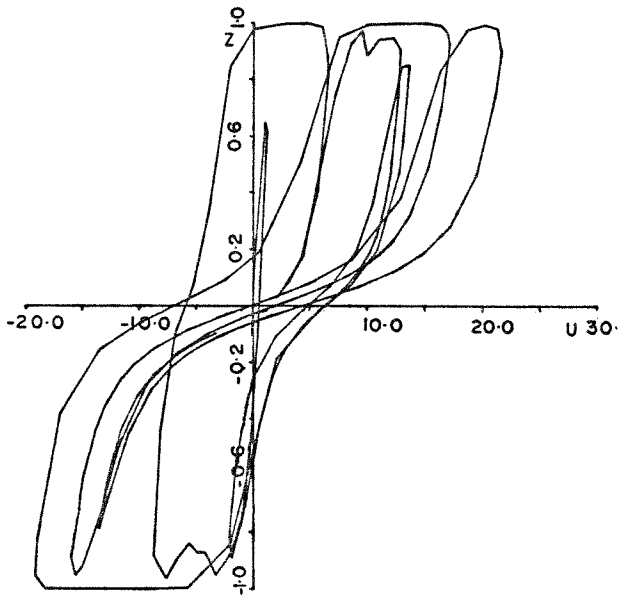

(c) $\xi_o = .15$. AND $\delta_\lambda = 0.2$.

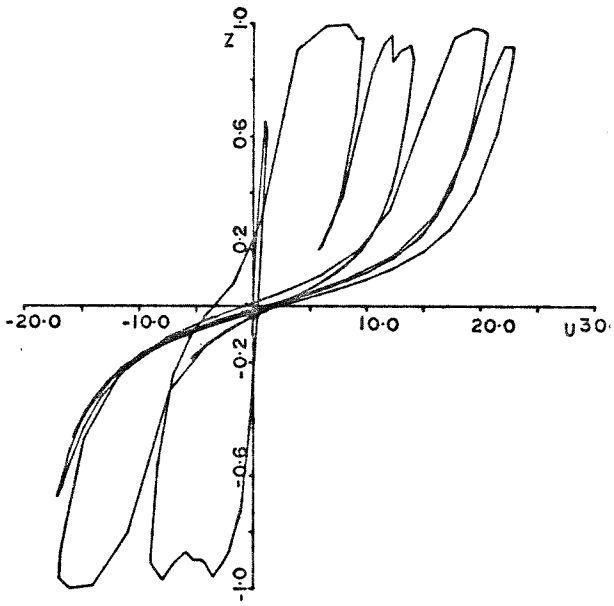

(d) $\xi_o = .15$. AND $\delta_\lambda = 0.5$.

FIG. 2.10 - PINCHING BEHAVIOR OF N-B MODEL UNDER WHITE NOISE EXCITATION. PSD = 0.2. $\zeta = 0.1$. $\lambda_o = 0.0$. AND $\delta_\xi = 0.0$.

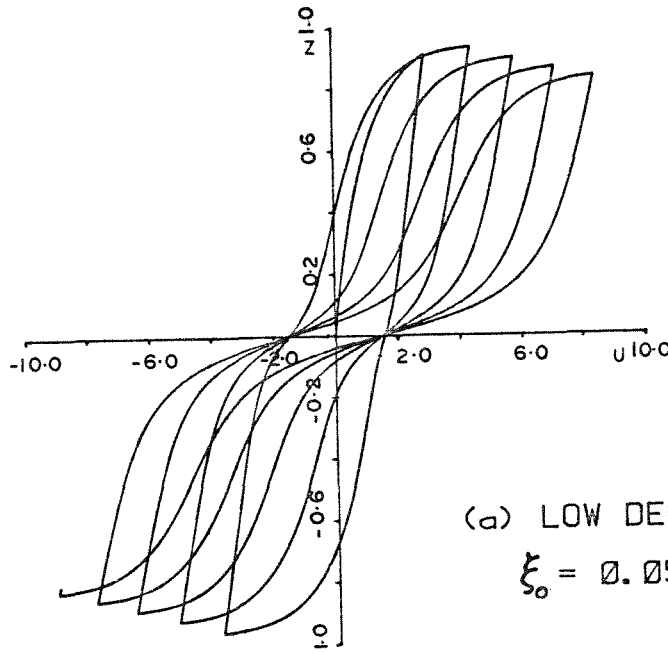

(a) LOW DEGRADATION RATE.
ξ_o = Ø.Ø5. AND δ_λ = Ø.2.

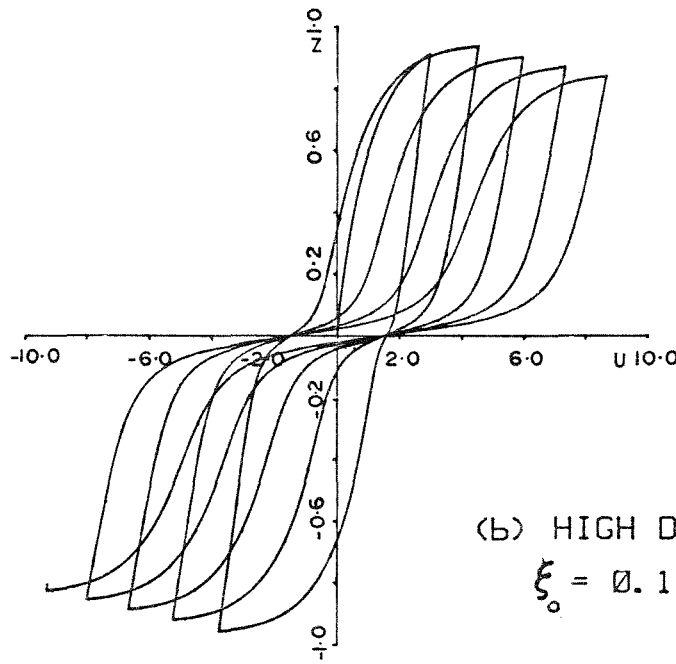

(b) HIGH DEGRADATION RATE.
ξ_o = Ø.1Ø. AND δ_λ = Ø.2.

FIG. 2.11 - PINCHING BEHAVIOR OF N-B MODEL UNDER COMBINED STRENGTH AND STIFFNESS DEGRADATION. δ_ξ = Ø.Ø. AND λ_o = Ø.Ø.

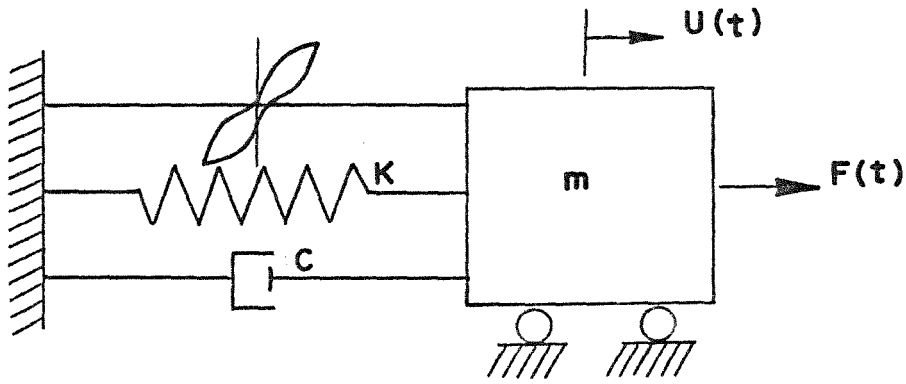

FIG. 2.12 - SDOF SYSTEM FOR SINGLE-ELEMENT-PINCHING MODEL.

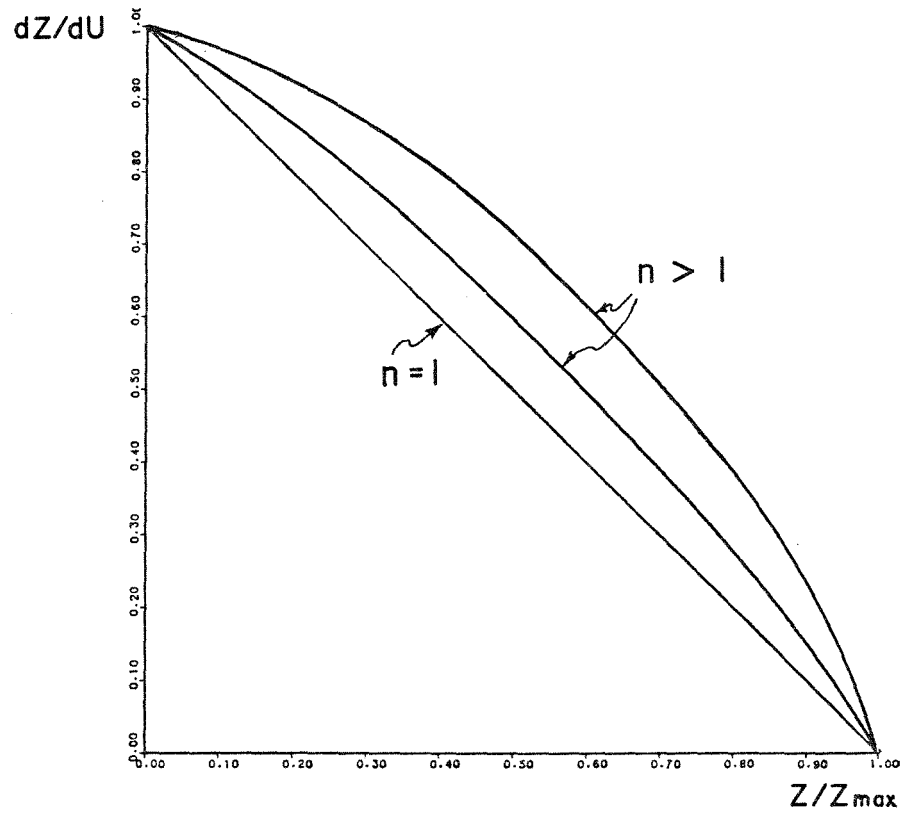

FIG. 2.13 - BEHAVIOR OF dZ/dU VS Z FOR SMOOTH HYSTERESIS (B-B-W).

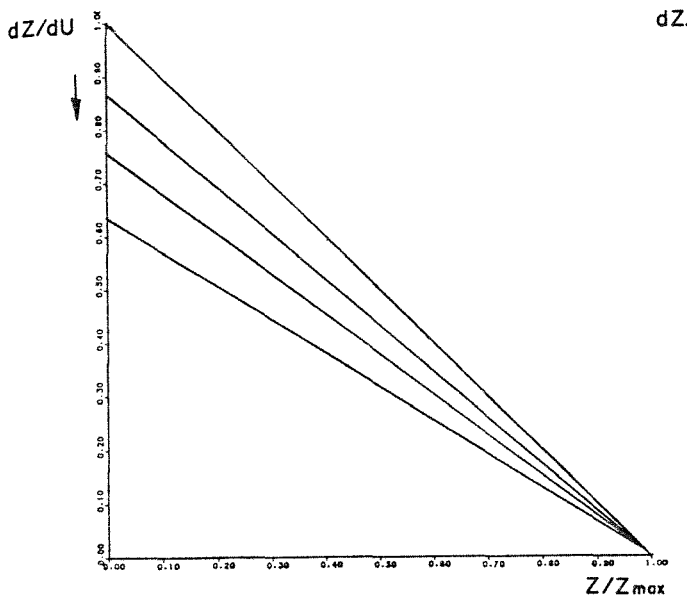

(a) ONLY η IS DEGRADING.

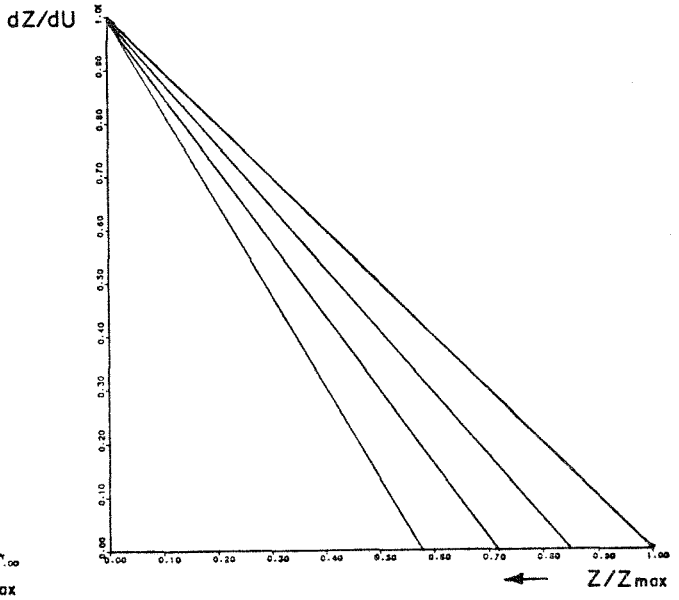

(b) ONLY ν IS DEGRADING.

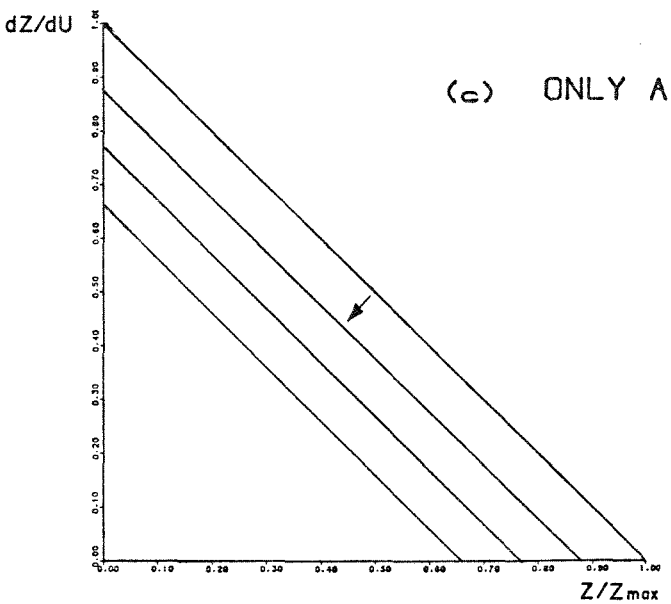

(c) ONLY A IS DEGARDING.

FIG. 2.14 - THE EFFECT OF VARIATION OF DEGRADATION PARAMETERS A, ν, AND η ON THE BEHAVIOR OF dZ/dU VS Z PLOT FOR SMOOTH HYSTERESIS OF B-B-W.

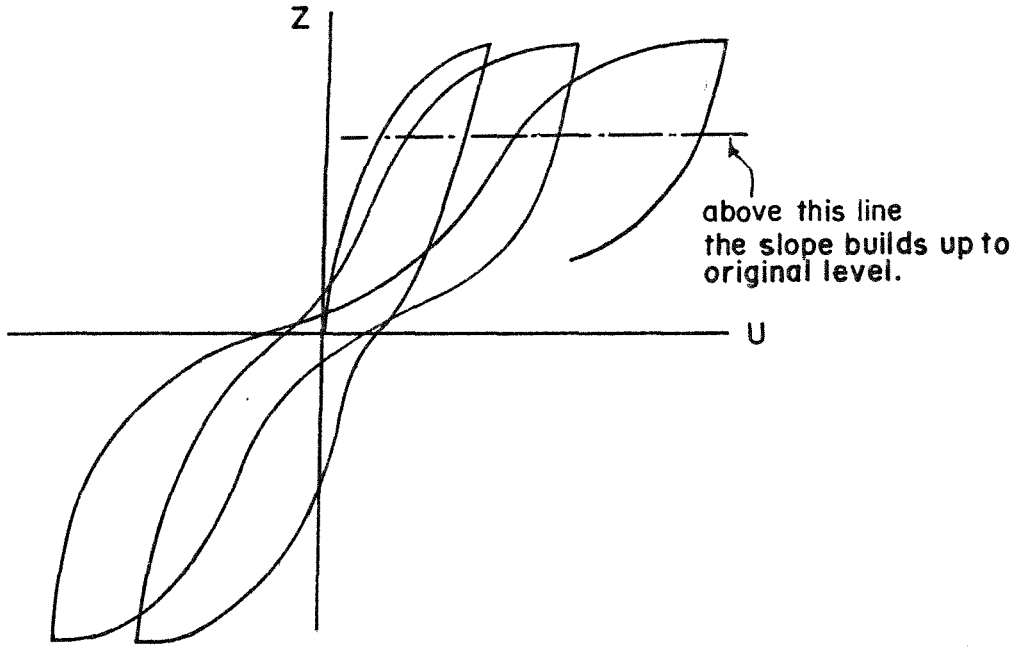

(a) Cycles of Loop-Pinching Hysteresis

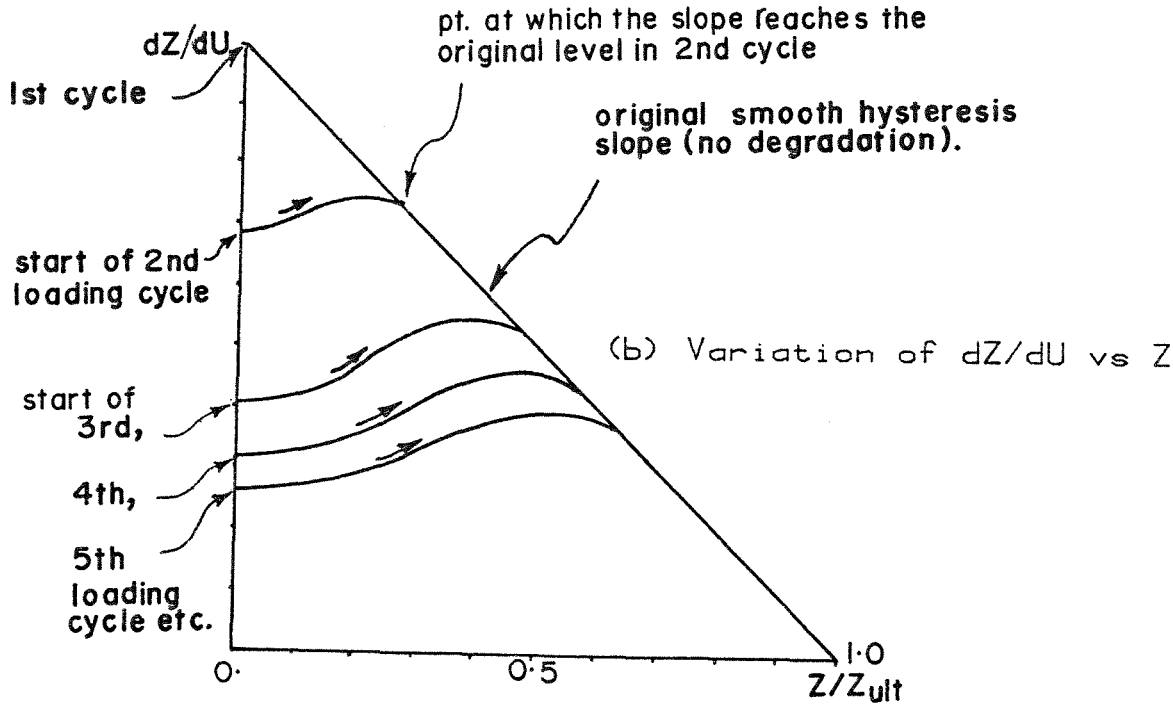

(b) Variation of dZ/dU vs Z

Figure 2.15 - Hysteretic Loop-Pinching Behavior and the Corresponding Effect on the Variation of dZ/dU vs Z.

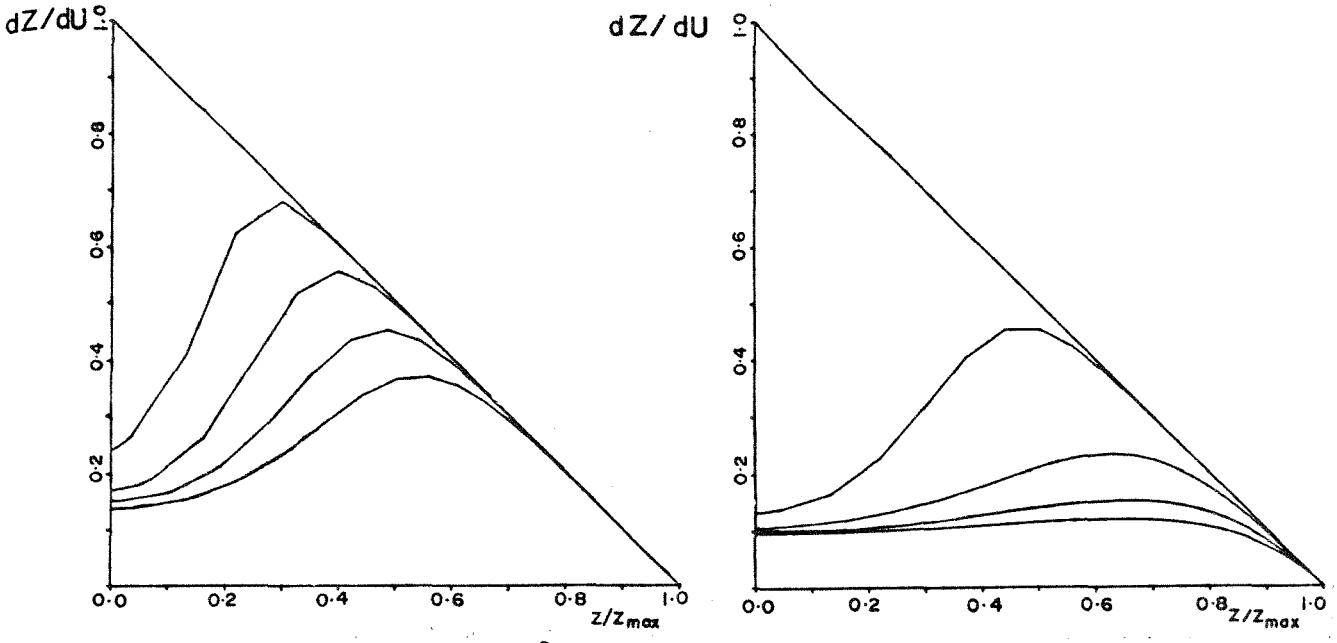

(a) Low Pinching Rate, σ = Ø.Ø7, δ_d = Ø.1, and δ_σ = Ø.ØØ9

(b) High Pinching Rate, σ = Ø.Ø7, δ_d = Ø.4, and δ_σ = Ø.Ø3

Figure 2.16 - Variation of dZ/dU vs Z for BN Slip-Lock Model Subjected to Cyclic Displacement.

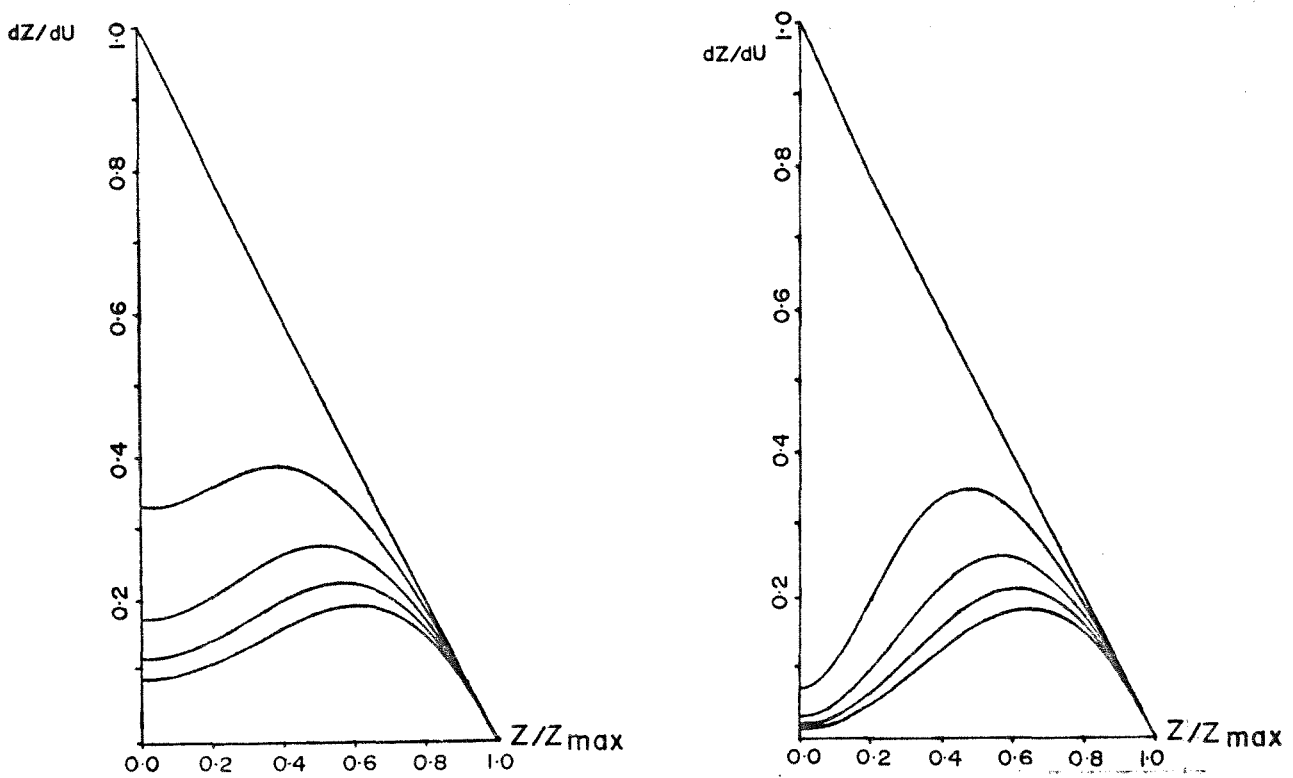

(a) Low Pinching Rate, λ_o = Ø., δ_λ = Ø.1, ξ_o = Ø.1, and δ_ξ = Ø.

(b) High Pinching Rate, λ_o = Ø., δ_λ = Ø.4, ξ_o = Ø.Ø2, and δ_ξ = Ø.

Figure 2.17 - Variation of dZ/dU vs Z for NB Slip-Lock Model Subjected to Cyclic Displacement.

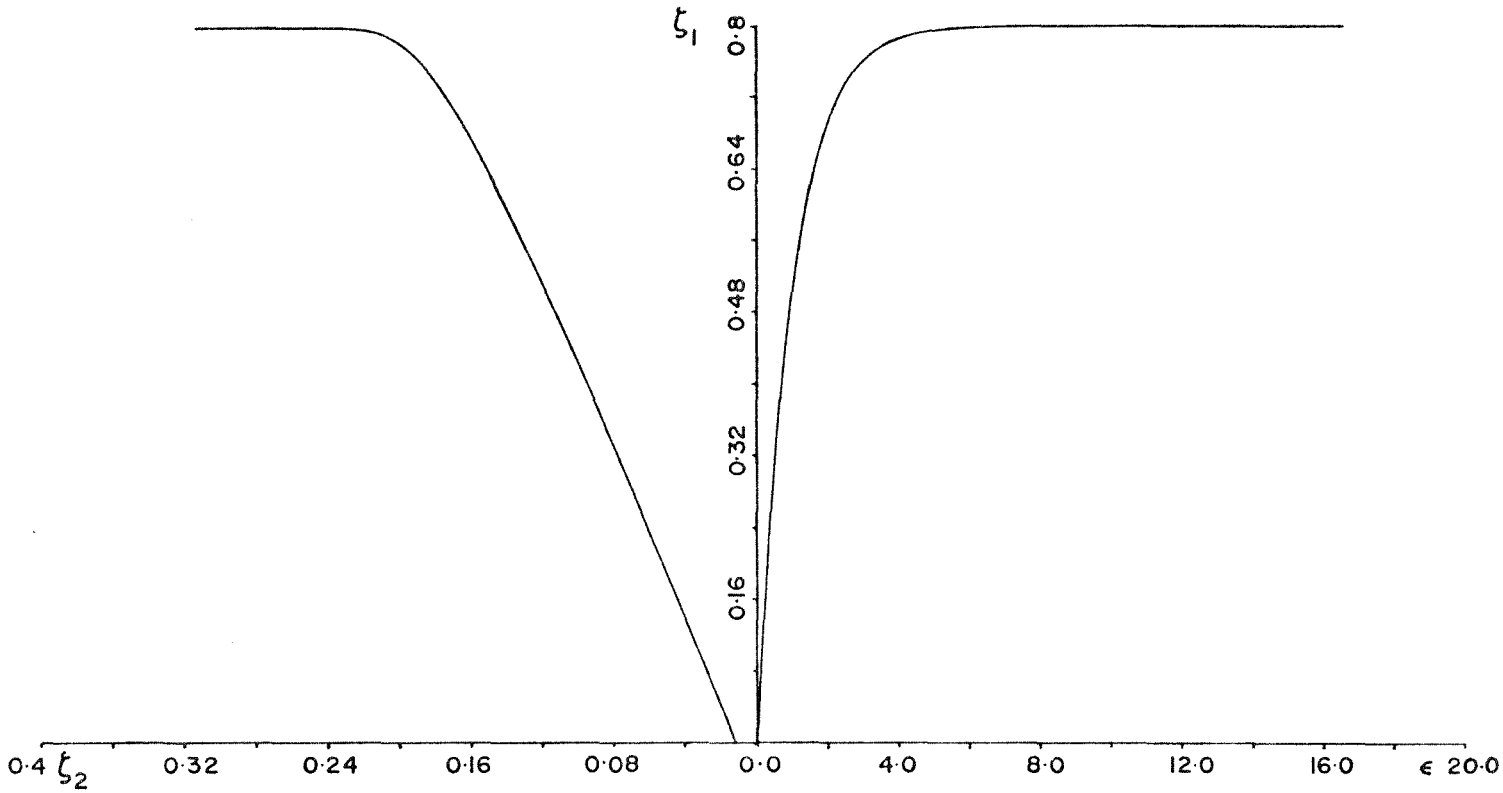

FIG. 2.18 - Variation of Parameters ζ_1 and ζ_2 as Given by Equations [2.21]-[2.23].

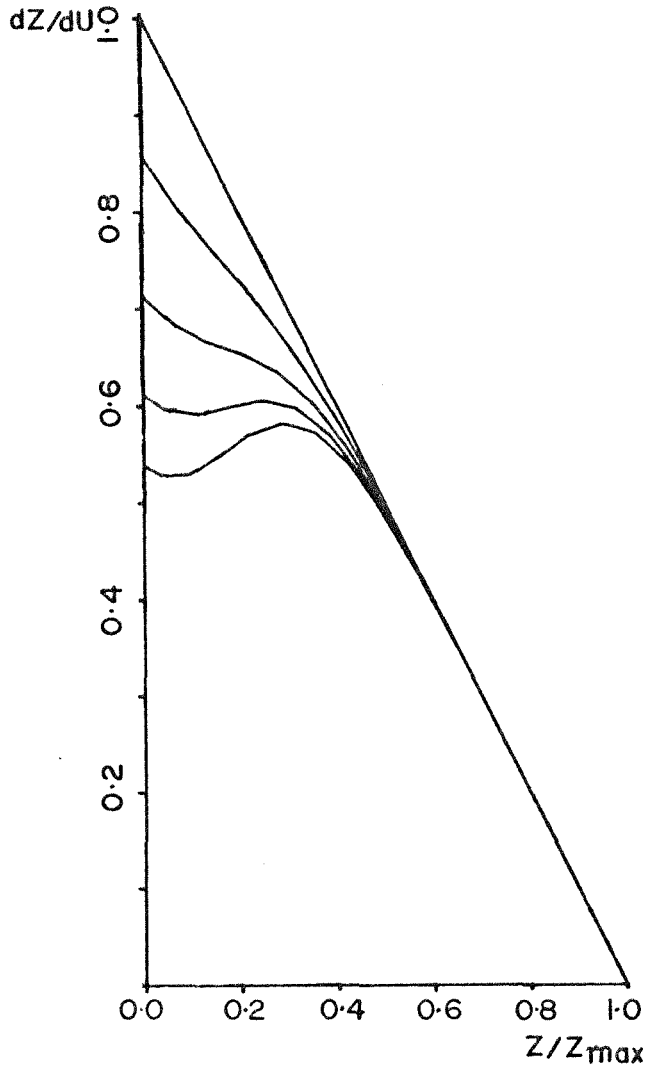

FIG. 2.19 - The Effect of Variation of ζ_1 on dz/du vs z When ζ_2 is Kept Constant.

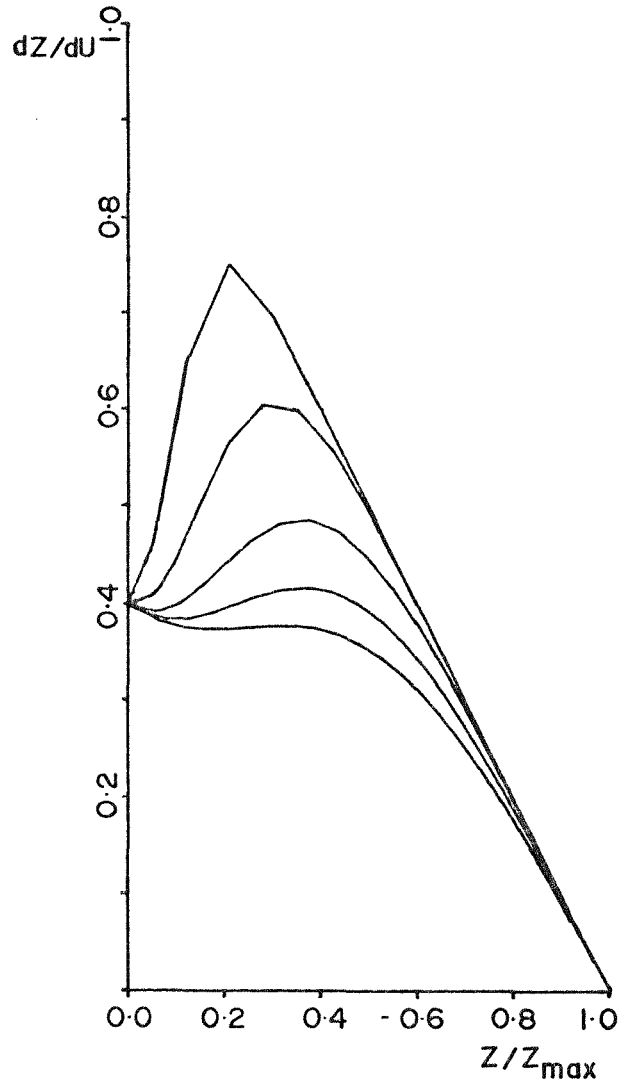

FIG. 2.20 - The Effect of Variation of ζ_2 on dz/du vs z When ζ_1 is Kept Constant.

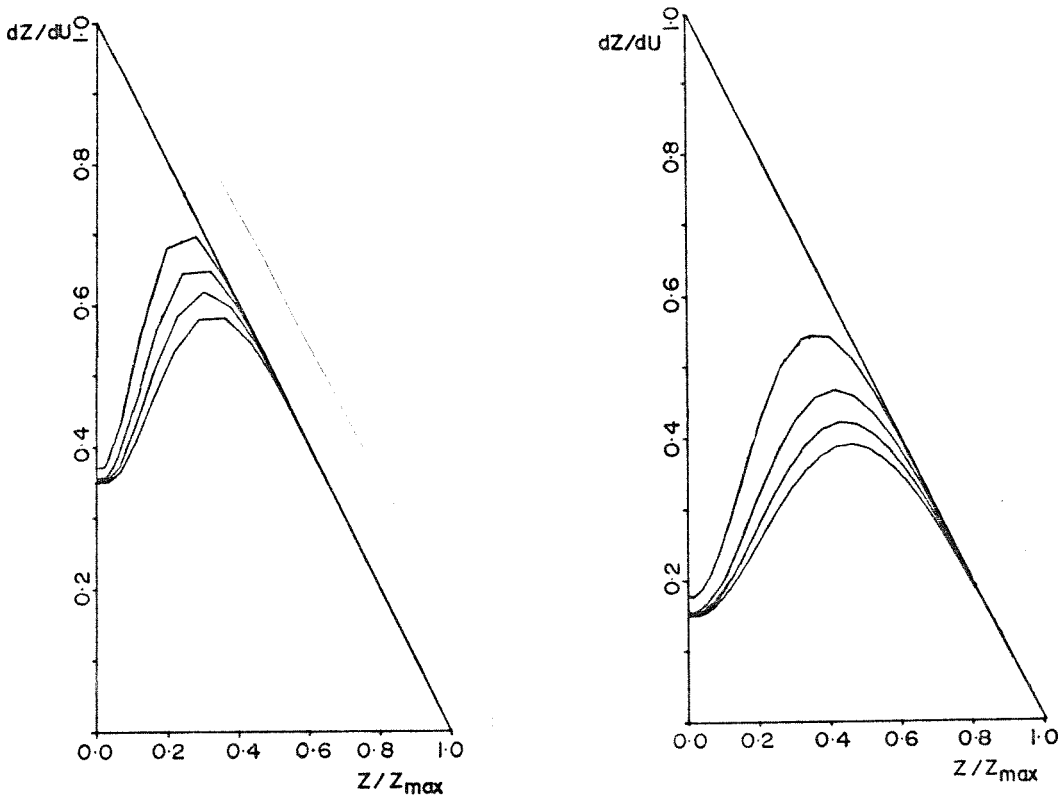

(a) Low Pinching Rate (b) High Pinching Rate

Figure 2.21 - dZ/dU vs Z Behavior for SEP Model Subjected to a Cyclic Displacement.

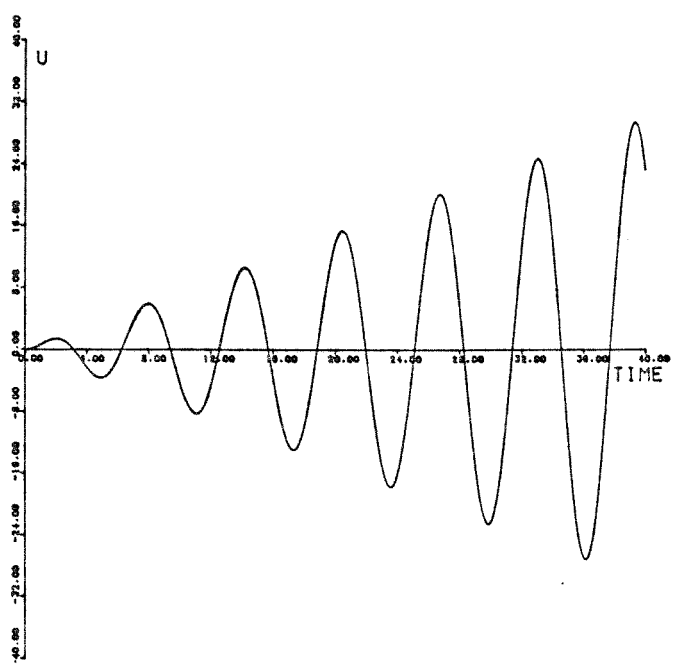

FIG·2·22 - INPUT CYCLIC DISPLACEMENT USED TO TEST SEP MODEL.

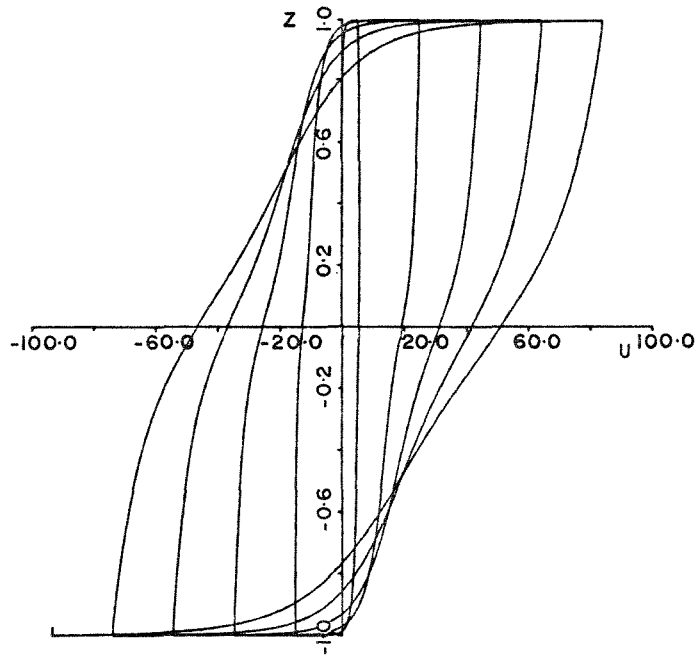

(a) Low Pinching Rate, $\zeta_{10} = 0.8$, $\lambda = 0.05$, $\xi_0 = 0.2$, and $\delta_\xi = 0.01$.

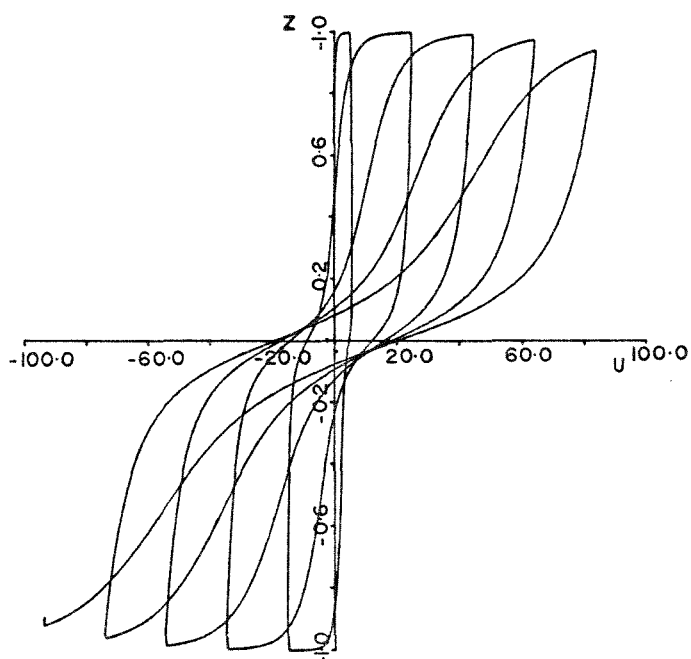

(b) High Pinching Rate, $\zeta_{10} = 0.95$, $\lambda = 0.3$, $\xi_0 = 0.2$, and $\delta_\xi = 0.01$.

Figure 2.23 - Loop-Pinching Behavior of SEP Model under the Cyclic Displacement Shown in Figure 2.22, ζ = 1%.

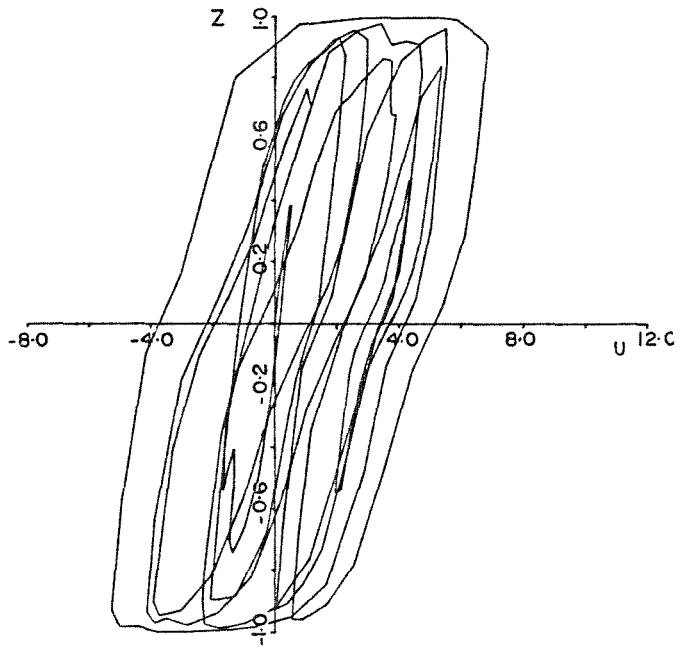

(a) Low Pinching Rate, $\zeta_{l_0} = 0.8$, and $\lambda = 0.05$.

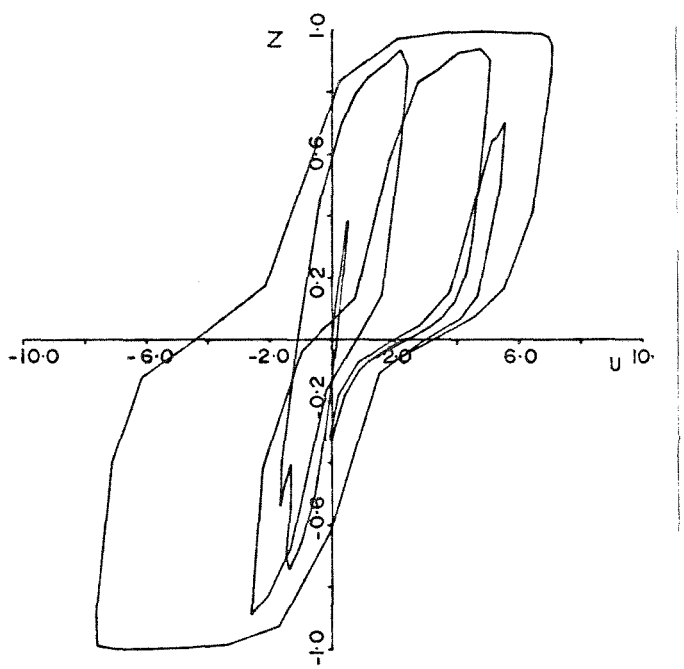

(b) High Pinching Rate, $\zeta_{l_0} = 0.95$, and $\lambda = 0.3$.

Figure 2.24 - Loop-Pinching Behavior of SEP Model under White Noise Input, PSD = 0.1, $\xi_0 = 0.2$, and $\delta\xi = 0.01$.

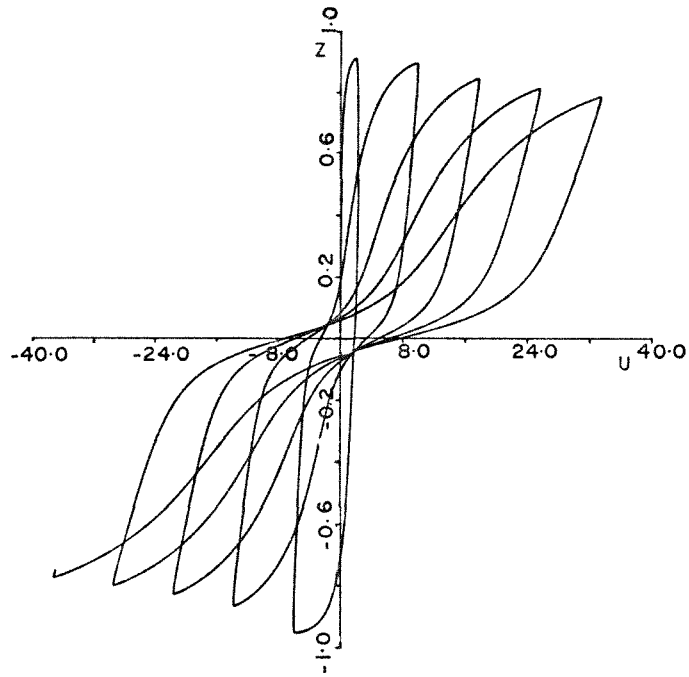

(a) Low Strength/Stiffness Degradation Rates.

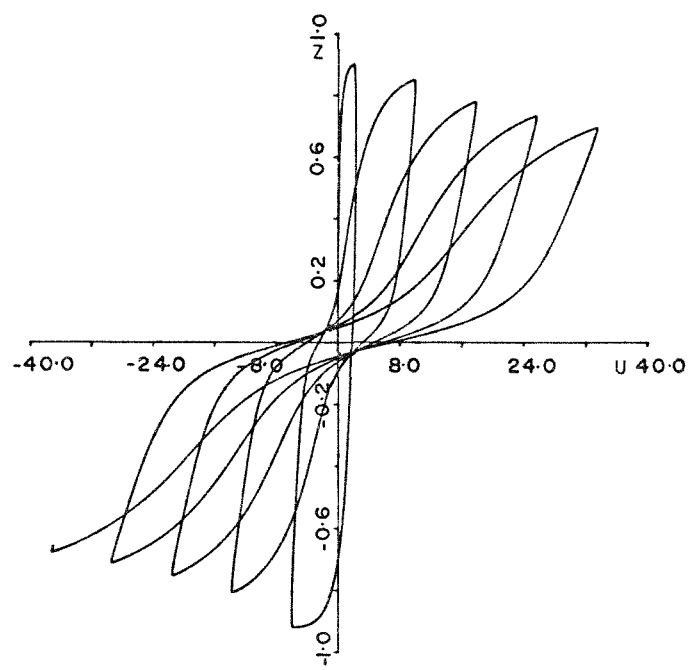

(b) High Strength/Stiffness Degradation Rates.

Figure 2.25 - Loop-Pinching Behavior of SEP Model under Cyclic Displacement and with Combined Stiffness and Strength Degradation, $\zeta_{1_0} = 0.9$, $\xi_0 = 0.2$, $\lambda = 0.06$, and $\delta_\xi = 0.01$.

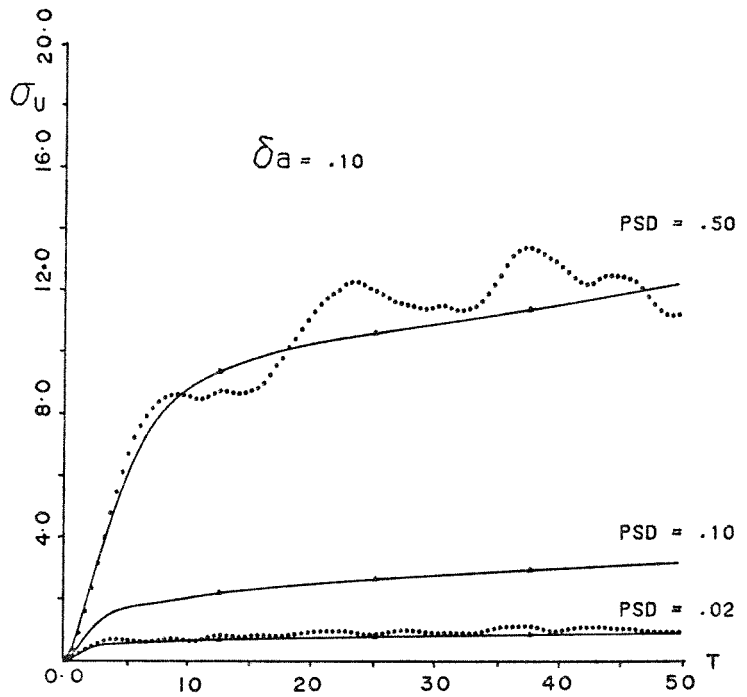

FIG. 3-1 - NONSTATIONARY RMS DISPLACEMENT RESPONSE OF SDOF SYSTEM UNDER STATIONARY WHITE NOISE INPUT. (LOW PINCHING RATE). (BN MODEL)

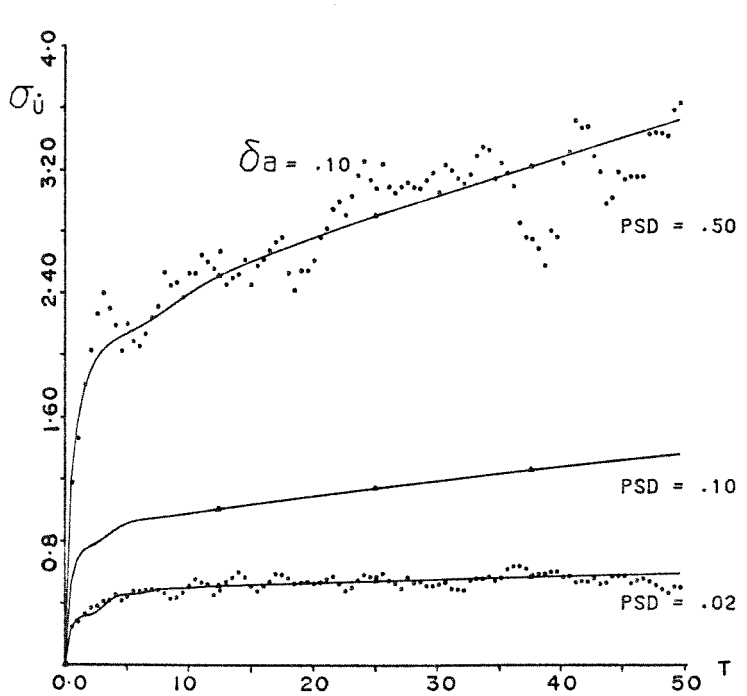

FIG. 3-2 - NONSTATIONARY RMS VELOCITY RESPONSE OF SDOF SYSTEM UNDER STATIONARY WHITE NOISE INPUT. (LOW PINCHING RATE). (BN MODEL)

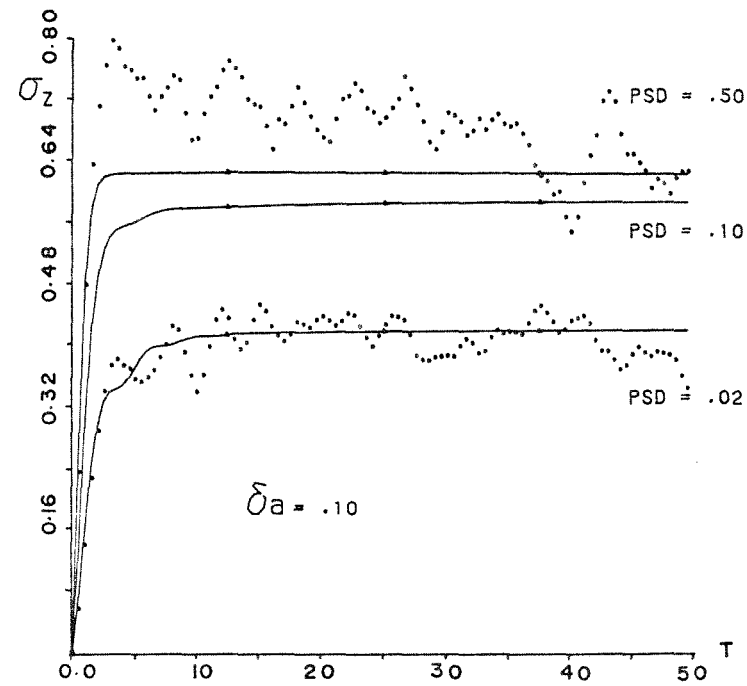

FIG.3.3- RMS PREDICTION OF RESTORING FORCE UNDER STATIONARY WHITE NOISE, (LOW PINCHING RATE). (BN MODEL)

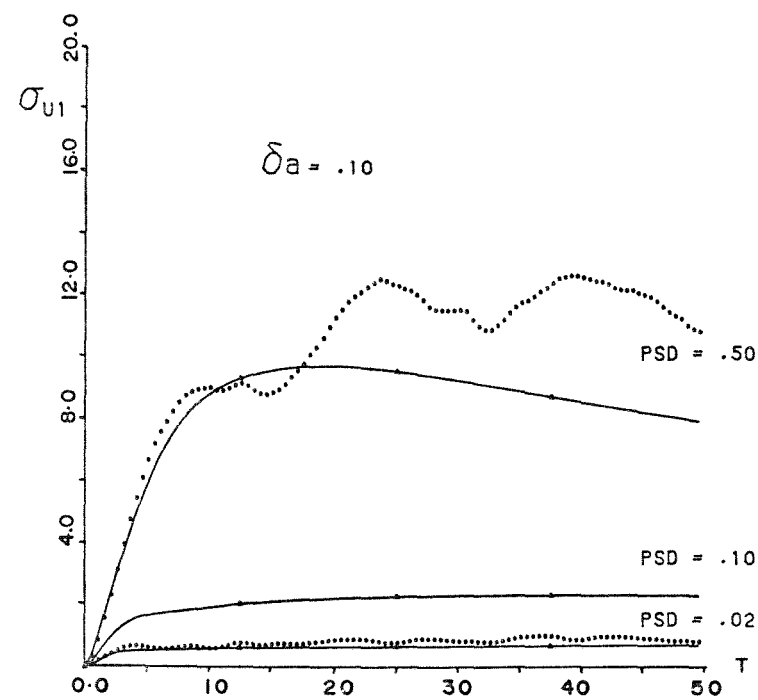

FIG.3.4 - NONSTATIONARY RMS DISPLACEMENT RESPONSE FOR THE SMOOTH ELEMENT UNDER STATIONARY WHITE NOISE INPUT, (LOW PINCHING RATE). (BN MODEL)

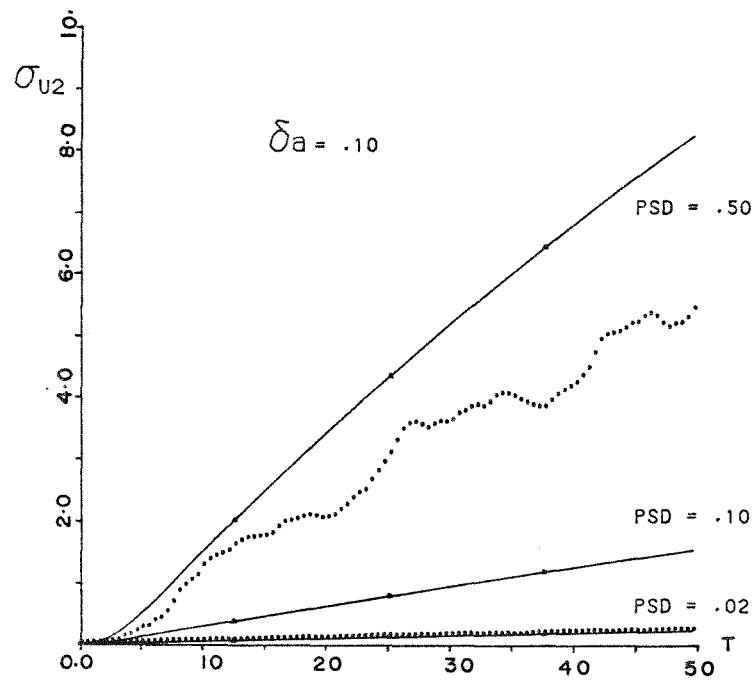

FIG.3.5- NONSTATIONARY RMS DISPLACEMENT RESPONSE FOR THE SLIP-LOCK ELEMENT UNDER STATIONARYWHITE NOISE. (LOW PINCHING RATE). (BN MODEL)

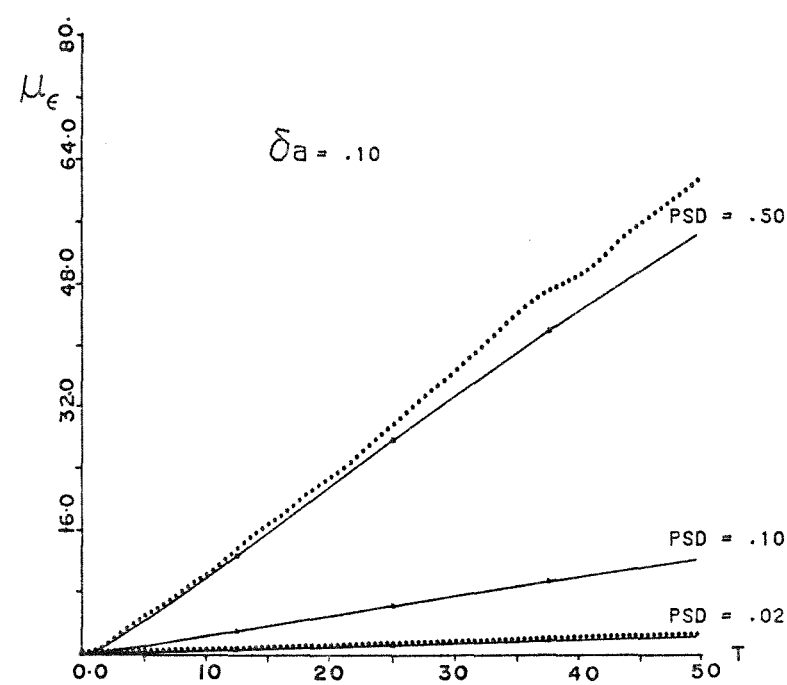

FIG.3.6- VARIATION OF DISSIPATION ENERGY FOR SDOF SYSTEM UNDER STATIONARY WHITE NOISE.(LOW PINCHING RATE). (BN MODEL)

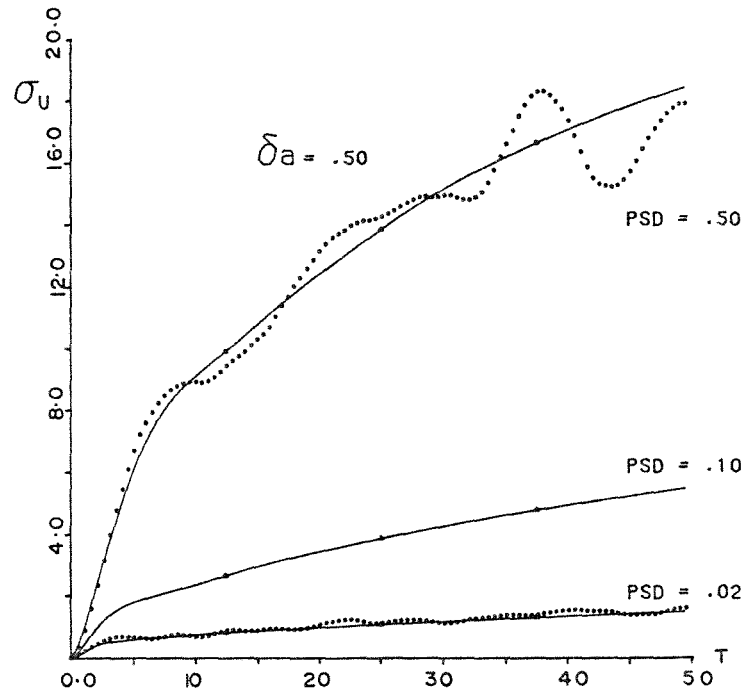

FIG. 3·7- NONSTATIONARY RMS DISPLACEMENT RESPONSE OF SDOF SYSTEM UNDER STATIONARY WHITENOISE INPUT. (HIGH PINCHING RATE). (BN MODEL)

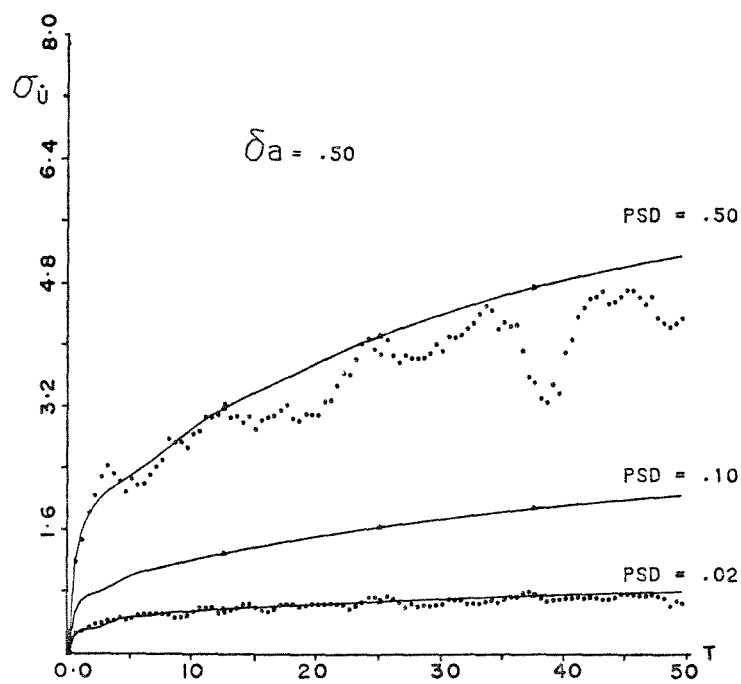

FIG. 3·8 - NONSTATIONARY RMS VELOCITY RESPONSE OF SDOF SYSTEM UNDER STATIONARY WHITENOISE INPUT. (HIGH PINCHING RATE). (BN MODEL)

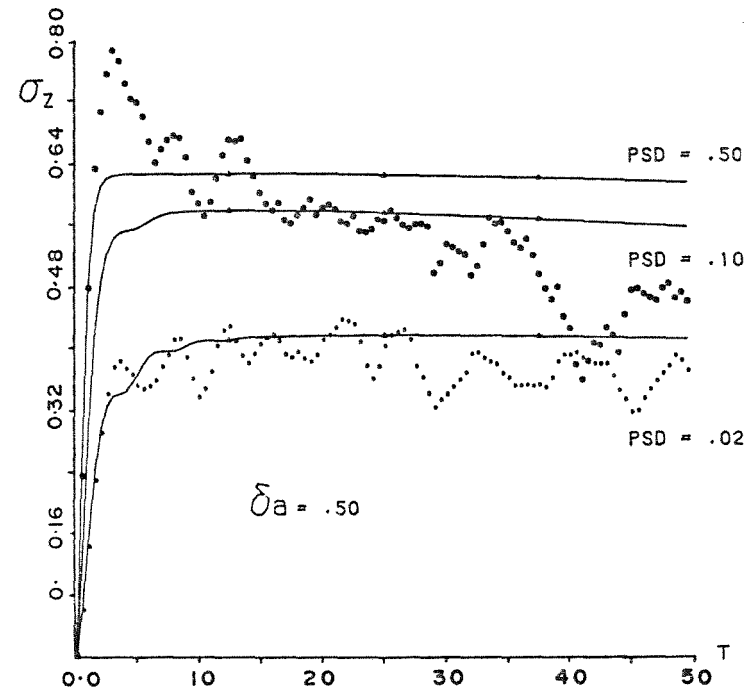

FIG. 3·9- RMS PREDICTION OF RESTORING FORCE UNDER STATIONARY WHITE NOISE.(HIGH PINCHING RATE). (BN MODEL)

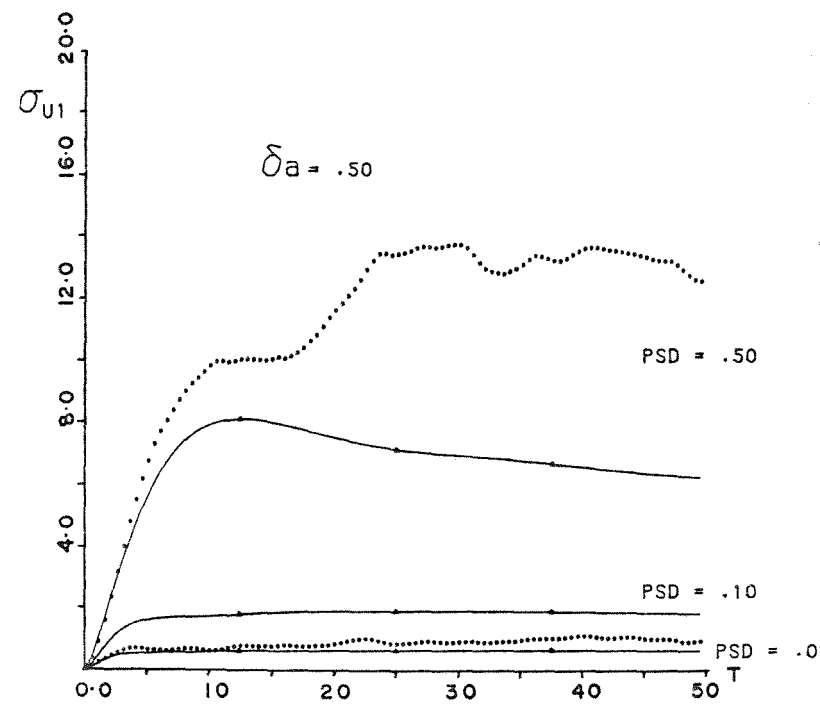

FIG. 3·10- NONSTATIONARY RMS DISPLACEMENT RESPONSE FOR THE SMOOTH ELEMENT UNDER STATIONARY WHITE NOISE INPUT. (HIGH PINCHING RATE). (BN MODEL)

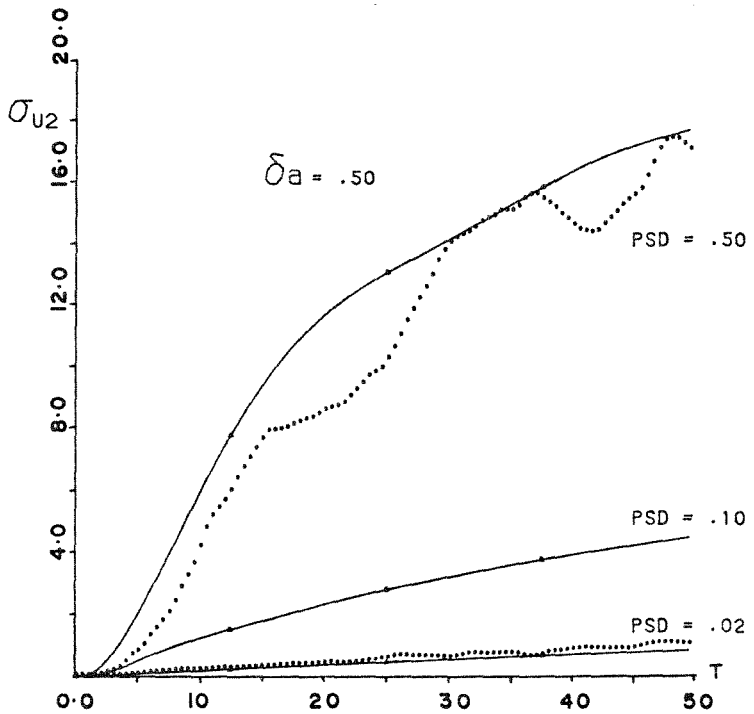

FIG. 3·11- NONSTATIONARY RMS DISPLACEMENT RESPONSE FOR THE SLIP-LOCK ELEMENT UNDER STATIONARYWHITE NOISE, (HIGH PINCHING RATE). **(BN MODEL)**

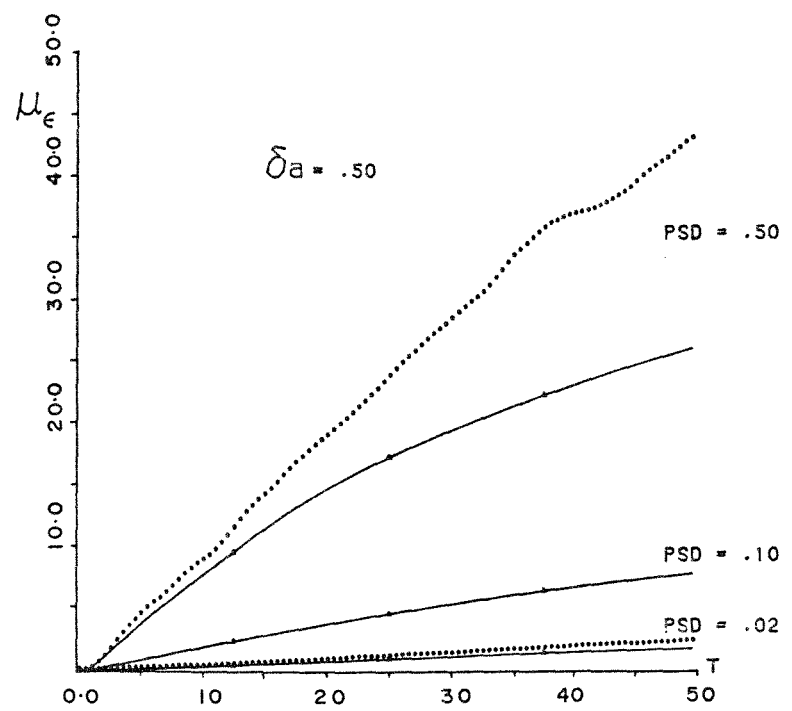

FIG. 3·12- VARIATION OF DISSIPATION ENERGY FOR SDOF SYSTEM UNDER STATIONARY WHITE NOISE, (HIGH PINCHING RATE). **(BN MODEL)**

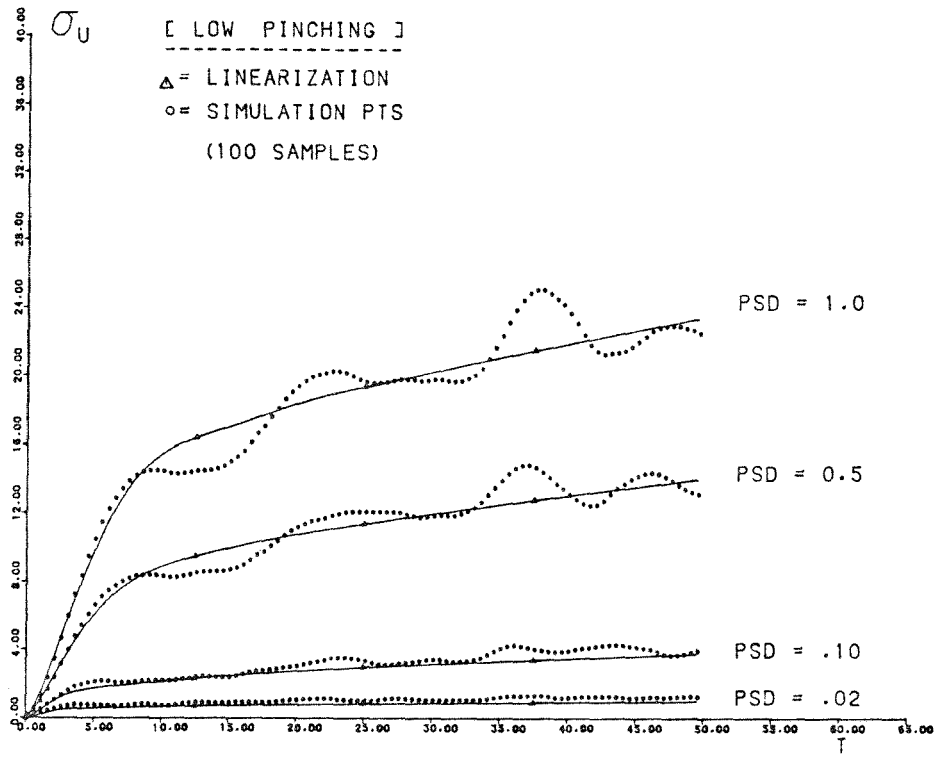

FIG.3-13 - NONSTATIONARY RMS DISPLACEMENT RESPONSE OF SDOF SYSTEM UNDER STATIONARY WHITE NOISE INPUT. ζ = .02, λ_o = 0.0, ξ_o = .350, δ_λ = 0.2, AND δ_ξ = 0.0. (NB MODEL)

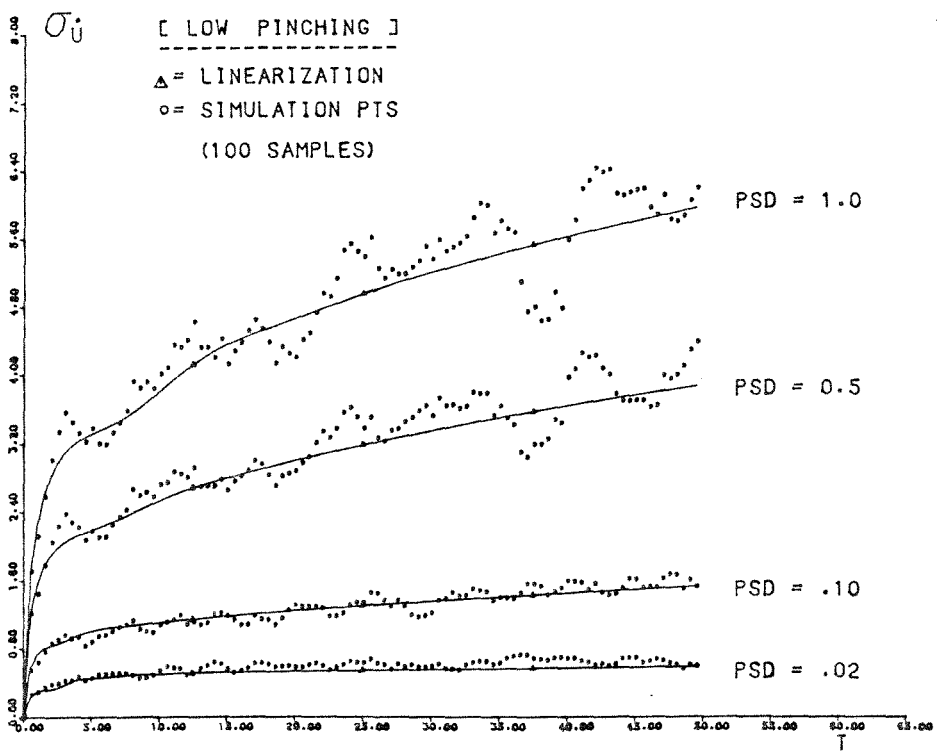

FIG.3-14 - NONSTATIONARY RMS VELOCITY RESPONSE OF SDOF SYSTEM UNDER STATIONARY WHITE NOISE INPUT. ζ = .02, λ_o = 0.0, ξ_o = .350, δ_λ = 0.2, AND δ_ξ = 0.0. (NB MODEL)

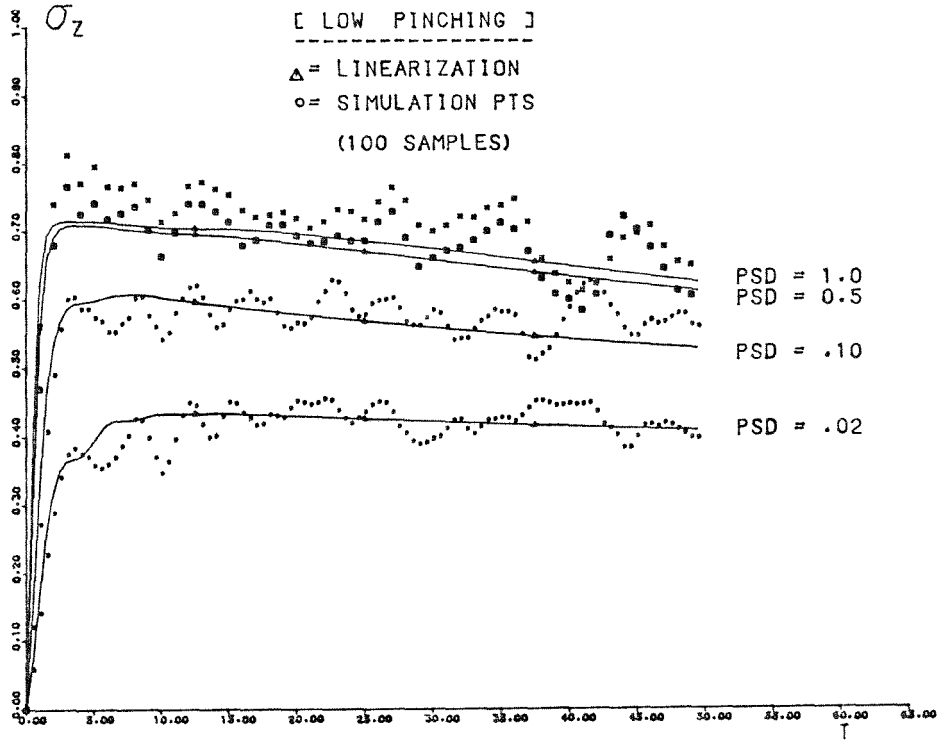

FIG.3-15 - RMS PREDICTION OF THE RESTORING FORCE OF SDOF SYSTEM UNDER STATIONARY WHITE NOISE INPUT. ζ = .02, λ_o = 0.0, ξ_o = .350, δ_λ = 0.2, AND δ_ξ = 0.0. (NB MODEL)

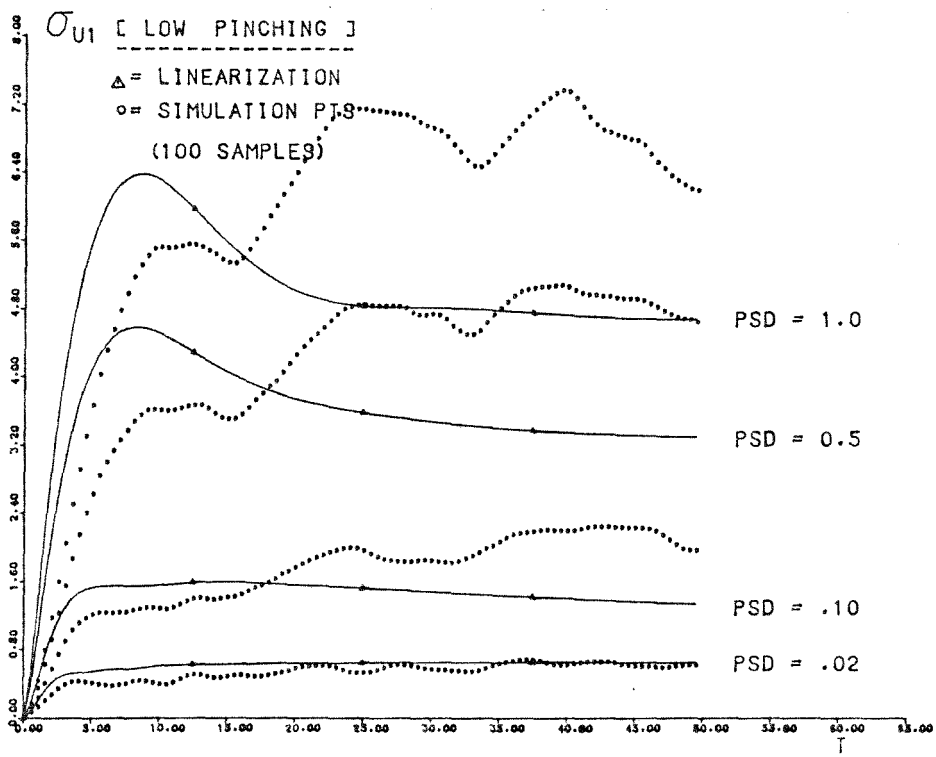

FIG.3-16 - NONSTATIONARY RMS DISPLACEMENT RESPONSE FOR THE SMOOTH ELEMENT UNDER STATIONARY WHITE NOISE INPUT. ζ = .02, λ_o = 0.0, ξ_o = .350, δ_λ = 0.2, AND δ_ξ = 0.0. (NB MODEL)

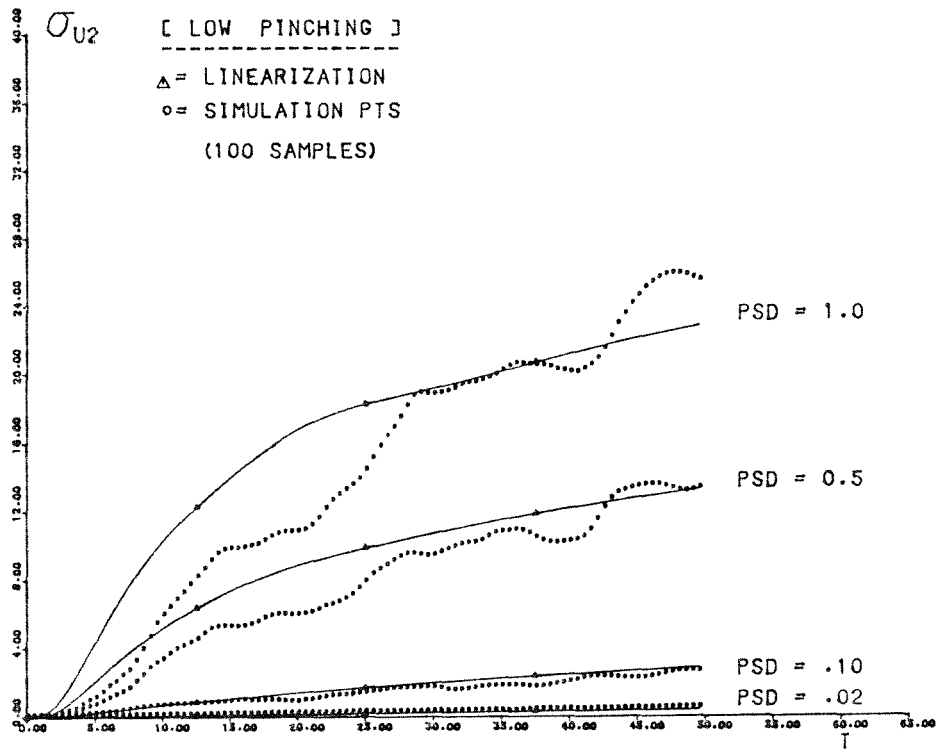

FIG.3-17- NONSTATIONARY RMS DISPLACEMENT RESPONSE FOR THE S-L ELEMENT UNDER STATIONARY WHITE NOISE INPUT. ζ = .02, λ_o = 0.0, ξ_o = .350, δ_λ = 0.2, AND δ_ξ = 0.0. (NB MODEL)

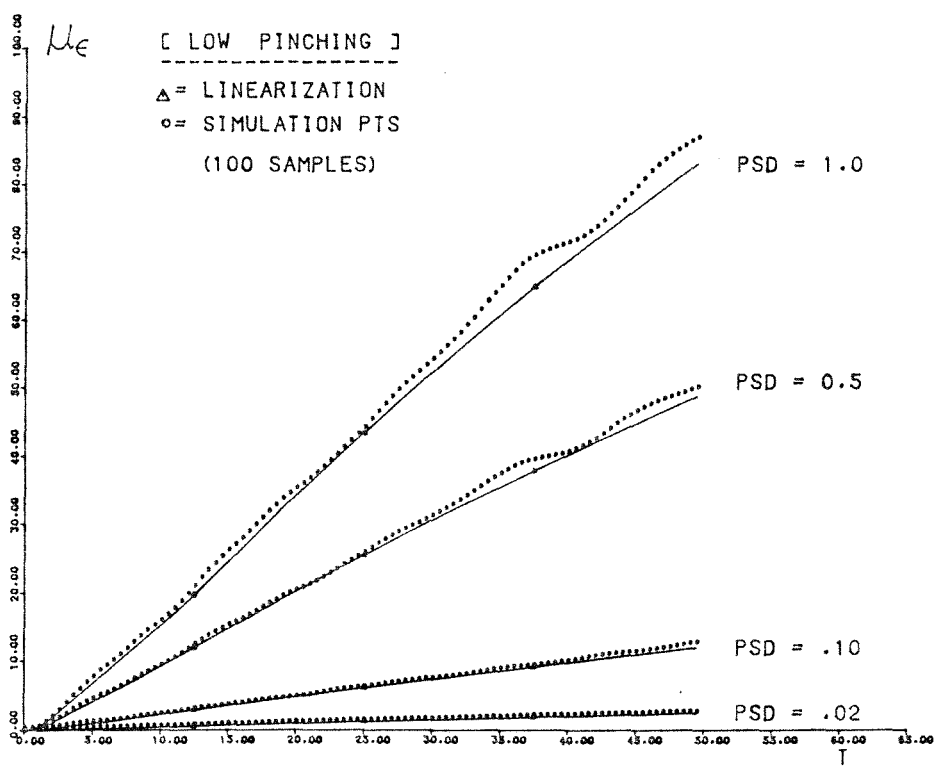

FIG.3-18- VARIATINON OF DISSIPATION ENERGY FOR SDOF SYSTEM(N-B MODEL) UNDER STATIONARY WHITE NOISE INPUT. ζ = .02, λ_o = 0.0, ξ_o = .350, δ_λ = 0.2, AND δ_ξ = 0.0. (NB MODEL)

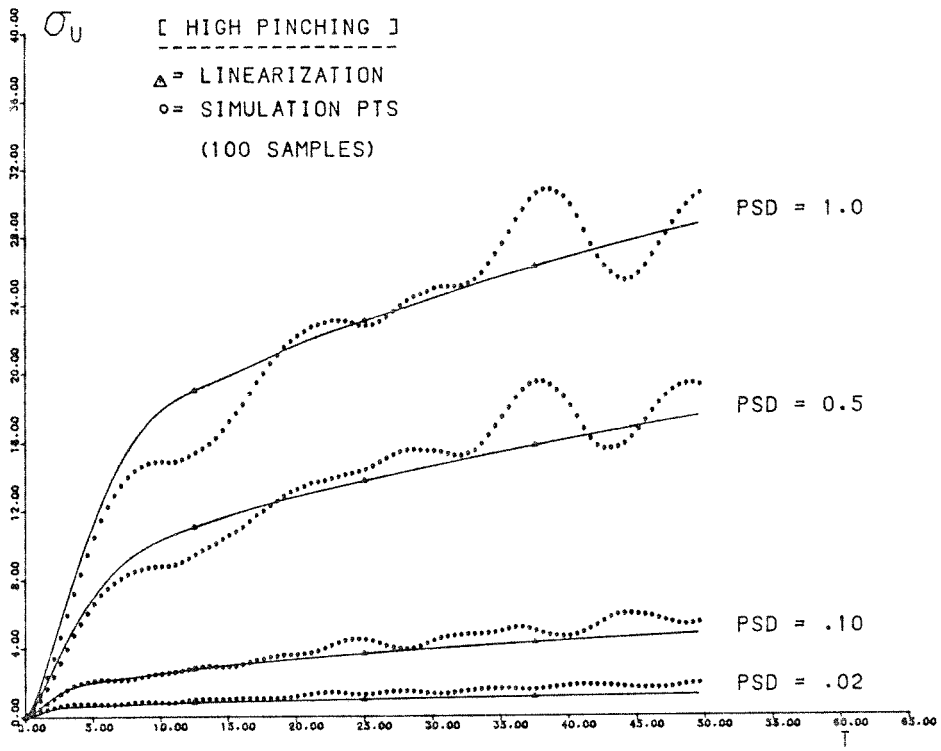

FIG.3·19 - NONSTATIONARY RMS DISPLACEMENT RESPONSE OF SDOF SYSTEM UNDER STATIONARY WHITE NOISE INPUT. ζ = .02, λ_o = 0.0, ξ_o = .125, δ_λ = 0.5, AND δ_ξ = 0.0. (NB MODEL)

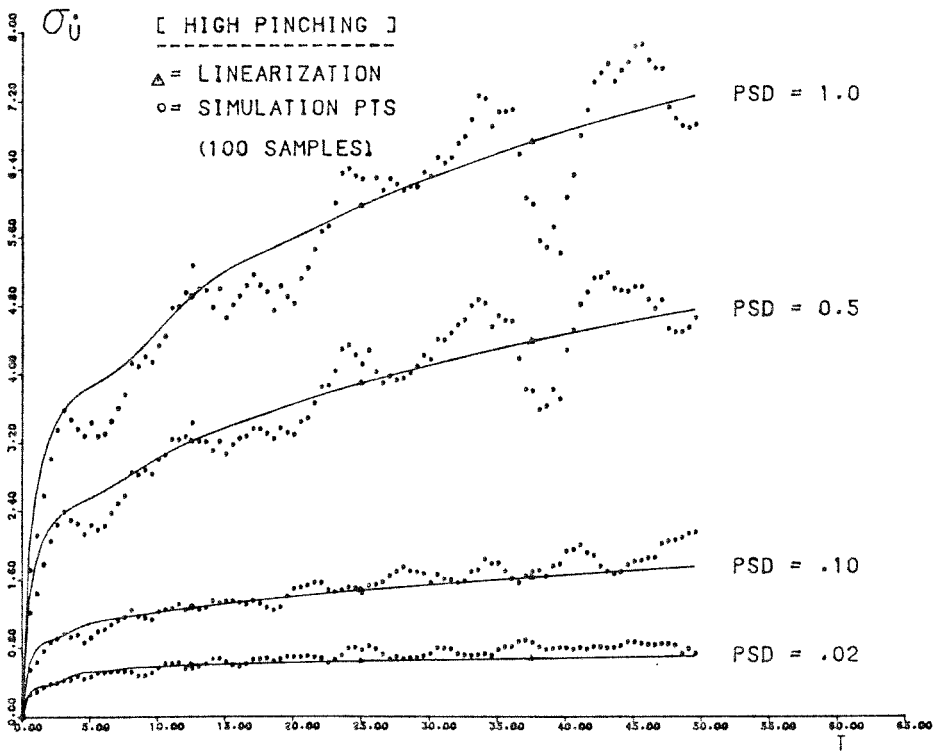

FIG.3·20 - NONSTATIONARY RMS VELOCITY RESPONSE OF SDOF SYSTEM UNDER STATIONARY WHITE NOISE INPUT. ζ = .02, λ_o = 0.0, ξ_o = .125 δ_λ = 0.5, AND δ_ξ = 0.0. (NB MODEL)

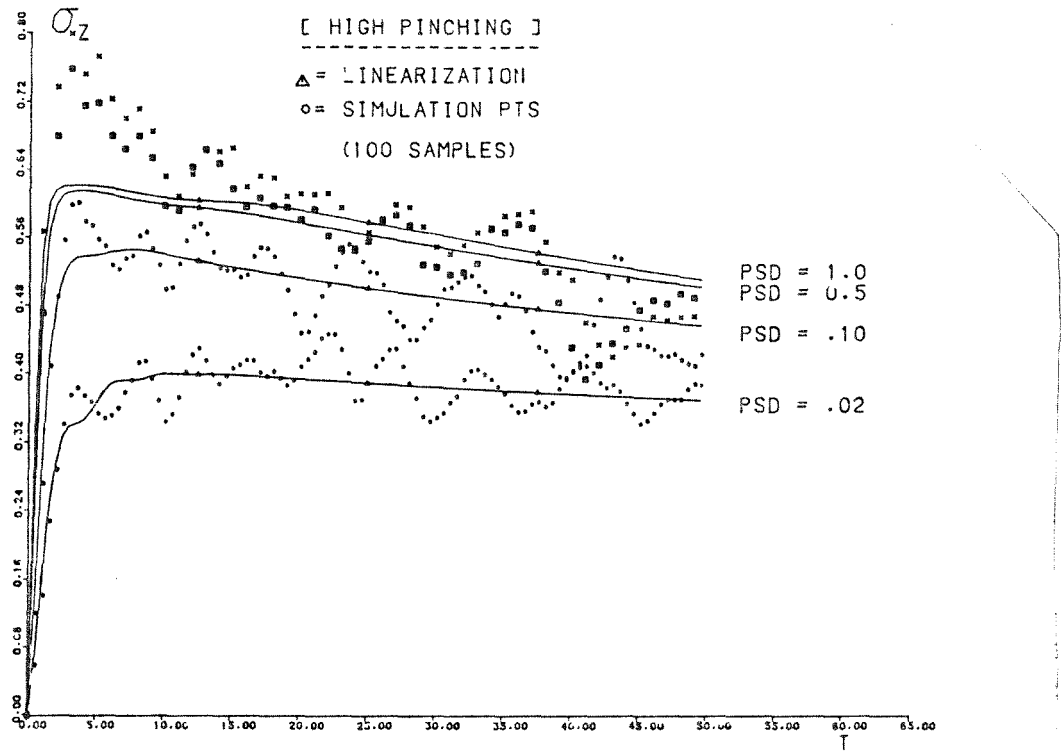

FIG.3-21- RMS PREDICTION OF THE RESTORING FORCE OF SDOF SYSTEM UNDER STATIONARY WHITE NOISE INPUT. ζ = .02, λ_o = 0.0, ξ_o = .125, δ_λ = 0.5, AND δ_ξ = 0.0. (NB MODEL)

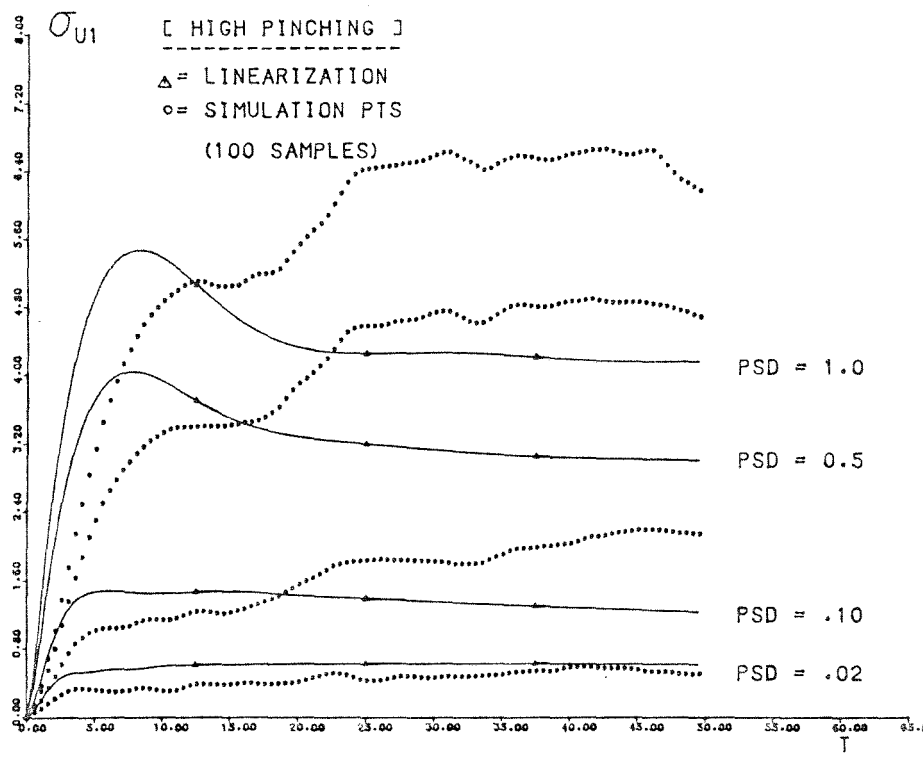

FIG.3-22- NONSTATIONARY RMS DISPLACEMENT RESPONSE FOR THE SMOOTH ELEMENT UNDER STATIONARY WHITE NOISE INPUT. ζ = .02, λ_o = 0.0, ξ_o = .125, δ_λ = 0.5, AND δ_ξ = 0.0. (NB MODEL)

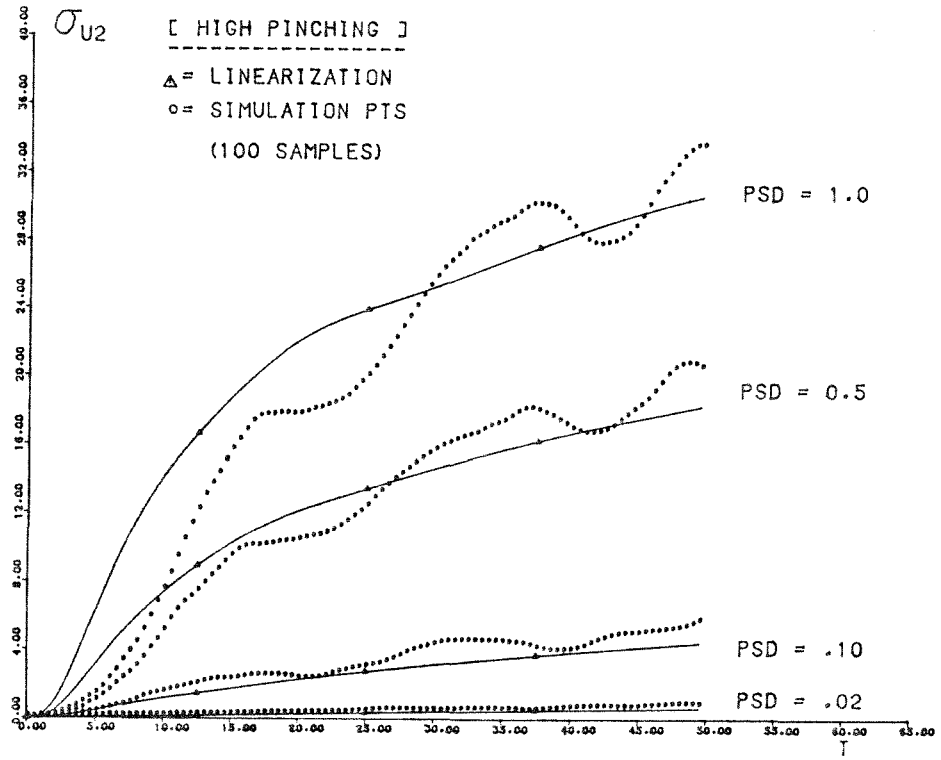

FIG.3-23- NONSTATIONARY RMS DISPLACEMENT RESPONSE FOR THE S-L ELEMENT UNDER STATIONARY WHITE NOISE INPUT. ζ = .02, λ_o = 0.0, ξ_o = .125, δ_λ = 0.5, AND δ_ξ = 0.0. (NB MODEL)

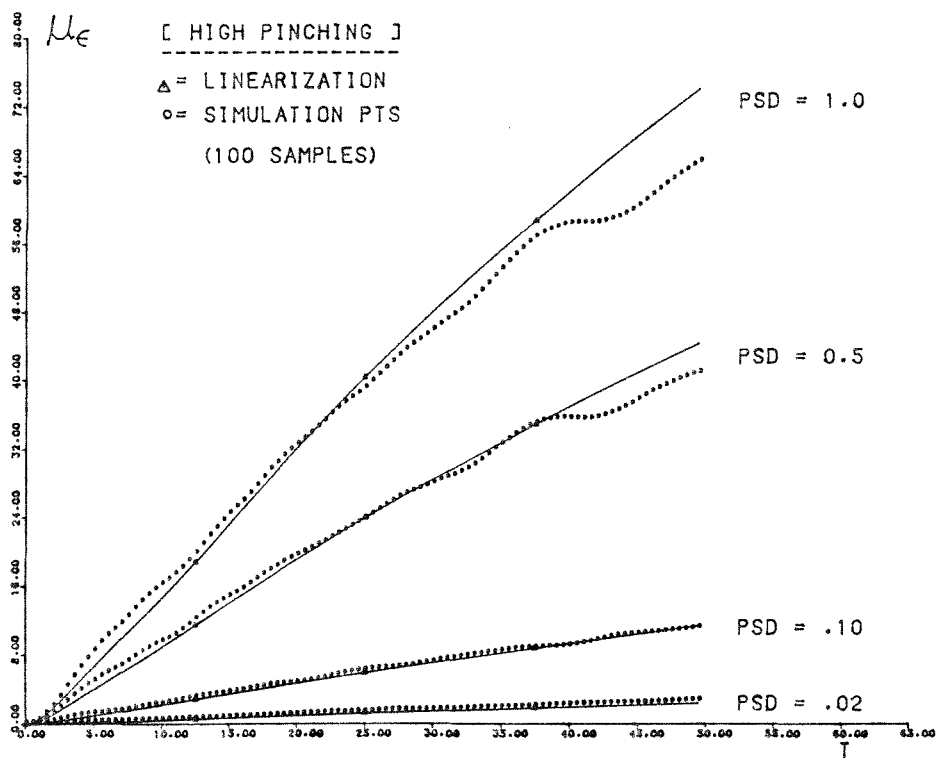

FIG.3-24- VARIATION OF DISSIPATION ENERGY FOR SDOF SYSTEM (N-B MODEL) UNDER STATIONARY WHITE NOISE INPUT. ζ = .02, λ_o = 0.0, ξ_o = .125, δ_λ = 0.5, AND δ_ξ = 0.0. (NB MODEL)

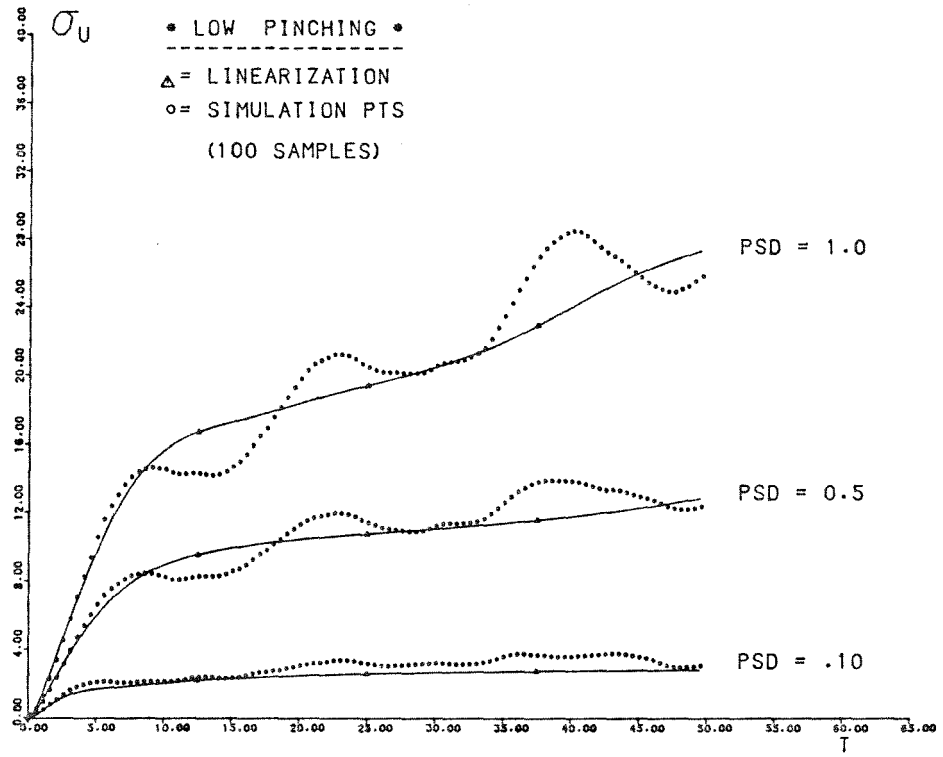

FIG.3·25- NONSTATIONARY RMS DISPLACEMENT RESPONSE OF SDOF SYSTEM UNDER STATIONARY WHITE NOISE INPUT. ζ_{I_o} = .80, λ = .05, ξ_o = 0.20, AND δ_ξ = .01. (SEP MODEL)

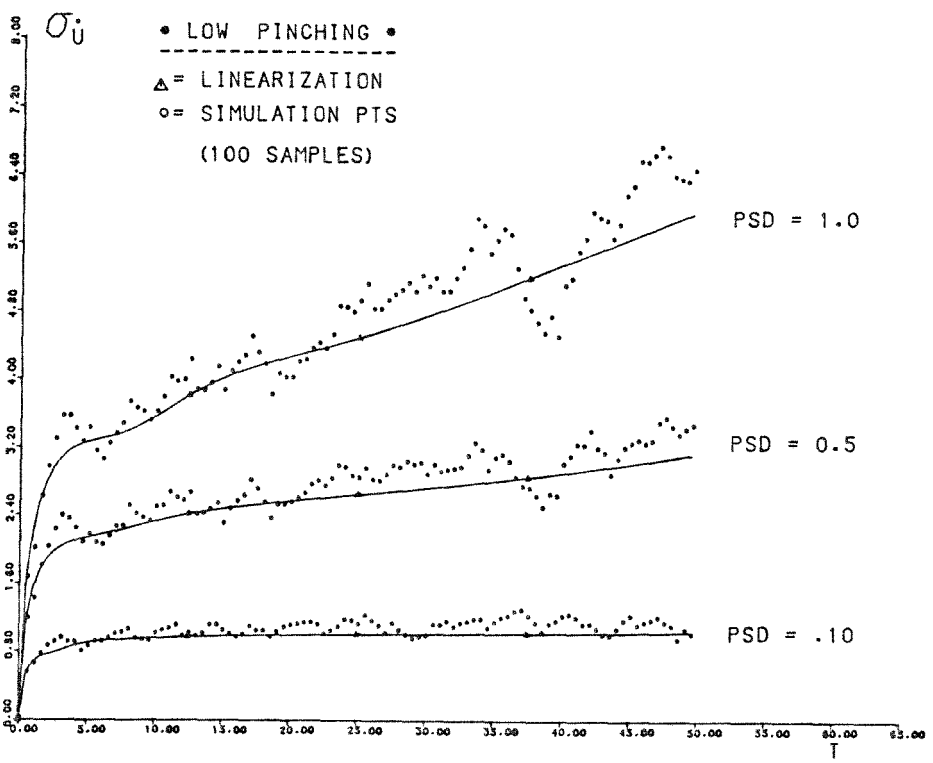

FIG.3·26- NONSTATIONARY RMS VELOCITY RESPONSE OF SDOF SYSTEM UNDER STATIONARY WHITE NOISE INPUT. ζ_{I_o} = 0.8, λ = .05, ξ_o = 0.20, AND δ_ξ = .01. (SEP MODEL)

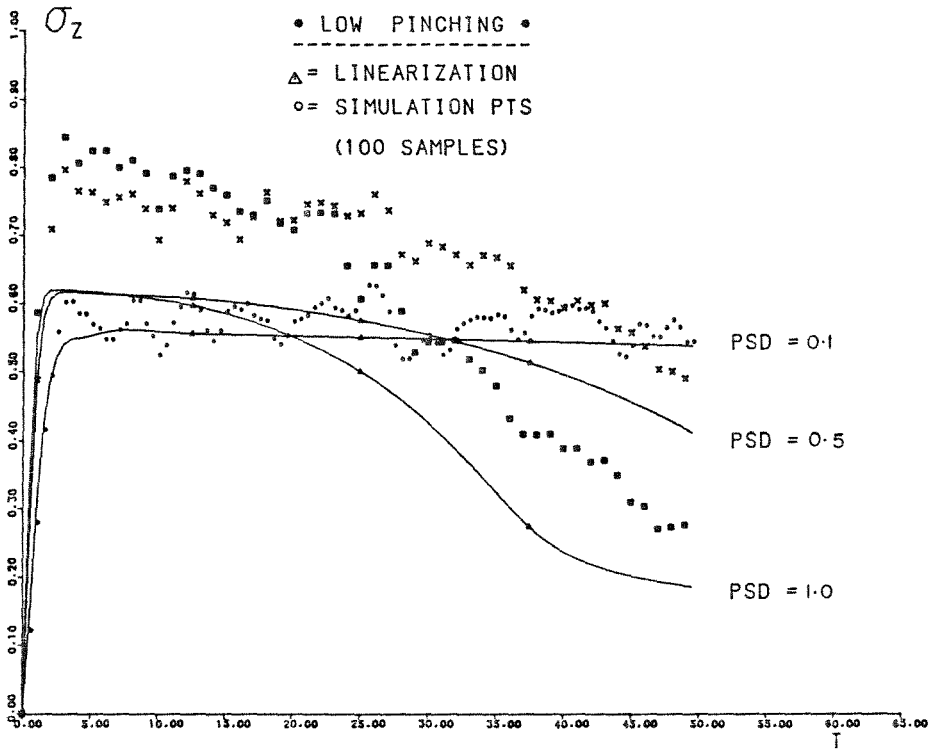

FIG.3·27- RMS PREDICTION OF THE RESTORING FORCE OF SDOF SYSTEM UNDER STATIONARY WHITE NOISE INPUT. ζ_{1_0} = .80, λ = .05, ξ_0 = 0.20, AND δ_ξ = .01. (SEP MODEL)

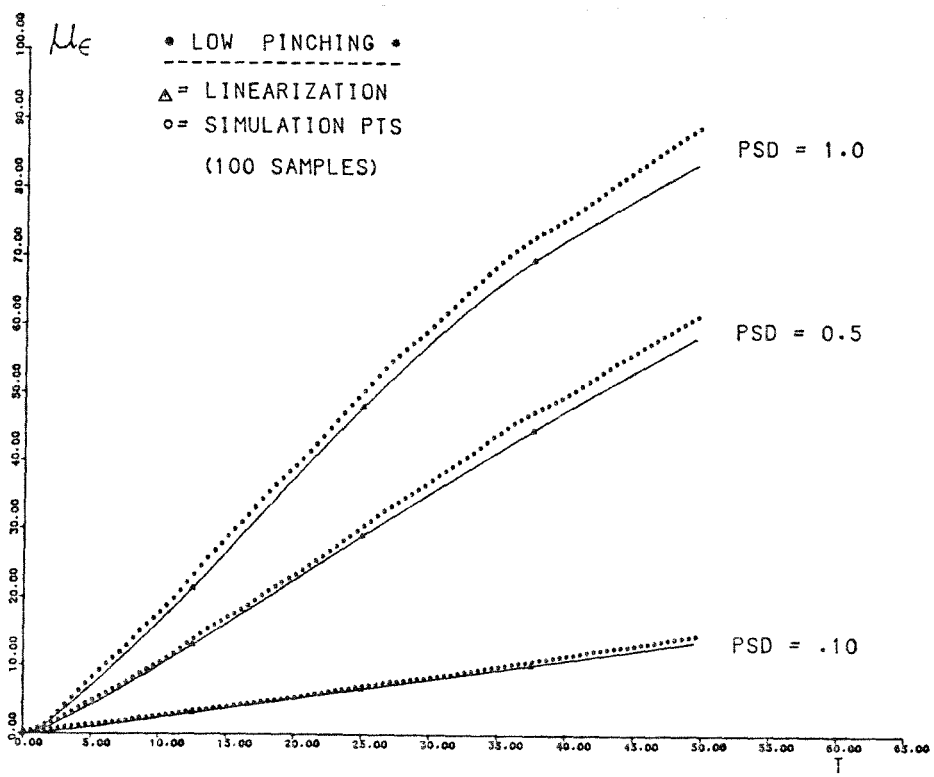

FIG.3·28- VARIATION OF DISSIPATION ENERGY FOR SDOF SYSTEM(SEP MODEL) UNDER STATIONARY WHITE NOISE INPUT. ζ_{1_0} = 0.8, λ = .05, ξ_0 = 0.20, AND δ_ξ = .01. (SEP MODEL)

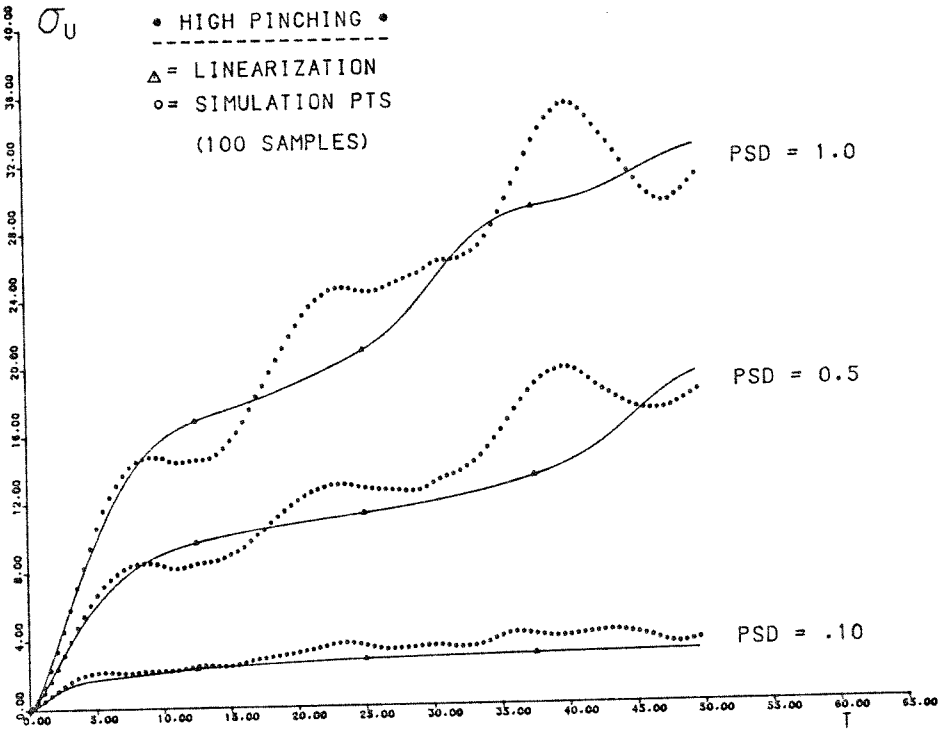

FIG.3-29- NONSTATIONARY RMS DISPLACEMENT RESPONSE OF SDOF SYSTEM UNDER STATIONARY WHITE NOISE INPUT. ζ_{I_o} = .90, λ = .15, ξ_o = 0.20, AND δ_ξ = .01. (SEP MODEL)

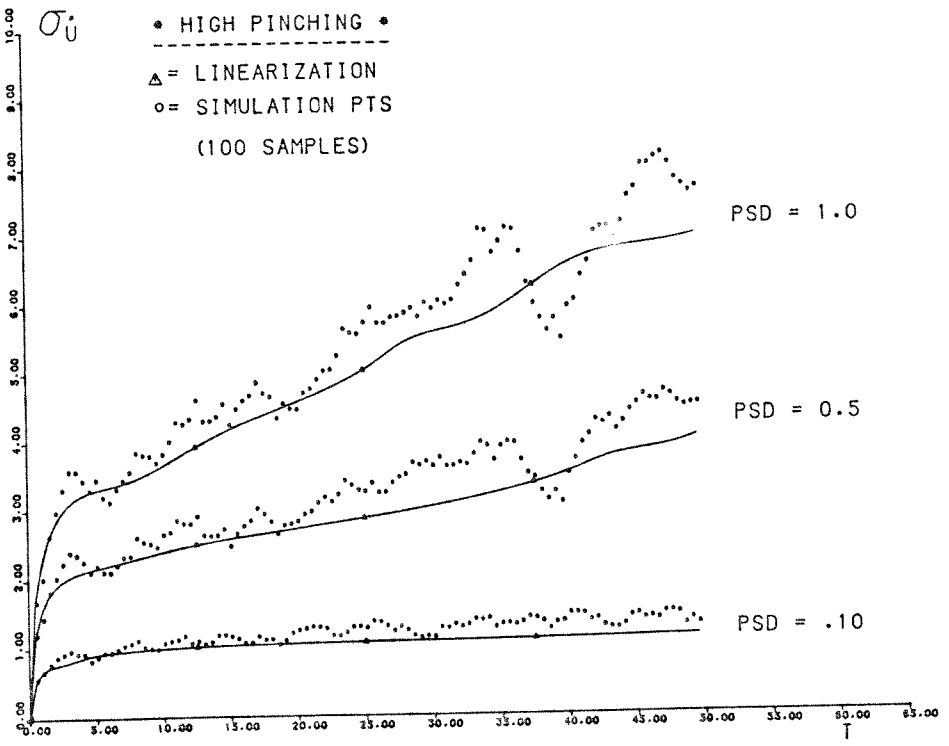

FIG.3-30- NONSTATIONARY RMS VELOCITY RESPONSE OF SDOF SYSTEM UNDER STATIONARY WHITE NOISE INPUT. ζ_{I_o} = 0.9, λ = .15, ξ_o = 0.20, AND δ_ξ = .01. (SEP MODEL)

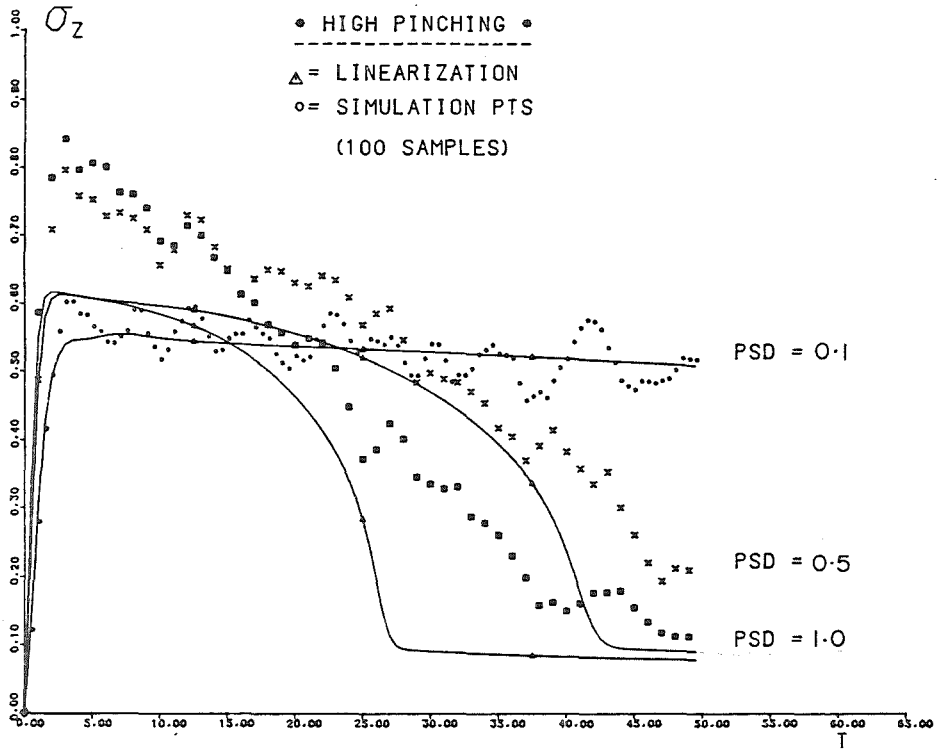

FIG.3-31 - RMS PREDICTION OF THE RESTORING FORCE OF SDOF SYSTEM UNDER STATIONARY WHITE NOISE INPUT. ζ_{1_o} = .90, λ = .15, ξ_o = 0.20, AND δ_ξ = .01. (SEP MODEL)

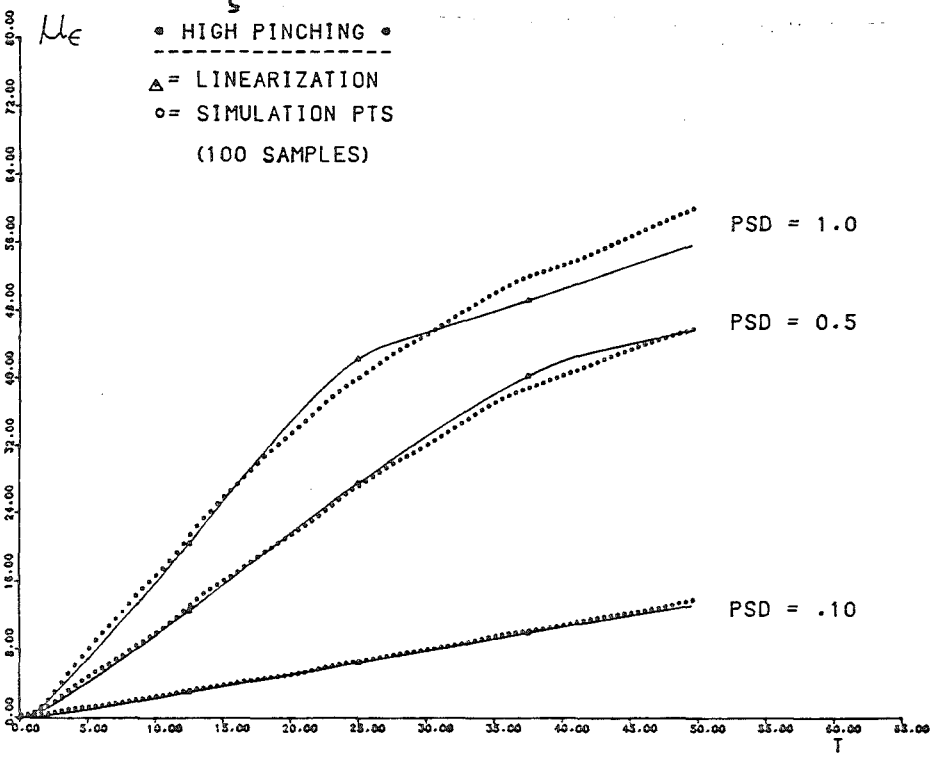

FIG.3-32- VARIATION OF DISSIPATION ENERGY FOR SDOF SYSTEM(SEP MODEL) UNDER STATIONARY WHITE NOISE INPUT. ζ_{1_o} = 0.9, λ = .15, ξ_o = 0.20, AND δ_ξ = .01. (SEP MODEL)

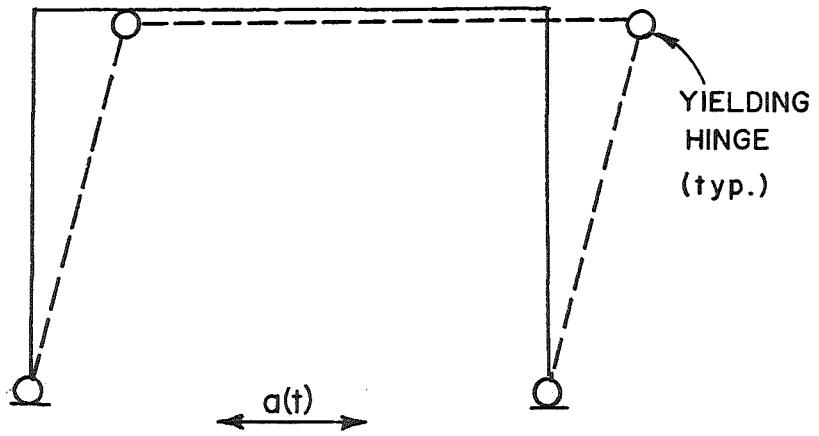

(a)- Response Without Gravity Load

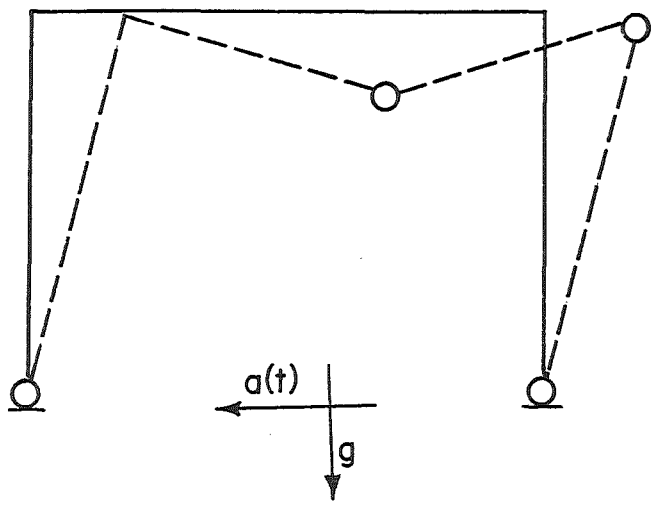

(b)- Response Including Gravity Load

FIG. 4.1- GRAVITY EFFECT ON RESPONSE TO LATERAL LOADS.

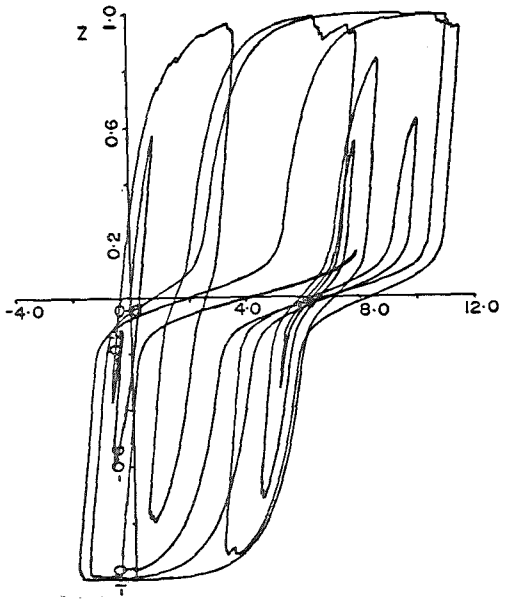

(a)- $\delta_a = 0.1$, $\mu_F = 0.2$

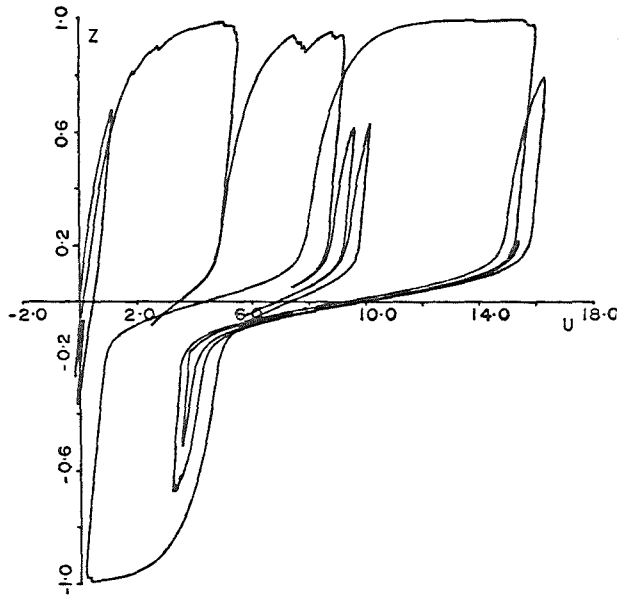

(b)- $\delta_a = 0.3$, $\mu_F = 0.4$

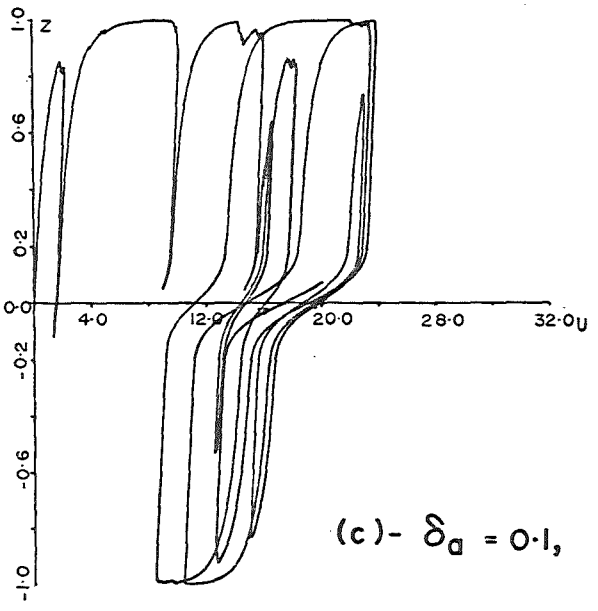

(c)- $\delta_a = 0.1$, $\mu_F = 0.8$

FIG. 4.2- PINCHING BEHAVIOR OF BN MODEL UNDER NONZERO MEAN STATIONARY WHITE NOISE INPUT. PSD = 0. , $\sigma_o = 0.8$, $\zeta = 0.1$.

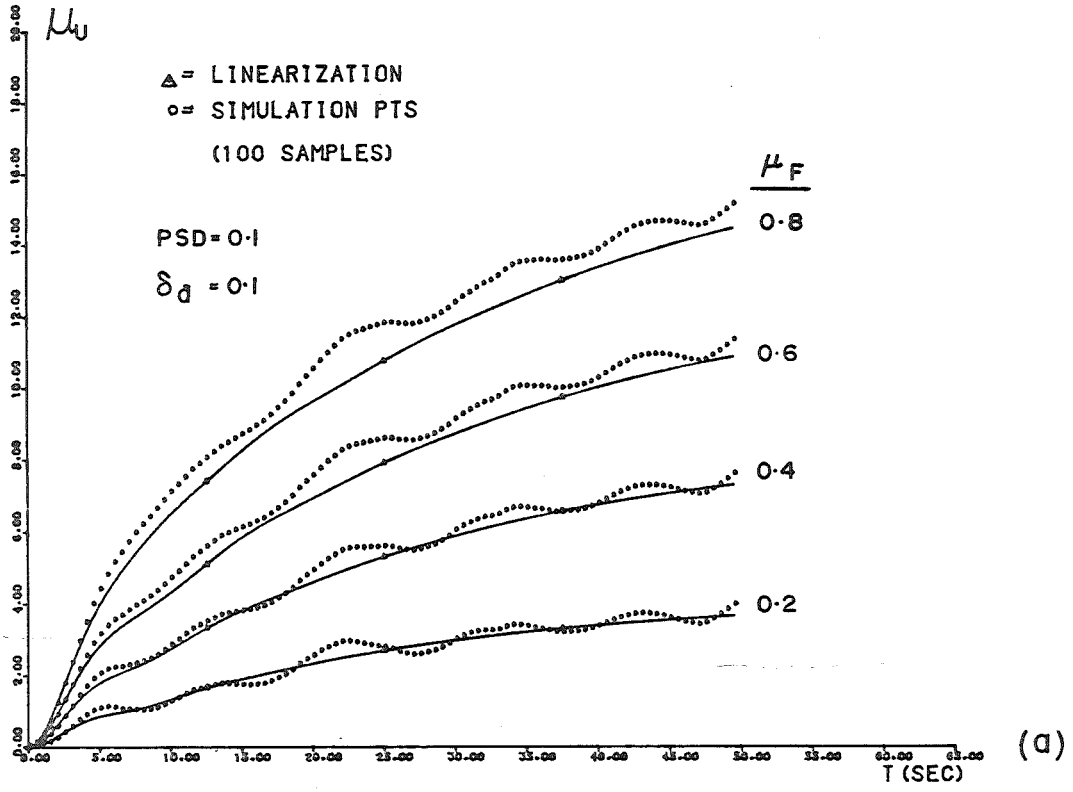

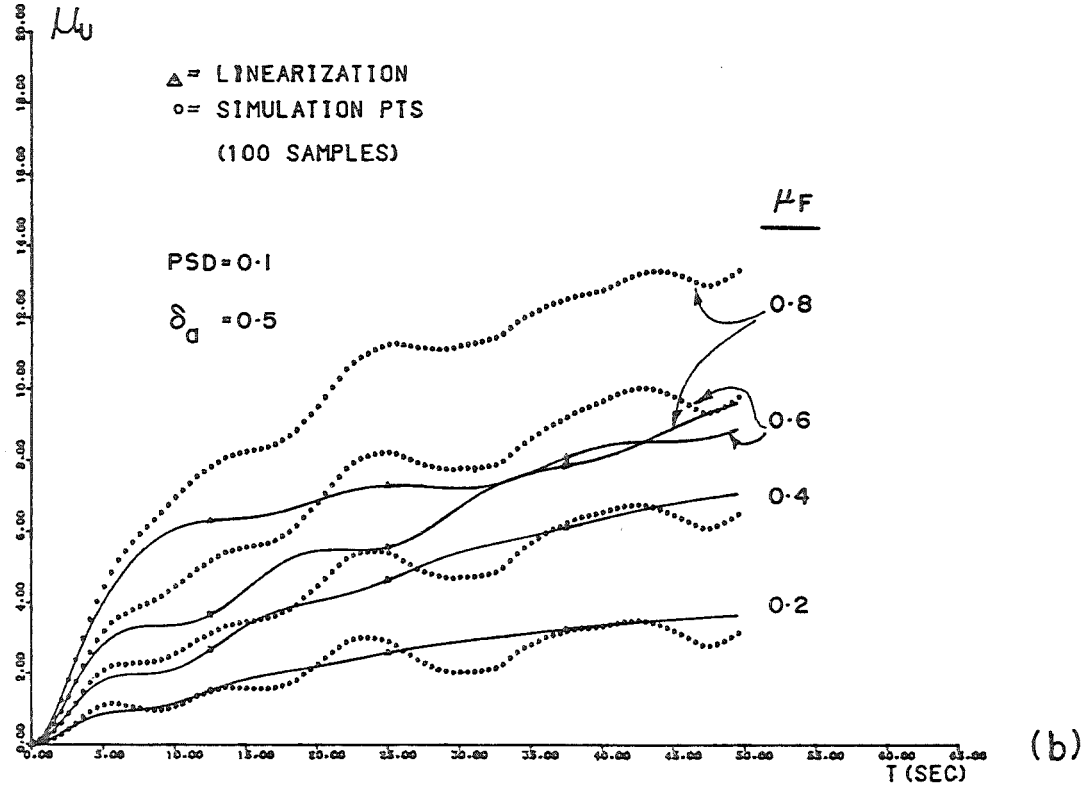

FIG. 4.3 - MEAN DISPLACEMENT RESPONSE OF SDOF B-N SLIP-LOCK MODEL UNDER NONZERO MEAN STATIONARY WHITE NOISE INPUT. $\sigma_0 = 0.08$, $\delta_\sigma = 0.$

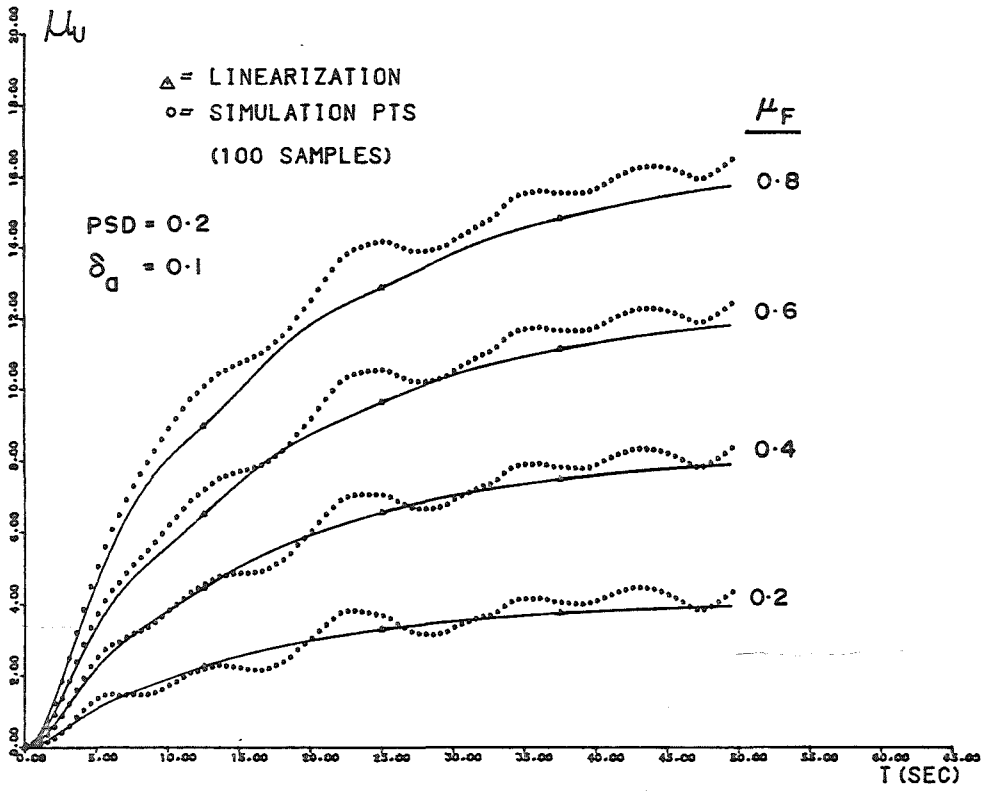

(c)

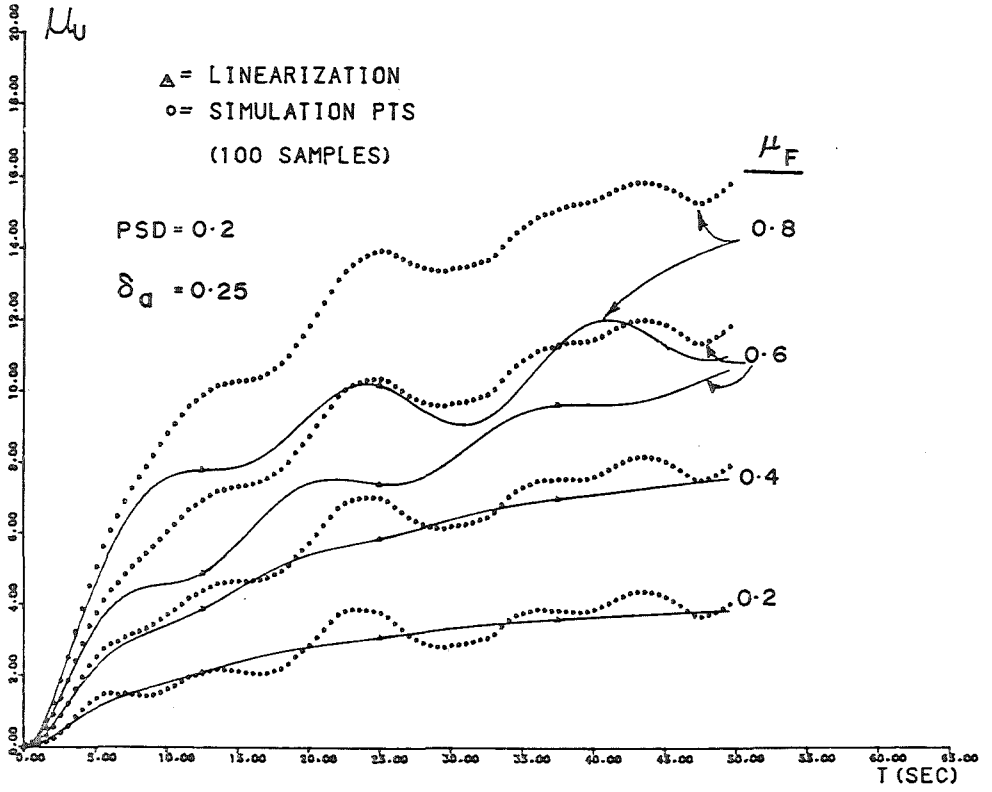

(d)

FIG. 4.3 (Cont'd)

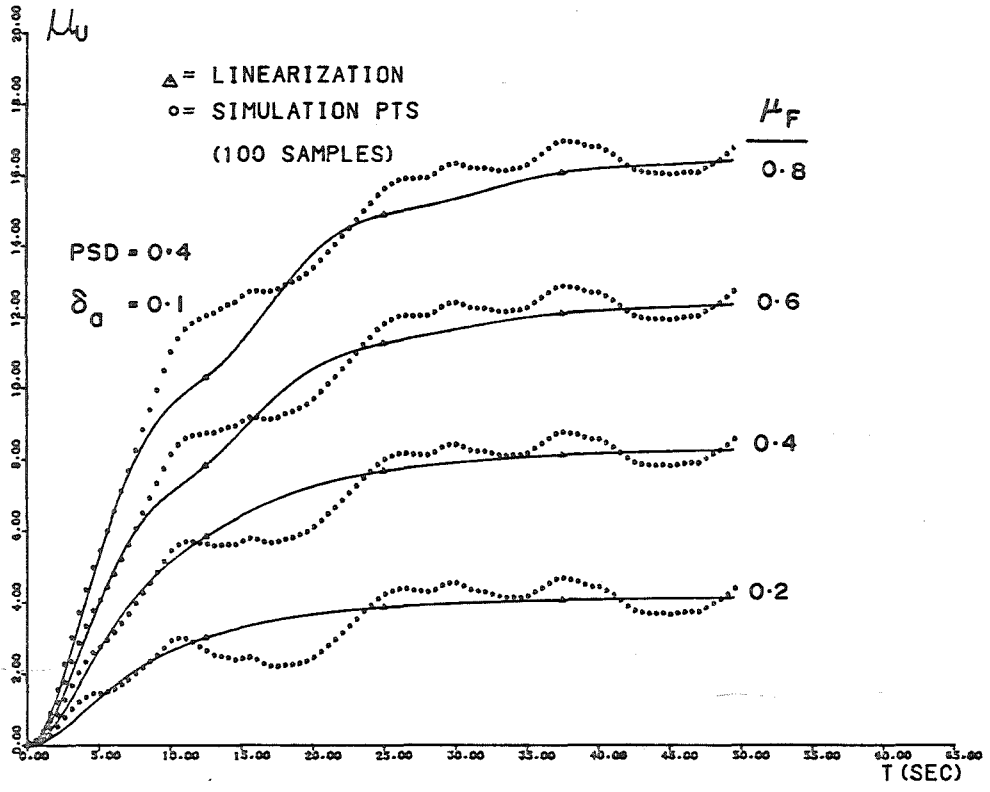

(e)

FIG. 4.3 (Cont'd)

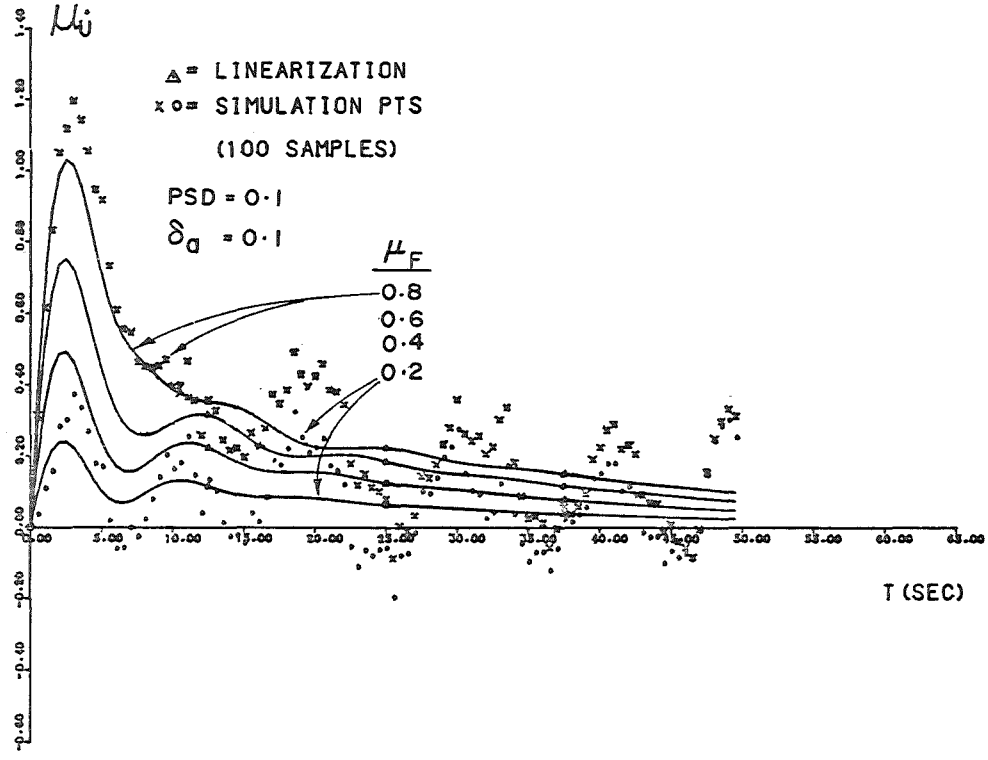

(a)

FIG. 4.4 - MEAN VELOCITY RESPONSE OF SDOF B-N SLIP-LOCK MODEL UNDER NONZERO MEAN STATIONARY WHITE NOISE INPUT. $\sigma = 0{\cdot}08$, $\delta_\sigma = 0$.

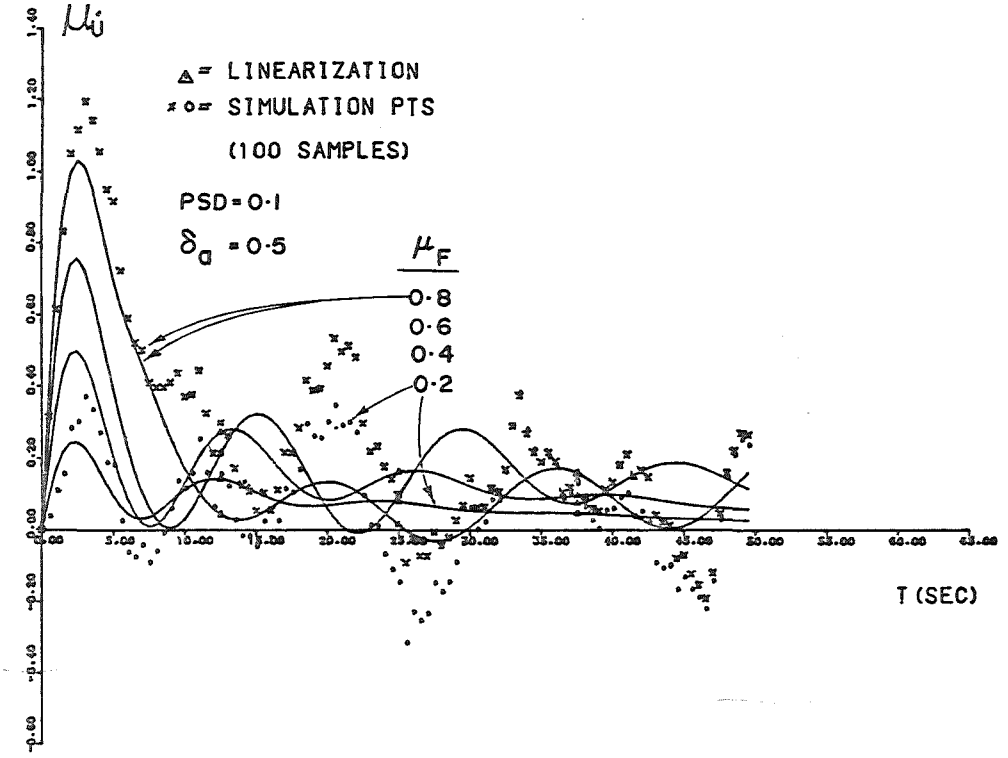

(b)

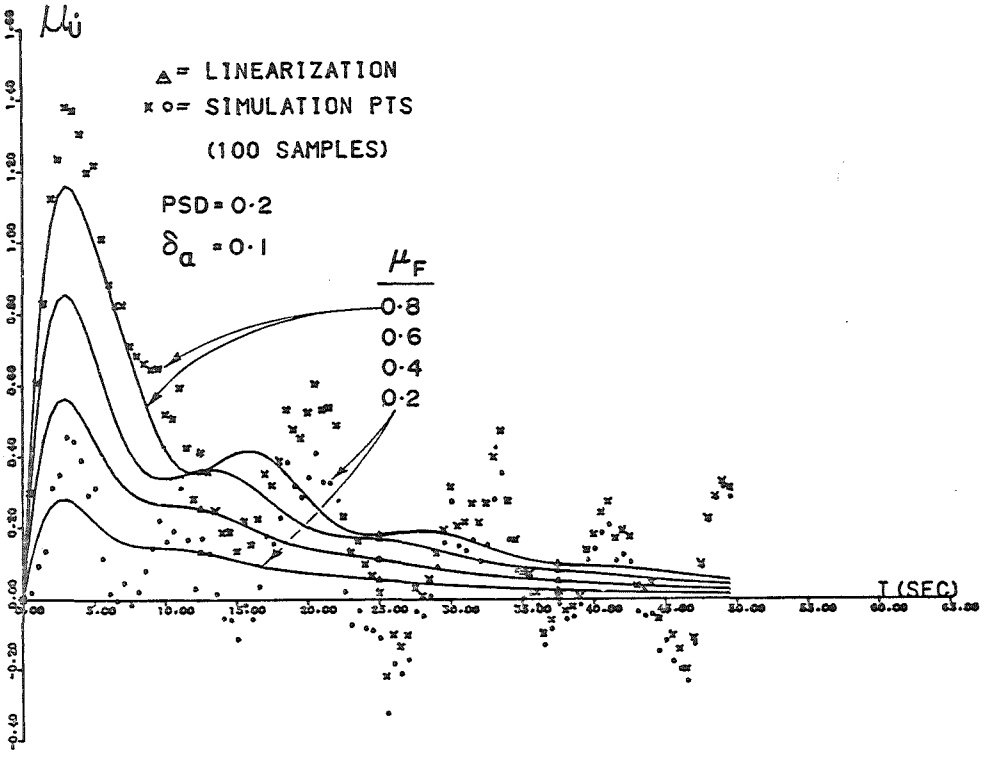

(c)

FIG. 4.4 (Cont'd)

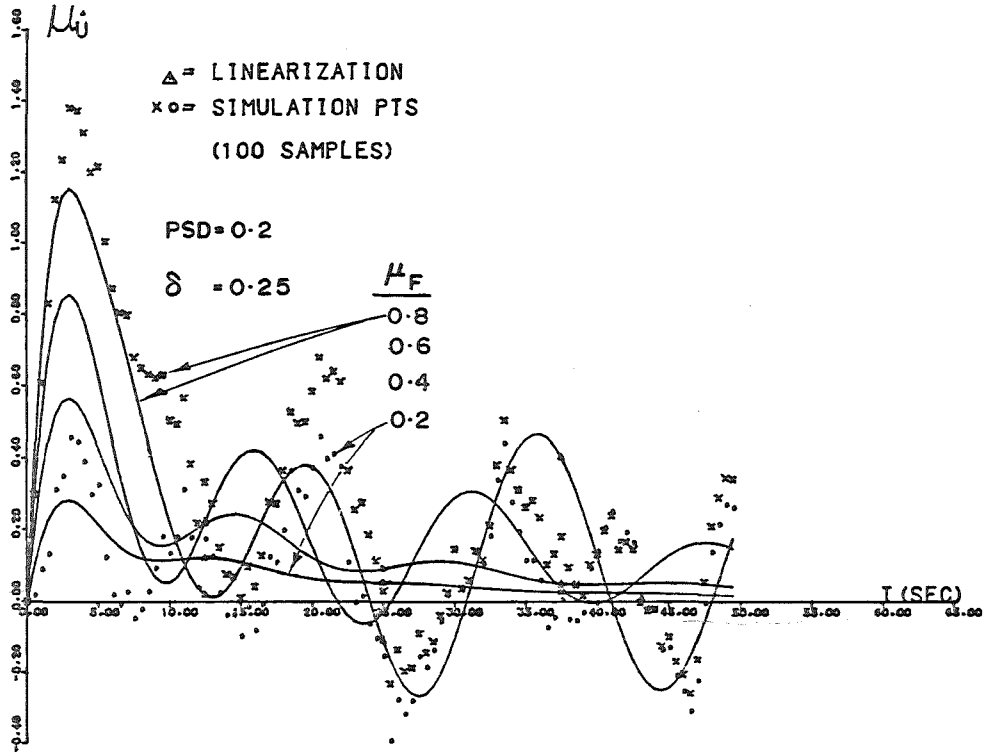

(d)

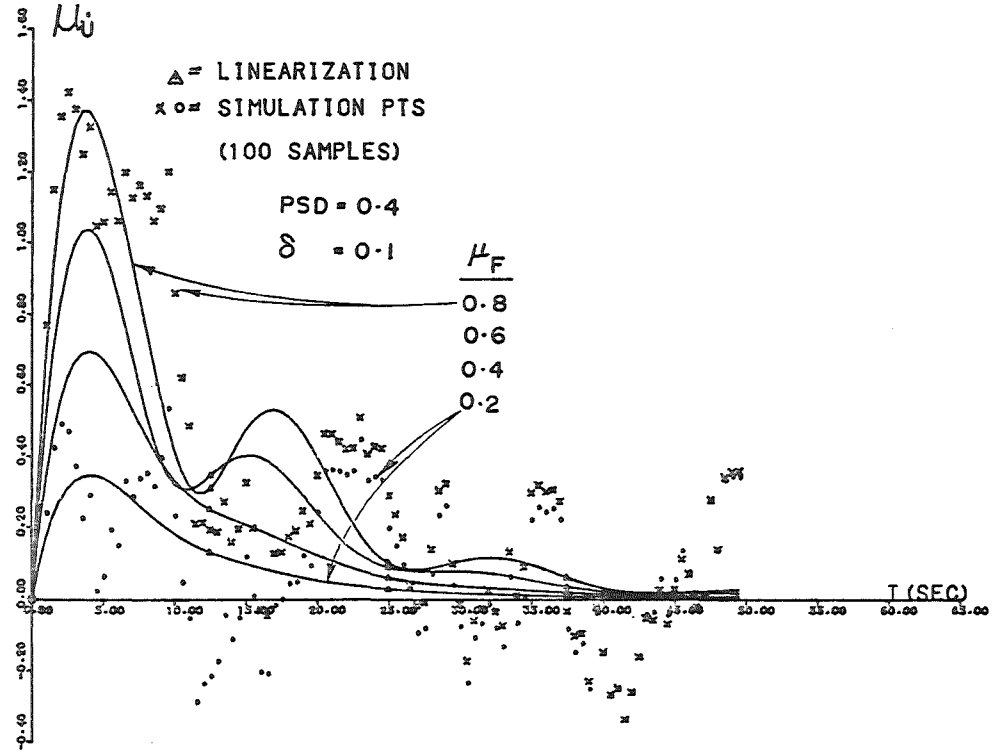

(e)

FIG. 4.4 (Cont'd)

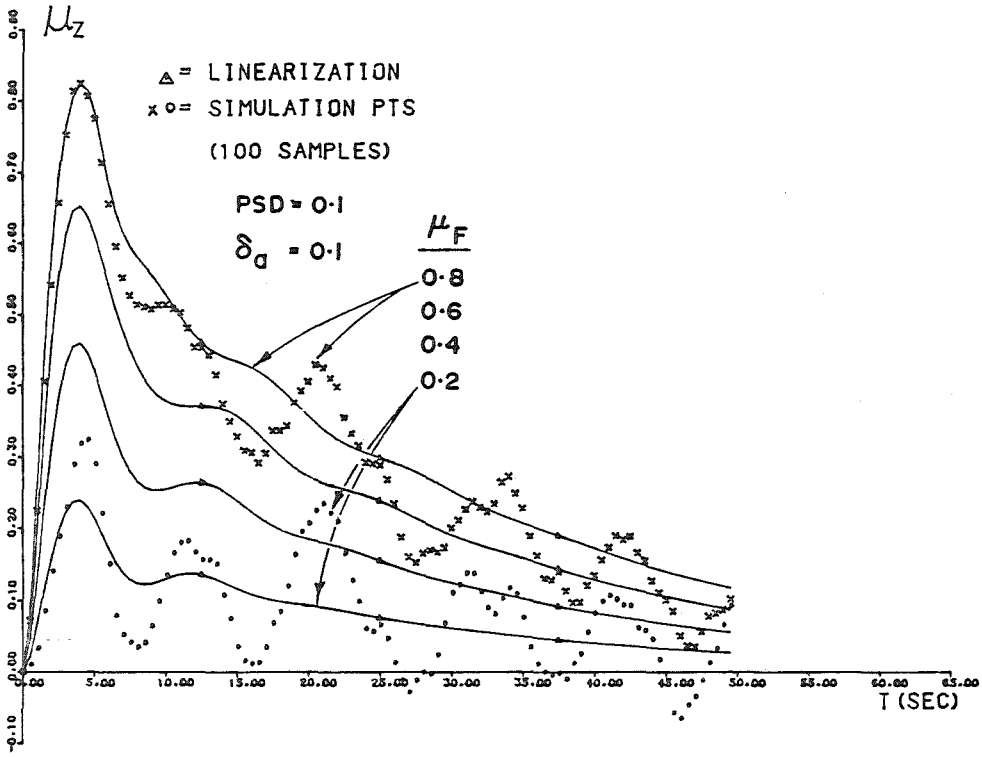

(a)

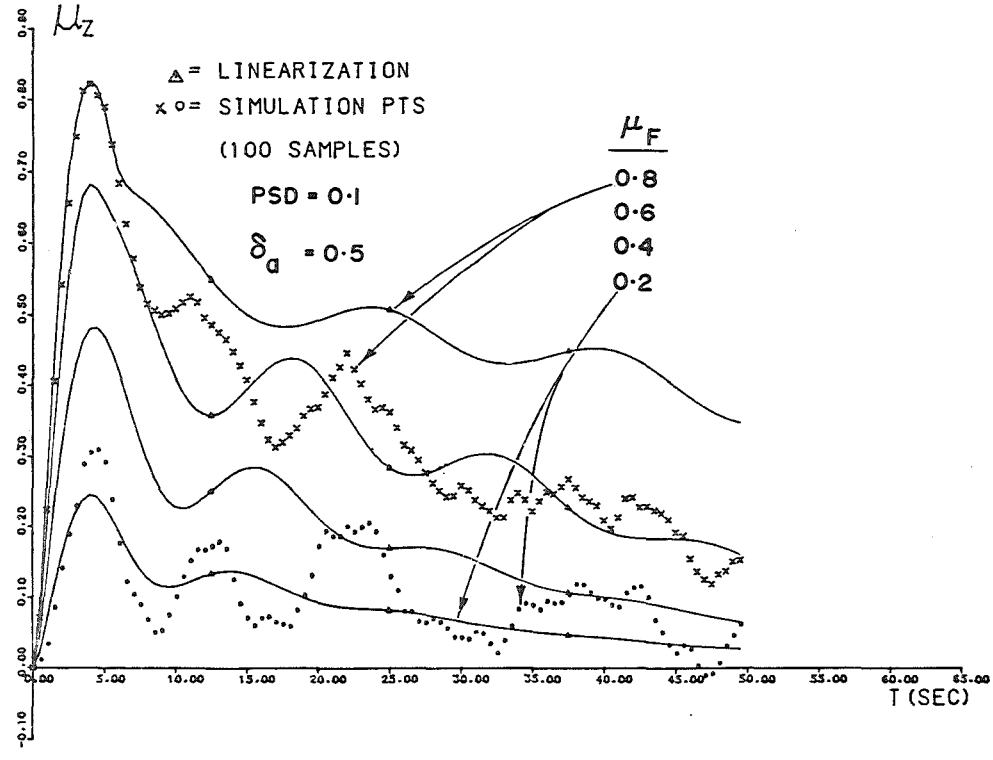

(b)

FIG. 4.5 - MEAN HYSTERETIC RESTORING FORCE RESPONSE FOR B-N MODEL UNDER NONZERO MEAN STATIONARY WHITE NOISE INPUT. $\sigma = 0.08$, $\delta_\sigma = 0.$

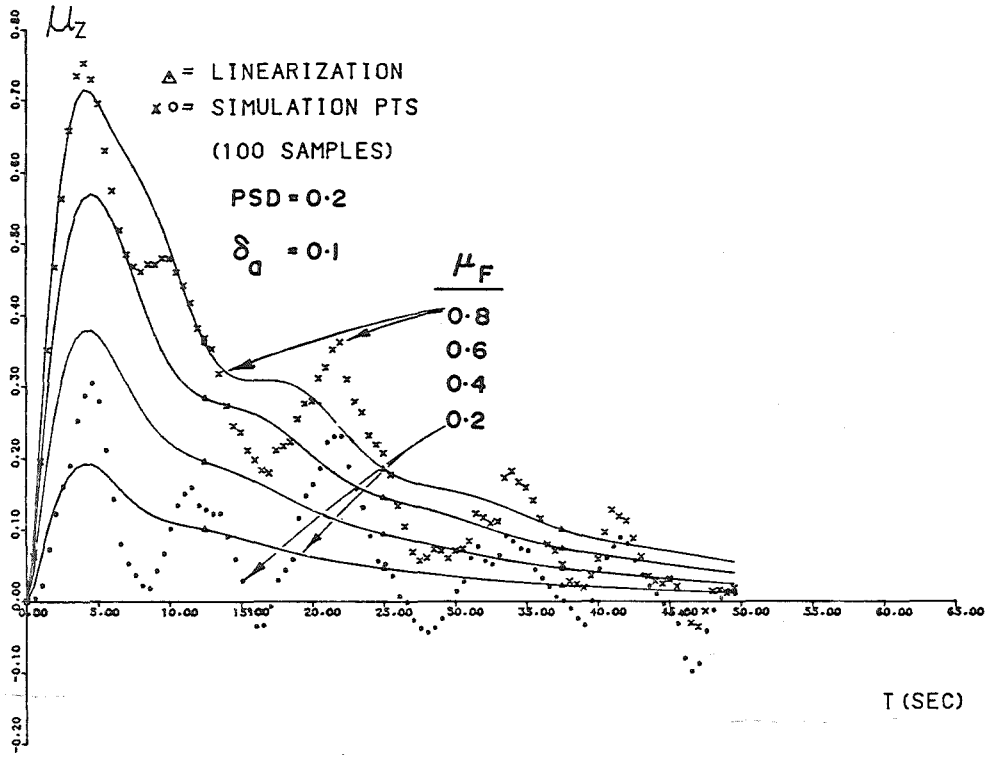

(c)

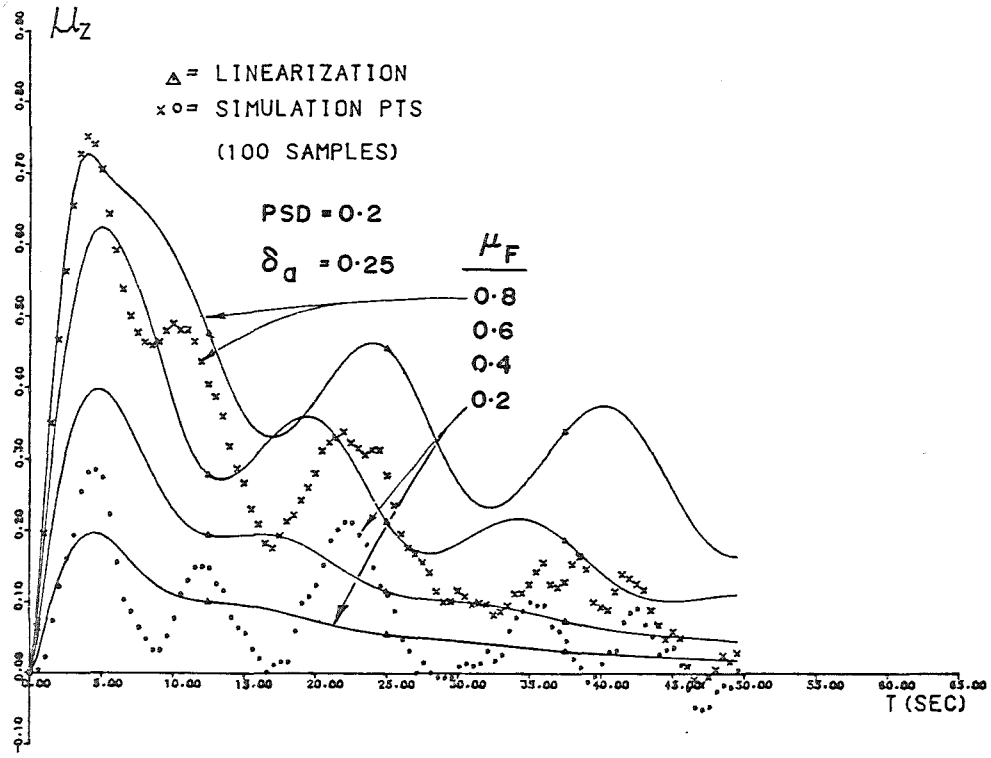

(d)

FIG. 4.5 (Cont'd)

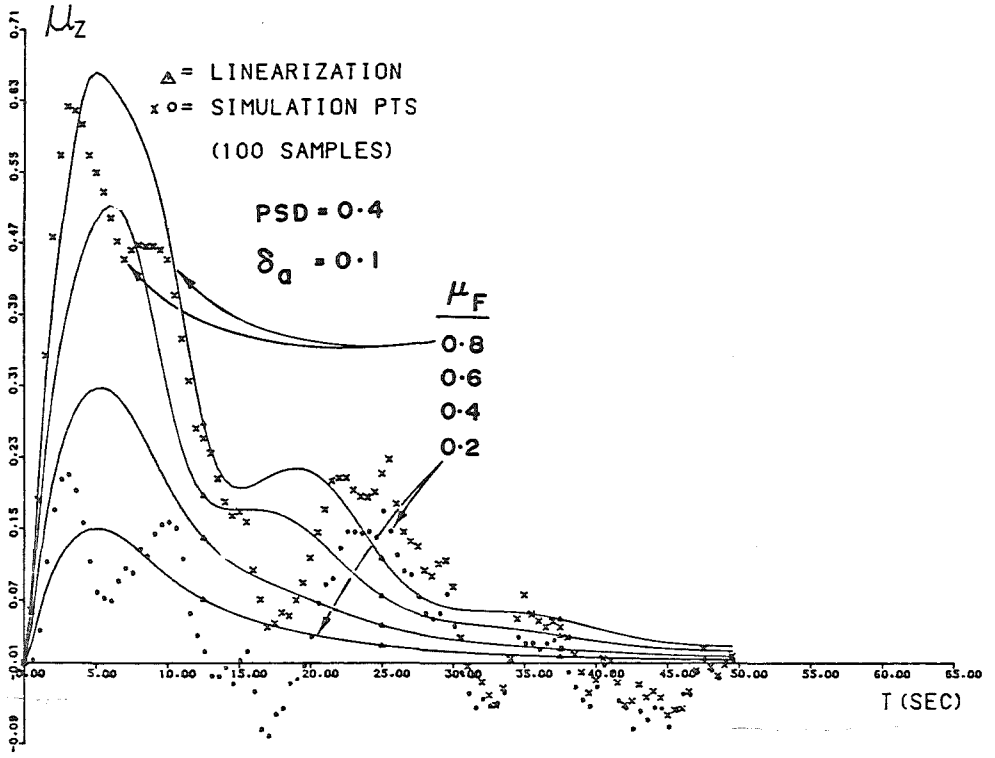

(e)

FIG. 4.5 (Cont'd)

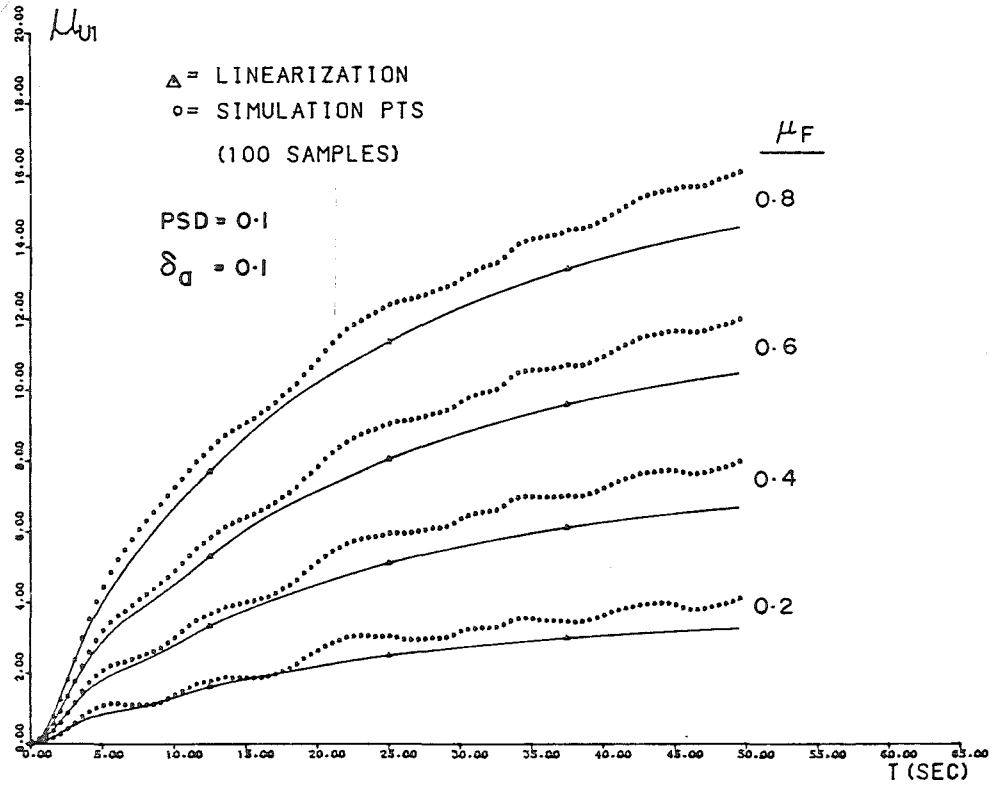

(a)

FIG. 4.6 - MEAN DISPL. RESPONSE FOR SMOOTH ELEMENT COMPONENT OF MODEL UNDER NONZERO MEAN STATIONARY WHITE NOISE INPUT. $\sigma = 0.08$, $\delta_\sigma = 0$.

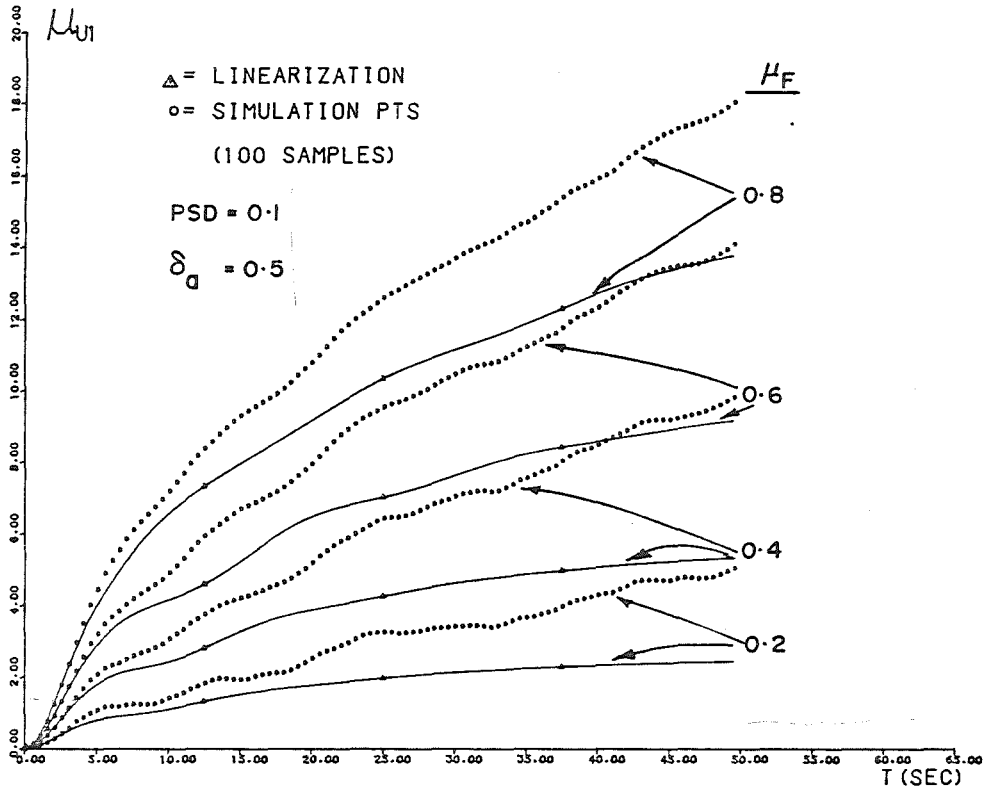

(b)

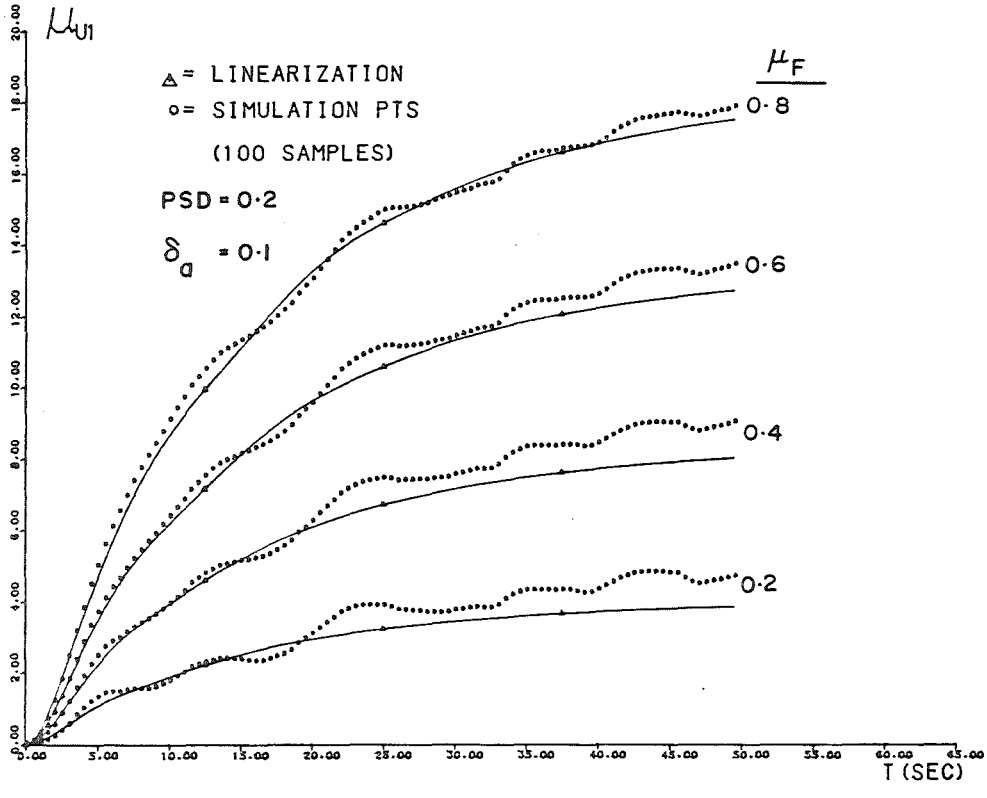

(c)

FIG. 4.6 (Cont'd)

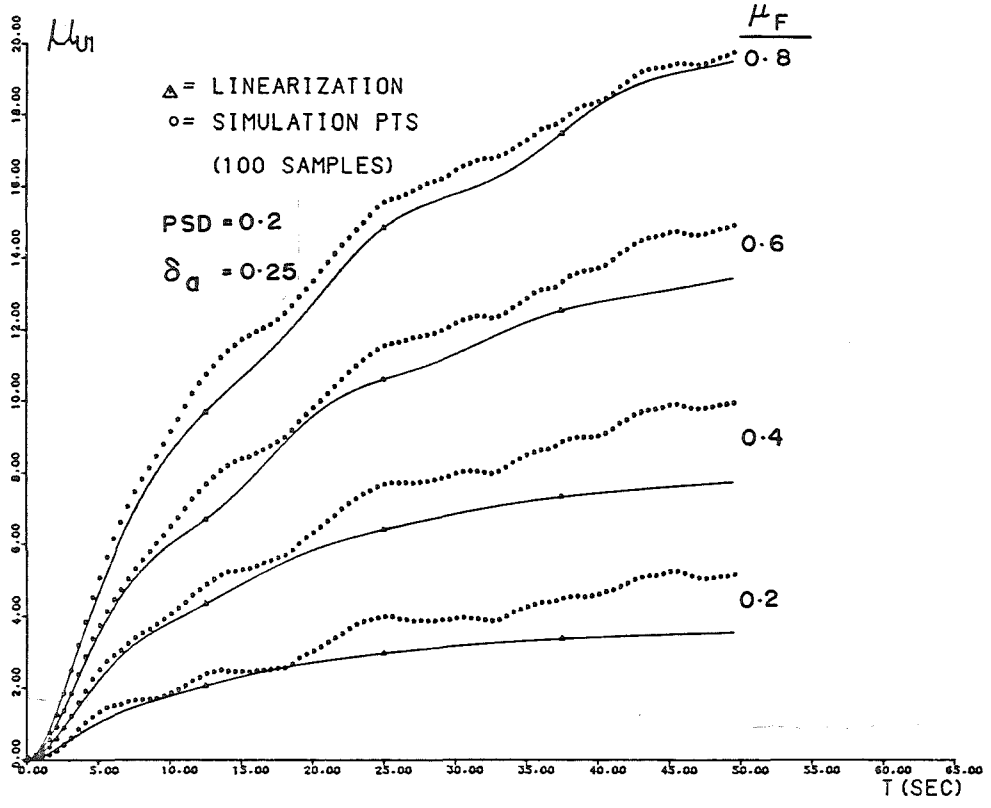

(d)

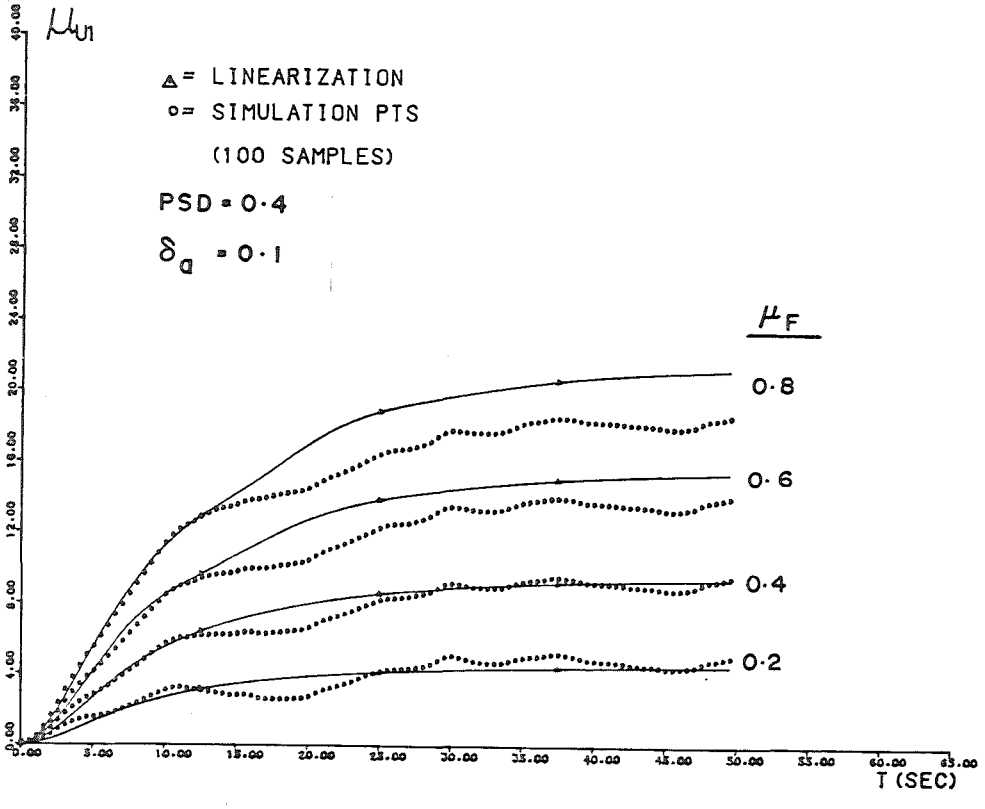

(e)

FIG. 4.6 (Cont'd)

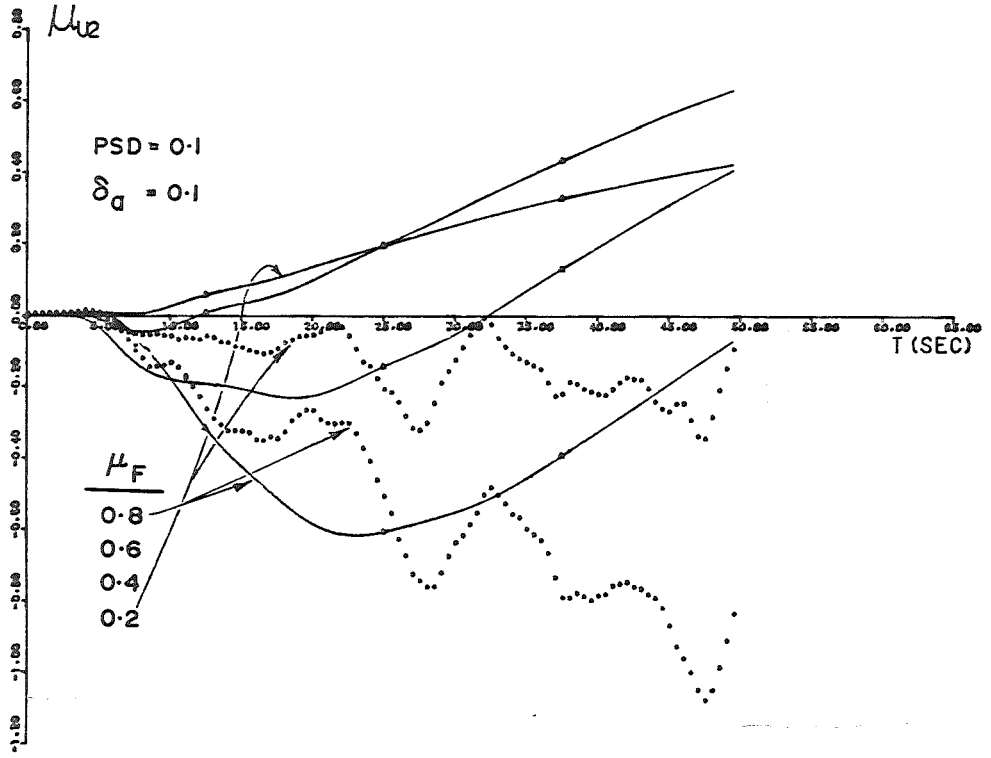

(a)

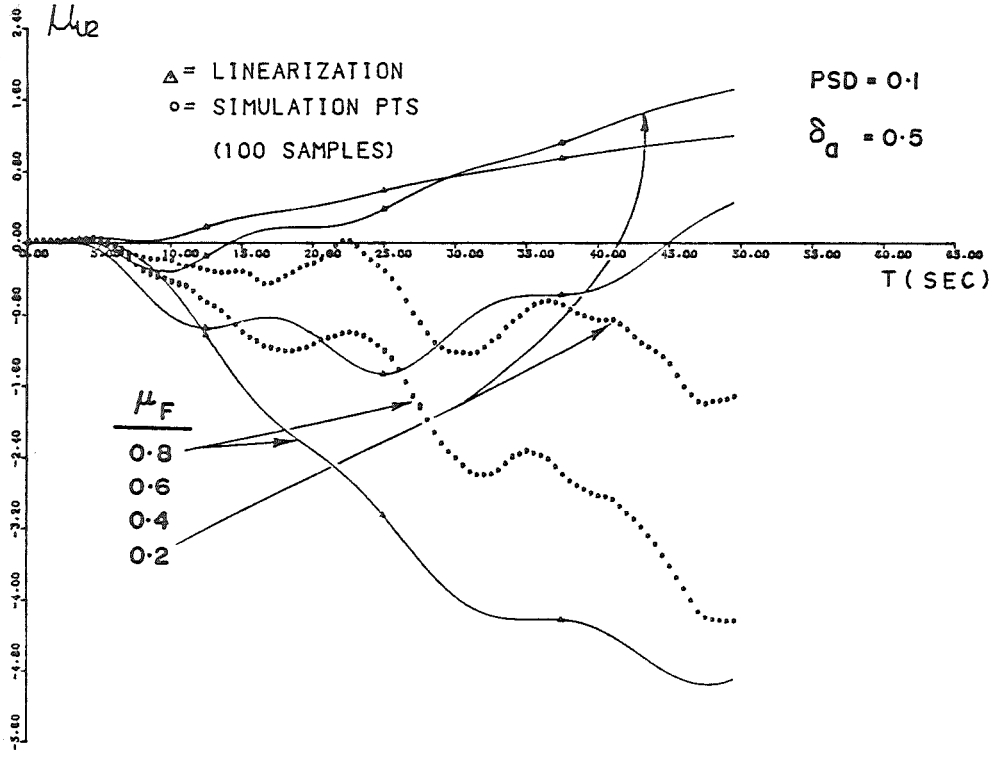

(b)

FIG. 4.7 - MEAN DISPLACEMENT RESPONSE OF S-L COMPONENT OF MODEL UNDER NONZERO MEAN STATIONARY WHITE NOISE INPUT. $\sigma = 0.08$, $\delta_\sigma = 0$.

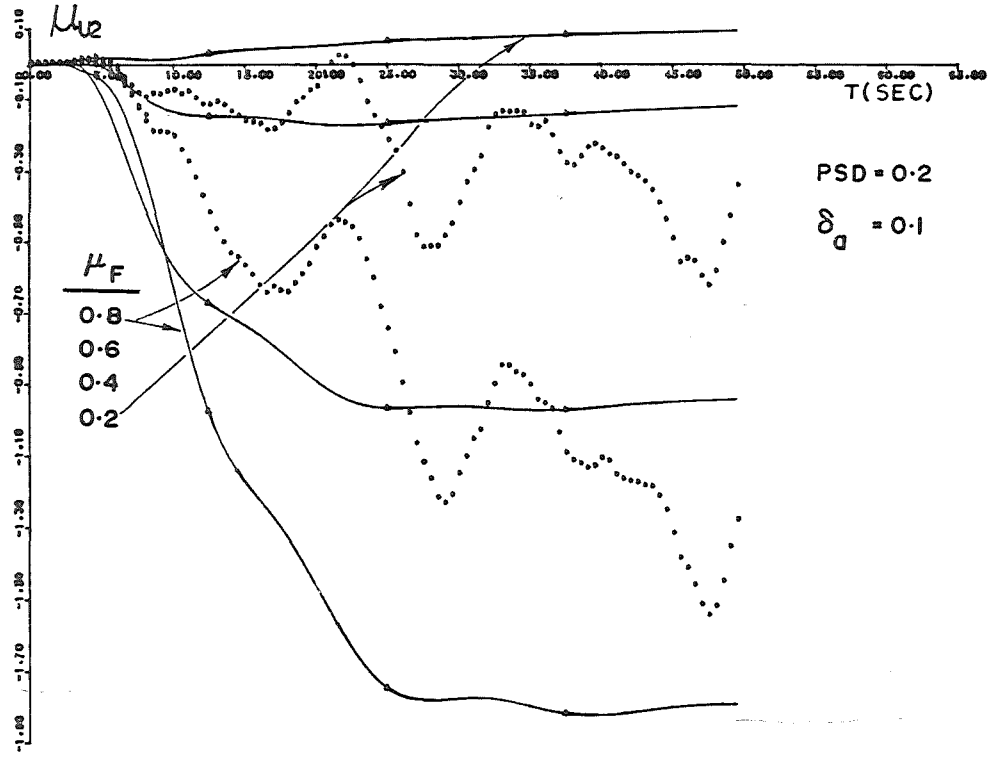

(c)

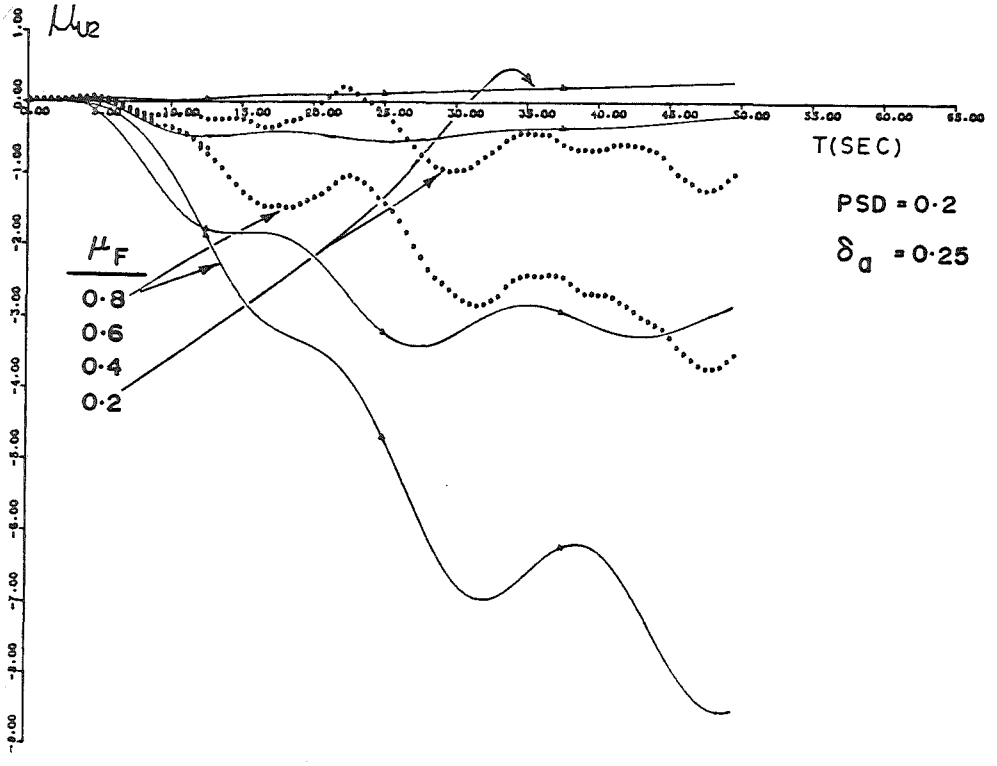

(d)

FIG. 4.7 (Cont'd)

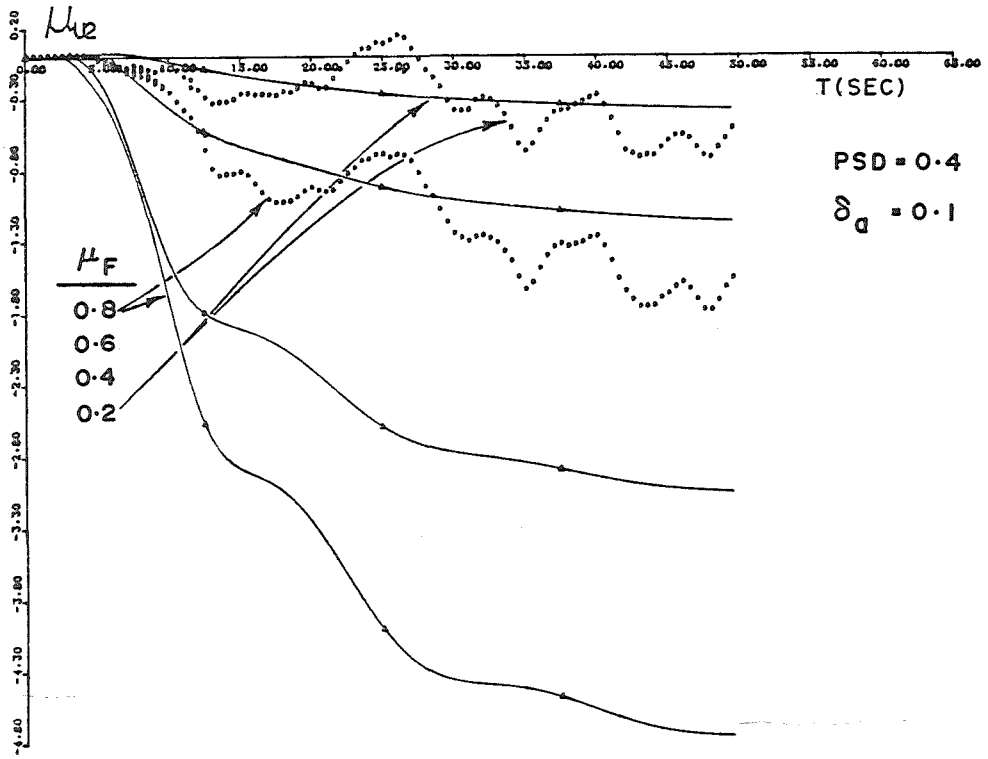

(e)

FIG. 4.7 (Cont'd)

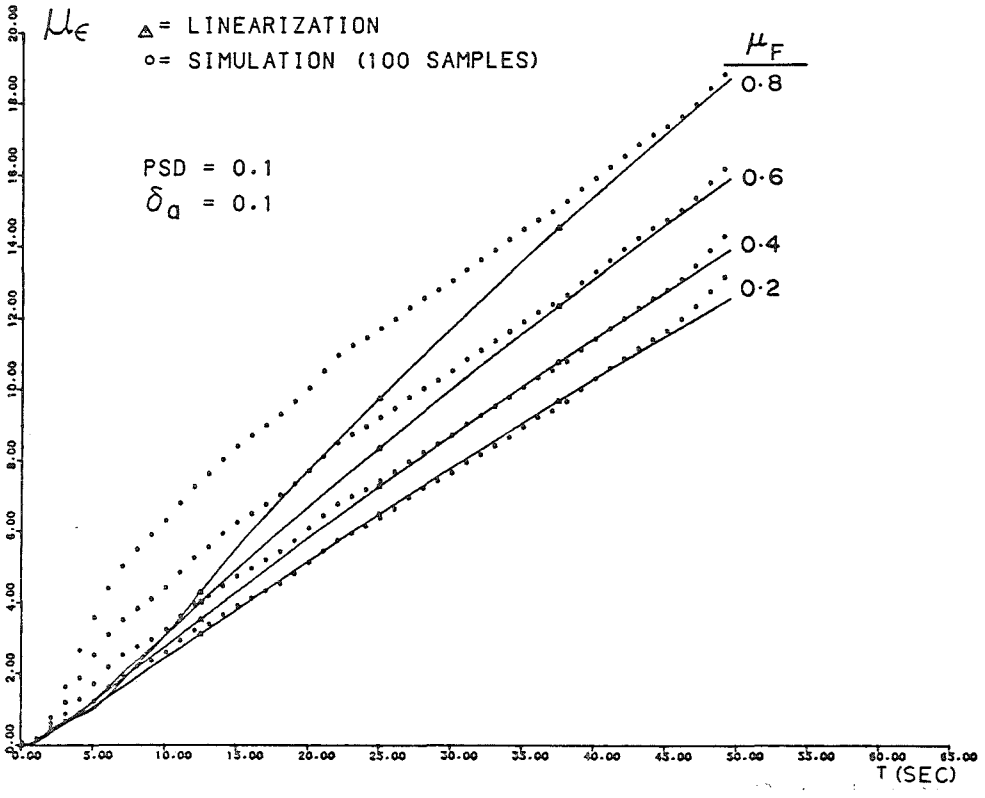

(a)

FIG. 4.8 - MEAN ENERGY DISSIPATION OF A SDOF BN MODEL UNDER NONZERO MEAN STATIONARY WHITE NOISE INPUT. $\sigma = 0.08$, $\delta_{\sigma=0}$.

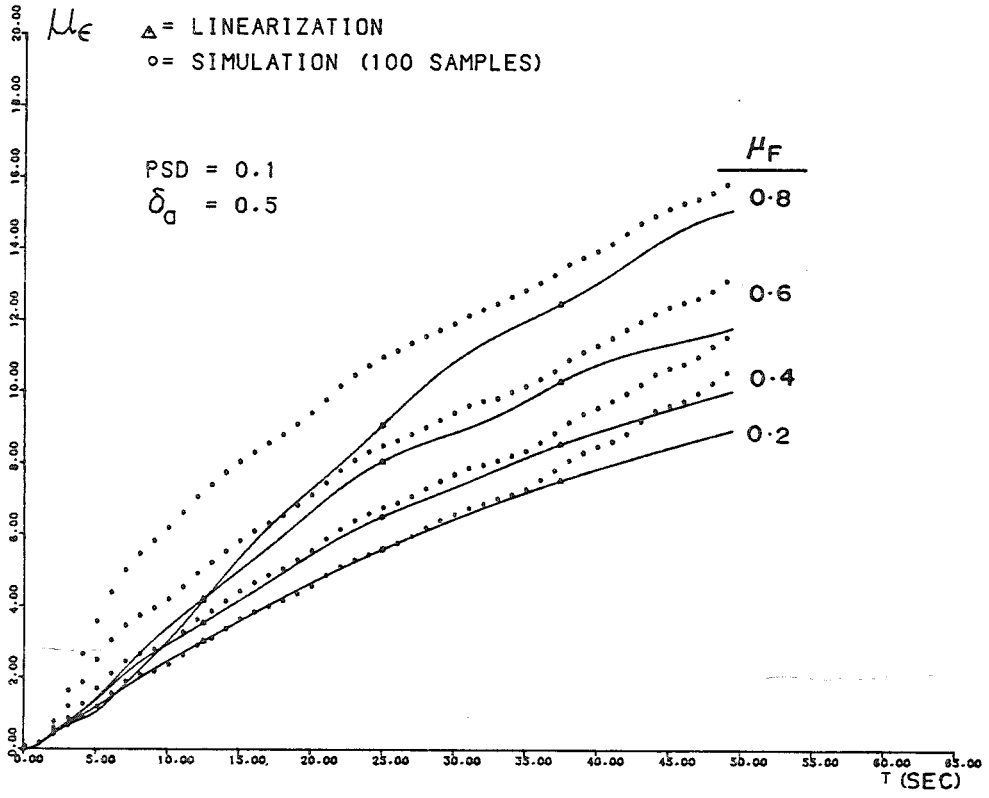

(b)

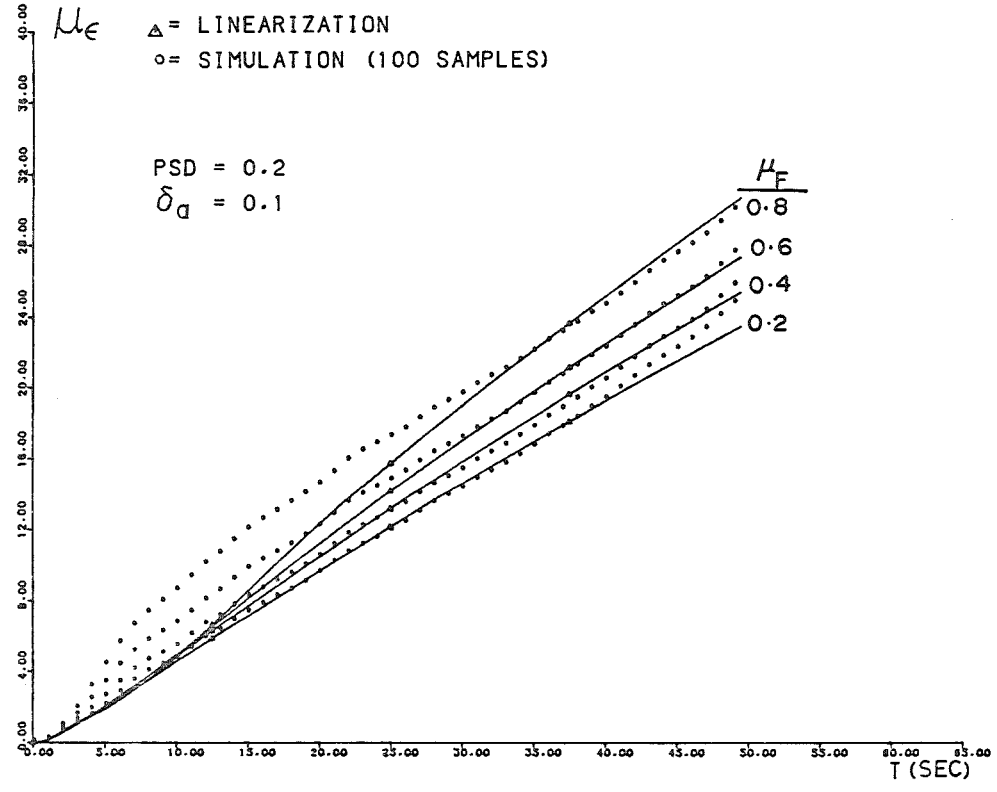

(c)

FIG. 4.8 (Cont'd)

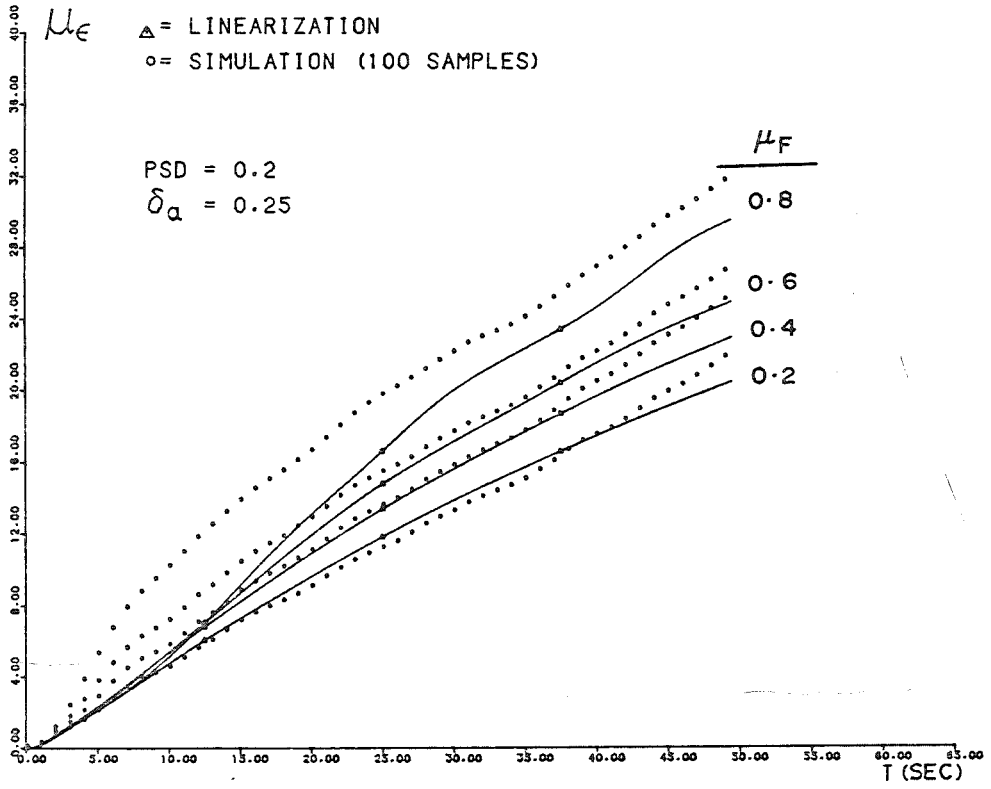

(d)

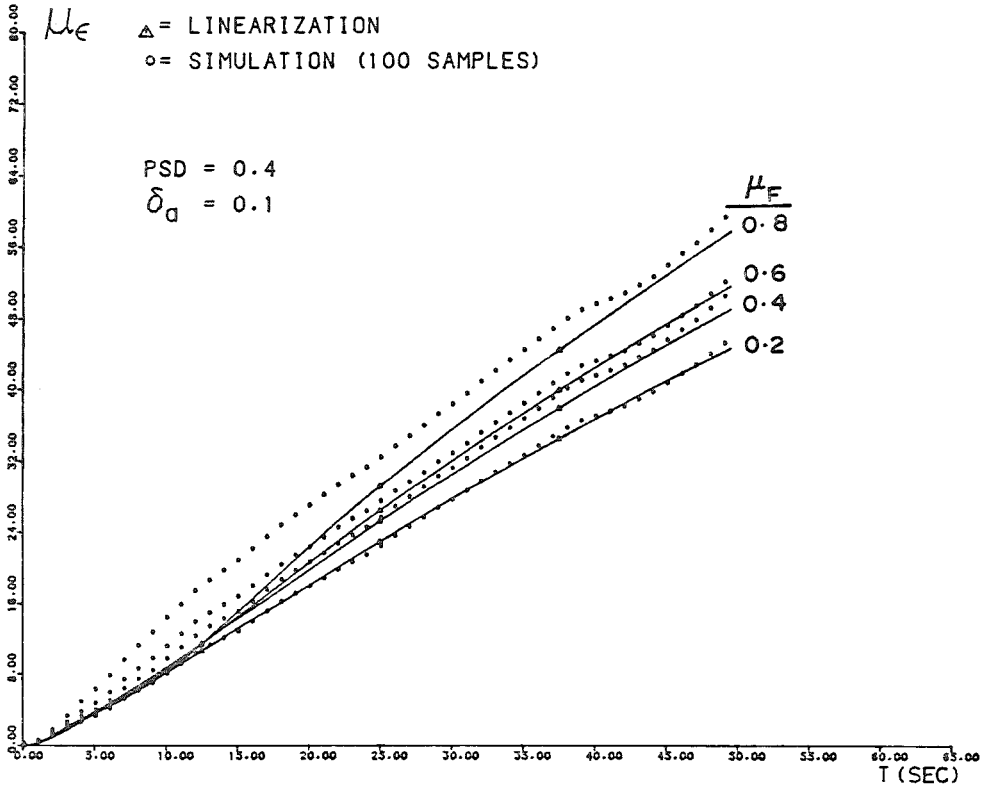

(e)

FIG. 4.8 (Cont'd)

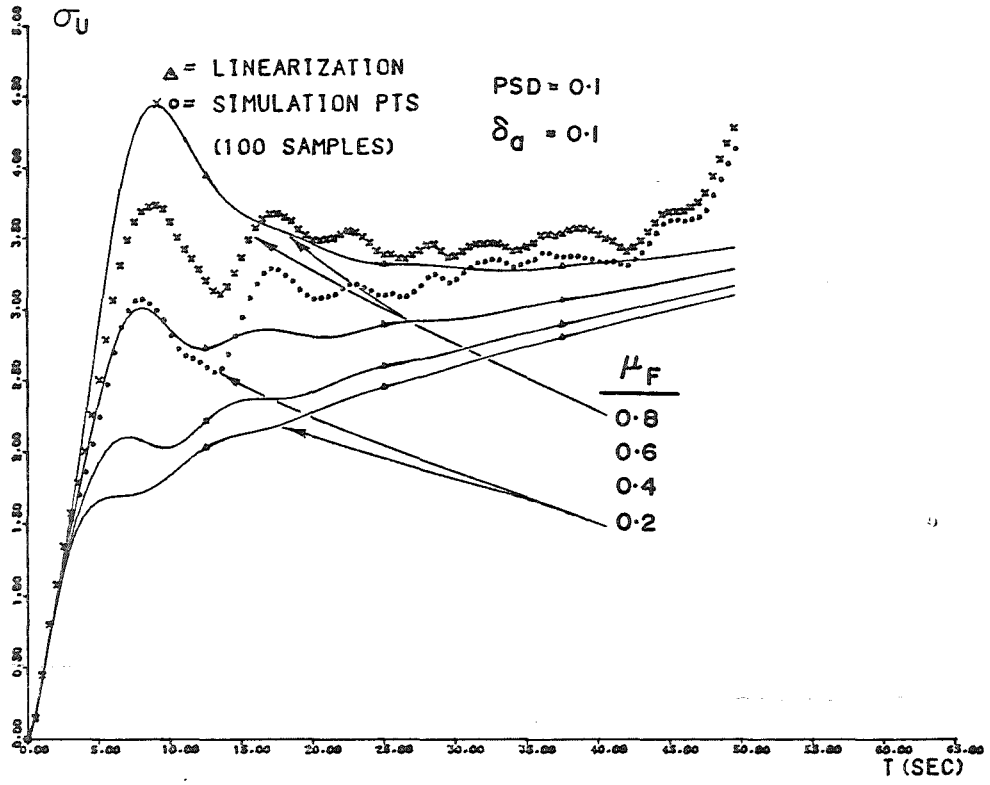

(a)

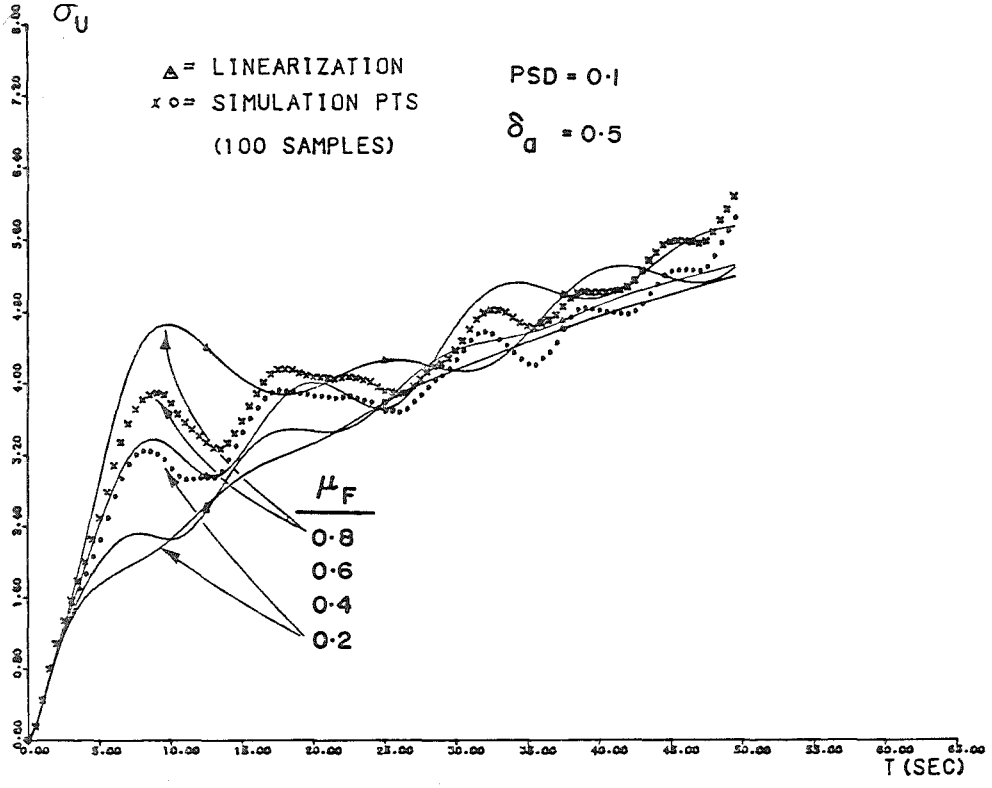

(b)

FIG. 4.9 - NONSTATIONARY RMS DISPLACEMENT RESPONSE OF SDOF B-N MODEL UNDER NONZERO MEAN STATIONARY WHITE NOISE INPUT. $\sigma = 0.08$, $\delta_\sigma = 0$.

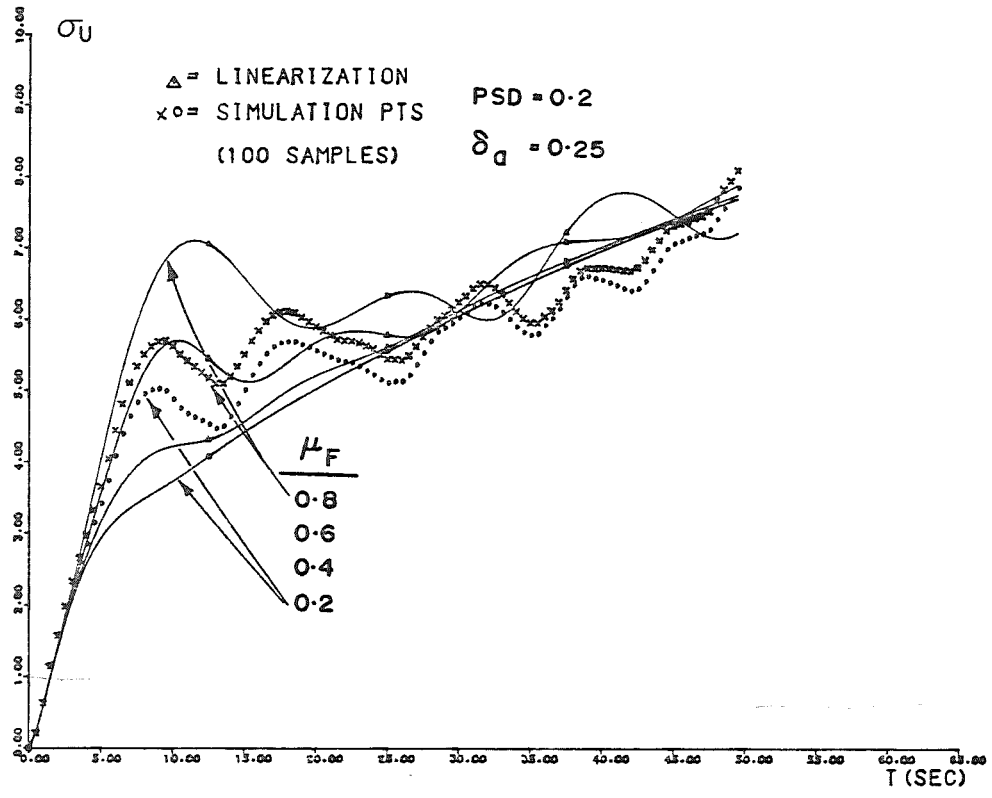

(c)

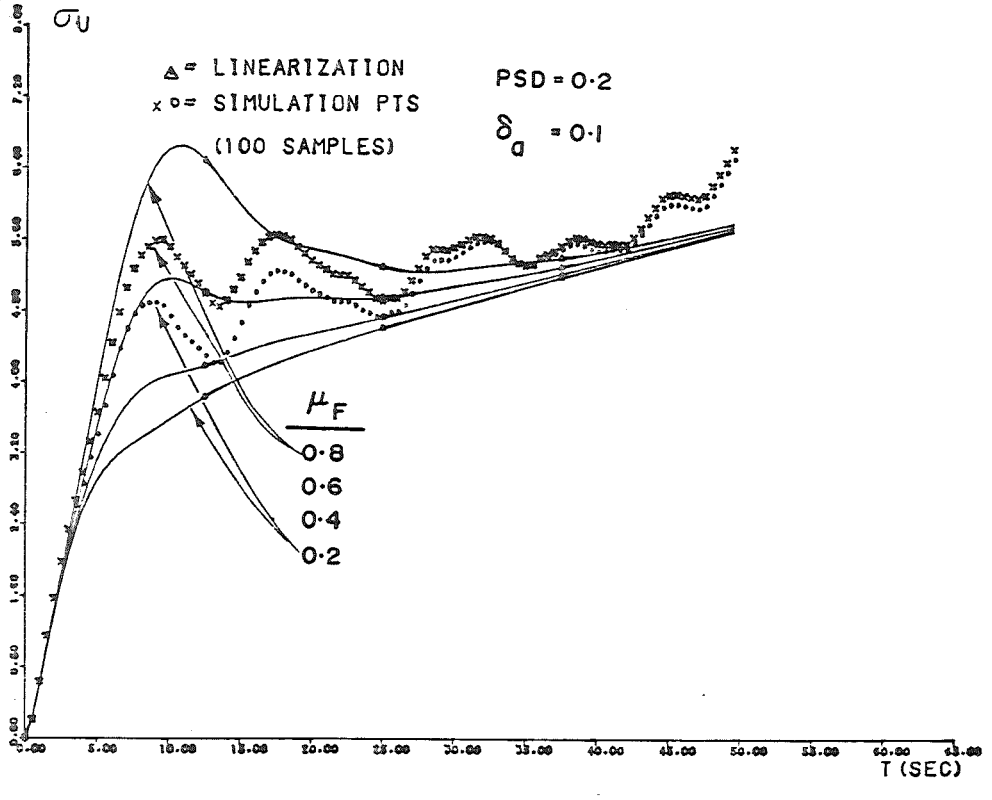

(d)

FIG. 4.9 (Cont'd)

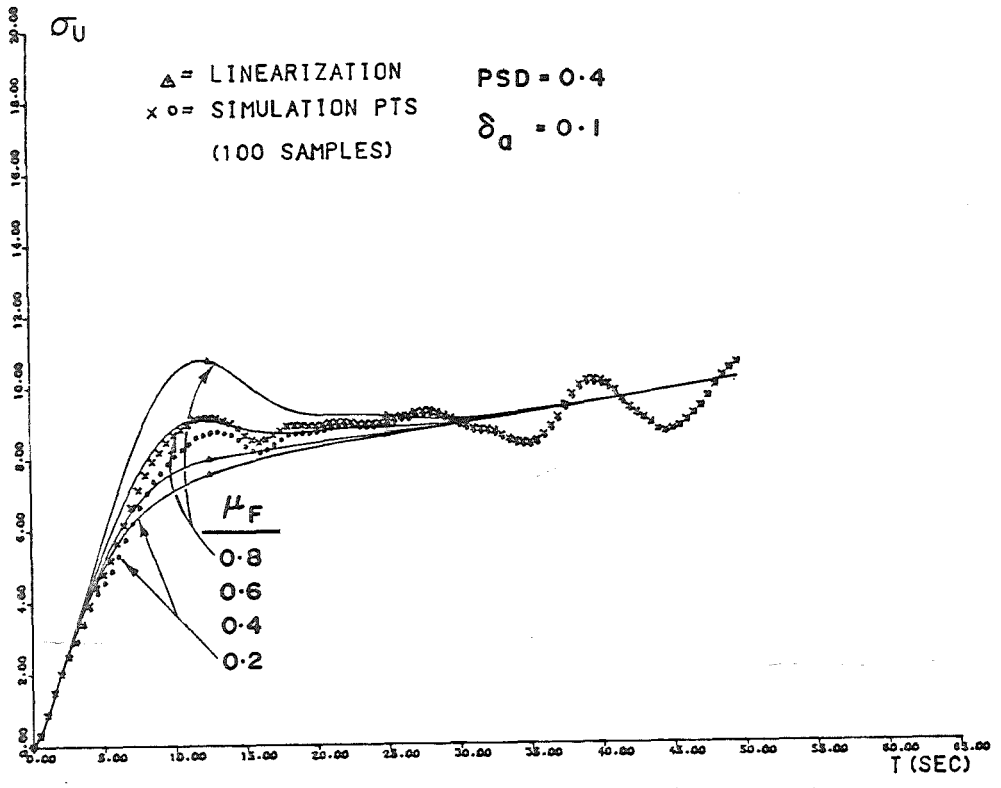

(e)

FIG. 4.9 (Cont'd)

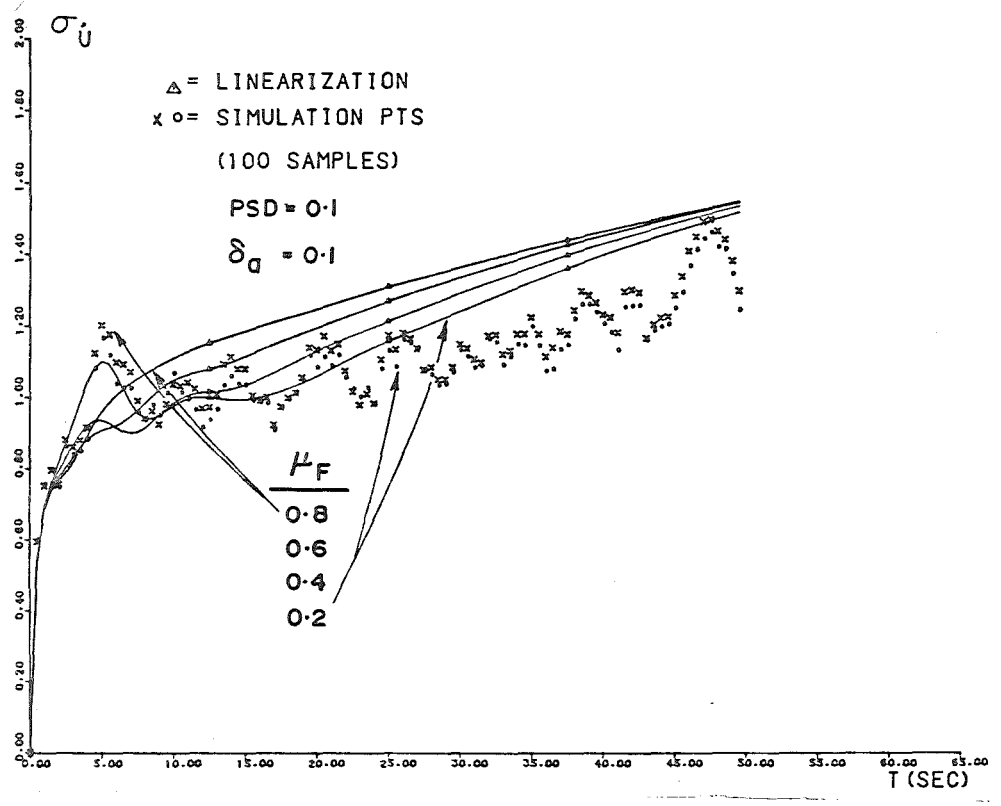

(a)

FIG. 4.10 - NONSTATIONARY RMS VELOCITY RESPONSE OF SDOF B-N MODEL UNDER NONZERO MEAN STATIONARY WHITE NOISE INPUT. σ=0·08, δ_σ = 0.

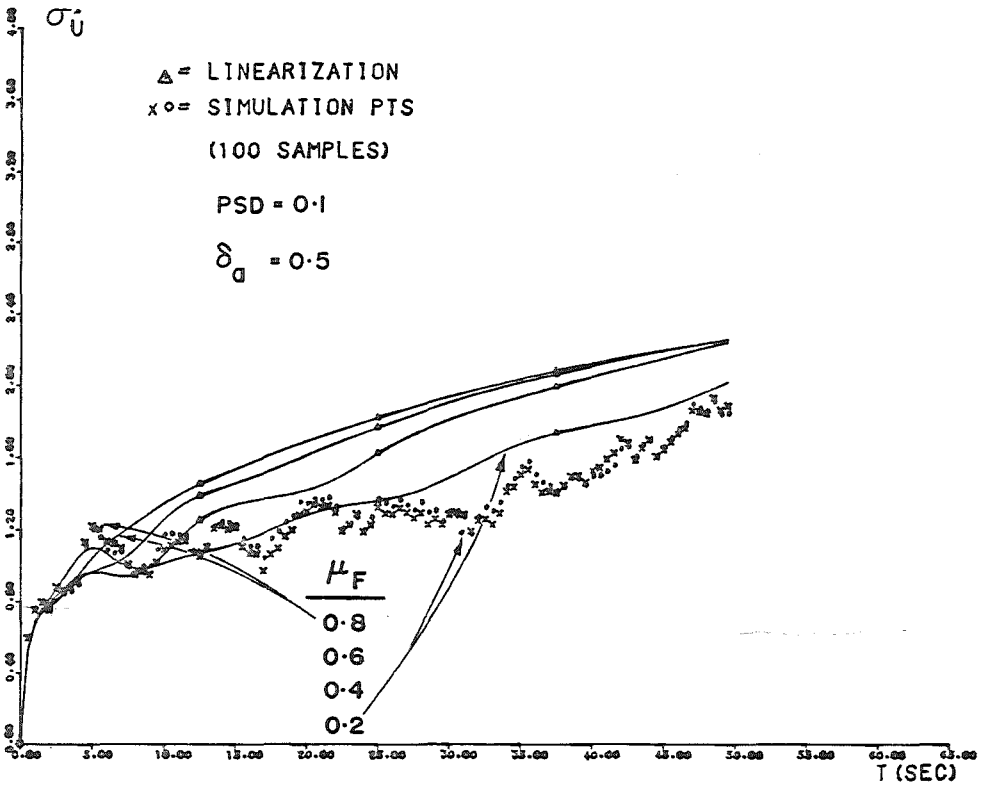

(b)

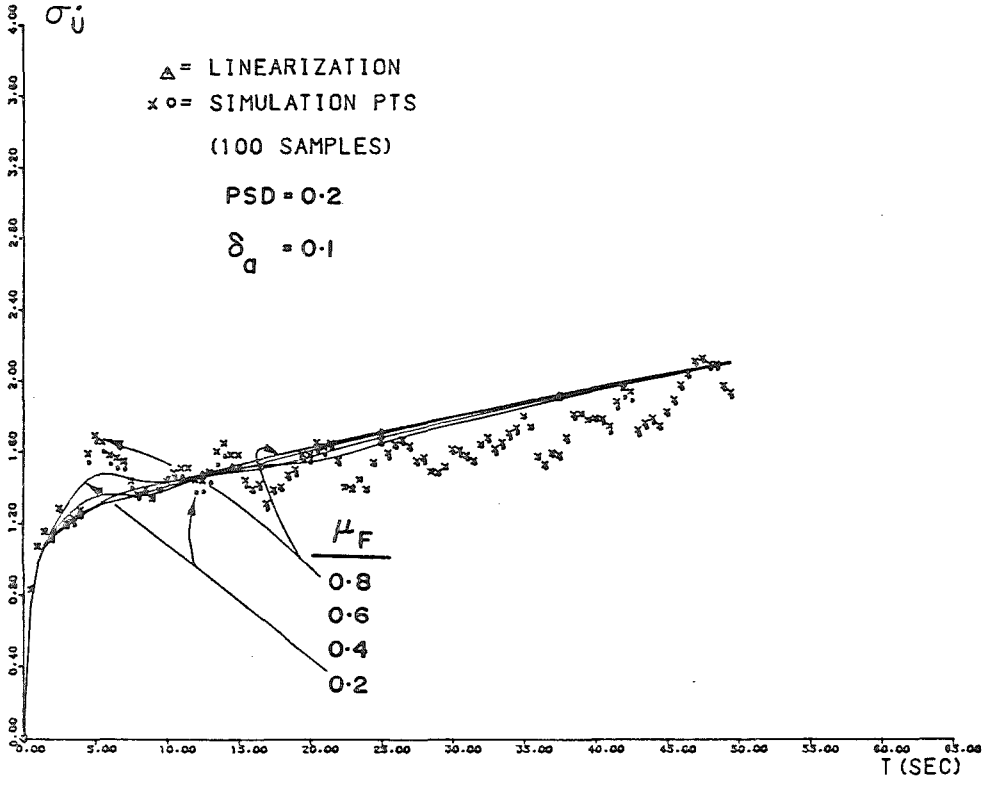

(c)

FIG. 4.10 (Cont'd)

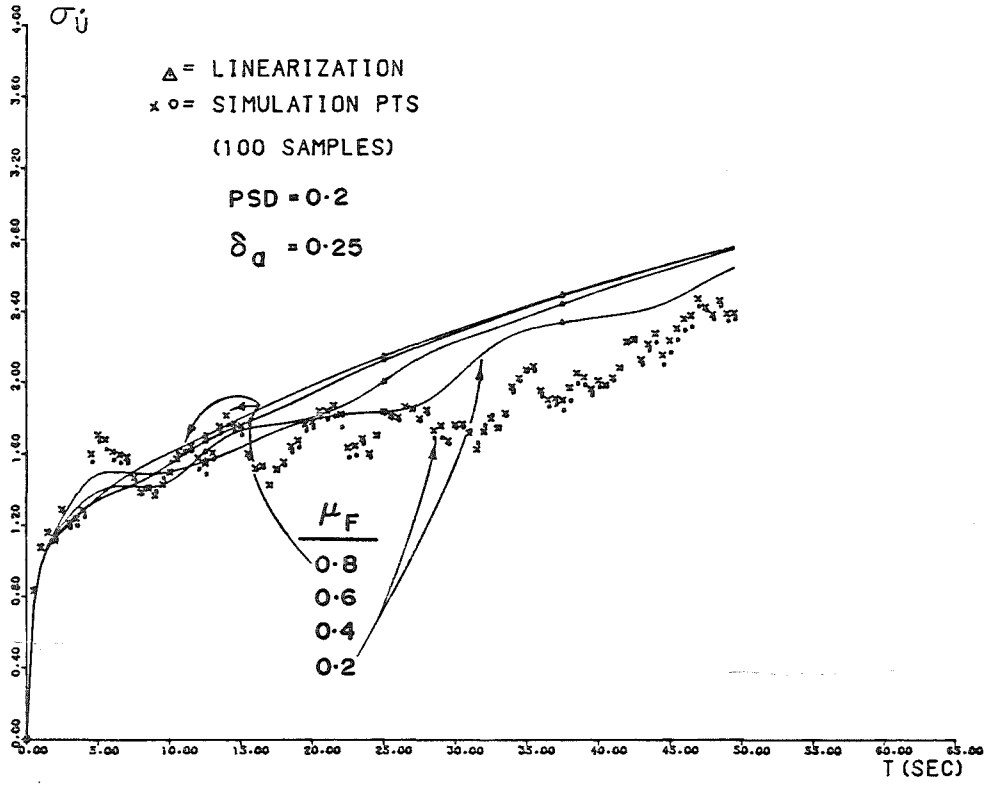

(d)

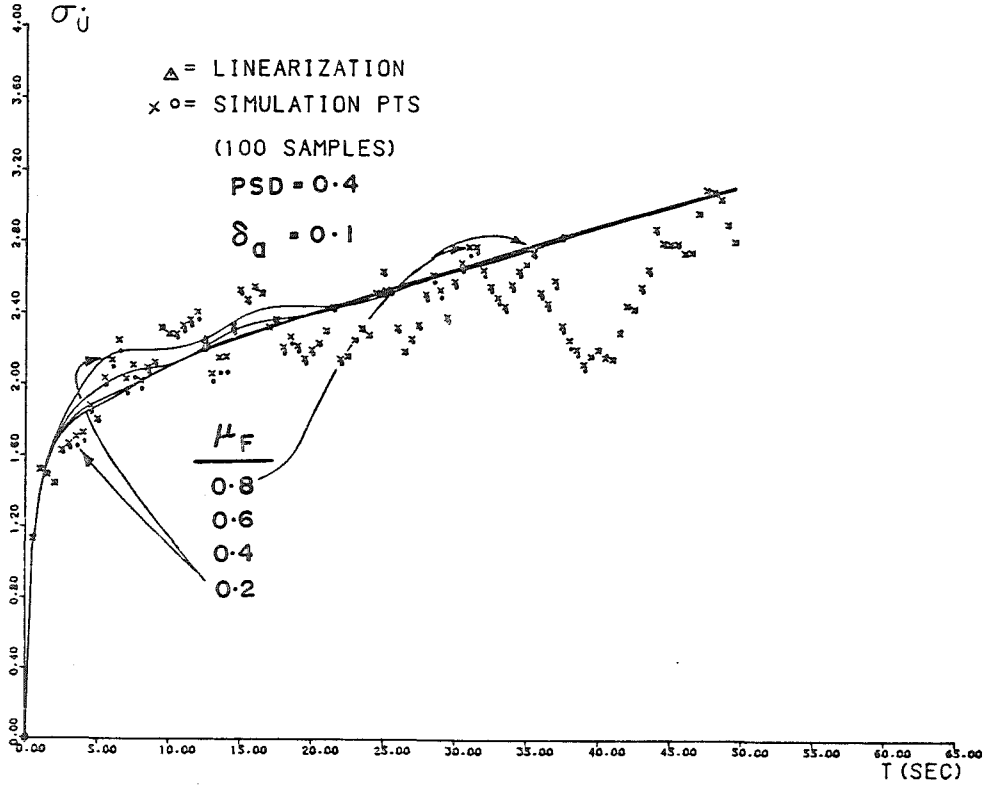

(e)

FIG. 4.10 (Cont'd)

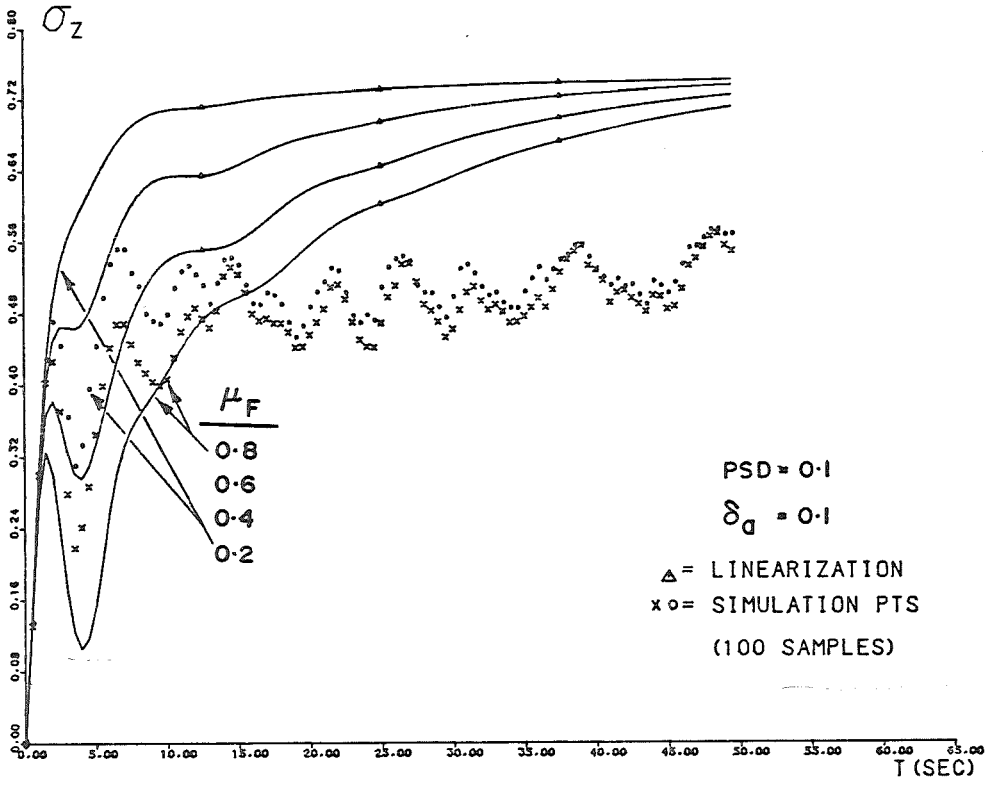

(a)

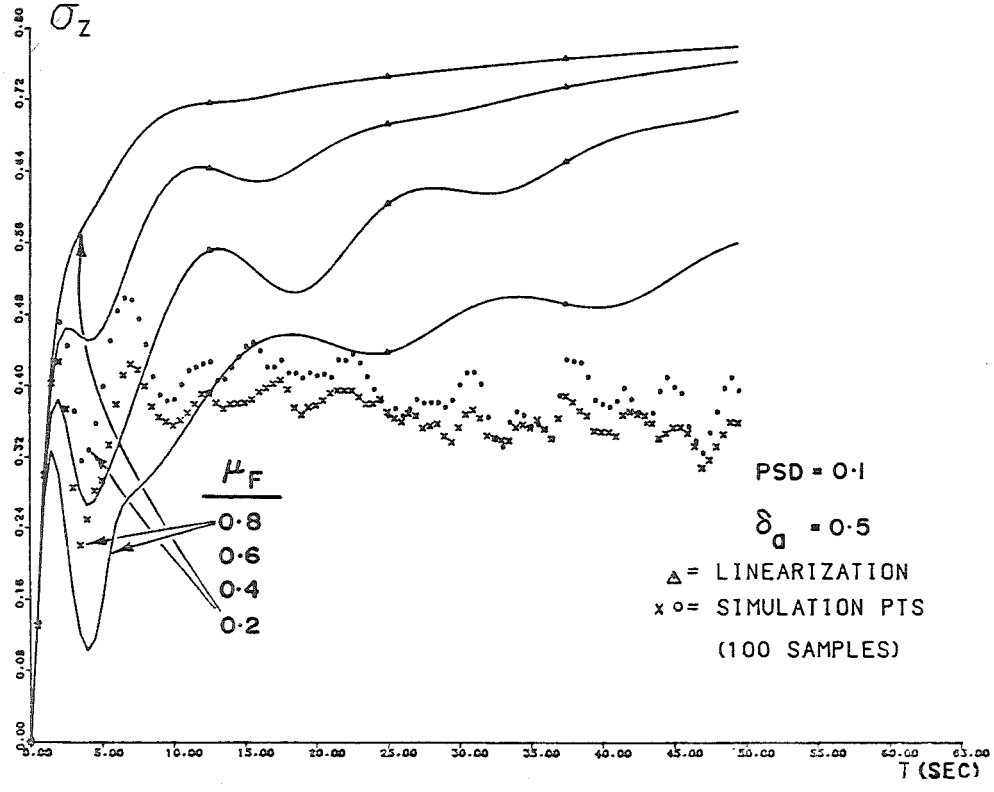

(b)

FIG. 4.11 - RMS HYSTERETIC RESTORING FORCE RESPONSE OF SDOF B-N MODEL UNDER NONZERO MEAN STATIONARY WHITE NOISE INPUT. $\sigma = 0.08$, $\delta_\sigma = 0$.

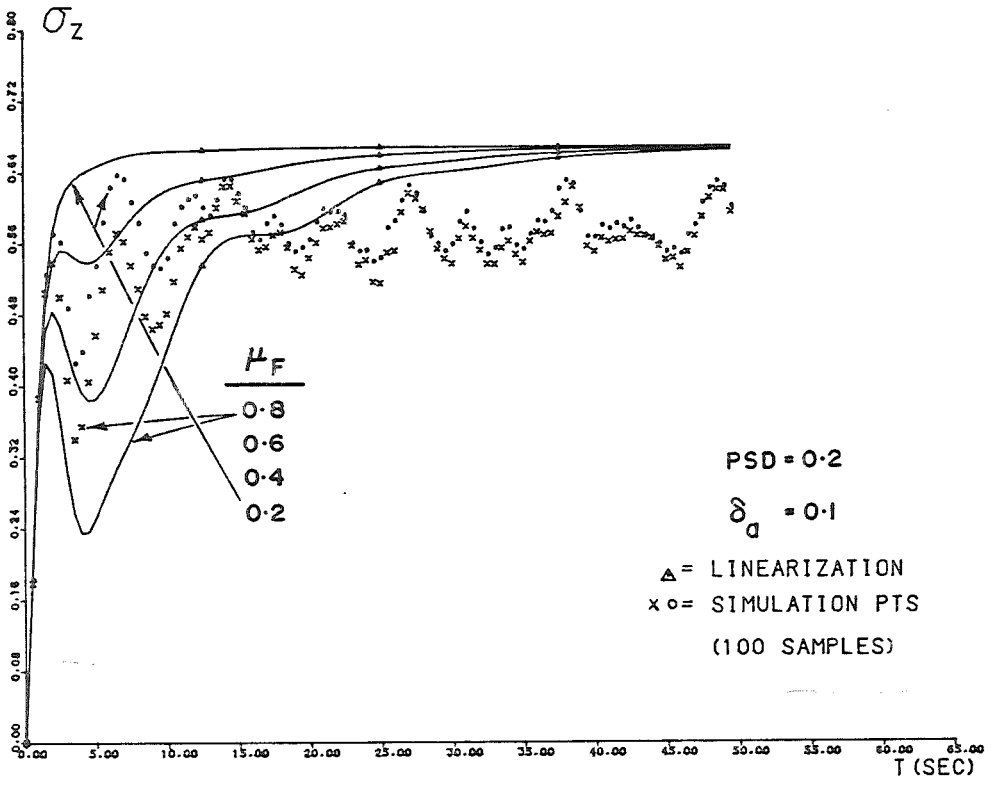

(c)

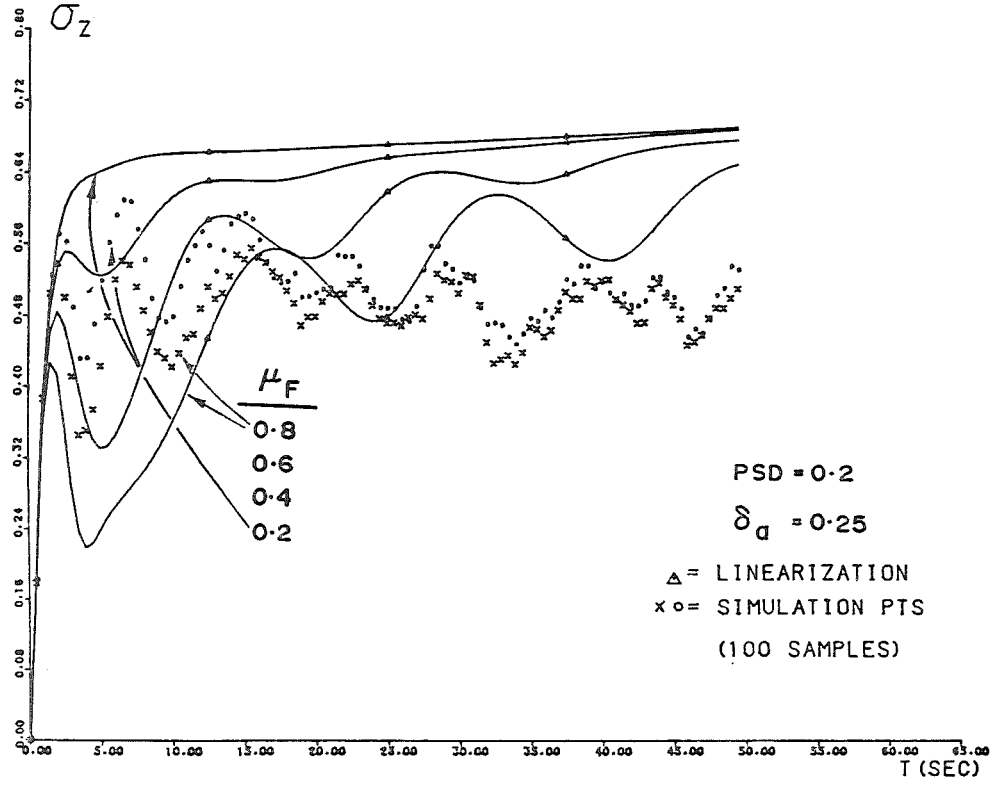

(d)

FIG. 4.11 (Cont'd)

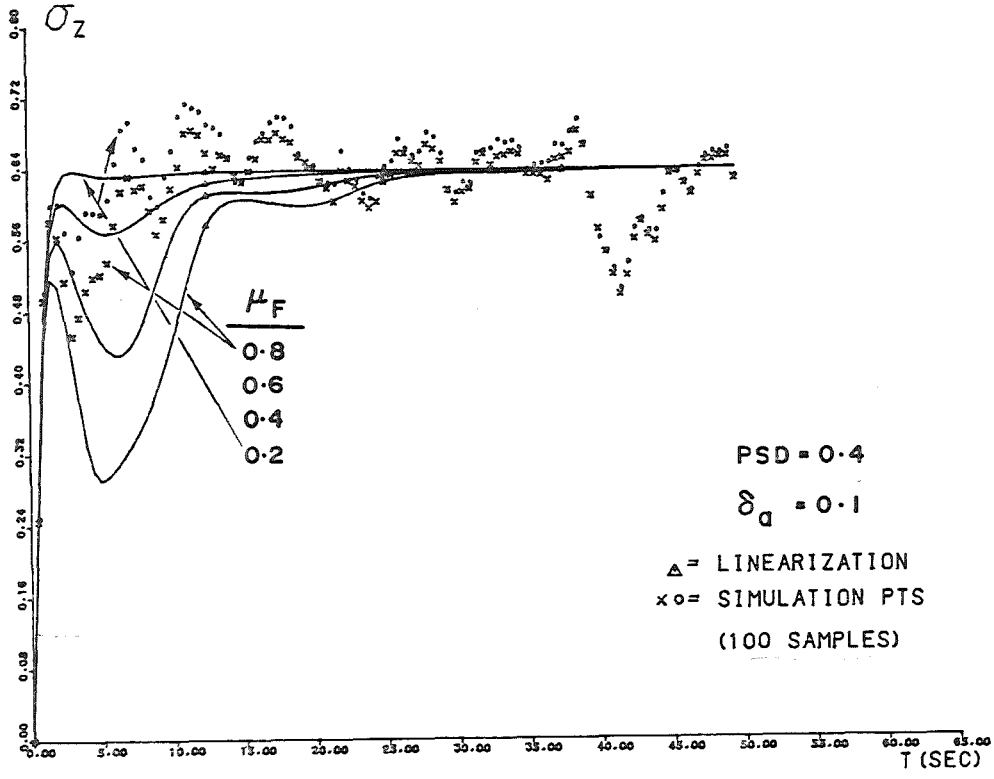

(e)

FIG. 4.11 (Cont'd)

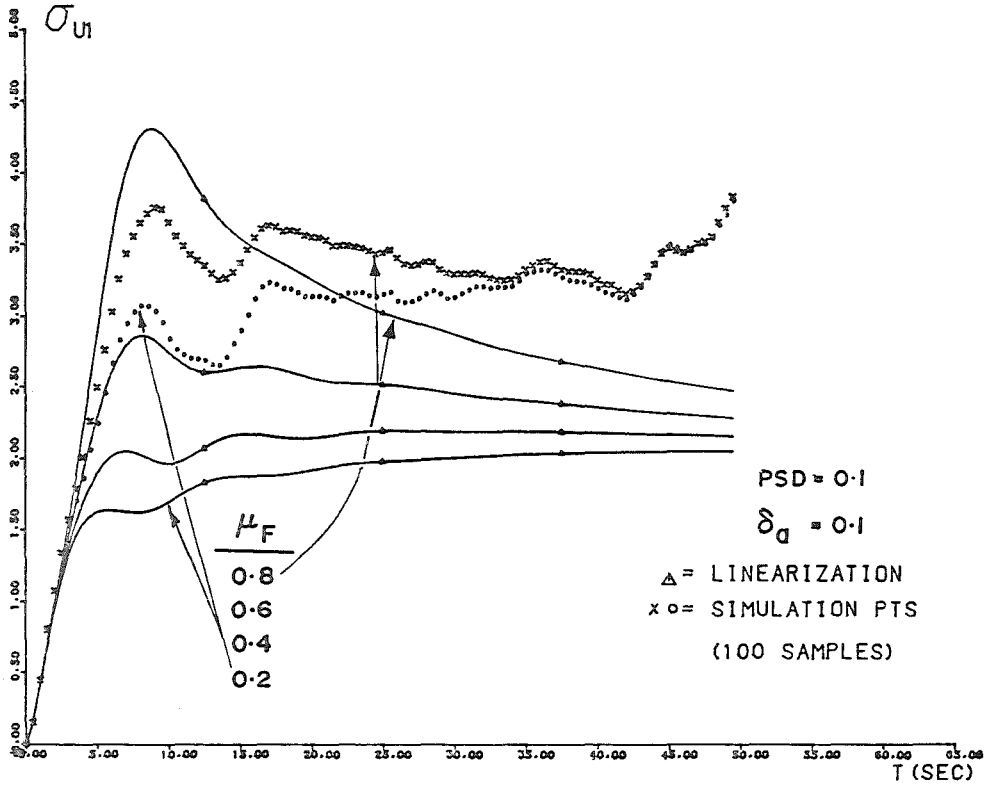

(a)

FIG. 4.12- RMS DISPLACEMENT RESPONSE OF SMOOTH ELEMENT IN MODEL UNDER NONZERO MEAN STATIONARY WHITE NOISE INPUT. $\sigma = 0.08$, $\delta_\sigma = 0.$

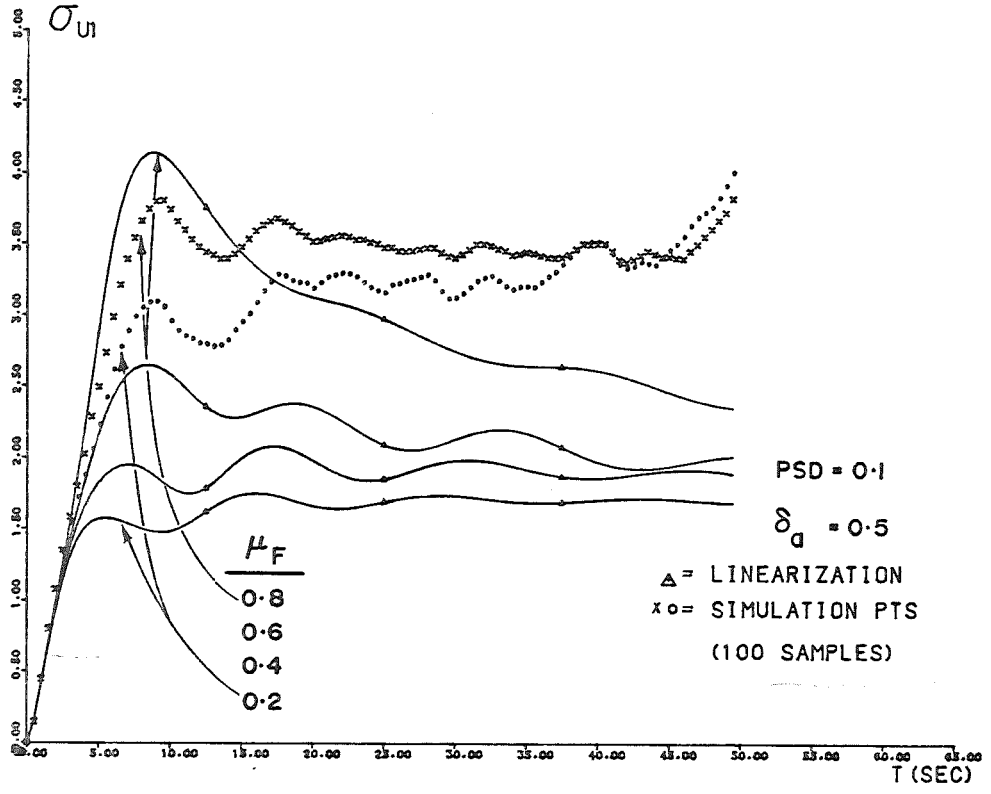

(b)

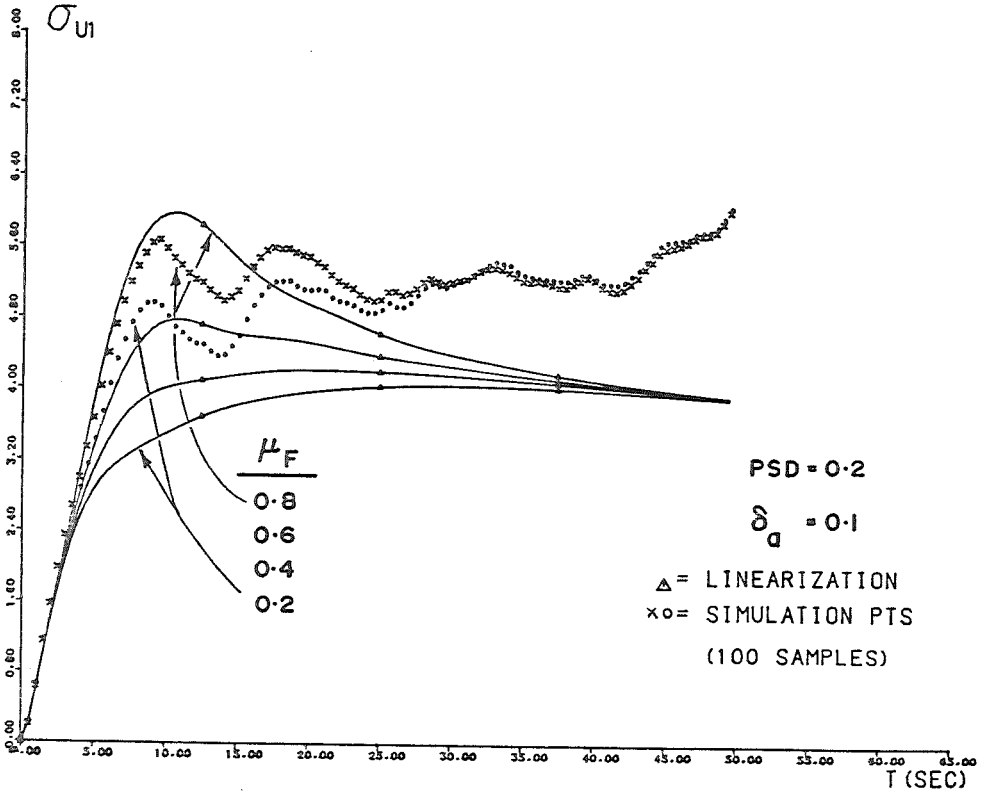

(c)

FIG. 4.12 (Cont'd)

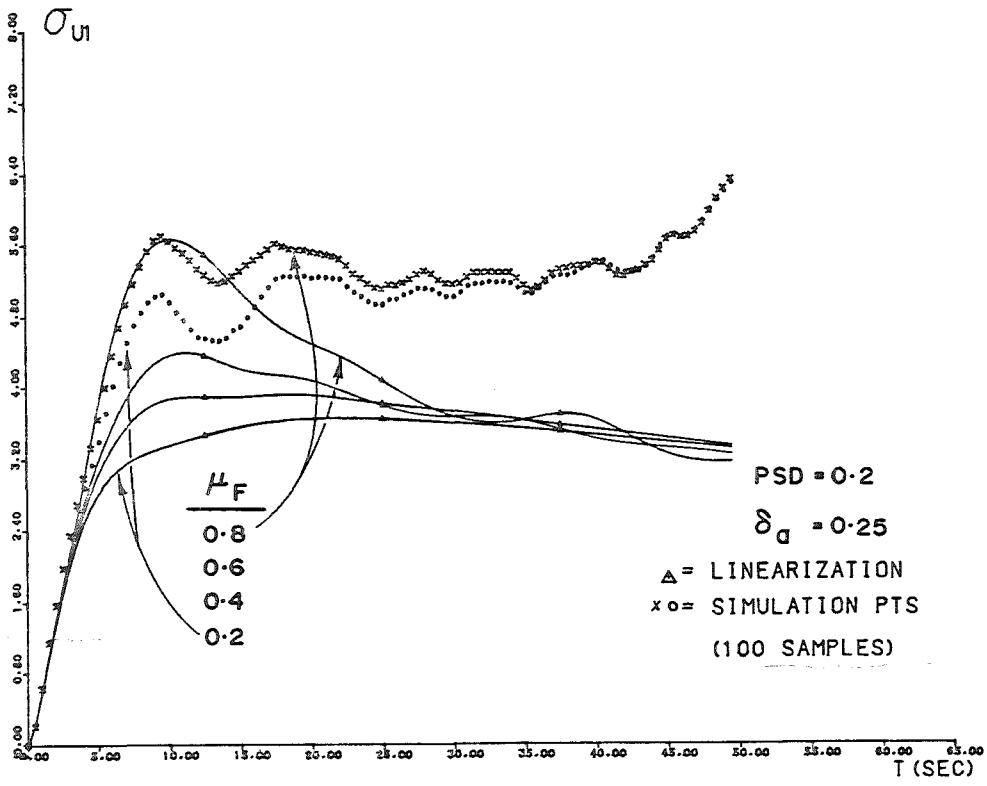

(d)

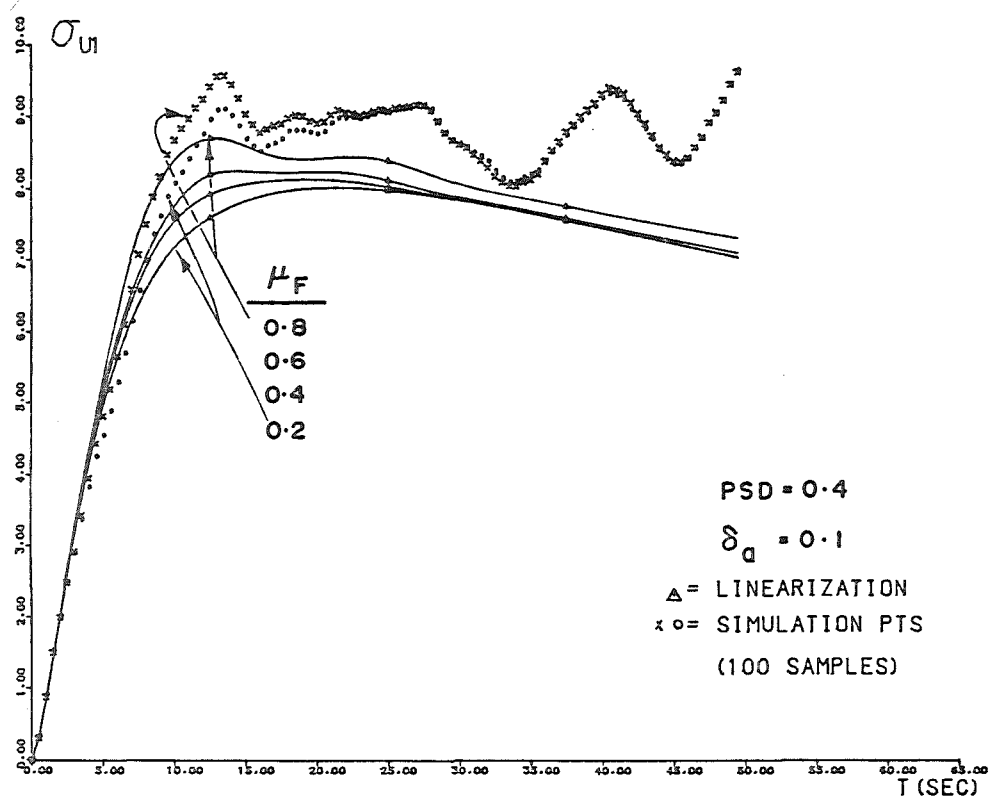

(e)

FIG. 4.12 (Cont'd)

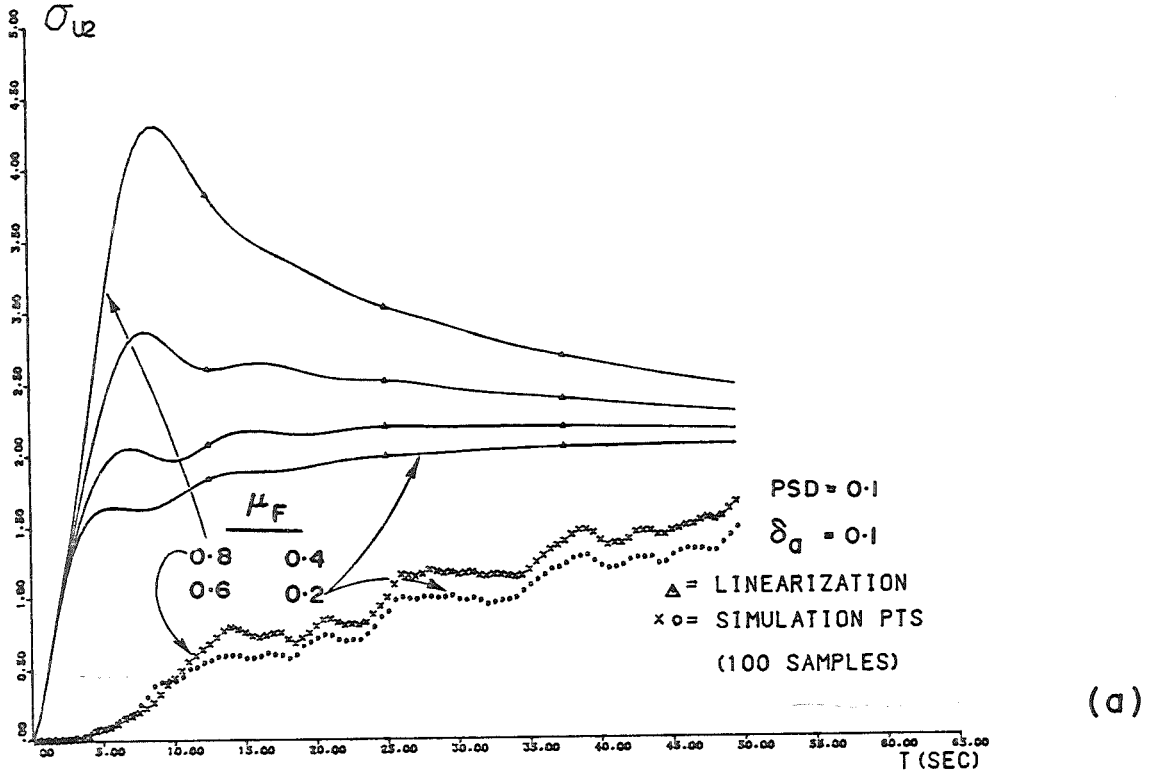

(a)

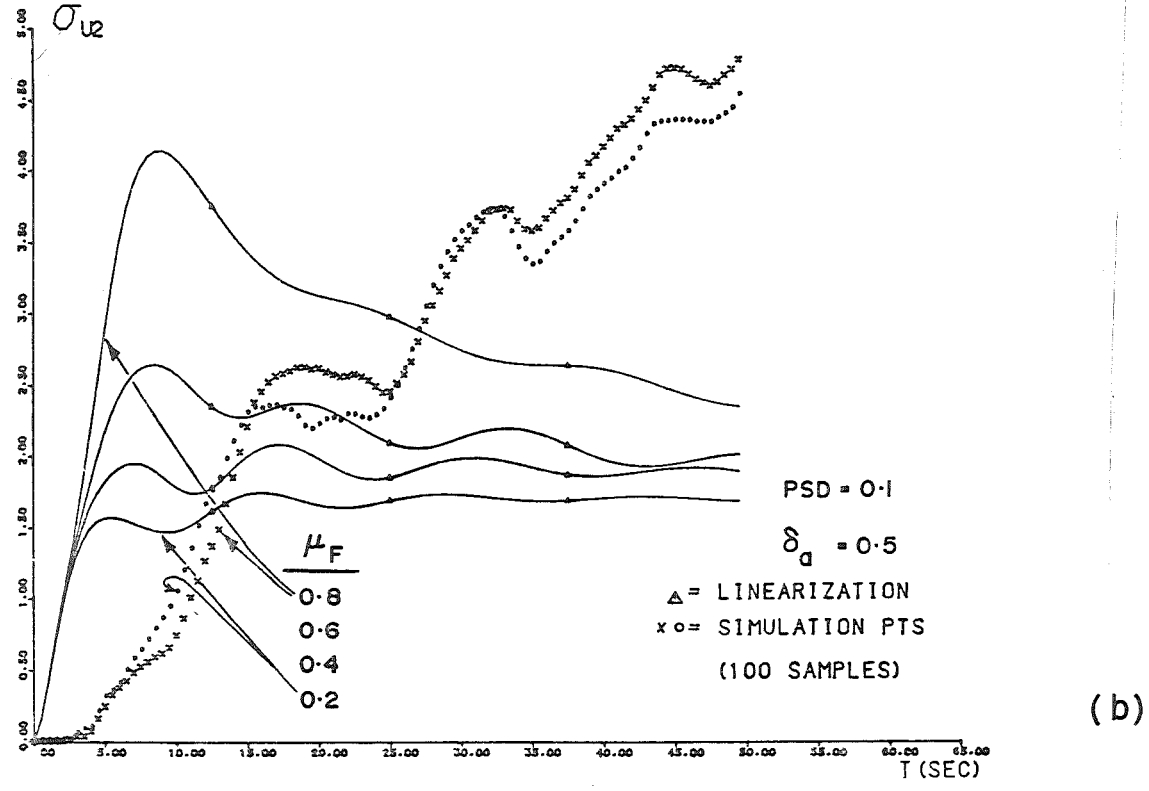

(b)

FIG. 4.13 - RMS DISPLACEMENT RESPONSE OF S-L COMPONENT OF BN MODEL UNDER NONZERO MEAN STATIONARY WHITE NOISE INPUT. $\sigma = 0.08$, $\delta_\sigma = 0$.

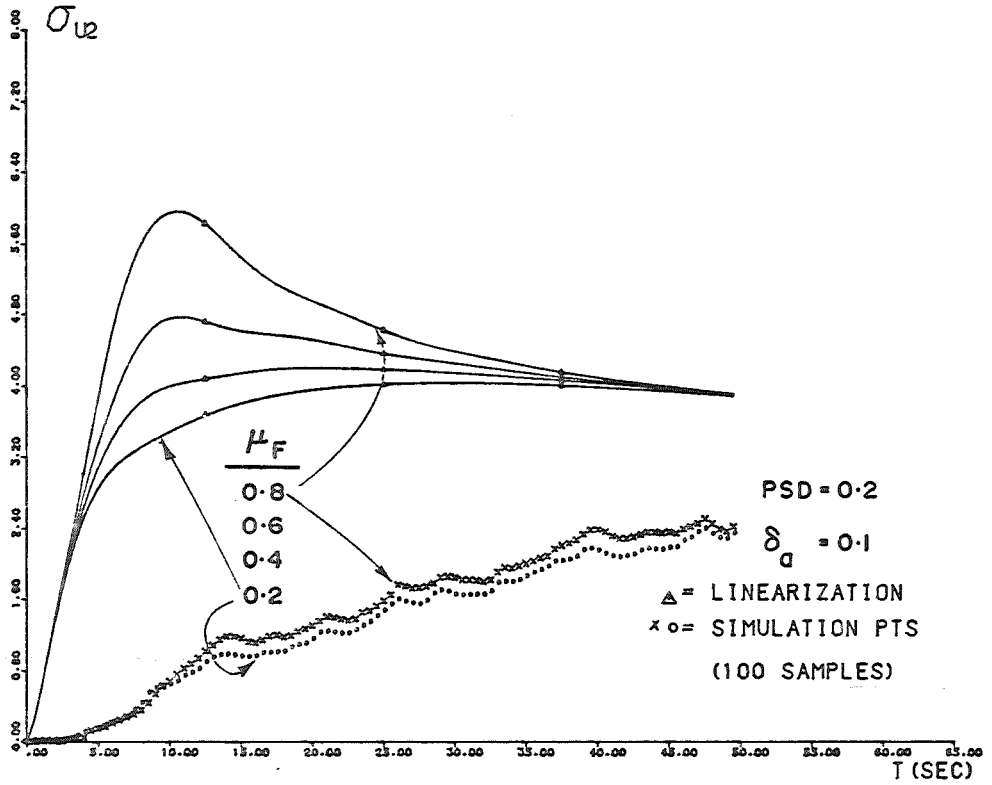

(c)

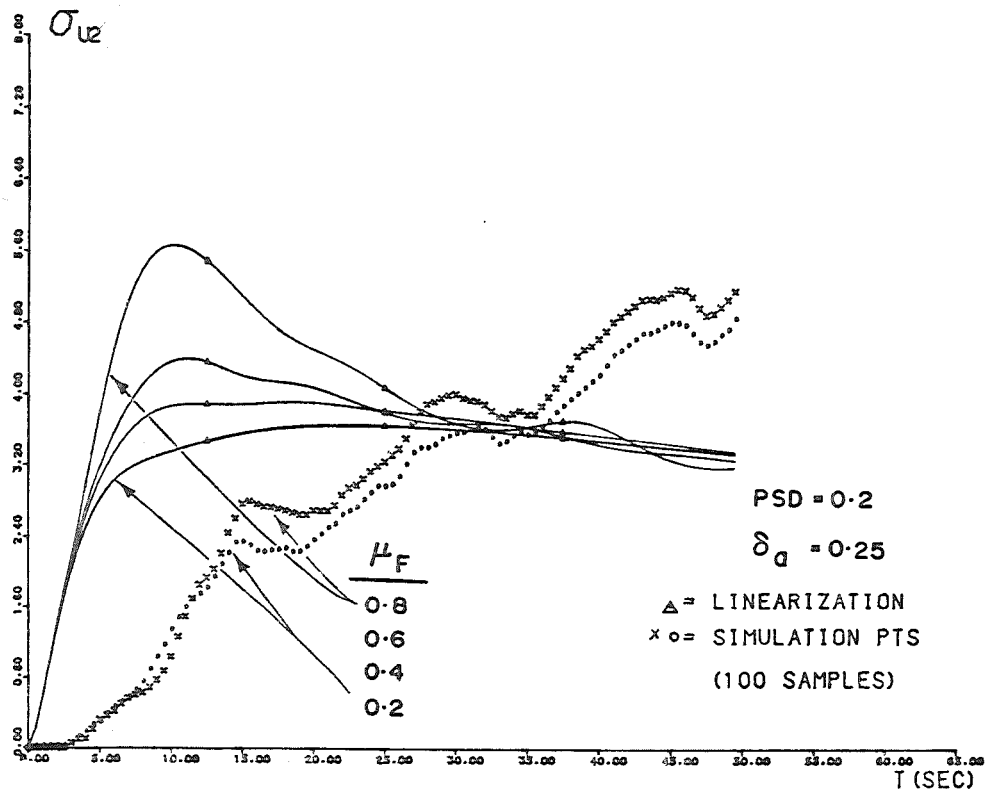

(d)

FIG. 4.13 (Cont'd)

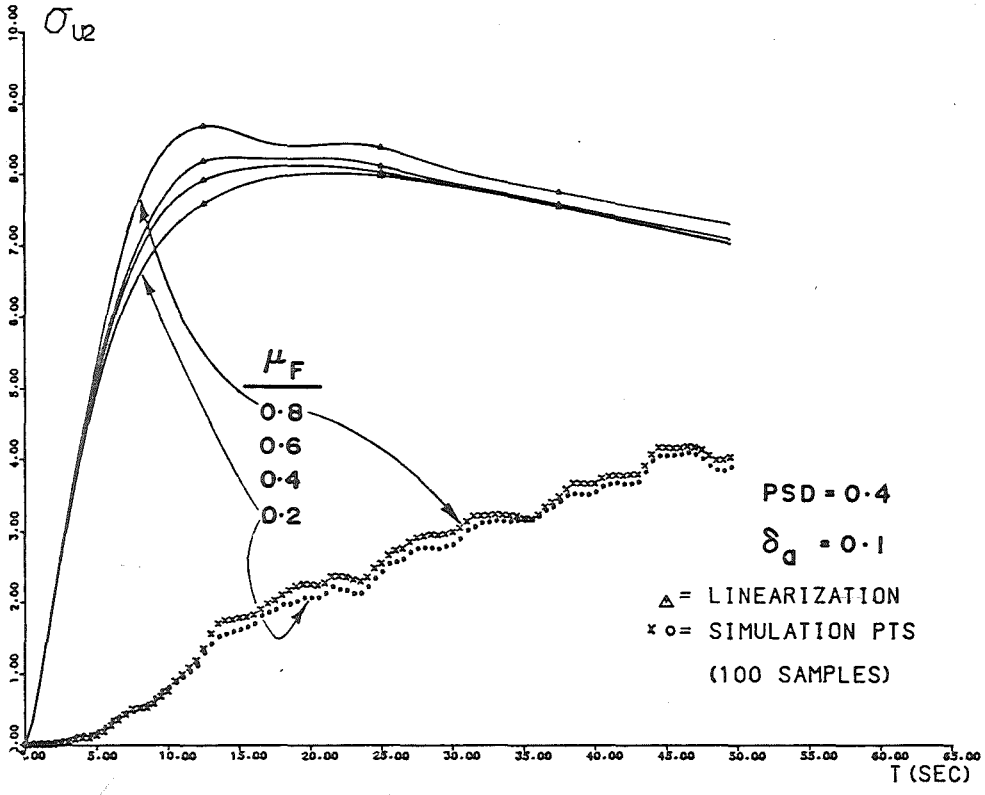

(e)

FIG. 4.13 (Cont'd)

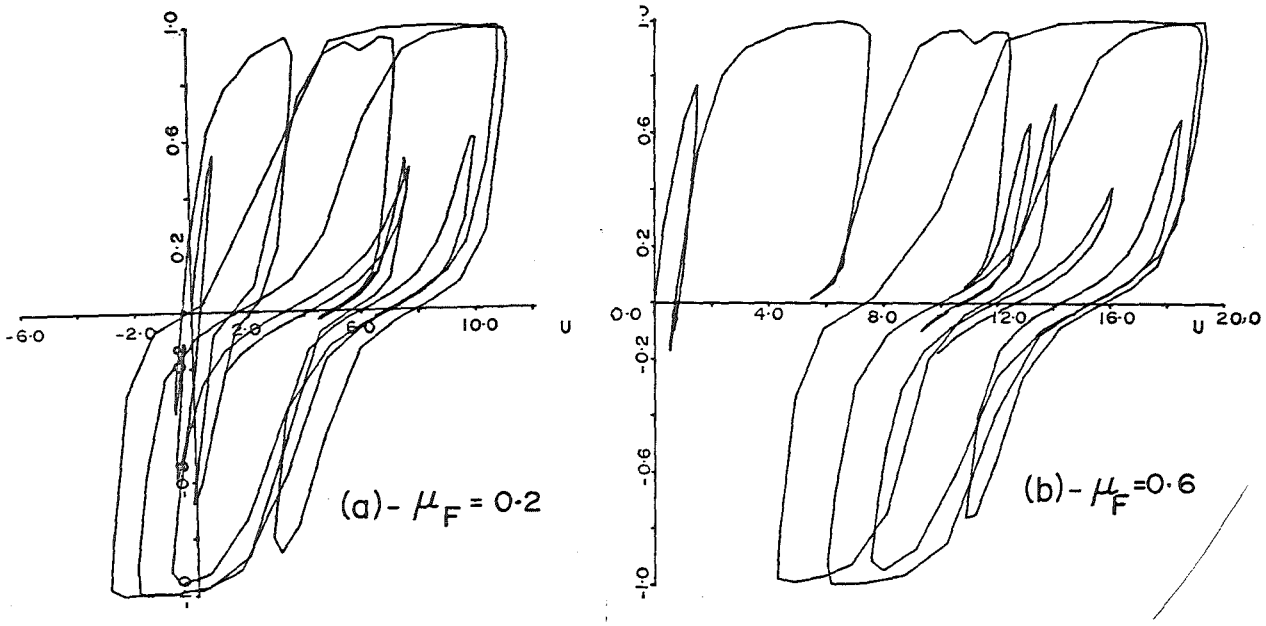

FIG.4·14- PINCHING BEHAVIOR OF SEP MODEL UNDER NONZERO MEAN STATIONARY WHITE NOISE INPUT. PSD = 0.1, ζ = .02, ζ_{10} = .95, AND λ = 0.15.

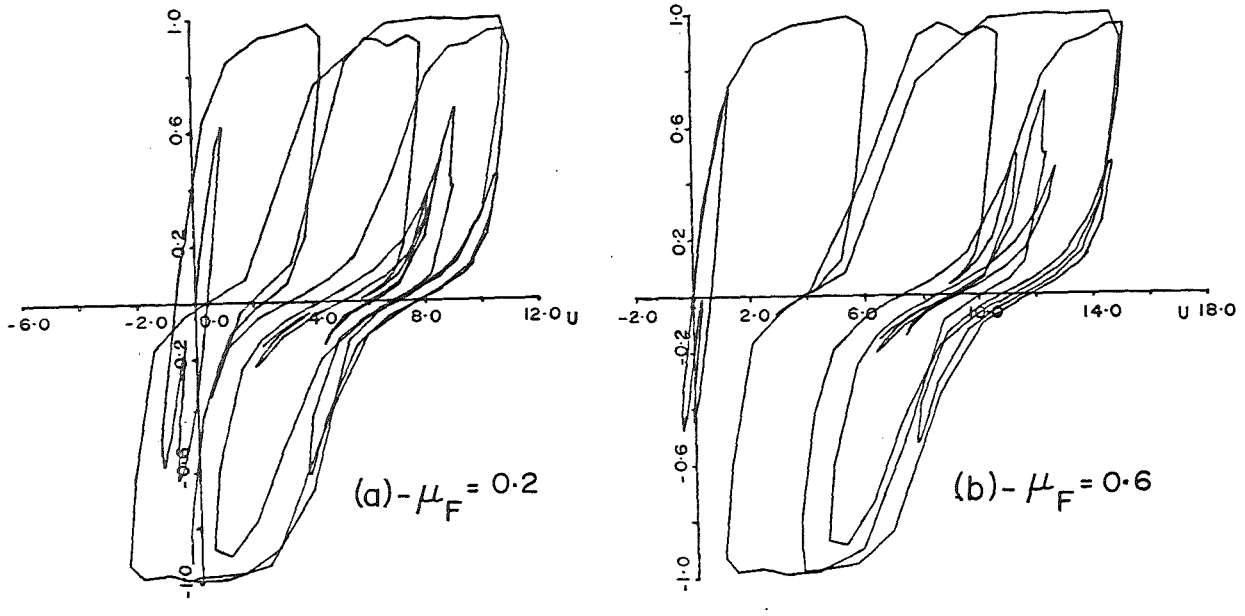

FIG.4·15- PINCHING BEHAVIOR OF SEP MODEL UNDER NONZERO MEAN STATIONARY WHITE NOISE INPUT. PSD = 0.2, ζ = 0.1, ζ_{10} = .95, AND λ = 0.15.

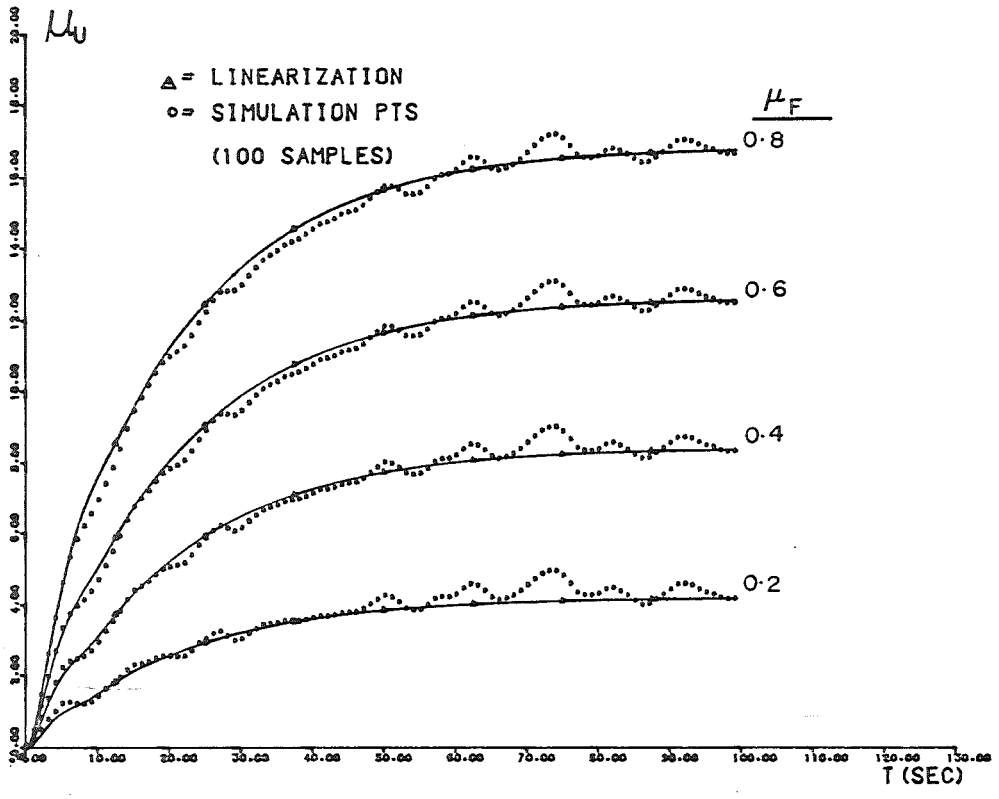

(a)

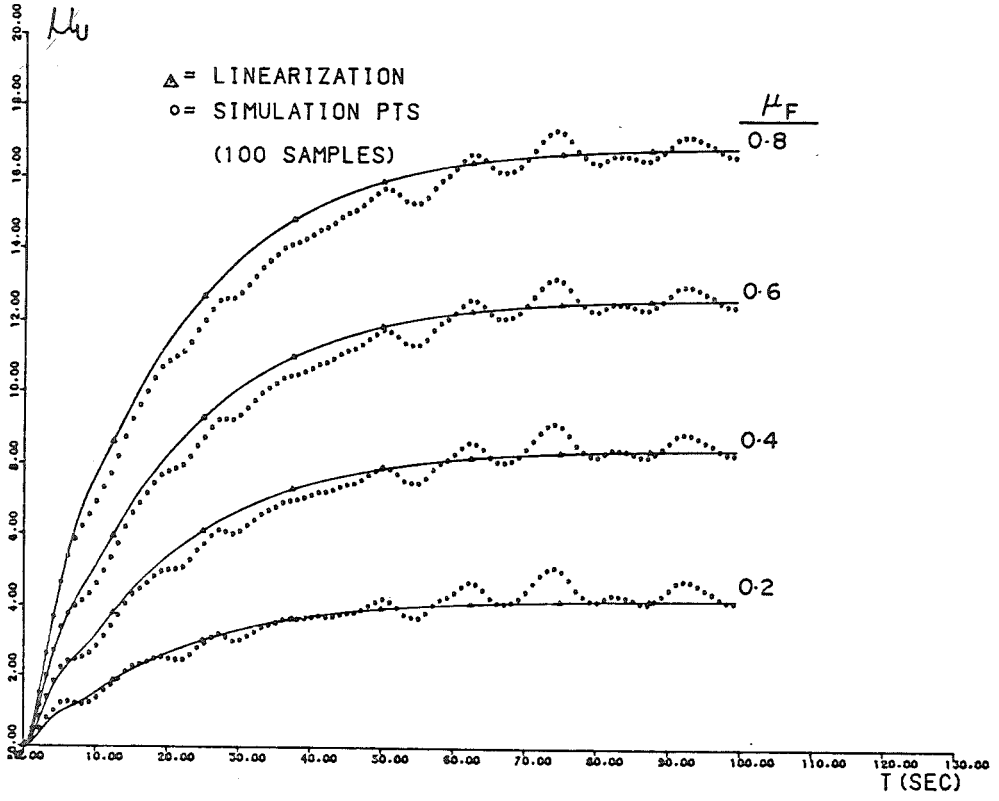

(b)

FIG. 4.16 - MEAN DISPLACEMENT RESPONSE OF A SDOF SEP MODEL UNDER NONZERO MEAN STATIONARY WHITE NOISE INPUT. $\xi = 0{\cdot}2$, $\delta_\xi = 0{\cdot}01$.

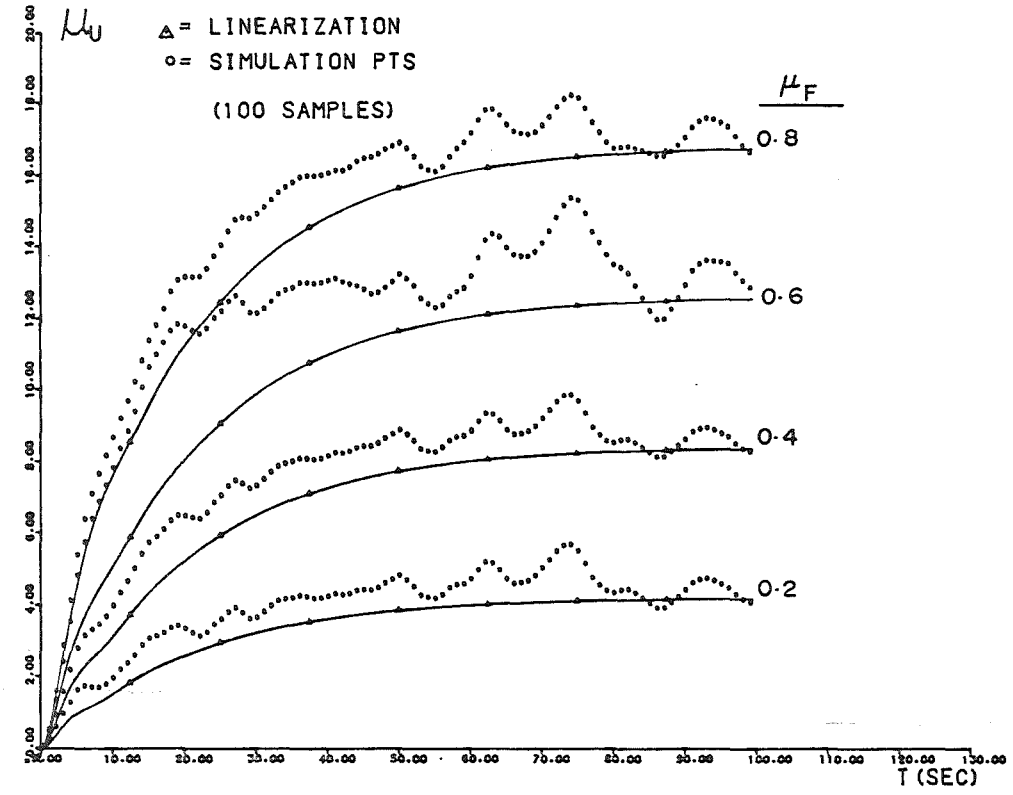

(c)

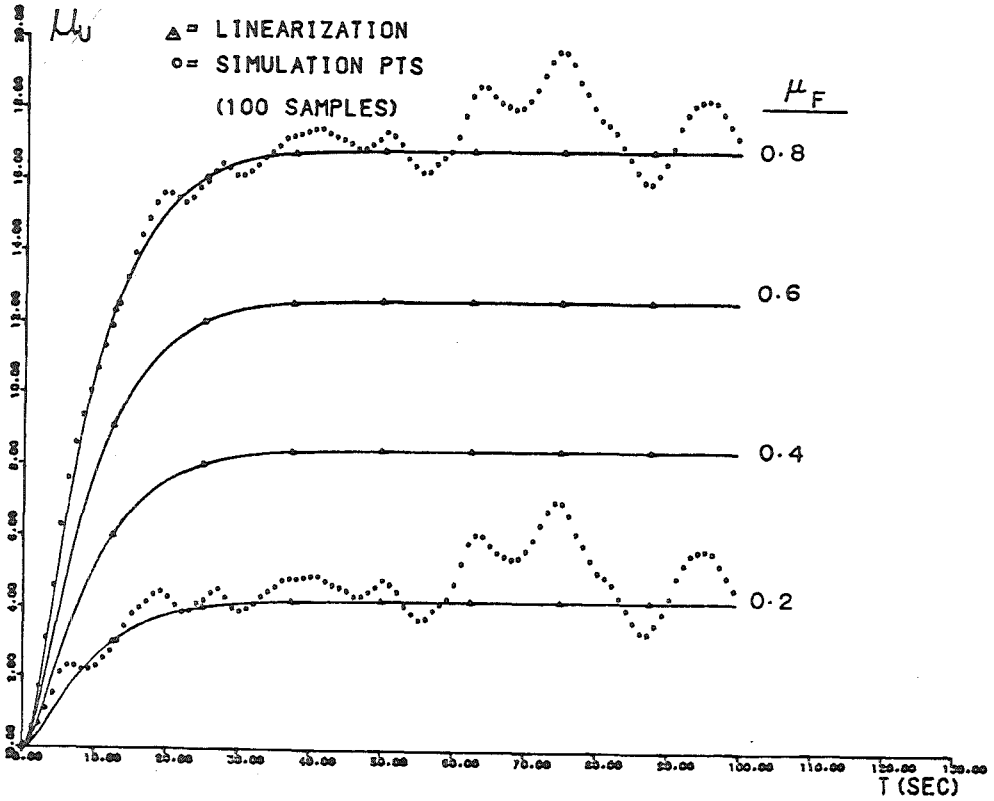

(d)

FIG. 4.16 (Cont'd)

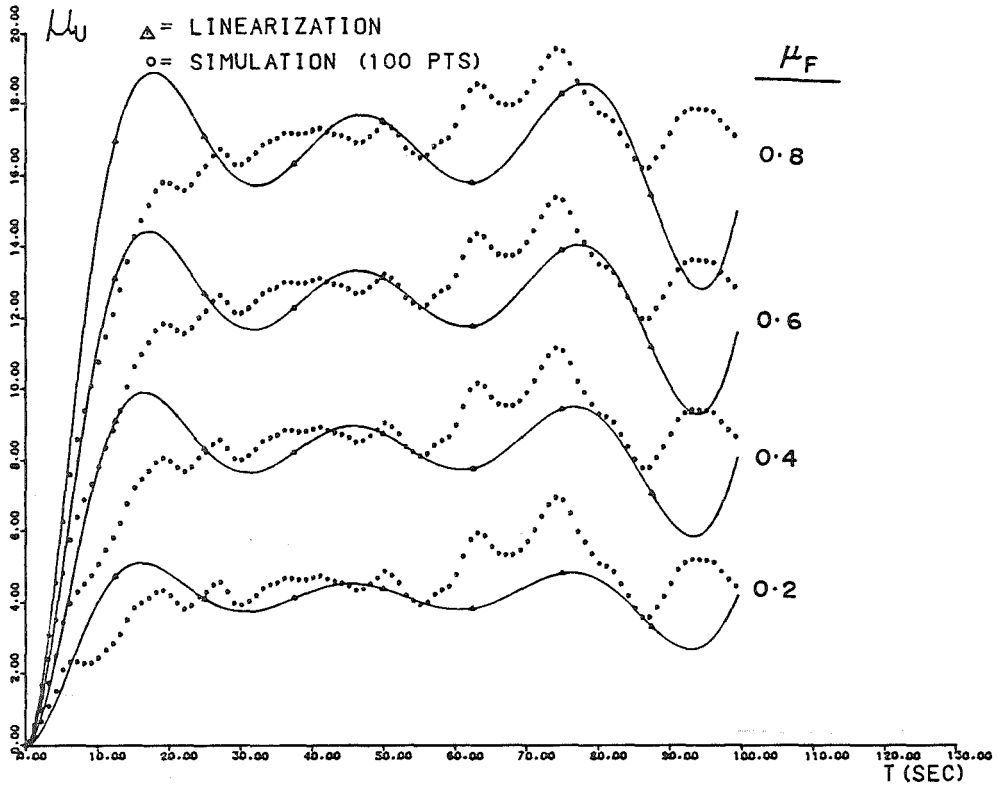

(e)

FIG. 4.16 (Cont'd)

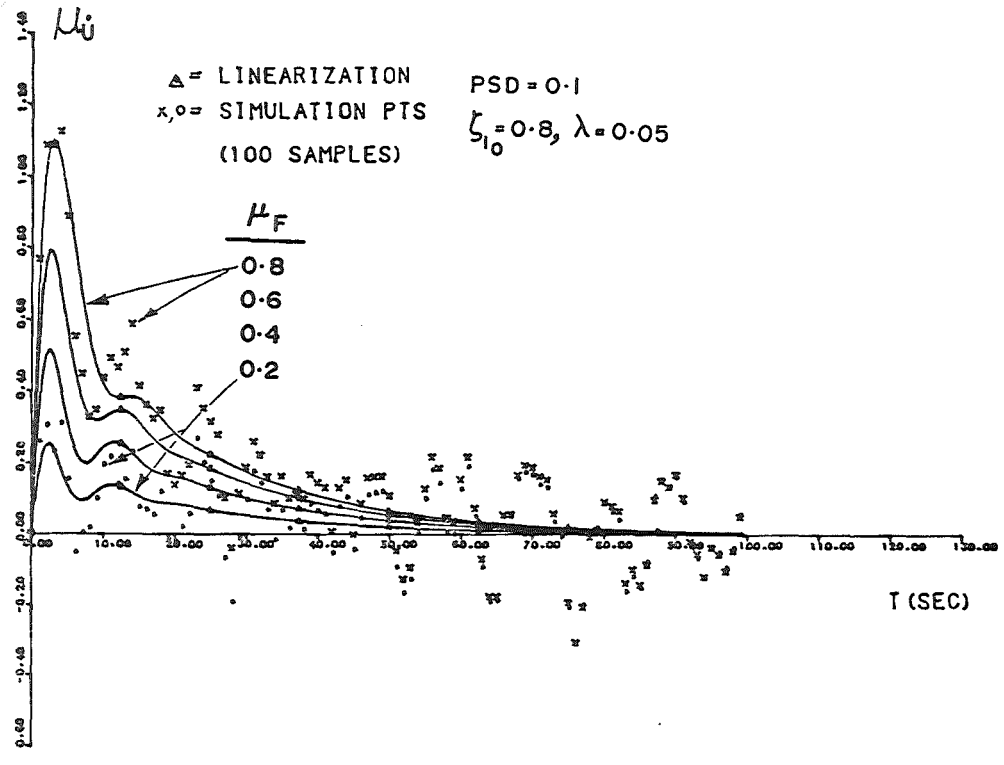

(a)

FIG. 4.17 - MEAN VELOCITY RESPONSE OF A SDOF SEP MODEL UNDER NONZERO MEAN STATIONARY WHITE NOISE INPUT. δ_ξ = 0·01, ξ = 0.2.

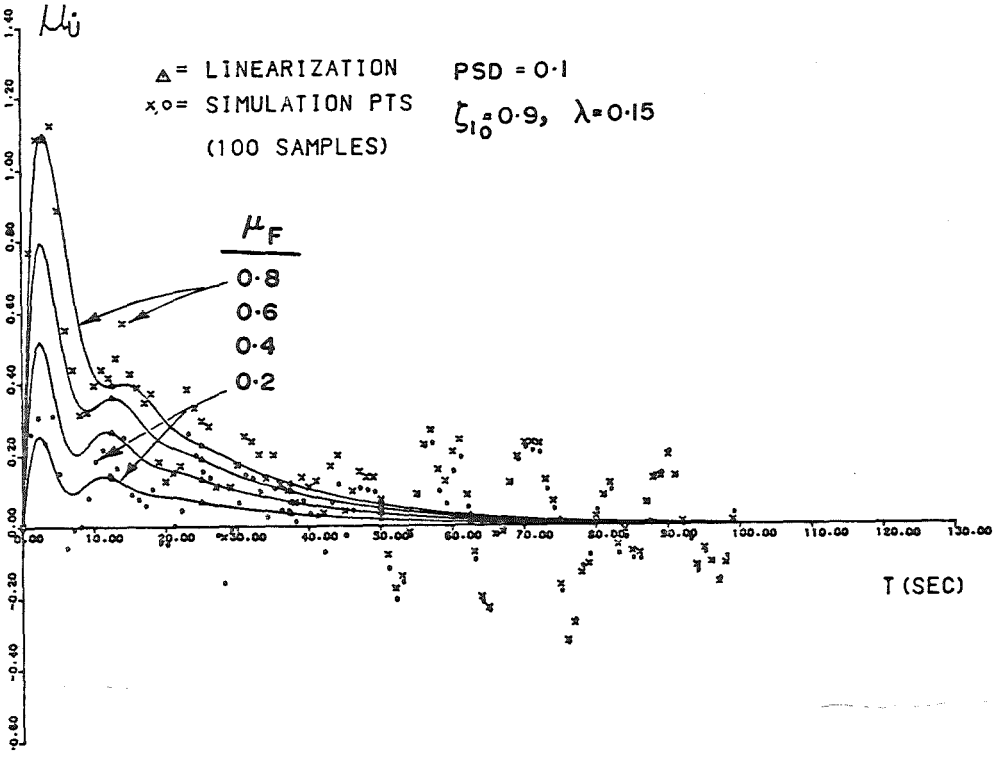

(b)

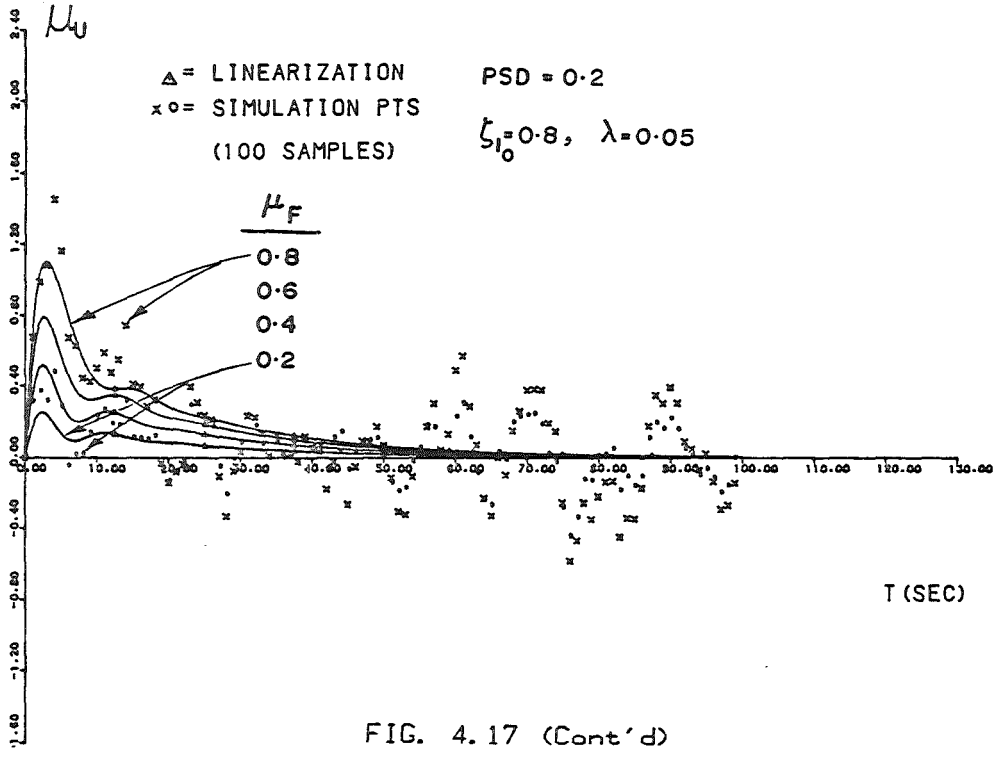

(c)

FIG. 4.17 (Cont'd)

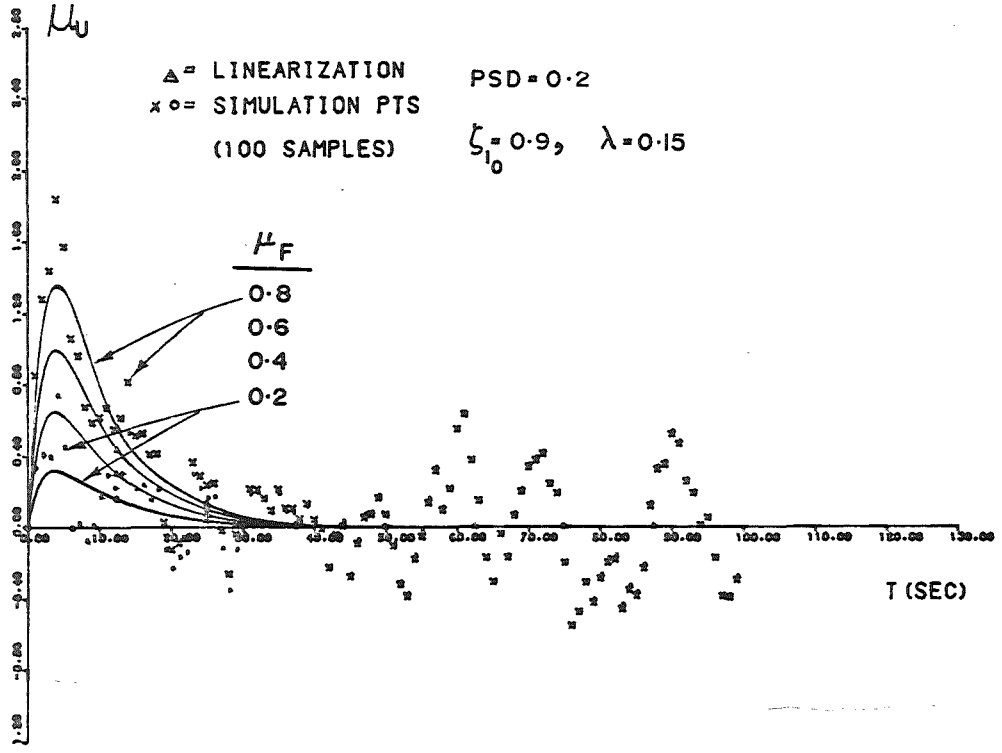

(d)

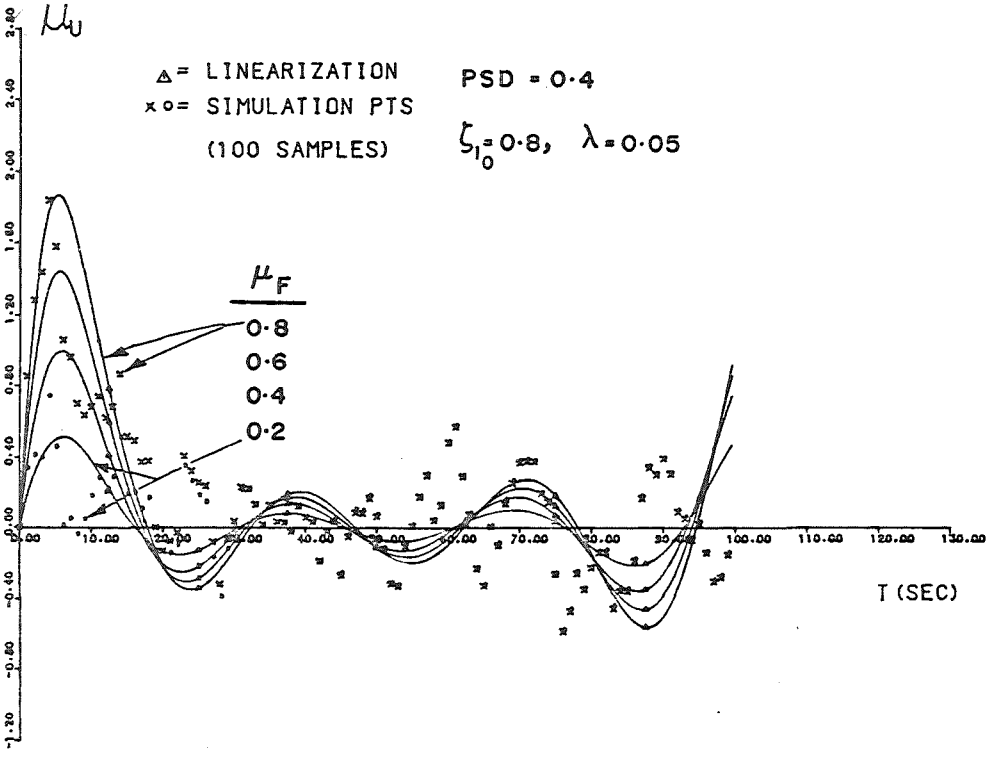

(e)

FIG. 4.17 (Cont'd)

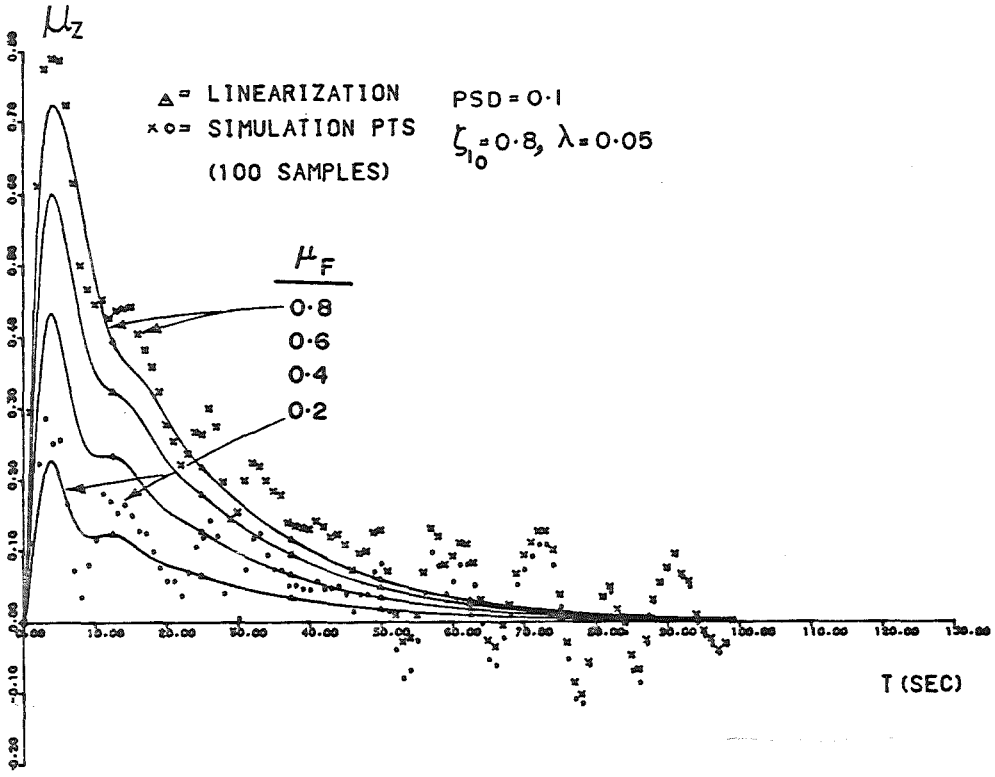

(a)

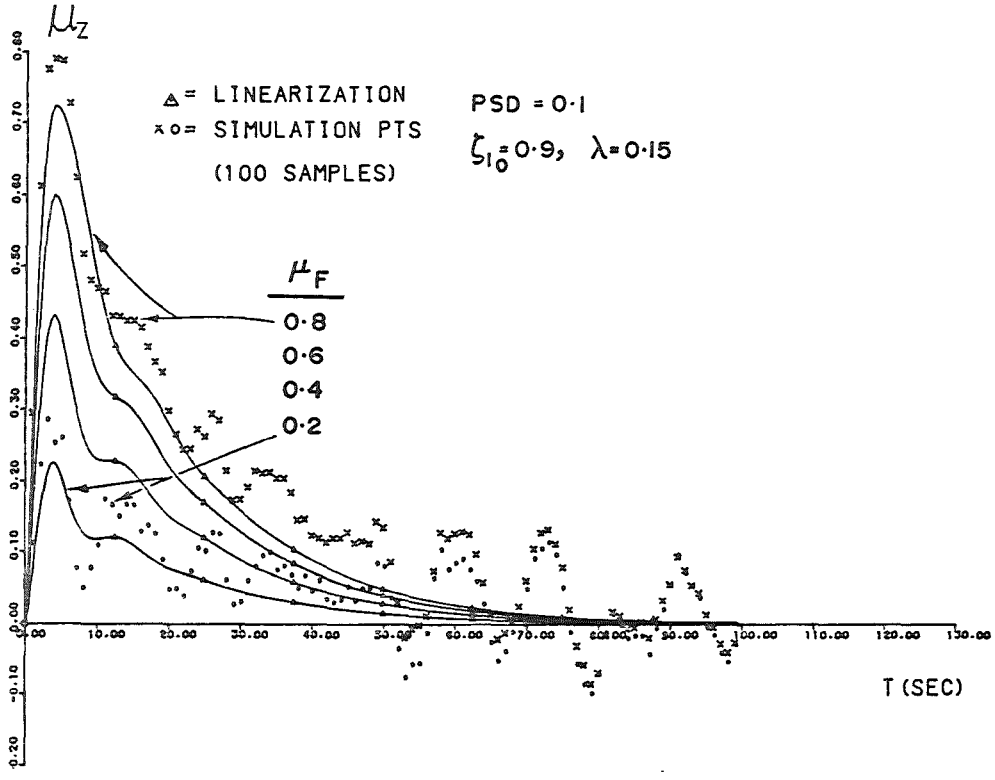

(b)

FIG. 4.18 - MEAN HYSTERETIC REST. FORCE RESPONSE OF A SDOF SEP MODEL UNDER NONZERO MEAN STATIONARY WHITE NOISE INPUT. δ_ξ = 0·01, ξ = 0.2.

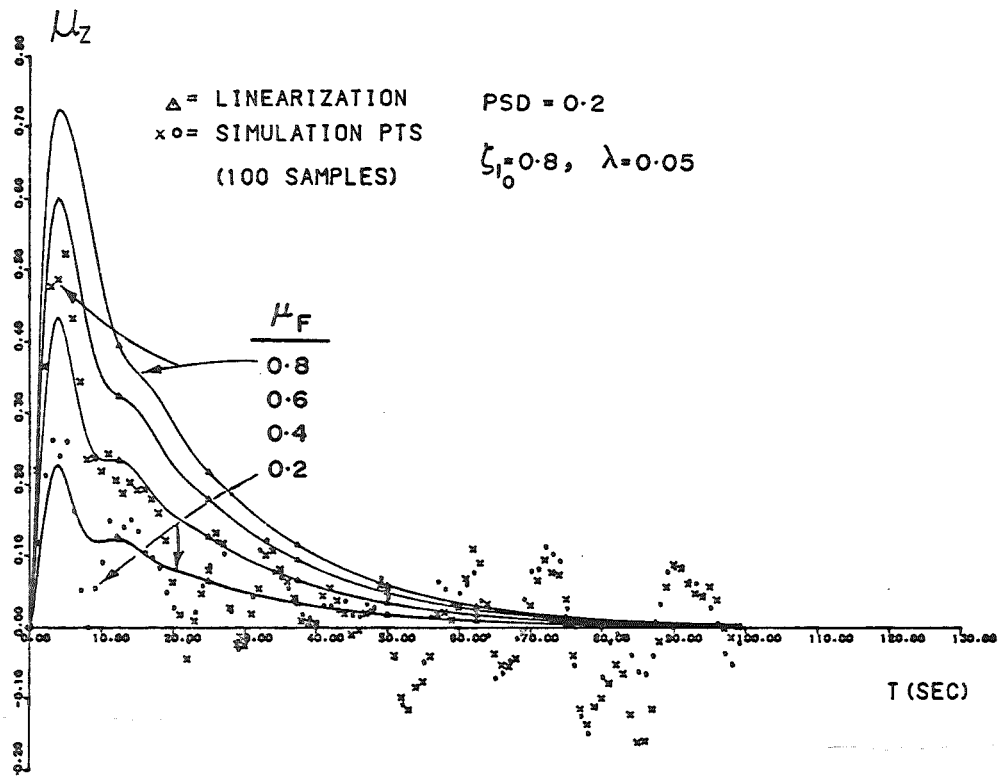

(c)

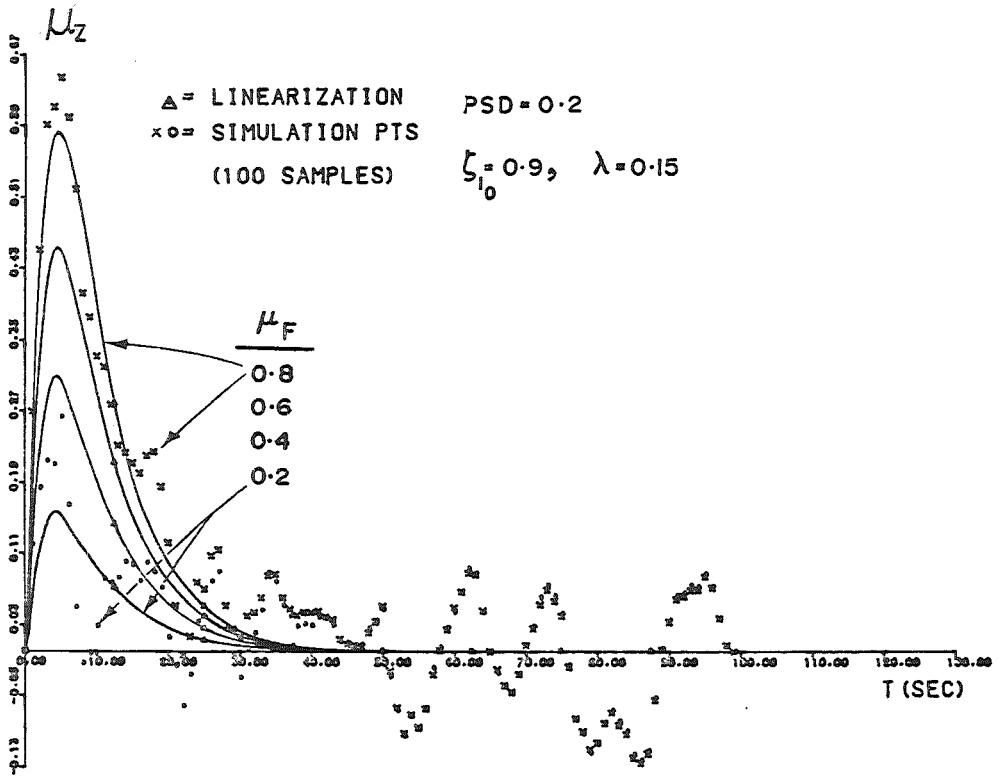

(d)

FIG. 4.18 (Cont'd)

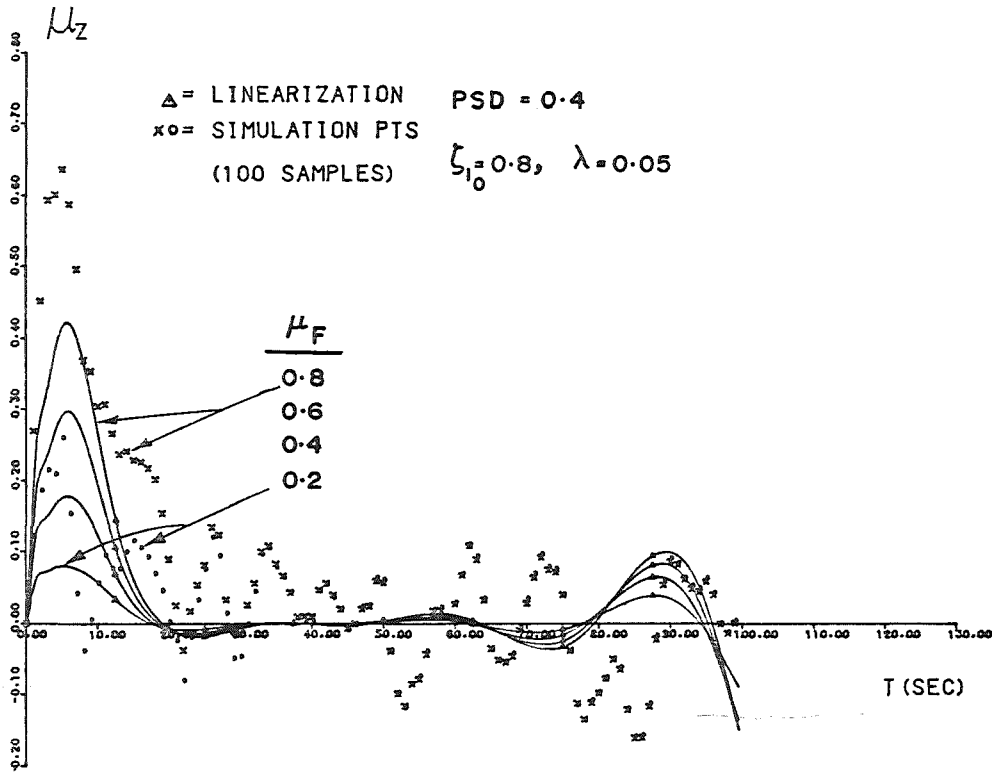

(e)

FIG. 4.18 (Cont'd)

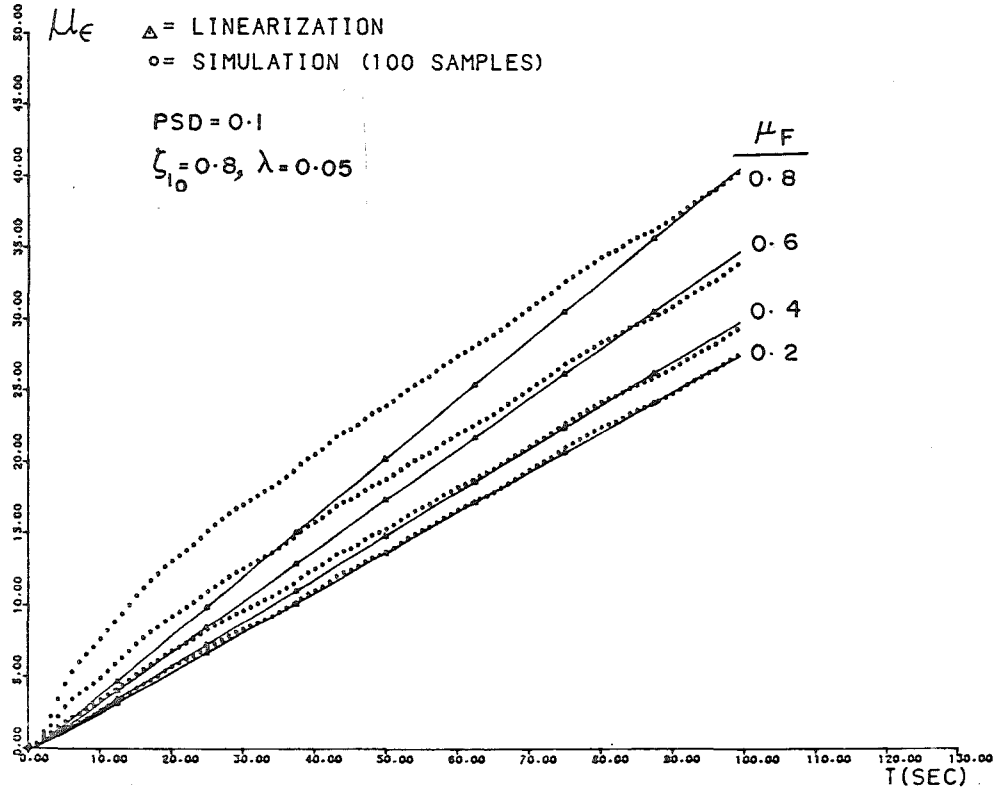

(a)

FIG. 4.19- MEAN ENERGY DISSIPATION OF A SDOF SEP MODEL UNDER NONZERO MEAN STATIONARY WHITE NOISE INPUT. δ_ξ=0·01, ξ = 0.2.

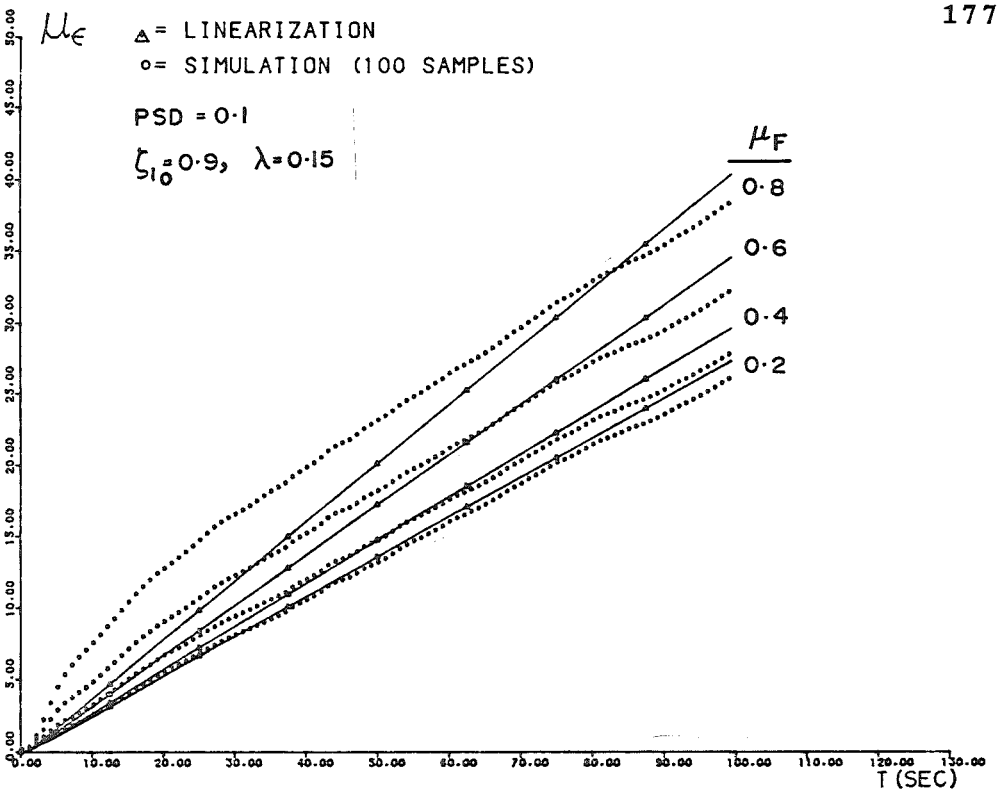

(b)

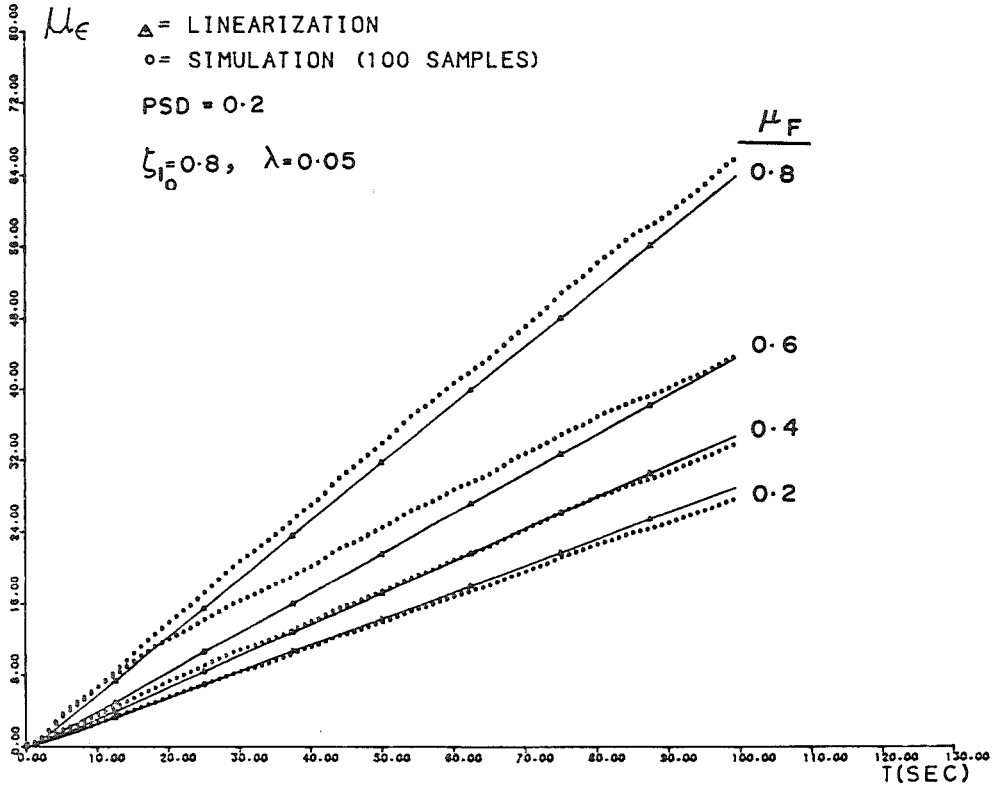

(c)

FIG. 4.19 (Cont'd)

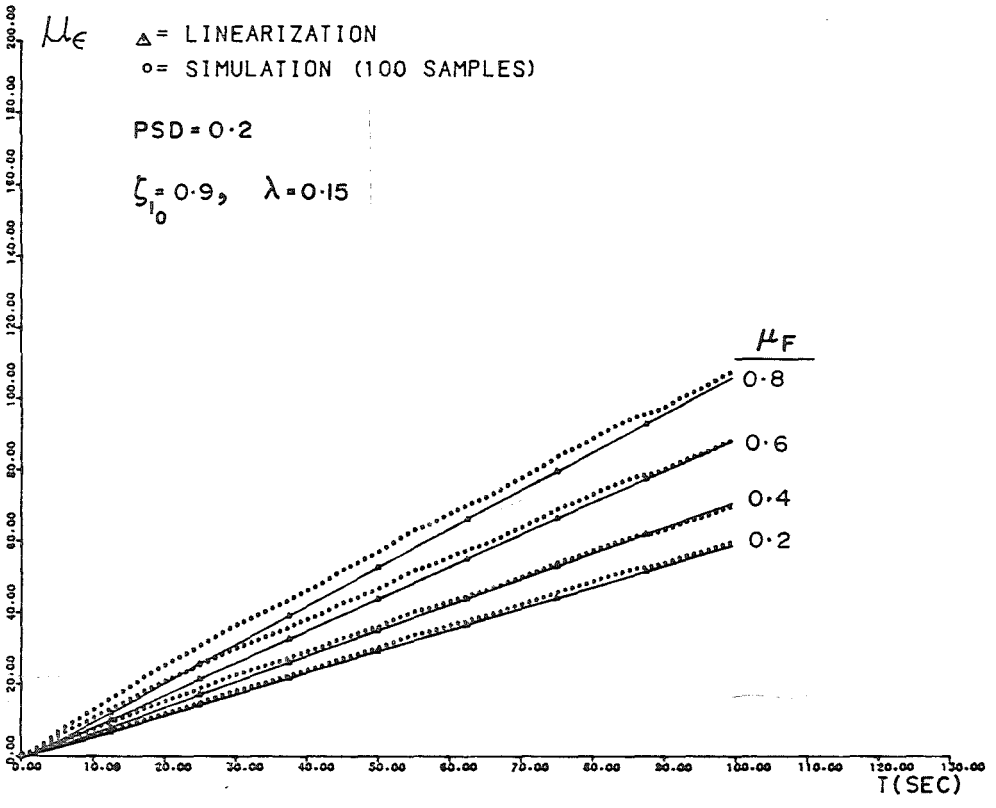

(d)

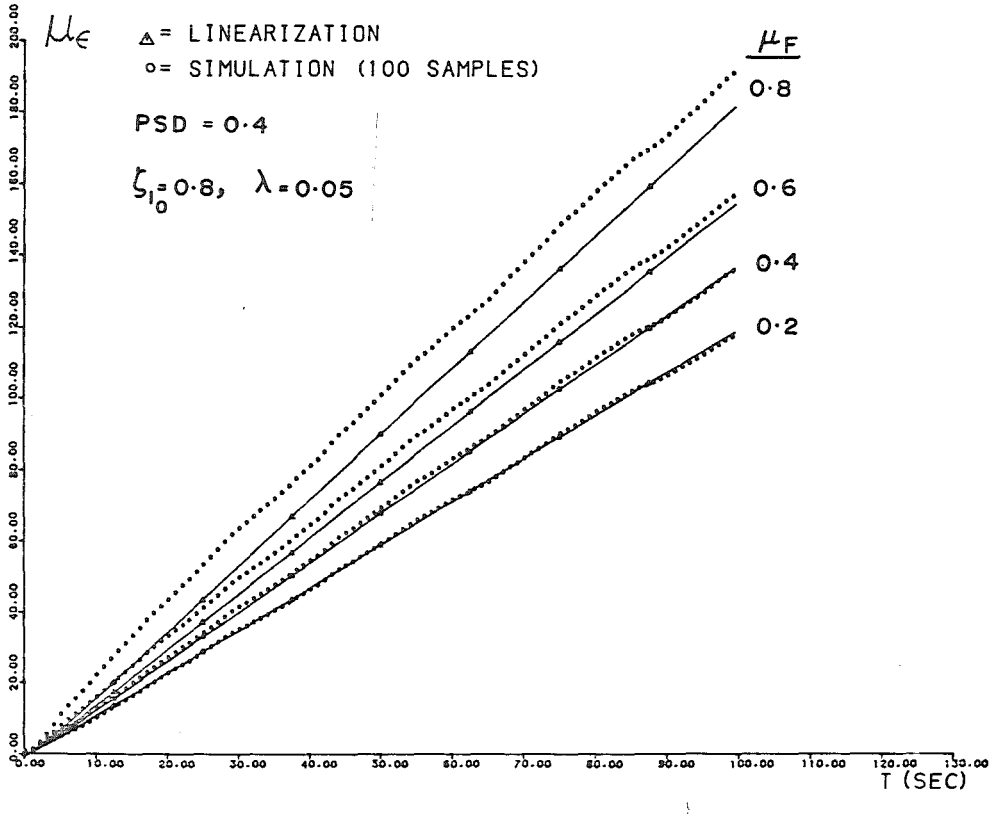

(e)

FIG. 4.19 (Cont'd)

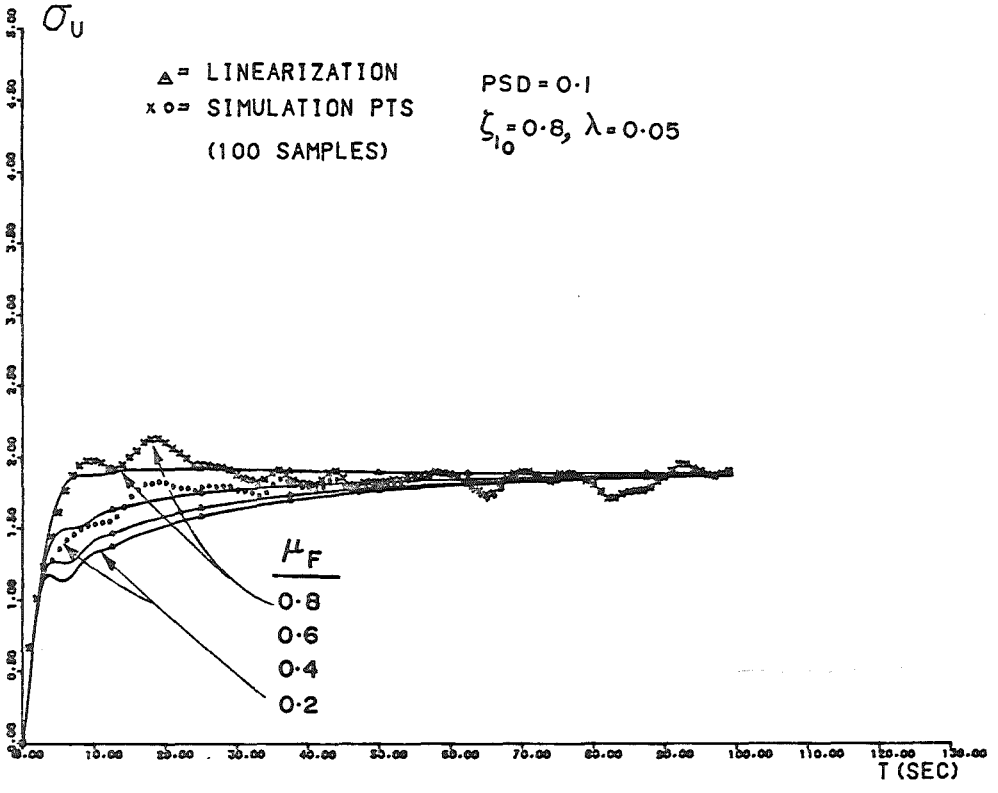

(a)

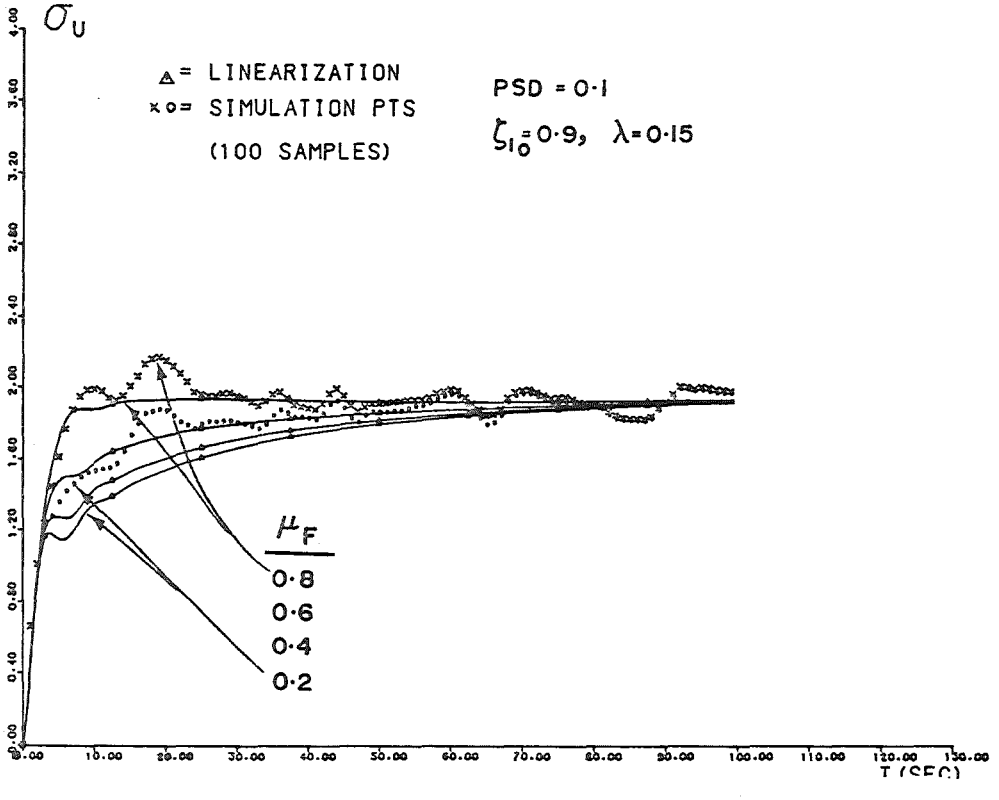

(b)

FIG. 4.20 - RMS DISPLACEMENT RESPONSE OF A SDOF SEP MODEL UNDER NONZERO MEAN STATIONARY WHITE NOISE INPUT. δ_ξ = 0·01, ξ = 0.2.

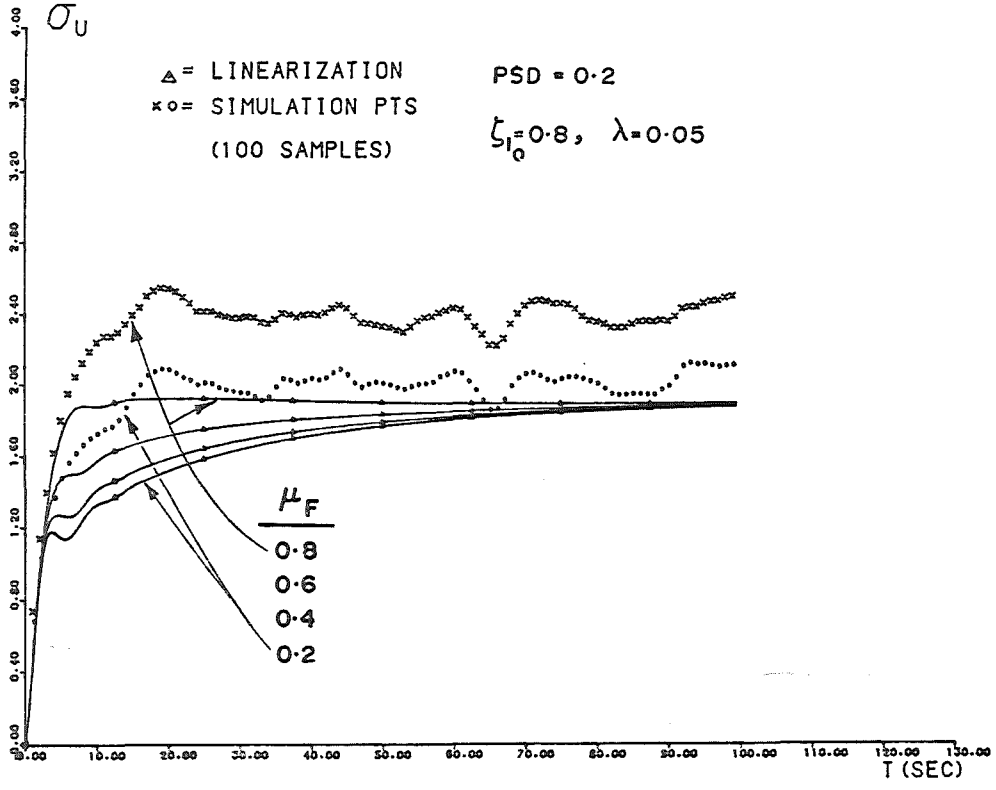

(c)

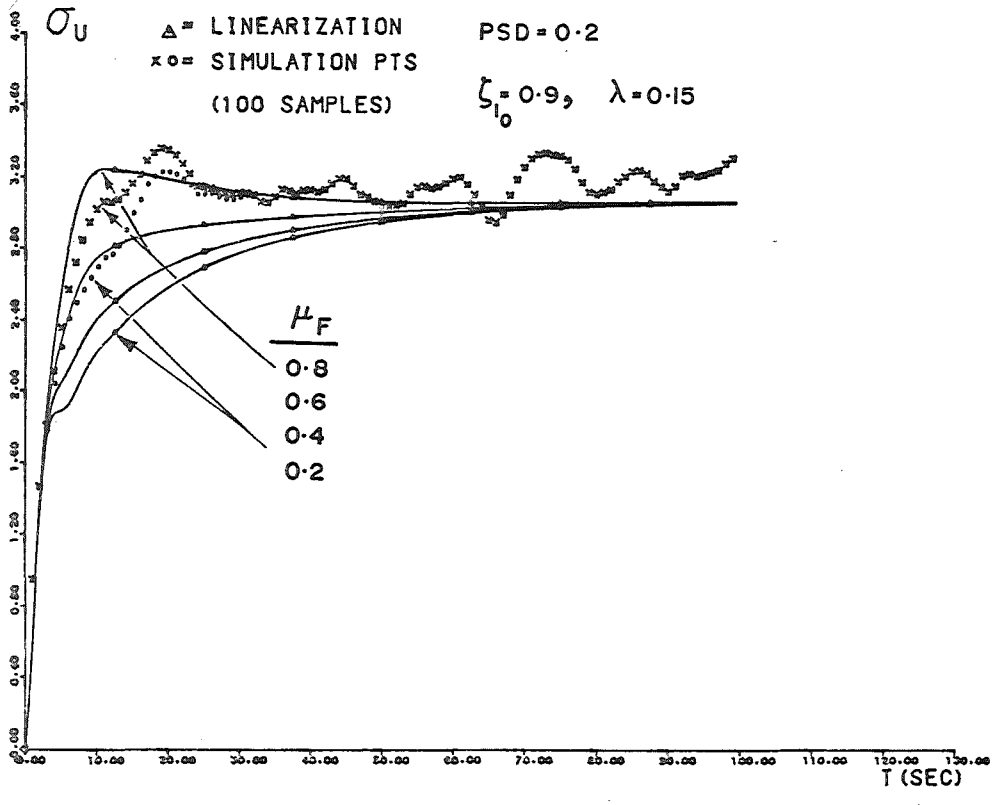

(d)

FIG. 4.20 (Cont'd)

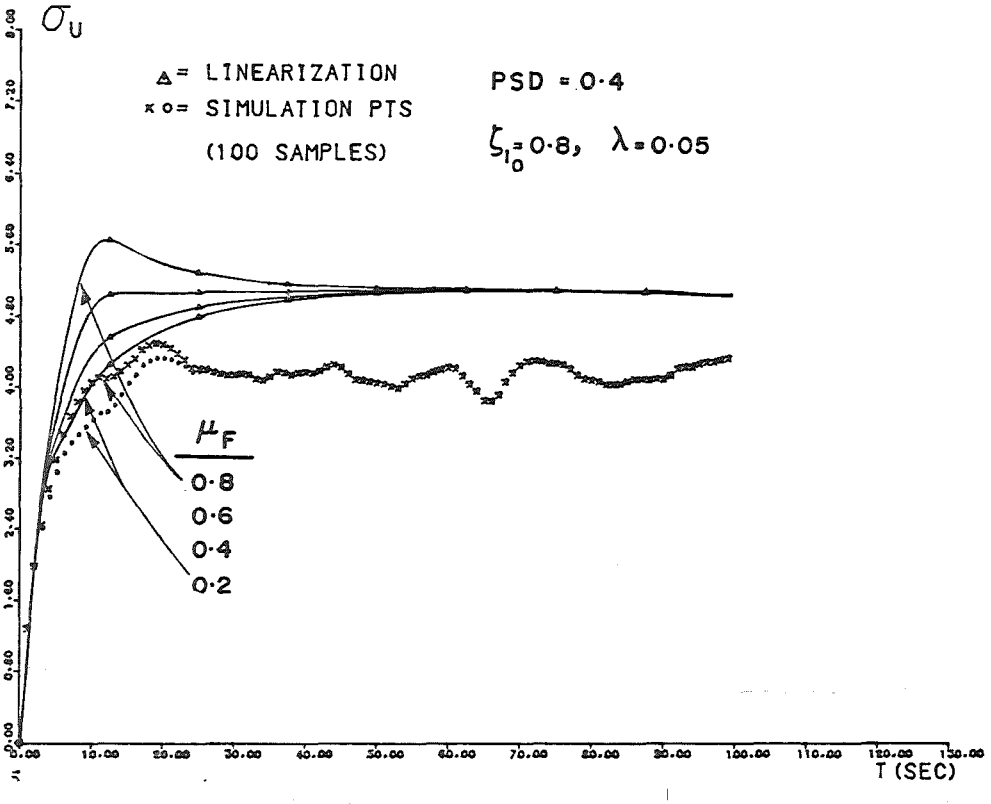

(e)

FIG. 4.20 (Cont'd)

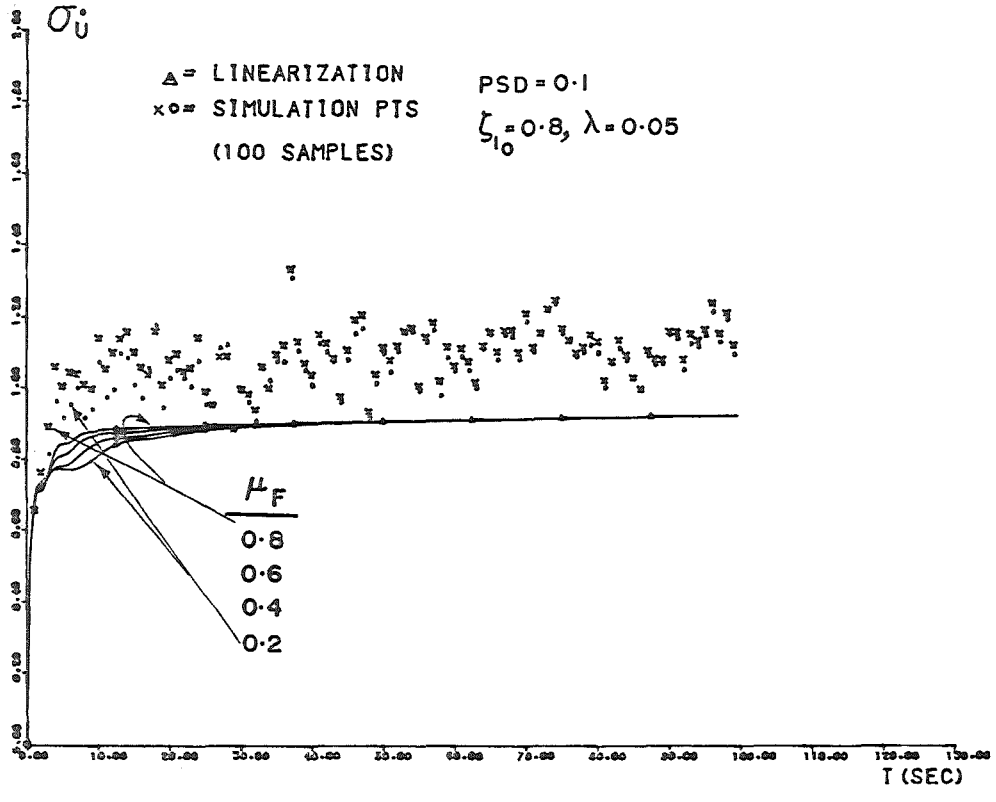

(a)

FIG. 4.21- RMS VELOCITY RESPONSE OF A SDOF SEP MODEL UNDER NONZERO MEAN STATIONARY WHITE NOISE INPUT. δ_ξ = 0·01, ξ = 0.2.

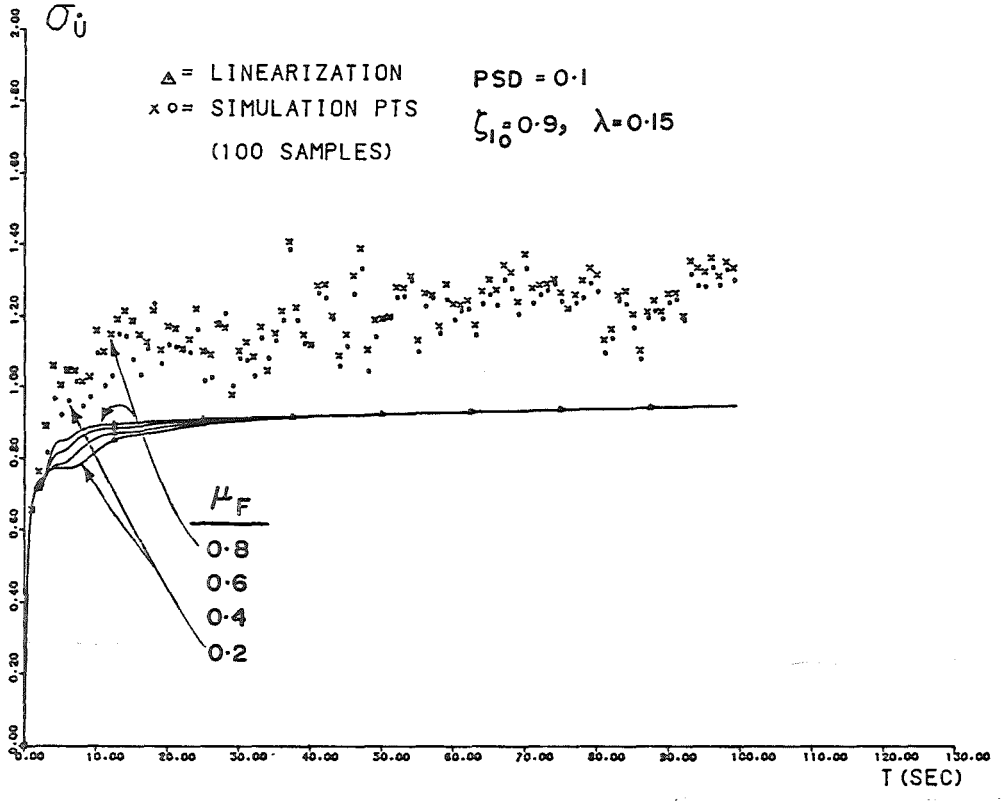

(b)

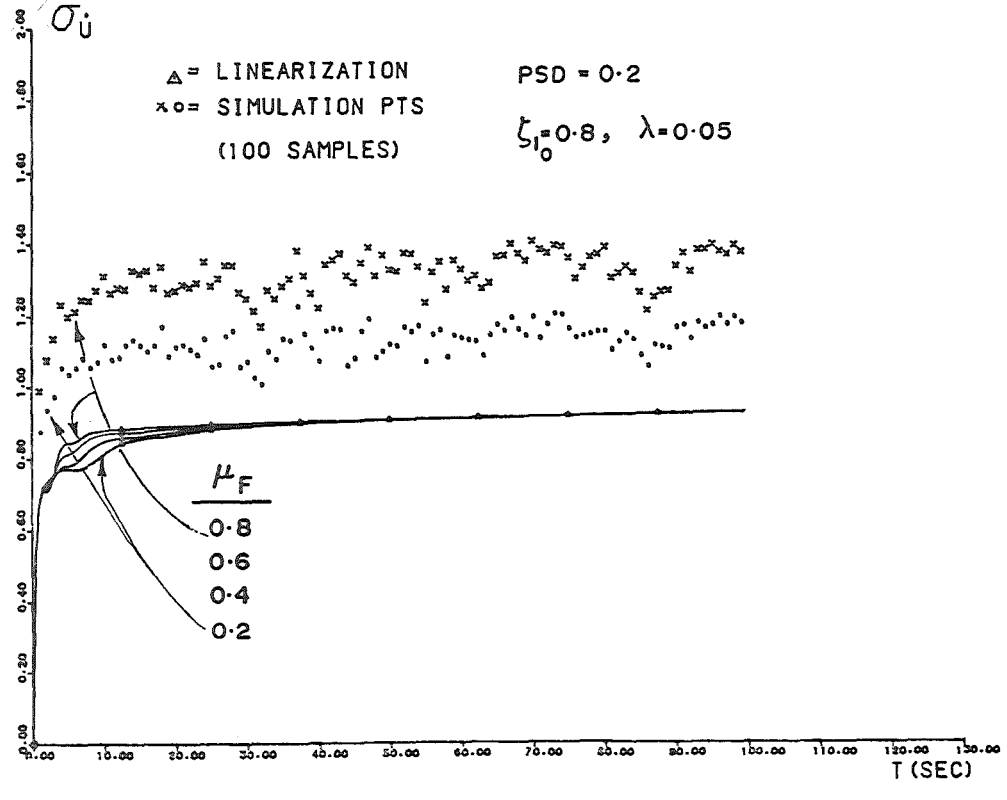

(c)

FIG. 4.21 (Cont'd)

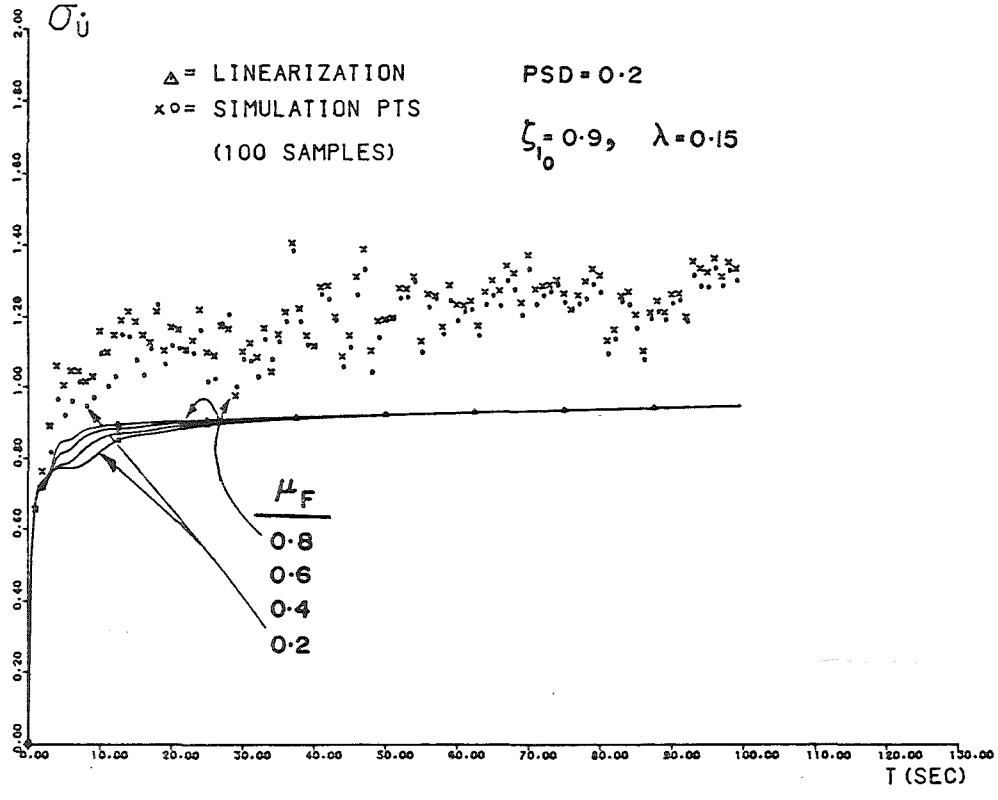

(d)

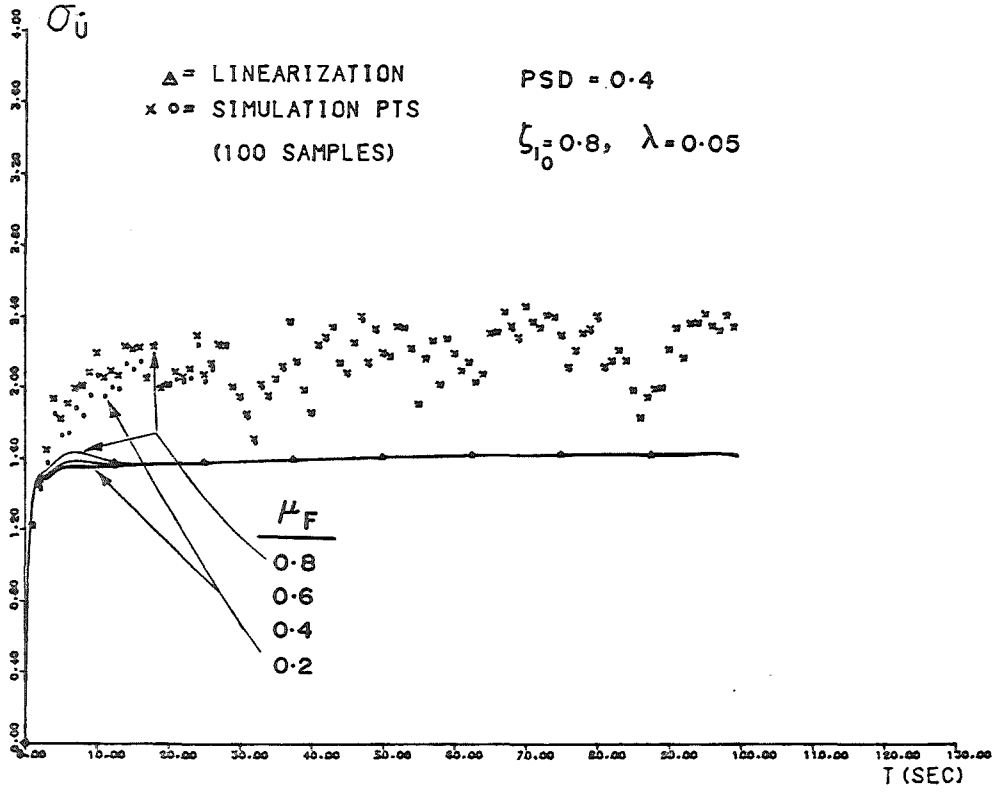

(e)

FIG. 4.21 (Cont'd)

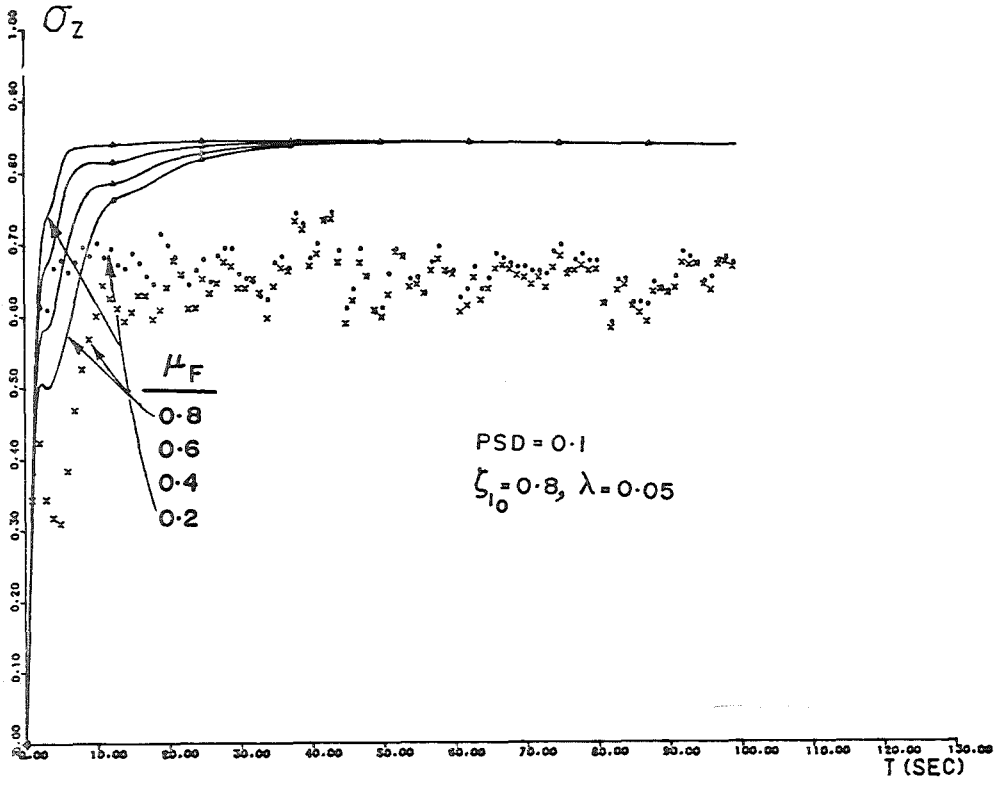

(a)

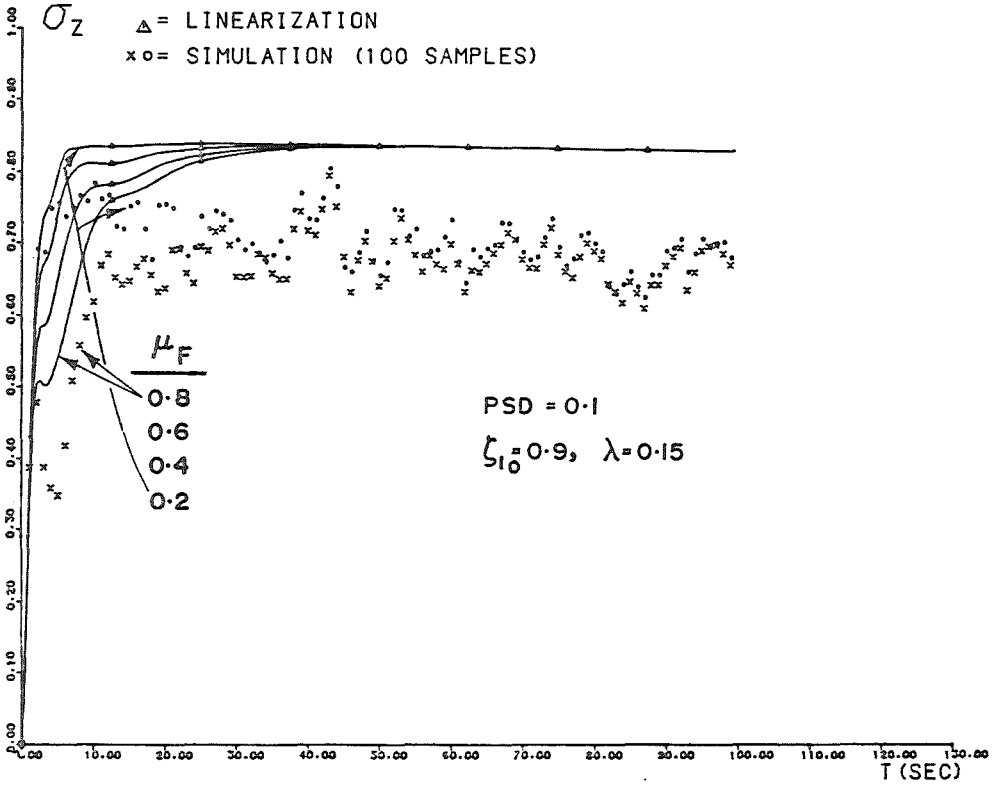

(b)

FIG. 4.22 - RMS HYSTERETIC FORCE RESPONSE OF A SDOF S MODEL UNDER NONZERO MEAN STATIONARY WHITE NOISE INPUT. δ_ξ = 0·01, ξ = 0.2.

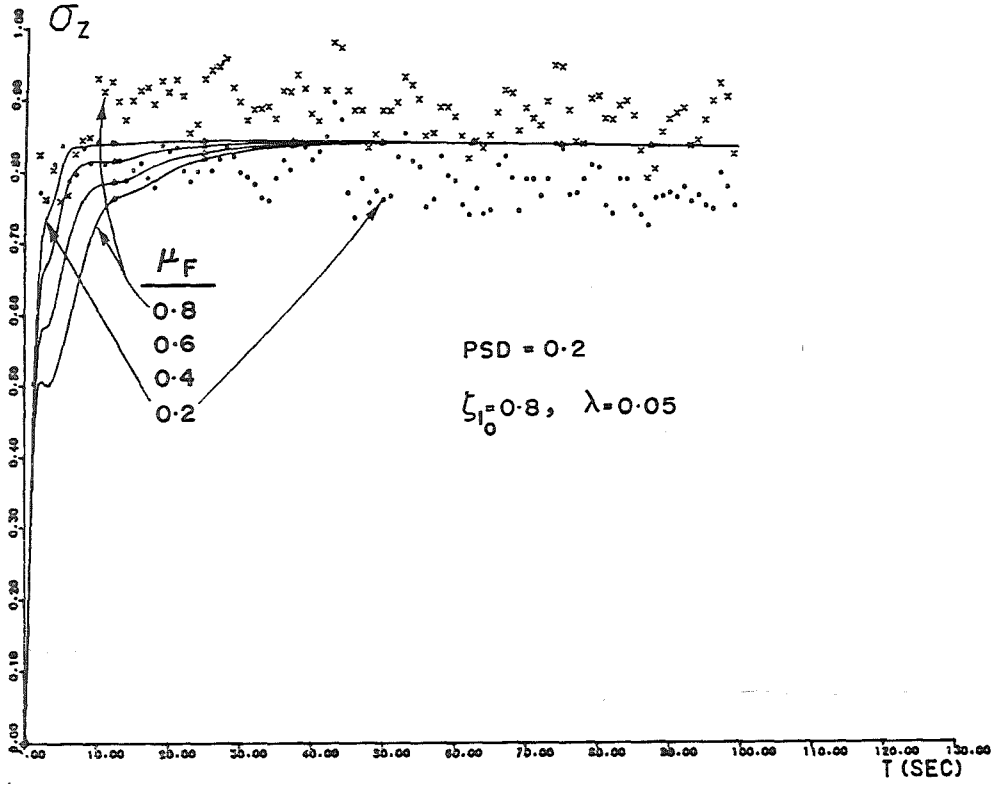

(c)

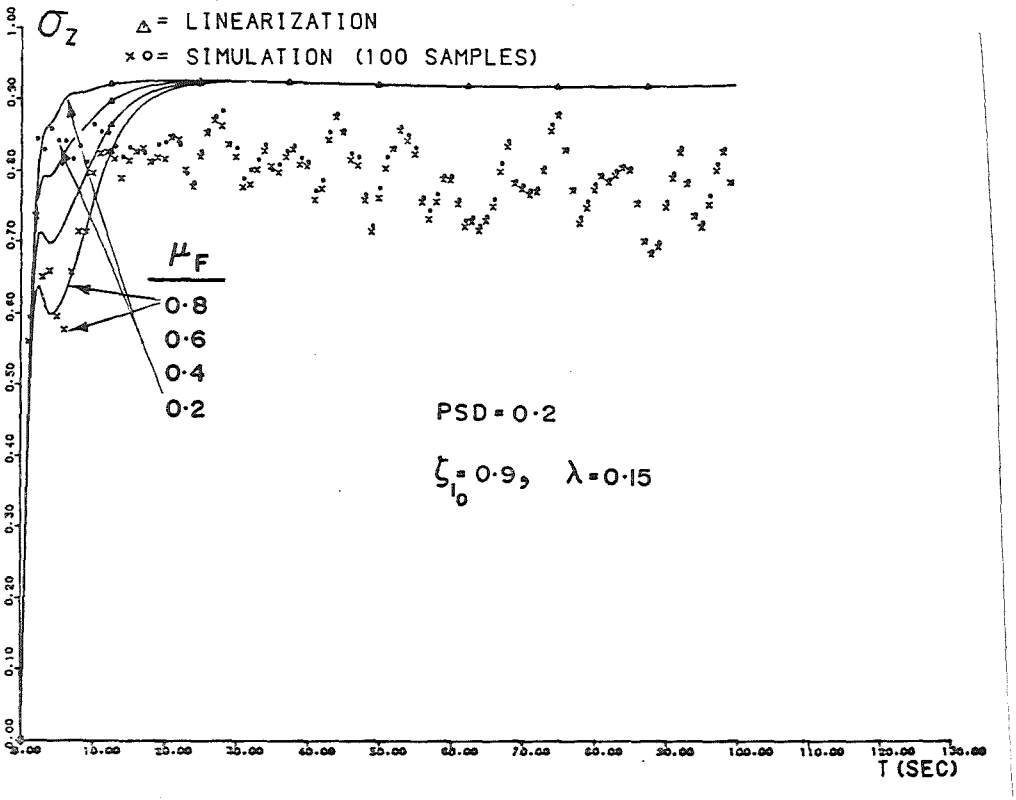

(d)

FIG. 4.22 (Cont'd)

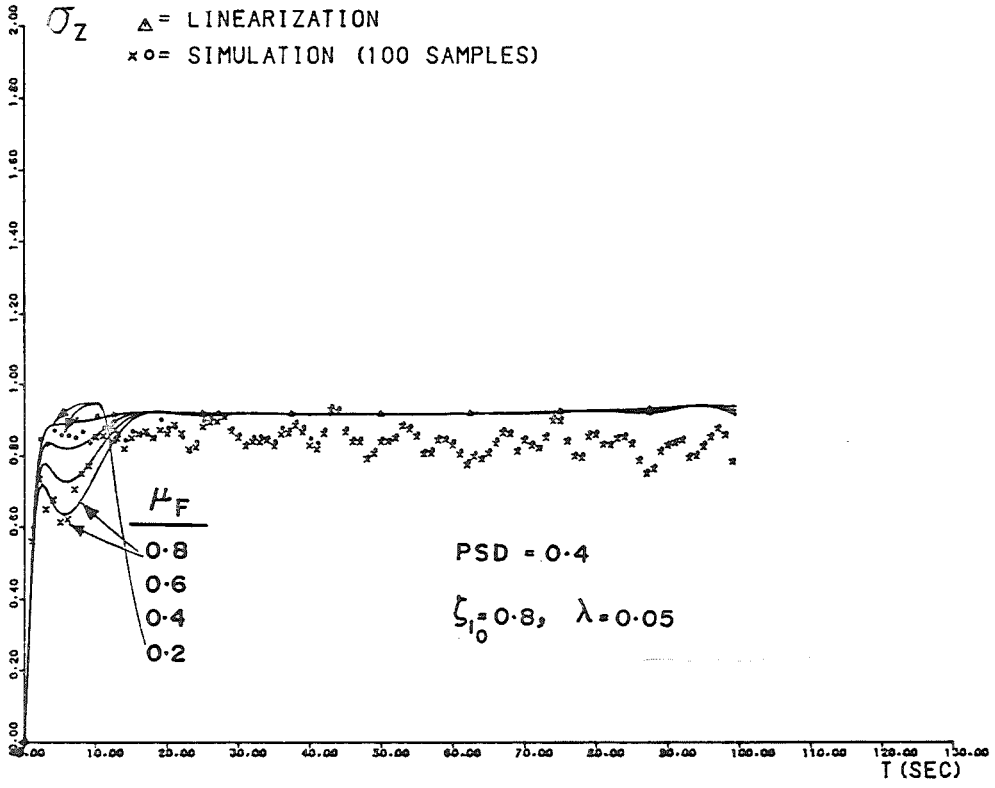

(e)

FIG. 4.22 (Cont'd)

APPENDIX A

DETAILS OF DERIVATION OF LINEARIZED COEFFICIENTS FOR BN MODEL (Zero Mean Case).

The expected values specified in Equation [3.5] gives, upon substitution of the appropriate $g_i(y_3, y_4)$ functions

$$
\begin{aligned}
C_{e3} &= E\{(\partial/\partial \dot{y}_4)[A\dot{y}_4 - \nu(\beta|y_3|^{(n-1)}y_3|\dot{y}_4| + \gamma|y_3|^n\dot{y}_4)]/\eta\} \\
K_{e3} &= E\{(\partial/\partial y_3)[A\dot{y}_4 - \nu(\beta|y_3|^{(n-1)}y_3|\dot{y}_4| + \gamma|y_3|^n\dot{y}_4)]/\eta\} \\
C_{e5} &= E\{(\partial/\partial \dot{y}_4)(2a/\sqrt{2\pi}\sigma)\exp[-y_3^2/(2\sigma^2)]\cdot \\
&\quad [A\dot{y}_4 - \nu(\beta|y_3|^{(n-1)}y_3|\dot{y}_4| + \gamma|y_3|^n\dot{y}_4)]/\eta\} \qquad [A\text{-}1] \\
K_{e5} &= E\{(\partial/\partial y_3)(2a/\sqrt{2\pi}\sigma)\exp[-y_3^2/(2\sigma^2)] \\
&\quad [A\dot{y}_4 - \nu(\beta|y_3|^{(n-1)}y_3|\dot{y}_4| + \gamma|y_3|^n\dot{y}_4)]/\eta\}
\end{aligned}
$$

Using the approximation for the deterioration control parameters given by Equations [2.4], [2.10] and [3.13] together with the assumption that A, , η and a can be replaced by

$$
\begin{aligned}
\mu_A &= A_0 - \delta_A\mu_\varepsilon \\
\mu_\nu &= \nu_0 + \delta_\nu\mu_\varepsilon \\
\mu_\eta &= \eta_0 + \delta_\eta\mu_\eta \qquad [A\text{-}2] \\
\mu_a &= \delta_a\mu_\eta
\end{aligned}
$$

allows the equations for C_{e3} and K_{e3} to be written as

$$
C_{e3} = \{\mu_A - \mu_\nu[\beta E(|y_3|^{(n-1)}y_3\,\mathrm{sgn}(\dot{y}_4)) + \gamma E(|y_3|^n)]\}/\mu_\eta \qquad [A\text{-}3]
$$

$$
K_{e3} = (-\mu_\nu/\mu_\eta)\{\beta E[n|y_3|^{(n-1)}|\dot{y}_4| + \gamma E[n|y_3|^{(n-2)}y_3\dot{y}_4]\}
$$

The expected values in [A-3] have been previously evaluated (15).

Hence

$$C_{e3} = [\mu_A - \mu_\nu(\beta F_1 + \gamma F_2)]/\mu_\eta$$
$$K_{e3} = [-\mu_\nu(\beta F_3 + \gamma F_4)]/\mu_\eta \qquad [A-4]$$

where

$$F_1 = \sigma_3^n \Gamma[(n+2)/2] 2^{n/2}(I_{s1} - I_{s2})/\pi$$
$$F_2 = \sigma_3^n \Gamma[(n+1)/2] 2^{n/2}/\sqrt{\pi}$$
$$F_3 = n\sigma_3^{(n-1)}\sigma_{\dot{4}}\Gamma[(n+2)/2]2^{n/2} \qquad [A-5]$$
$$\{2[(1-\rho_{3\dot{4}}^2)/n]^{(n+1)/2} + \rho_{3\dot{4}}(I_{s1} - I_{s2})\}/\pi$$
$$F_4 = n\rho_{3\dot{4}}\sigma_3^{(n-1)}\sigma_{\dot{4}}\Gamma[(n+1)/2]\ 2^{n/2}/\ \pi$$

In [A-5], $\Gamma(.)$ is the gamma function,

$$I_{s1} = \int_0^{\phi} \sin^n\theta d\theta \qquad [A-6]$$

$$I_{s2} = \int_{\phi}^{\pi} \sin^n\theta d\theta \qquad [A-7]$$

and

$$\phi = \arctan[-\sqrt{1-\rho_{3\dot{4}}^2}/\rho_{3\dot{4}}] \qquad [A-8]$$

In a similar manner, C_{e5} and K_{e5} are given by

$$C_{e5} = 2\mu_a/(\sqrt{2\pi}\sigma\mu_\eta)\{\mu_A E[\exp(-y_3^2/(2\sigma^2))] -$$
$$\mu_\nu\left[\beta E[y_3|y_3|^{(n-1)}\exp(-y_3^2/(2\sigma_2))\partial|\dot{y}_4|/\partial\dot{y}_4] + \right.$$
$$\left.\gamma E[\ y_3\ ^n \exp(-y_3^2/(2\sigma^2))]\right]\}$$
$$K_{e5} = 2\mu_a/(\sqrt{2\pi}\sigma\mu_\eta)\{-(\mu_A/\sigma^2)E[y_4 y_3 \exp(-y_3^2/(2\sigma^2))] +$$
$$\beta\mu_\nu\left[(1/\sigma^2)E[|\dot{y}_4||y_3|^{(n+1)}\exp(-y_3^2/(2\sigma^2))] - \right.$$
$$\left.E[|\dot{y}_4|\exp(-y_3^2/(2\sigma^2))(\partial/\partial y_3)(y_3|y_3|^{(n-1)})]\right] +$$
$$\gamma\mu_\nu\left[(1/\sigma^2)E[y_3|y_3|^n\dot{y}_4\ \exp(-y_3^2/(2\sigma^2))\right] -$$
$$\left.E[|\dot{y}_4|\exp(-y_3^2/(2\sigma^2))\partial|y_3|^n/\partial y_3]\right]\}$$

or

$$C_{e5} = 2\mu_a/(\sqrt{2\pi}\sigma\mu_\eta)\ \{\mu_A F_5/\sigma_z - \mu_\nu[\beta F_6(I_{s3} - I_{s4}) + \gamma F_7]\}$$

$$K_{e5} = 2\mu_a/(\sqrt{2\pi}\sigma\mu_\eta)\{-(\mu_A/\sigma^2)F_{16} + \beta\mu_\nu[(F_8/\sigma^2)(F_{17}F_{18}^{(n+2)}/(n+2) + F_{12}) - F_9(F_{17}F_{18}^{n}/n + F_{13})] + \gamma\mu_\nu[F_{10}(F_{14}/\sigma^2 - F_{15}/2)]\} \qquad [A-9]$$

where

$$F_5 = \sigma_3\sigma/\sqrt{\sigma^2 + \sigma_3^2}$$

$$F_6 = [F_5^{n+1}/(\pi\sigma_3)2^{n/2}\Gamma[(n+2)/2]$$

$$F_7 = [F_5^{n+1}/(\sqrt{\pi}\sigma_3)2^{n/2}\Gamma[(n+1)/2]$$

$$F_8 = [F_5^{n+2}/(\pi\sigma_3)\sigma_4^{\circ}\Gamma[(n+4)/2]2^{(n+2)/2}$$

$$F_9 = [nF_5^{n}/(\pi\sigma_3)\sigma_4^{\circ}\Gamma[(n+2)/2]2^{n/2}$$

$$F_{10} = \rho_{34}^{\circ}\ 2^{(n+2)/2}\ \sigma_4^{\circ}/(\pi\sigma_3)$$

$$F_{12} = (\rho_{34}^{\circ}/\sigma_3)(I_{s5} - I_{s6})F_5$$

$$F_{13} = (\rho_{34}^{\circ}/\sigma_3)F_5(I_{s3} - I_{s4}) \qquad [A-10]$$

$$F_{14} = (F_5^{n+3}/\sigma_3)\Gamma[(n+3)/2]$$

$$F_{15} = (n\ F_5^{n+1}/\sigma_3)\Gamma[(n+1)/2]$$

$$F_{16} = \rho_{34}^{\circ}\sigma_4^{\circ}\ F_5^{3}/\sigma_3^{2}$$

$$F_{17} = 2\sqrt{1 - \rho_{34}^{\circ 2}}$$

$$F_{18} = F_{17}/(2\ \sqrt{(F_{17}^{2}/4) + \rho_{34}^{\circ 2}F_5^{2}/\sigma_3^{2}}\ )$$

In the above relations

$$I_{s3} = \int_0^{\Omega}\sin^n\theta d\theta \qquad [A-11]$$

$$I_{s4} = \int_{\Omega}^{\pi}\sin^n\theta d\theta \qquad [A-12]$$

$$I_{s5} = \int_0^{\Omega}\sin^{n+2}\theta d\theta \qquad [A-13]$$

$$I_{s6} = \int_{\Omega}^{\pi}\sin^{n+2}\theta d\theta \qquad [A-14]$$

where

$$\Omega = \arctan[-\sigma_3 \sqrt{1-\rho_{3\dot{4}}^2}/(\rho_{3\dot{4}} F_5)] \qquad [A-15]$$

If, in the above, it is decided to generalize the degradation still further, by allowing σ to vary, then σ must be replaced approximately by μ_σ.

APPENDIX B

DETAILS OF DERIVATION OF LINEARIZED COEFFICIENTS FOR NB MODEL (Zero Mean Case).

The expected values in Equation [3.5] give the same relationships for C_{e3} and K_{e3}. For C_{e5}' and K_{e5}'

$$\begin{aligned} C_{e5}' &= E\{\partial/\partial\dot{y}_4[\lambda\xi/(\xi^2+ y_3^2)] \\ &\quad [A\dot{y}_4 - \nu(\beta|y_3|^{(n-1)}y_3|\dot{y}_4| + \gamma|y_3|^n\dot{y}_4)]/\eta\} \\ K_{e5}' &= E\{\partial/\partial y_3[\lambda\xi/(\xi^2+ y_3^2)] \\ &\quad [A\dot{y}_4 - \nu(\beta|y_3|^{(n-1)}y_3|\dot{y}_4| + \gamma|y_3|^n\dot{y}_4)]/\eta\} \end{aligned} \qquad [B-1]$$

Using the relations for the degradation control parameters A, , and η given by [A-2] together with assumption that λ and ξ can be replaced by

$$\begin{aligned} \mu_\lambda &= \delta_\lambda\mu_\varepsilon \\ \mu_\xi &= \xi_0 + \delta_\xi\mu_\varepsilon \end{aligned} \qquad [B-2]$$

allows that C_{e5}' and K_{e5}' be written in the form

$$\begin{aligned} C_{e5}' &= (\mu_\lambda\mu_\xi/\mu_\eta)\{\mu_A\, E[1/(\mu_\xi^2+ y_3^2)] - \\ &\quad \mu_\nu[\beta E[y_3|y_3|^{(n-1)}/(\mu_\xi^2+ y_3^2)\partial|\dot{y}_4|/\partial\dot{y}_4] + \\ &\quad \gamma E[|y_3|^n/(\mu_\xi^2+ y_3^2]]\} \\ K_{e5}' &= (\mu_\lambda\mu_\xi/\mu_\eta)\{-2\mu_A\, E[\dot{y}_4 y_3/(\mu_\xi^2+ y_3^2)^2] + \\ &\quad 2\mu_\nu[\beta E[y_3^2|y_3|^{(n-1)}|\dot{y}_4|/(\mu_\xi^2+ y_3^2)^2] + \\ &\quad \gamma E[y_3|y_3|^n\dot{y}_4/(\mu_\xi^2+ y_3^2)^2]] - \\ &\quad \mu_\nu[\beta E[|\dot{y}_4|/(\mu_\xi^2+ y_3^2)\partial/\partial y_3(y_3|y_3|^{(n-1)})] + \\ &\quad \gamma E[\dot{y}_4/(\mu_\xi^2+ y_3^2)\partial|y_3|^n/\partial y_3]]\} \end{aligned} \qquad [B-3]$$

or

$$C_{e5}' = (\mu_\lambda \mu_\xi / \mu_\eta)\{\mu_A E_1 - \mu_\nu[\beta E_2 + \gamma E_3]\}$$
$$K_{e5}' = (\mu_\lambda \mu_\xi / \mu_\eta)\{ -2\mu_A E_4 + 2\mu_\nu[\beta E_5 + \gamma E_6] - \mu_\nu[\beta E_7 + \gamma E_8]\} \qquad [B-4]$$

where

$$E_1 = [\sqrt{\pi/2}\,/(\mu_\xi \sigma_3)][1-\mathrm{erf}(\mu_\xi/\sqrt{2}\sigma_3)]\exp(\mu_\xi^2/2\sigma_3^2)$$
$$E_2 = 1/(\sqrt{2\pi}\sigma_3)\{\int_0^\infty (y_3^n/\alpha_1)\exp(\alpha_2)[1-\mathrm{erf}(\phi)]dy_3 - (-1)^n \int_0^\infty (y_3^n/\alpha_1)\exp(\alpha_2)\,[1-\mathrm{erf}(-\phi)]dy_3\}$$
$$E_3 = 2/(\sqrt{2\pi}\sigma_3)\int_0^\infty (y_3^n/\alpha_1)\exp(\alpha_2)dy_3 \qquad [B-5]$$
$$E_4 = 2\rho_{34}[\sigma_4/(\sqrt{2\pi}\sigma_3^2)]\int_0^\infty (y_3^2/\alpha_1^2)\exp(\alpha_2)dy_3$$
$$E_5 = 1/(\sqrt{2\pi}\sigma_3)\{\int_0^\infty (y_3^{(n+1)}/\alpha_1^2)[1-\mathrm{erf}(\phi)]dy_3 - \int_0^\infty (y_3^{(n+1)}/\alpha_1^2)\exp(\alpha_2)\,[1-\mathrm{erf}(-\phi)]dy_3\}$$
$$E_6 = 2\rho_{34}\,\sigma_4/(\sqrt{2\pi}\sigma_3^2)\int_0^\infty (y_3^{(n+2)}/\alpha_1^2)\exp(\alpha_2)dy_3$$

$$E_7 = [n/(\sqrt{2\pi}\sigma_3)]\{\int_0^\infty (1/\alpha_1)y_3^{(n-1)}\exp(\alpha_2)[1-\mathrm{erf}(\phi)]dy_3 - \int_0^\infty (1/\alpha_1)y_3^{(n-1)}\exp(\alpha_2)[1-\mathrm{erf}(-\phi)]dy_3\}$$
$$E_8 = 2n\,\rho_{34}\,\sigma_4/(\sqrt{2\pi}\sigma_3^2)\int_0^\infty (y_3^n/\alpha_1)\exp(\alpha_2)dy_3$$

In these numerical quadrature equations, expressions for α_1, α_2 and ϕ are

$$\alpha_1 = \mu_\xi^2 + y_3^2$$
$$\alpha_2 = -y_3^2/(2\sigma_3^2) \qquad [B-6]$$
$$\phi = -\rho_{34}\,y_3/[\sigma_3\sqrt{2(1-\rho_{34}^2)}]$$

and erf(.) is the error function.

APPENDIX C

DETAILS OF DERIVATION OF LINEARIZED COEFFICIENT FOR SEP MODEL (Zero Mean Case).

The expected values in Equation [3.5] give the following relationships for C_{e3}' and K_{e3}'

$$C_{e3}' = E\{\partial/\partial y_2[1-\zeta_1\exp(-y_3^2/\zeta_2^2)]$$
$$[Ay_2 - \nu(\beta|y_2\|y_3|^{(n-1)}y_3 + \gamma|y_3|^n y_2)]/\eta\}$$
$$K_{e3}' = E\{\partial/\partial y_3[1-\zeta_1\exp(-y_3^2/\zeta_2^2)]$$
$$[Ay_2 - \nu(\beta|y_2\|y_3|^{(n-1)}y_3 + \gamma|y_3|^n y_2)]/\eta\}$$

or

$$C_{e3}' = \{A[1-\zeta_1\exp(-y_3^2/\zeta_2^2)] -$$
$$[1-\zeta_1\exp(-y_3^2/\zeta_2^2)][\beta(\partial/\partial y_2)\, y_2\, y_3^{(n-1)}y_3 +$$
$$\gamma\, y_3^n]\}/\mu_\eta$$
$$K_{e3}' = (2/\mu_\eta)(\zeta_1 y_3/\zeta_2^2)\exp(-y_3^2/\zeta_2^2) \qquad [C\text{-}1]$$
$$\{Ay_2 - \mu_\nu[\beta\, y_2\, y_3^{(n-1)}y_3 + \gamma y_2\, y_3^n]\} - (1/\mu_\eta)\cdot$$
$$[1-\zeta_1\exp(-y_3^2/\zeta_2^2)]\{\mu_\nu[\beta\, y_2\, \partial/\partial y_3(y_3^{(n-1)}y_3) +$$
$$\gamma y_2\, \partial/\partial y_3\, y_3^n]\}$$

Using the relations for A, ν, and η given by [A-2] together with assumption that ζ_1 and ζ_2 can be replaced by their mean values, allows that C_{e3}' and K_{e3}' be written in the form

$$C_{e3}' = \mu_A/\mu_\eta - (\mu_A/\mu_\eta)\mu_{\zeta_1} E[\exp(-y_3^2/\mu_{\zeta_2}^2)] -$$
$$(\mu_\nu/\mu_\eta)\{\beta E[\partial/\partial y_2|y_2\|y_3|^{(n-1)}y_3] + \gamma E[|y_3|^n]\} +$$
$$(\mu_{\zeta_1}\mu_\nu/\mu_\eta)\{\beta E[\exp(-y_3^2/\mu_{\zeta_2}^2)\partial/\partial y_2|y_2\|y_3|^{(n-1)}y_3] +$$
$$\gamma E[\exp(-y_3^2/\mu_{\zeta_2}^2)|y_3|^n]\}$$

$$K_{e3}' = (2\mu_A\mu_{\zeta_1}/\mu_\eta\mu_{\zeta_2}^2)\, E[y_3y_2\exp(-y_3^2/\mu_{\zeta_2}^2)] - \qquad [C\text{-}2]$$
$$(\mu_\nu/\mu_\eta)\,\{\beta E[|y_2|\partial/\partial y_3(|y_3|^{(n-1)}y_3)] +$$
$$\gamma E[y_2\,\partial/\partial y_3|y_3|^n]\} + (\mu_{\zeta_1}\mu_\nu/\mu_\eta)\cdot$$
$$\{\beta E\exp(-y_3^2/\mu_{\zeta_2}^2)\,|y_2|\partial/\partial y_3(|y_3|^{(n-1)}|y_3|)] +$$
$$\gamma E[\exp(-y_3^2/\mu_{\zeta_2}^2)y_2\partial/\partial y_3|y_3|^n]\} -$$
$$2(\mu_{\zeta_1}\mu_\nu/\mu_{\zeta_2}^2\mu_\eta)\{\beta E[\exp(-y_3^2/\mu_{\zeta_2}^2)|y_2\,\|y_3|^{(n+1)}] +$$
$$\gamma E[\exp(-y_3^2/\mu_{\zeta_2}^2)y_3y_2|y_3|^n]\}$$

Hence

$$C_{e3}' = (\mu_A/\mu_\eta) - (\mu_A/\mu_\eta)\mu_{\zeta_1}F_5' -$$
$$(\mu_\nu/\mu_\eta)\{\beta F_1' + \gamma F_2'\} +$$
$$(\mu_{\zeta_1}\mu_\nu/\mu_\eta)[\beta F_6'(I_{s3}' - I_{s4}') + \gamma F_7']$$
$$K_{e3}' = 2[\mu_A\mu_{\zeta_1}/(\mu_\eta\mu_{\zeta_2}^2)]\,F_{16}' - (\mu_\nu/\mu_\eta)\{\beta F_3' + \gamma F_4'\} + \qquad [C\text{-}3]$$
$$(\mu_{\zeta_1}\mu_\nu/\mu_\eta)\{\beta F_9'(F_{17}'F_{18}^n/n + F_{13}') +$$
$$(\gamma/2)F_{10}'F_{15}'\} -$$
$$2(\mu_{\zeta_1}\mu_\nu/\mu_\eta)\{\beta F_8'[F_{17}'F_{18}^{n+2}/(n+2) + F_{12}'] +$$
$$\gamma F_{10}'F_{14}'\}$$

where the values for $F_1' - F_{10}'$ and $F_{12}' - F_{18}'$ in the above equations can be obtained from the same relationships given for $F_1 - F_{10}$ and $F_{12} - F_{18}$ in [A-5], [A-8], [A-10], and [A-15] respectively with the following modifications

$$F_5' = \mu_{\zeta_2}\sigma_3/\sqrt{2\sigma_3^2 + \mu^2}$$

must replace F5 in all those expressions and ρ_{23} will replace ρ_{34}.

APPENDIX D

DETAILS OF DERIVATION OF THE CALCULATION OF EXPECTED VALUES FOR BN MODEL (Nonzero Mean Case).

Solution of the differential equations for mean response requires evaluation of the expected values [4.5]. These may be rewrittenin terms of the variables $y_i = v_i - \mu_i$ as follows

$$
\begin{aligned}
E_1 &= E[\,|y_3+\mu_3|^{(n-1)}(y_3+\mu_3)\,|\dot{y}_4+\dot{\mu}_4|\,] \\
E_2 &= E[\,|y_3+\mu_3|^{n}(\dot{y}_4+\dot{\mu}_4)\,] \\
E_3 &= E[\exp(-[y_3+\mu_3]^2/(2\sigma^2))(\dot{y}_4+\dot{\mu}_4)\,] \\
E_4 &= E[\exp(-[y_3+\mu_3]^2/(2\sigma^2))\,|y_3+\mu_3|^{(n-1)}(y_3+\mu_3)\,|\dot{y}_4+\dot{\mu}_4|\,] \\
E_5 &= E[\exp(-[y_3+\mu_3]^2/(2\sigma^2))\,|y_3+\mu_3|^{n}(\dot{y}_4+\dot{\mu}_4)\,]
\end{aligned}
\qquad [D\text{-}1]
$$

Substituting the appropriate nonlinear functions into Equations [4.8] leads to

$$
\begin{aligned}
C_{e3} &= \{\mu_A-\mu_\nu[\beta E_6+\gamma E_7]\}/\mu_\eta \\
K_{e3} &= -\mu_\nu[\beta E_8+\gamma E_9]/\mu_\eta \\
C_{e5} &= 2\mu_a/(\sqrt{2\pi}\sigma)\{\mu_A E_{10}-\mu_\nu[\beta E_{11}+\gamma E_{12}]\}/\mu_\eta \\
K_{e5} &= 2\mu_a/(\sqrt{2\pi}\sigma)\{-(\mu_A/\sigma^2)E_{13}-\mu_\nu[\beta(-E_{14}/\sigma^2+E_{15}) + \\
&\qquad \gamma(-E_{16}/\sigma_2+E_{17})]\}/\mu_\eta
\end{aligned}
\qquad [D\text{-}2]
$$

where

$$
\begin{aligned}
E_6 &= E[\,|y_3+\mu_3|^{(n-1)}(y_3+\mu_3)\,\mathrm{sgn}(\dot{y}_4+\dot{\mu}_4)\,] \\
E_7 &= E[\,|y_3+\mu_3|^{n}\,] \\
E_8 &= nE[\,|y_3+\mu_3|^{(n-1)}\,|\dot{y}_4+\dot{\mu}_4|\,] \\
E_9 &= nE[\,|y_3+\mu_3|^{(n-2)}(y_3+\mu_3)(\dot{y}_4+\dot{\mu}_4)\,] \\
E_{10} &= E[\exp(-[y_3+\mu_3]^2/(2\sigma^2))\,]
\end{aligned}
$$

$$E_{11} = E[\exp(-[y_3+\mu_3]^2/(2\sigma^2))|y_3+\mu_3|^{(n-1)}\cdot (y_3+\mu_3)\,\mathrm{sgn}(\dot{y}_4+\dot{\mu}_4)]$$

$$E_{12} = E[\exp(-[y_3+\mu_3]^2/(2\sigma^2))|y_3+\mu_3|^{n}] \qquad [D-3]$$

$$E_{13} = E[\exp(-[y_3+\mu_3]^2/(2\sigma^2))(y_3+\mu_3)(\dot{y}_4+\dot{\mu}_4)]$$

$$E_{14} = E[\exp(-[y_3+\mu_3]^2/(2\sigma^2))|y_3+\mu_3|^{(n+1)}|\dot{y}_4+\dot{\mu}_4|]$$

$$E_{15} = nE[\exp(-[y_3+\mu_3]^2/(2\sigma^2))|y_3+\mu_3|^{(n-1)}|\dot{y}_4+\dot{\mu}_4|]$$

$$E_{16} = E[\exp(-[y_3+\mu_3]^2/(2\sigma^2))|y_3+\mu_3|^{n}\cdot (y_3+\mu_3)(\dot{y}_4+\dot{\mu}_4)]$$

$$E_{17} = nE[\exp(-[y_3+\mu_3]^2/(2\sigma^2))|y_3+\mu_3|^{(n-2)} (y_3+\mu_3)(\dot{y}_4+\dot{\mu}_4)]$$

These expected values are evaluated in several distinct groups as follows

CASE 1- n = odd:

In this case, all integrals can be evaluated in closed form. For computational purposes, it is appropriate to categorize the integrals to the number of summation required.

(a) No Summation Integrals

$$E_3 = (\alpha/\sigma_3)\dot{\sigma_4}\,\Delta_1\Delta_2$$

$$E_{10} = (\alpha/\sigma_3)\Delta_1$$

$$E_{13} = (\alpha/\sigma_3)^2\,\dot{\sigma_4}\,\alpha\Delta_1[\beta_3\Delta_2+\rho_{3\dot{4}}]$$

(b) Single Summation Integrals

$$E_2 = \dot{\sigma_4}\sigma_3{}^n\{\sum_{k=0}^{n}\binom{n}{k}\beta_3{}^{(n-k)}[\rho_{3\dot{4}}\;I_{s2}(k+1,\beta_3) +$$

$$\beta_4^{\circ} \quad I_{s2}(k,\beta_3)]\}$$

$$E_5 = (\alpha^{n+1}/\sigma_3)\sigma_4^{\circ}\Delta_1\{\sum_{k=0}^{n}\binom{n}{k}\Delta_3^{(n-k)}\cdot$$

$$[(\rho_{34}^{\circ}\alpha/\sigma_3)I_{s2}(k+1,-\Delta_3) + \Delta_2 I_{s2}(k,-\Delta_3)]\}$$

$$E_7 = -\sigma_3^{n}\{\sum_{k=0}^{n}\binom{n}{k}\beta_3^{(n-k)} \quad I_{s2}(k,\beta_3)\}$$

$$E_9 = n\sigma_4^{\circ}\sigma_3^{(n-1)}\{\sum_{k=0}^{n-1}\binom{n-1}{k}\beta_3^{(n-k-1)}\cdot$$

$$[\rho_{34}^{\circ} \quad I_{s2}(k+1,\beta_3) + \beta_4^{\circ} \quad I_{s2}(k,\beta_3)]\}$$

$$E_{12} = (\alpha^{n+1}/\sigma_3)\Delta_1\{\sum_{k=0}^{n}\binom{n}{k}\Delta_3^{(n-k)} \quad I_{s2}(k,-\Delta_3)\}$$

$$E_{16} = (\alpha^{n+2}/\sigma_3)\sigma_4^{\circ}\Delta_1\{\sum_{k=0}^{n+1}\binom{n+1}{k}\Delta_3^{(n+1-k)}[\rho_{34}^{\circ}(\alpha/\sigma_3)\cdot$$

$$I_{s2}(k+1,-\Delta_3) + \Delta_2 I_{s2}(k,-\Delta_3)]\}$$

$$E_{17} = (\alpha^{n}/\sigma_3)\sigma_4^{\circ}\Delta_1\{\sum_{k=0}^{n-1}\binom{n-1}{k}\Delta_3^{(n-k-1)}[(\rho_{34}^{\circ} \alpha/\sigma_3)\cdot$$

$$I_{s2}(k+1,-\Delta_3) + \Delta_2 I_{s2}(k,-\Delta_3)]\}$$

(c) Double Summation Integrals

$$E_1 = \sigma_4^{\circ}\sigma_3^{n}\{\sum_{k=0}^{n}\binom{n}{k}(\sqrt{1-\rho_{34}^{\circ 2}})^{k} \quad I_{s1}(k)\cdot$$

$$\sum_{m=0}^{n-k}[\binom{n-k}{m}\rho_{34}^{\circ m}\beta_3^{(n-k-m)}I_{s2}(m+1,\beta_4^{\circ}) + \beta_4^{\circ}I_{s2}(m,\beta_4^{\circ})]\}$$

$$E_4 = (\alpha_\rho^{n+1}/\sigma_3)\sigma_4^{\circ}\Delta_4\Delta_7\{\sum_{k=0}^{n}\binom{n}{k}(\sqrt{1-\rho_{34}^{\cdot 2}})^k\cdot$$

$$(\alpha_\rho/\sigma_3)^{(n-k)}\ I_{s1}(k)\ \sum_{m=0}^{n-k}\binom{n-k}{m}\Delta_5^{\,m}\ \Delta_6^{(n-k-m)}\cdot$$

$$[\Delta_7 I_{s2}(m+1,\Delta_8) + \Delta_9 I_{s2}(m,\Delta_8)]\}$$

$$E_6 = \sigma_3^{\,n}\{\sum_{k=0}^{n}\binom{n}{k}(1-\rho_{34}^{\cdot 2})^k\ I_{s1}(k)\ \cdot$$

$$\sum_{m=0}^{n-k}\binom{n-k}{m}\rho_{34}^{\cdot m}\ \beta_3^{(n-k-m)} I_{s2}(m,\beta_4^{\circ})\}$$

$$E_8 = n\sigma_4^{\circ}\sigma_3^{(n-1)}\{\sum_{k=0}^{n-1}\binom{n-1}{k}(\sqrt{1-\rho_{34}^{\cdot 2}})^k\ I_{s1}(k)\ \cdot$$

$$\sum_{m=0}^{n-k-1}\binom{n-k-1}{m}\rho_{34}^{\cdot m}\ \beta_3^{(n-k-m-1)}[I_{s2}(m+1,\beta_4^{\circ}) +$$

$$\beta_4^{\circ}\ I_{s2}(m,\beta_4^{\circ})]\}$$

$$E_{11} = (\alpha_\rho^{n+1}/\sigma_3)\Delta_4\Delta_7\{\sum_{k=0}^{n}\binom{n}{k}(\sqrt{1-\rho_{34}^{\cdot 2}})^k(\alpha_\rho/\sigma_3)^{(n-k)}\cdot$$

$$I_{s1}(k)\ \sum_{m=0}^{n-k}\binom{n-k}{m}\rho_{34}^{\cdot m}\ \Delta_7^{\,m}\ \Delta_6^{(n-k-m)} I_{s2}(m,\Delta_8)]\}$$

$$E_{14} = (\alpha_\rho^{n+2}/\sigma_3)\sigma_4^{\circ}\Delta_4\Delta_7\{\sum_{k=0}^{n+1}\binom{n+1}{n}(\sqrt{1-\rho_{34}^{\cdot 2}})^k\cdot$$

$$(\alpha_\rho/\sigma_3)^{(n-k+1)} I_{s1}(k)\ \sum_{m=0}^{n-k+1}\binom{n-k+1}{m}[\rho\Delta_7]^m\ \Delta_6^{(n-k-m+1)}\cdot$$

$$[\Delta_7 I_{s2}(m+1,\Delta_8) + \Delta_9 I_{s2}(m,\Delta_8)]\}$$

$$E_{15} = (\alpha_\rho/\sigma_3)\sigma_4^{\cdot}\alpha_\rho^{(n-1)}\Delta_4\Delta_7\{\sum_{k=0}^{n-1}\binom{n-1}{k}(\sqrt{1-\rho_{34}^{\cdot 2}})^k \cdot$$

$$(\alpha_\rho/\sigma_3)^{(n-k-1)} I_{s1}(k) \sum_{m=0}^{n-k-1}\binom{n-k-1}{m}[\rho_{34}^{\cdot}\Delta_7]^m \Delta_6^{(n-k-m-1)} \cdot$$

$$[\Delta_7 I_{s2}(m+1,\Delta_8) + \Delta_9 I_{s2}(m,\Delta_8)]\}$$

In the above,

$$\alpha = \sigma\sigma_3/\sqrt{\sigma^2 + \sigma_3^2} \quad ; \quad \alpha_\rho = \sigma\sigma_3/\sqrt{(1-\rho_{34}^{\cdot 2})\sigma_3^2 + \sigma^2}$$

$$\beta_3 = \mu_3/\sigma_3 \quad ; \quad \beta_4 = \dot{\mu}_4//\sigma_4^{\cdot}$$

$$\beta_\rho = \sqrt{1-(\alpha_\rho/\sigma_3)^2} \quad ; \quad \hat{\beta}_\rho = 1/[1-\rho_{34}^{\cdot 2}(1-\beta_\rho^2)]$$

and the Δ's are given by

$$\Delta_1 = \exp\{\beta_3^2[(\alpha/\sigma_3)^2-1]\}$$

$$\Delta_2 = \beta_4^{\cdot} + \rho_{34}^{\cdot}[(\alpha/\sigma_3)^2-1]\beta_3$$

$$\Delta_3 = (\alpha/\sigma_3)\beta_3$$

$$\Delta_4 = \exp\{\beta_\rho^2\beta_3^2[\rho_{34}^{\cdot 2}\hat{\beta}_\rho^2\beta_\rho^2 - 1]/[2(1-\rho_{34}^{\cdot 2})]\}$$

$$\Delta_5 = \rho_{34}^{\cdot}\hat{\beta}_\rho\sqrt{1-\rho_{34}^2}$$

$$\Delta_6 = \beta_3 - \rho_{34}^{\cdot}\hat{\beta}_\rho^2\beta_\rho^2\beta_3$$

$$\Delta_7 = \hat{\beta}_\rho\sqrt{1-\rho_{34}^{\cdot 2}}$$

$$\Delta_8 = -\Delta_9/\Delta_7$$

$$\Delta_9 = \beta_4^{\cdot} - \rho_{34}^{\cdot}\hat{\beta}_\rho^2\beta_\rho^2\beta_3$$

The standard integrals are

$$I_{s1}(k) = (1/\sqrt{2\pi})\int_\infty^\infty \zeta^k \exp(-\zeta^2/2)\,d\zeta$$

$$I_{s2}(k,\beta_i) = (1/\sqrt{2\pi})\int_\infty^\infty \zeta^k \mathrm{sgn}(\zeta+\beta_i)\exp(-\zeta^2/2)\,d\zeta$$

The integrals I_{s1} and I_{s2} can be evaluated in closed form

giving

$$I_{s1}(k) = \begin{cases} 0 & \text{(odd } k\text{)} \\ 1 & (k=0) \\ \{(k-1)!/[(k-2)/2]!\}[2^{(k-2)/2}] & \text{(even } k\text{)} \end{cases}$$

$$I_{s2}(k,\beta_i) = \begin{cases} (\sqrt{2/\pi})(-1)^{(k-1)}\beta_i^{(k-1)}\exp(-\beta_i^2/2)+ \\ (k-1)I_{s2}(k-2,\beta_i) & (k > 2) \\ (\sqrt{2/\pi})\exp(-\beta_i^2/2) & (k = 1) \\ 1 - 2\phi(-\beta_i) & (k = 0) \end{cases}$$

Where $\phi(.)$ is the Gaussian cumulative distribution function.

CASE 2- n = even:

Several integrals are simplified but other integrals reduce to a sum of two Gauss-Laguerre quadratures.

(a) No Summation Integrals

E_3, E_{10}, and E_{13} do not depend on 'n' and therefore, do not change.

(b) Single Summation Integrals

$$E_2 = \sigma_4^{\cdot}\sigma_3^{\,n}\{\sum_{n=0}^{k}\binom{n}{k}\beta_3^{(n-k)}[\rho_{34}^{\cdot}\, I_{s1}(k+1) + \beta_4^{\cdot}\, I_{s1}(k)]\}$$

$$E_5 = (\alpha^{n+1}/\sigma_3)\sigma_4^{\cdot}\Delta_1\{\sum_{n=0}^{k}\binom{n}{k}\Delta_3^{(n-k)}\cdot$$

$$[\rho_{34}^{\cdot}(\alpha/\sigma_3)\, I_{s1}(k+1) + \Delta_2 I_{s1}(k)]\}$$

$$E_7 = \sigma_3^n \{ \sum_{k=0}^{n} \binom{n}{k} \beta_3^{(n-k)} I_{s1}(k)] \}$$

$$E_9 = n\sigma_4^* \sigma_3^{(n-1)} \{ \sum_{k=0}^{n-1} \binom{n-1}{k} \beta_3^{(n-k-1)} \cdot [\rho_{34}^* I_{s1}(k+1) + \beta_4^* I_{s1}(k)] \}$$

$$E_{12} = (\alpha^{n+1}/\sigma_3)\Delta_1 \{ \sum_{k=0}^{n} \binom{n}{k} \Delta_3^{(n-k)} I_{s1}(k) \}$$

$$E_{16} = (\alpha^{n+2}/\sigma_3)\sigma_4^* \Delta_1 \{ \sum_{k=0}^{n+1} \binom{n+1}{k} \Delta_3^{(n+1-k)} \cdot [\rho_{34}^* (\alpha/\sigma_3) I_{s1}(k+1) + \Delta_2 I_{s1}(k)]$$

$$E_{17} = (\alpha^n/\sigma_3)\sigma_4^* \Delta_1 \{ \sum_{k=0}^{n-1} \binom{n-1}{k} \Delta_3^{(n-k-1)} \cdot [(\rho_{34}^* \alpha/\sigma_3) I_{s1}(k+1) + \Delta_2 I_{s1}(k)] \}$$

(c) Numerical Quadratures

The double summation integrals can no longer be evaluated in closed form, but can be reduced to the following quadratures

$$E_1 = (\sigma_4^* \sigma_3^n / \sqrt{2\pi}) \{ \int_{-\infty}^{0} |\zeta|^{(n-1)} \zeta \, \theta_2 \exp(\gamma_3) \exp(\zeta) d\zeta + \int_0^{\infty} \zeta^n \theta_2 \exp(\gamma_2) \exp(-\zeta) d\zeta \}$$

$$E_4 = (\sigma_4^* \sigma_3^n / \sqrt{2\pi}) \{ \int_{-\infty}^{0} |\zeta|^{(n-1)} \zeta \, \theta_3 \exp(\zeta) d\zeta + \int_0^{\infty} \zeta^n \theta_4 \exp(-\zeta) d\zeta \}$$

$$E_6 = (\sigma_3^n / 2\pi) \{ \int_{-\infty}^{0} |\zeta|^{(n-1)} \zeta \, \theta_1 \exp(\gamma_3) \exp(\zeta) d\zeta + \int_0^{\infty} \zeta^n \theta_1 \exp(\gamma_2) \exp(-\zeta) d\zeta \}$$

$$E_8 = n(\sigma_4^{\cdot}\sigma_3^{n-1}/\sqrt{2\pi})\{\int_{-\infty}^{0} |\zeta|^{(n-1)}\ \theta_2 \exp(\gamma_3)\exp(\zeta)d\zeta\ +$$
$$\int_0^{\infty} \zeta^{(n-1)}\ \theta_1 \exp(\gamma_2)\exp(-\zeta)d\zeta\ \}$$

$$E_{11} = (\sigma_3^{n}/\sqrt{2\pi})\{\int_{-\infty}^{0} |\zeta|^{(n-1)}\ \theta_5 \exp(\zeta)d\zeta\ +$$
$$\int_0^{\infty} \zeta^{n}\ \theta_6 \exp(-\zeta)d\zeta\ \}$$

$$E_{14} = (\sigma_4^{\cdot}\sigma_3^{n+1}/\sqrt{2\pi})\{\int_{-\infty}^{0} |\zeta|^{(n+1)}\ \theta_3 \exp(\zeta)d\zeta\ +$$
$$\int_0^{\infty} \zeta^{(n+1)}\ \theta_4 \exp(-\zeta)d\zeta\ \}$$

$$E_{15} = (\sigma_4^{\cdot}\sigma_3^{n-1}/\sqrt{2\pi})\{\int_{-\infty}^{0} |\zeta|^{(n-1)}\ \theta_3 \exp(\zeta)d\zeta\ +$$
$$\int_0^{\infty} \zeta^{(n+1)}\ \theta_4 \exp(-\zeta)d\zeta\ \}$$

In these numerical quadratures

$$\gamma_1 = [\beta_4^{\cdot} - \rho_{34}(\zeta - \beta_3)]/\sqrt{1 - \rho_{34}^{\cdot 2}}$$
$$\gamma_2 = -0.5(\zeta - \beta_3)^2 + \zeta$$
$$\gamma_3 = -0.5(\zeta - \beta_3)^2 - \zeta$$
$$\gamma_4 = \rho_{34}^{\cdot}(\zeta - \beta_3) + \beta_4^{\cdot}$$
$$\theta_1 = [1 - 2\phi(-\gamma_1)]$$
$$\theta_2 = (\sqrt{2/\pi})\ \sqrt{1-\rho_{34}^{\cdot 2}}\ \exp(-\gamma_1^2/2) + \gamma_4\theta_1$$
$$\theta_3 = \theta_2\exp(\gamma_3)\exp[-\sigma_3^2\zeta^2/(2\sigma^2)]$$
$$\theta_4 = \theta_2\exp(\gamma_2)\exp[-\sigma_3^2\zeta^2/(2\sigma^2)]$$
$$\theta_5 = \theta_3\theta_1/\theta_2$$
$$\theta_6 = \theta_4\theta_1/\theta_2$$

CASE 3- n = Non-Integer Value

If 'n' is not an integer, the no summation integrals still remain unchanged. The numerical quadratures of Case 2(c) will also remain unchanged, but the single summation quadratures are

no longer feasible. Then the following additional numerical quadratures are required.

$$E_2 = (\sigma_4^{\cdot}\sigma_3^{\,n}/\sqrt{2\pi})\left[\int_{-\infty}^{0} |\zeta|^n \gamma_4 \exp(\gamma_3)\gamma_4 \exp(\zeta)\,d\zeta + \int_0^{\infty} \zeta^n \gamma_4 \exp(\gamma_2)\exp(-\zeta)\,d\zeta\right]$$

$$E_5 = (\sigma_4^{\cdot}\sigma_3^{\,n}/\sqrt{2\pi})\left[\int_{-\infty}^{0} |\zeta|^n \theta_7 \exp(\zeta)\,d\zeta + \int_0^{\infty} \zeta^n \theta_8 \exp(-\zeta)\,d\zeta\right]$$

$$E_7 = (\sigma_3^{\,n}/\sqrt{2\pi})\left[\int_{-\infty}^{0} |\zeta|^n \exp(\gamma_3)\exp(\zeta)\,d\zeta + \int_0^{\infty} \zeta^n \exp(\gamma_2)\exp(-\zeta)\,d\zeta\right]$$

$$E_9 = n(\sigma_4^{\cdot}\sigma_3^{\,n-1}/\sqrt{2\pi})\left[\int_{-\infty}^{0} |\zeta|^{(n-2)} \gamma_4 \exp(\gamma_3)\exp(\zeta)\,d\zeta + \int_0^{\infty} \zeta^{(n-1)} \gamma_4 \exp(\gamma_2)\exp(-\zeta)\,d\zeta\right]$$

$$E_{12} = (\sigma^n/\sqrt{2\pi})\left[\int_{-\infty}^{0} |\zeta|^n \theta_9 \exp(\zeta)\,d\zeta + \int_0^{\infty} \zeta^n \theta_{10} \exp(-\zeta)\,d\zeta\right]$$

$$E_{16} = (\sigma_4^{\cdot}\sigma_3^{\,n+1}/\sqrt{2\pi})\left[\int_{-\infty}^{0} |\zeta|^n \theta_7 \exp(\zeta)\,d\zeta + \int_0^{\infty} \zeta^{(n+1)} \theta_8 \exp(-\zeta)\,d\zeta\right]$$

$$E_{17} = (\sigma_4^{\cdot}\sigma_3^{\,n-1}/\sqrt{2\pi})\left[\int_{-\infty}^{0} |\zeta|^{(n-2)} \theta_7 \exp(\zeta)\,d\zeta + \int_0^{\infty} \zeta^{(n-1)} \theta_8 \exp(-\zeta)\,d\zeta\right]$$

where

$$\theta_7 = \exp[-\sigma_3^{\,2}\zeta^2/(2\sigma^2)]\exp(\gamma_3)\gamma_4$$

$$\theta_8 = \exp[-\sigma_3^{\,2}\zeta^2/(2\sigma^2)]\exp(\gamma_2)\gamma_4$$

$$\theta_9 = \theta_7/\gamma_4$$

$$\theta_{10} = \theta_8/\gamma_4$$

In the reduced forms, all of the numerical quadratures are

compatible with an N point Gauss-Laguerre formula.

APPENDIX E

DETAILS OF DERIVATION OF THE CALCULATION OF EXPECTED VALUES FOR SEP MODEL (Nonzero Mean Case).

The expected values needed for the solution of stochastic differential equations for the mean responses given in [4.26] can be rewritten as follows. Here, $y_i = v_i - \mu_i$ as before

$$
\begin{aligned}
E_1' &= E[\,|y_3+\mu_3|^{(n-1)}(y_3+\mu_3)\;\;|y_2+\mu_2|\,] \\
E_2' &= E[\,|y_3+\mu_3|^{n}(y_2+\mu_2)\,] \\
E_3' &= E[\exp(-\{y_3+\mu_3\}^2/\zeta_2^2)(y_2+\mu_2)\,] \\
E_4' &= E[\exp(-\{y_3+\mu_3\}^2/\zeta_2^2)\,|y_3+\mu_3|^{(n-1)}(y_3+\mu_3)\,|y_2+\mu_2|\,] \\
E_5' &= E[\exp(-\{y_3+\mu_3\}^2/\zeta_2^2)\,|y_3+\mu_3|^{n}(y_2+\mu_2)\,]
\end{aligned}
\qquad [E\text{-}1]
$$

Also substitution of the appropriate nonlinear functions into Equation [4.29] results

$$
\begin{aligned}
C_e &= \{\mu_A - \mu_\nu[\beta E_6' + \gamma E_7']\}/\mu_\eta - \\
&\quad (\mu_{\zeta_1}/\mu_\eta)\{AE_{10}' - \mu_\nu[\beta E_{11}' + \gamma E_{12}']\}
\end{aligned}
\qquad [E\text{-}2]
$$

$$
\begin{aligned}
K_e &= (-\mu_\nu/\mu_\eta)[\beta E_8' + \gamma E_9'] + (\mu_{\zeta_1}/\mu_\eta)\{\mu_\nu[\beta E_{15}' + \gamma E_{17}'] + \\
&\quad (2\mu_A/\mu_{\zeta_2}^2)E_{13}' - (2\mu_\nu/\mu_{\zeta_2}^2)[\beta E_{14}' + \gamma E_{16}']\}
\end{aligned}
$$

where

$$
\begin{aligned}
E_6' &= E[\,|y_3+\mu_3|^{(n-1)}(y_3+\mu_3)\;\mathrm{sgn}(y_2+\mu_2)\,] \\
E_7' &= E[\,|y_3+\mu_3|^{n}\,] \\
E_8' &= nE[\,|y_2+\mu_2\,\|y_3+\mu_3|^{(n-1)}\,] \\
E_9' &= nE[\,|y_3+\mu_3|^{(n-2)}(y_3+\mu_3)(y_2+\mu_2)\,] \\
E_{10}' &= E[\exp(-\{y_3+\mu_3\}^2/\zeta_2^2)\,]
\end{aligned}
$$

$$E_{11}' = E[\,|y_3+\mu_3|^{(n-1)}(y_3+\mu_3)\ \mathrm{sgn}(y_2+\mu_2)\exp(-\{y_3+\mu_3\}^2/\zeta_2^2)]$$
$$E_{12}' = E[\,|y_3+\mu_3|^{n}\ \exp(-\{y_3+\mu_3\}^2/\zeta_2^2)] \qquad [E-3]$$
$$E_{13}' = E[(y_3+\mu_3)(y_2+\mu_2)\ \exp(-\{-y_3+\mu_3\}^2/\zeta_2^2)]$$
$$E_{14}' = E[\,|y_3+\mu_3|^{(n+1)}\,|y_2+\mu_2|\exp(-\{y_3+\mu_3\}^2/\zeta_2^2)]$$
$$E_{15}' = nE[\,|y_3+\mu_3|^{(n-1)}\,|y_2+\mu_2|\exp(-\{y_3+\mu_3\}^2/\zeta_2^2)]$$
$$E_{16}' = E[\,|y_3+\mu_3|^{n}(y_3+\mu_3)(y_2+\mu_2)\exp(-\{y_3+\mu_3\}^2/\zeta_2^2)]$$
$$E_{17}' = nE[\,|y_3+\mu_3|^{(n-2)}(y_3+\mu_3)(y_2+\mu_2)\exp(-\{y_3+\mu_3\}^2/\zeta_2^2)]$$

These expected values can be evaluated in the same three distinct categories established for BN model in Appendix D. The general form of these E_i's expected values are similar to respective E_i's values tabulated in the Appendix D. Therefore, with the following modifications same relations can be used for the evaluation of expected values in [E-2] and [E-3]. The necessary modifications are

$\rho_{34}^{\cdot}$ must be replaced with ρ_{23}

$\sigma_4^{\cdot}$ must be replaced with σ_2

$\beta_4^{\cdot}$ must be replaced with $\beta_2 = \mu_2/\sigma_2$

α must be replaced with $\alpha = \zeta_2\sigma_3/\sqrt{\zeta_2^2+2\sigma_3^2}$

α_ρ must be replaced with $\alpha_\rho = \zeta_2\sigma_3/\sqrt{2(1-\rho_{23}^2)+\zeta_2^2}$